The evolution and ecology of fungal symbionts in ant-associated mutualisms

by

Kirsten Leigh Gotting

A dissertation submitted in partial fulfillment of

The requirements for the degree of

Doctor of Philosophy

(Genetics)

at the

UNIVERSITY OF WISCONSIN – MADISON

2022

Date of final oral examination: 12/13/2022

Final Oral Committee:

Cameron R. Currie, Professor, Bacteriology

Nancy Keller, Professor, Medical Microbiology and Immunology, Bacteriology

Nicole Perna, Professor, Genetics

Chris Hittinger, Professor, Genetics

John Pool, Professor, Genetics

Dissertation Abstract

The evolution and ecology of fungal symbionts in ant-associated mutualisms

By Kirsten Leigh Gotting

Under the supervision of Professor Cameron R. Currie

At the University of Wisconsin – Madison

Fungi define and shape a multitude of organismal evolutionary trajectories. These fungi play a variety of roles in symbiosis and can have a multitude of ecologies ranging from parasites to mutualists. Many insects associate with fungi. Some insects eat fungi, and some fungi eat insects. The fungus-growing ant-microbe symbiosis is one example where fungal symbionts take on different roles. Fungus-growing ants are engaged in an obligate mutualism with fungi in the genus *Leucoagaricus*. The ants bring diverse substrates to their constructed fungal homes called 'fungus gardens' which digest these substrates. Additionally, these fungus gardens house a diverse array of bacteria, some which have various roles in the fungus garden such as nitrogen fixation. Another symbiont is the parasite *Escovopsis*, which infects nearly all fungus-growing ant colonies, and can potentially completely disrupt the colony. In response to this parasite, fungus-growing ants use weeding and grooming behaviors, as well as prophylactic application of antibiotics to prevent the growth of this parasite. In this dissertation, I used a variety of computational frameworks to explore the relationships of fungi amongst mutualism, one being the fungus-

growing ant microbe symbiosis. My main goal is to assess both the evolution and ecology of different fungal symbionts in the context of mutualisms.

My first chapter gives a broad overview of the biology of the fungus-growing ant-microbe symbiosis. I discuss the production of energy and exchange of nutrients, various symbiotic microbes that have been found in fungus-gardens, as well as parasites to the mutualism. Lastly, I discuss the different defenses that fungus-growing ants use to combat parasitic pressure. In my second chapter, I look at the evolution of the parasite *Escovopsis* across the evolutionary history of the symbiosis. I show that *Escovopsis* genomes diverge on a macro-evolutionary scale, with broad differences in dates of origin for major clades, genome sizes, and copy numbers and compositions of suites of functional genes. In my third chapter, I examine metagenomes from the fungus growing ant symbiosis. I show that metagenomes recapitulate some aspects of the ecology of the symbiosis, but often misses identifying key partners. In my fourth chapter, I took what I learned from fungus-growing ants into another insect-fungus symbiosis encapsulated within the *Azteca-Cecropia* symbiosis. I show that *Candida* associated with *Azteca* ants are within the CUG-Ser1 clade of yeasts and contain similar biosynthetic gene clusters that may play a role in the ecology of these fungi. Overall, the work in this dissertation expands our knowledge on the evolution and ecology of fungal symbioses.

Acknowledgements

The stages of my life leading into deciding to do a PhD are defined by the people and teams that created foundational moments in my life that define me as a scientist. These people shaped both how I think about science, and the way that I pursue scientific questions. They continuously encouraged my curiosity, challenged my assumptions, and pushed me to go beyond one stage of thinking.

I would like to start by thanking the team at The Zebrafish International Resource Center at University of Oregon, in particular, Jen-jen Huang Shum and Andrzej Nasiadka. In my undergrad, I needed paid work to get through financially. I am so lucky that I found a paid job with flexible hours that fully supported and prioritized my academic pursuits while also giving me the opportunity to work with a genetic model organism. I learned so much about biology, and developmental biology by working with these fish in a position where I got to put some of what I was learning in the classroom to practice.

I would like to thank the bioinformatics training program at the University of Oregon. This master's program gave me so many useful skills, and a way to put them into practice. I would like to thank Farrel Ford for training me in interviewing and resume prep, while also showing me how I strive to present myself professionally. These are skills that I continue to use to this day and was one of the most valuable learning experiences I had in the program. I also am grateful for this program for leading me to my first long-term research experience with my internship.

My internship through my master's program led me to The Stowers Institute for Medical Research, where I feel so lucky and fortunate to have gotten to work in Alejandro Sánchez's lab and get my first position as a bioinformaticist. I would particularly like to thank Eric Ross. Learning from you, laughing with you, and brainstorming with you was one of the best experiences, and I always remember those days fondly. Similarly, Sofia Robb, Malcolm Cook, Madelaine Gogal, Chris Seidel, and the rest of the bioinformatics scientists at Stowers created an excellent and encouraging learning environment during my time there. I'd also like to thank some of my lab mates from the time: Beth Duncan, Erin Davies, Stephanie Nowotarski, Christopher Arnold, Alice Accorsi, and Wei Wang. You are all amazing people and scientists, and your work continues to inspire me. Lastly, I thank Alejandro, because without you believing in me, I probably would have given up on this dream a long time ago.

This brings me to the wonderful people and communities that I've gotten to be a part of at the University of Wisconsin – Madison. I would like to start by thanking Martha Reck, Errol Wizda, Audrey Gasch, and Nicole Perna. Your administration of the Genetics Training Program has made this PhD a smooth road for me, and for that I am very grateful. I would also like to thank the administrative staff in the Bacteriology department, and in particular Kari Straus, Kim Best, and Janet Newlands for keeping me oriented while straddling two buildings and a lot of different funding situations. Additionally, my committee has been foundational in guiding my progress, thank you to Nancy Keller, Anne Pringle, Chris Hittinger, Nicole Perna, and John Pool.

I would like to thank my advisor Cameron Currie, for supporting me in a multitude of ways and without whom this work would not exist. Your mentorship instilled foundational ways of thinking about evolutionary biology and I'm excited to keep using the tools that I gained in the lab in my future research. You also allowed me a lot of freedom to pursue a wide range of interests, for which I will always be grateful. I would like to thank the many people in the Currie lab, who shaped my thinking and provided a lot of support for my research. Thank you to Lily Khadempour, Camila Carlos, Heidi Horn, Caitlin Carlson, Reed Stubbendieck, Marc Chevrette, Daniel May, Hongjie Li, Lindsay Wilson, Rachel Arrango, and Nat Zeng. I want to give a special thanks to Donny Hoang, Charlotte Francoeur, Soleil Young, and Jenny Bratburd; thank you for being wonderful friends and colleagues to me, and for supporting me, challenging me, and holding me together through the worst and best of these years together.

I was extremely fortunate to do fieldwork during the COVID19 pandemic. I am unendingly grateful to Bill Wicslo, Paula Gomez, and Isis Ochoa-Herrera for supporting my research during my Smithsonian Tropical Research Institute fellowship. I thank Scott Powell, for teaching me all about army ants. I hope to get to work on them again in the future! I want to specifically thank Donny Hoang (again), Maddy Foote, Amanda Savage, Finn Piatscheck, Logan James and Eleinis Ávila-Lovera for supporting me in Panama, and more importantly being awesome friends.

I have amazing collaborators that contributed to my projects. To Jeffrey Sosa-Calvo and Ted Schultz, thank you so much for your insight, advice, and instruction on phylogeny, dating, and the attine ant symbiosis. I learned so much from you and I am excited to keep using these

tools in the future. Thank you to Mônica Pupo for your support through the ICBG project, and your grace and kindness. Thank you to Tim Bugni for supporting our endeavors in chemistry. And thank you the Spencer Johnston, for your insight and contributions to *Escovopsis* genome sizes.

I also want to thank all my friends from the Genetics Training Program, in particular, my base-pair bud Mel Adams, and my committee comrade Mikey Kartje. I would also like to thank Elizabeth McDaniel, working with you on ComBEE was truly and amazing experience, and I learned so much about organizing and efficiency from you. I also want to acknowledge the COVID19 pandemic, which played a larger role than I would have ever wanted it to in shaping this thesis.

I would also like to thank my family, because while you may not fully understand what I'm doing at times, and I can't always answer questions about my career, I'm glad that you can appreciate and support me on one of the grandest adventures of my life. Thanks to my mom, Karen for always answering the phone and listening to whatever is on my mind. Thanks to my dad, Tad, for showing me and reminding me of how to live and enjoy my life. Thanks to my brothers Eric and Blake, for always having my back. I thank my dear friends Gwen and Eric, for propping me up when I could barely stand on two legs. And to Natasha Story, Vasha DuTell, Allison Orr, and Ashley Woodfin, thank you for always encouraging me to show up with my best self and for supporting me for the last ten years personally and professionally. This wouldn't have happened without any of you. Lastly, I would like to thank myself for persevering through personal and professional challenges and making this thing happen.

Table of Contents

Chapter 1: Evolution of fungal cultivation by ants

Kirsten Gotting[1] (gotting@wisc.edu)
Cameron Currie[1,2] (ccurrie@mcmaster.ca)

This chapter is in preparation for submission for publication, pending minor changes.

Affiliations:
[1]University of Wisconsin Madison, Department of Bacteriology, Madison, Wisconsin
[2]McMaster University, Department of Biochemistry and Biomedical Sciences, Hamilton, Ontario

1.1 Summary

Diverse fungi engage in complex symbioses with insects. One such symbiosis involves fungi that are cultivated for food by attine ants. This is an ancient and obligate nutritional mutualism, with the fungus (Basidomycota: Agaricales: Agaricaceae or Pterulaceae) growing on the vegetative substrate delivered by their ant hosts, and in exchange produces specialized hyphal swellings that the ants consume. This fungus-ant mutualism originated over 55 million years ago, with each fungus-ant symbiotic lineage coevolving over time. Other bacterial and fungal symbionts are associated with the system, occurring within the fungus garden matrix and in or on the ants themselves, including fungi in the genus *Escovopsis* (Ascomycota: Hypocreales: Hypocreaceae) that are specialized parasites of the fungus gardens and have co-diversified across fungus-ant symbiotic lineages. This chapter will focus on the complex interactions of these fungus-garden associations and our current understanding of co-evolution within this symbiosis.

1.2 Introduction

Fungi are ancient and extraordinary organisms that engage in symbiotic relationships with nearly all living organisms. By contributing to the colonization of land by plants, fungal symbionts have even helped space the formation of terrestrial ecosystems and have continued to evolve with and amongst the diversity of life forms on land. Within these communities, fungi play many roles across the spectrum of antagonism to mutualism. Fungi occur embedded within terrestrial systems occupied by a bevy of other cryptic life forms, from insects and other invertebrates to bacteria and viruses, as well as other fungi. The interactions fungi engage in within these terrestrial communities as well as within the context of a host microbiome remains poorly known, yet these interactions play important roles in organismal evolution and adaptation (Moran, 2007).

Among metazoans, insects are one of the most ubiquitous interactants with fungi. These interactions are often antagonistic, such as entomopathogenic fungi that kill and consume their insect hosts and mushroom fruiting bodies being eaten by fly larvae. But fungi also engage in mutualisms with insects, including serving as nutritional symbionts of insects. Although many fungi are consumed by insects in some capacity, whether as a primary or secondary food source (Hammond & Lawrence, 1989; Martin, 1992), specialized consumptive relationships that obligate mutualisms have evolved, such as those with fungus-growing termites, beetles, and ants (Li et al., 2021). These nutritional mutualism overcome certain barriers to herbivory: physical defenses prevent penetration of plant tissue, requiring either specific enzymes to degrade plant cell walls

or specific structures that can penetrate plant tissues (Mendgen et al., 1996), while chemical defenses often deter herbivorous insects, with many herbivorous insects requiring specific adaptations to overcome these chemical defenses and consume specific plants (Ehrlich & Raven, 1964).

A complex and relatively well-studied insect-fungal nutritional mutualism is the attine-ant microbiome symbiosis. This symbiosis is structured around the fungus-growing ant "attine" lineage and the basidiomycetous fungi they cultivate for food. The fungi cultivated by attine ants are phylogenetically diverse, with most fungal symbionts from the genus *Leucoagaricus* within the family Agaricaceae (order: Agaricales) (Chapela et al., 1994; Vo et al., 2009). As detailed below, there has been multiple evolutionary origins in the fungi, including the domestication of fungi in the genus *Myrmecopterula* in the family Pterulaceae (order: Agaricales) (Leal-Dutra et al., 2020). In addition to the phylogenetic diversity in the fungus, after a single evolution origin in the ants they have evolved into a diverse assemblage comprised of 20 genera and more than 240 species (Bolton, n.d.).

This ant-fungal association is an obligate mutualism, involving elaborate and intimate connections in the life history of each. This mutualism spans the American tropics, ranging from mid-latitudinal regions of the United States, the Caribbean, to the lower latitudes of Argentina (Sosa-Calvo et al., 2015). This mutualism, and the partnership between the fungus and the ants is predicated by co-transmission of the fungus with the ants. New colonies are established by ant queens that carry a piece of the fungus from their mother colony to a new location. Once colonies

are established, fungus-growing ants bring diverse plant substrate back to their nest where they house their 'fungus gardens' (Weber, 1966), the structural matrix of the fungal nest maintained by the ants. The ants maintain this structure by moving tufts of fungus onto newly foraged substrates, as well as grooming and cleaning foraged substrates and the fungus to remove potential parasites. Ants divide labor in the nest to ensure the success of the colony, which depends both on the survival of the ant queen, as well as the health and maintenance of the fungal cultivar (Hölldobler & Wilson, 2010). The fungus garden structure is the site of the decomposition of substrates that the ants feed to the fungus, with the fungus assimilating recalcitrant plant polymers. The fungal mutualists serve as a source of food for the ants, with the ants feeding on specialized food structures called 'gongylidia'. Together, the ant and fungus are mutually dependent on each other, the ants require the fungus for a food source, and the fungi make use of the ants for substrate acquisition and transmission. An emblematic example of this association is the leaf-cutter ants in the genera *Acromyrmex* and *Atta*, which can form colonies of hundreds-of-thousand to millions of workers, with hundreds of fungus-garden chambers (Hölldobler & Wilson, 2010).

Across the ~55-70 million year evolutionary history of the symbiosis, at least 5 lineages of both the ants and fungi have formed, representing distinct symbiotic pairings with important differences in the sizes of the nests, as well as the substrates used to manure the fungus garden (Branstetter et al., 2017; Hanisch et al., 2022). These differences are most concordant with the phylogeny of the monophyletic fungus-growing ants, with phylogenetic lineages taking on

different forms, while the cultivated fungi are polyphyletic but with specific lineages of fungi still being associated with specific lineages of ants. The earliest derived ants are referred to as “lower” attines engage in what is referred to as ‘lower attine agriculture’, which originated approximately 55-70 million years ago and involves the cultivation of Agaricaceae fungi in the genus *Leucocoprinus.* The domestication of *Leucocoprinus* by attine ants, from their saprobic litter specialist ancestors, likely occurred at the origin of the mutualism (U. G. Mueller et al., 2001; Schultz & Brady, 2008) but with subsequently involved novel acquisitions of *Leucocoprinus* from free-living lineages (Chapela et al., 1994; Ulrich G. Mueller et al., 1998; Schultz et al., 2015). “Yeast agriculture” originated ~36 million years ago from within “lower” attine ants and *Leucocoprinus* fungi and is characterized by the exclusive growth of the fungi as yeast. “Coral agriculture” originated from a switch to cultivating *Pterulaceae* fungi by ants in the genus *Apterostigma* and evolved ~25 million years ago. “Higher attine agriculture” originated around 28 million years ago, with “leafcutter” agriculture originating ~19 million years ago and is distinguished by the use of freshly cut leaves as the primary forage substrate (Hanisch et al., 2022). These lineages serve as a phylogenetic framework for assessing differences across fungus-ant pairings.

This chapter will overview both the details of how fungi in this symbiosis mediate production of nutrients in partnership with their ant counterparts, how these symbionts overcome plant defenses to herbivory, and which microbes contribute to the defense of this mutualism against pathogenic pressure

1.2 Energy production and nutrient exchange in fungus-ant mutualism

The energy hub of this ant-fungus mutualism are the so called 'fungus gardens', which have even been referred to as bioreactors because of their capacity for deconstructing plant matter (Somera et al., 2015). Within gardens, ants deliver foraged plant-based substrates for the fungus to decompose and convert into fungal biomass and eventually energy and other nutrients consumed by the ants. The combination of forage materials and fungal mycelia make up the structure of the fungus garden matrix. The fungus gardens are the interphase of this fungal mutualism, where energy and nutrient exchange with their ant hosts occurs.

Fungus gardens are first established at the initiation of new ant nests. Across the diversity of this ant-fungus mutualism this process involves new colonies being formed when queens produce reproductive females and males during a reproductive season, typically at the beginning of the rainy season. Reproductive females select a small mycelial plug from the fungus garden of their parent nest, carrying the fungal inoculum in their infrabuccal pocket. Over a short time-window, typically a few hours, synchronized by ant species and geographic region, the nuptial flight occurs, with reproductive ants leaving their parent nest to mate. After the flight, the males die, and the new founder females are queens that establish fungus garden within protective locations, often in small chambers underground. Once the new site is excavated, the queen spits out the mycelial plug and begins to cultivate it using her first eggs and fecal liquids. The first workers that eclose manage the fungus garden and forage for new plant substrate after collecting plant material and return to the nest, workers integrate the substrate it into the matrix of the

fungus garden. This plant substrate forms the structure of the fungus garden. The fungus is placed by workers on the plant substrate, and as the garden matures fungal tissue is collected from the older regions of the garden and placed on fresh inoculum. In at least some ant species, workers engage in masticating the substrate, a physical manipulation that likely facilitates the degradation of the plant substrate.

Attine ants, like all ants and most metazoans, cannot digest cellulosic plant substrates. The ants primarily consume and gain energy and nutrients from the fungal mutualist, while foraging workers can feed on plant sap (Quinlan & Cherrett, 1979). The 'magic sauce' of this mutualism for the ants is the ability of their fungal mutualist to degrade cellulosic substrate, converting it into usable energy for the ants. Indeed, in the leaf-cutter ant *Atta colombica* it has been shown that the abundance of various plant polysaccharides and cellulose decreases within the fungus garden, with the exception of lignin (Suen et al., 2010). Genomic studies of *Leucoagricus* spp. associated with leaf-cutter ants has revealed its capacity to encode enzymes that degrade cellulosic substrate (Aylward et al. 2013). Thus, these decreases are largely attributed to the fungal cultivar, which produces hemicellulases, pectinases, xylanases, and cellulases (Aylward et al., 2013) . Additionally, the cultivar has been shown to directly degrade cellulose and integrate it into its biomass (Conlon et al., 2022), but has changes in the domain in the enzyme responsible for lignin degradation which likely impacts its ability to degrade this substrate (Nygaard et al., 2016). *Leucoagricus* spp. produce enzymes in response to the types of substrates integrated into the garden, shifting the types of enzymes produced after a shift in the

type of substrate (Khadempour et al., 2016; Kooij et al., 2011). In addition, there are differences in abundances of these enzymatic profiles across the different types of fungi that engage in the fungus-growing ant symbioses (De Fine Licht et al., 2010), with different fungus-ant lineages utilizing different enzymatic suites. These data underscore the idea that the fungus engages in decomposition of diverse substrates, as well as dynamically shifts enzymatic production in response to substrate availability.

In addition to using these plant substrates to form more fungal biomass, *Leucoagaricus* spp. develop specialized hyphal swellings called gongylidia, which the ants consume (Quinlan & Cherrett, 1979). These hyphal swellings are enriched with nutrients such as lipids and carbohydrates (Martin & Martin, 1970; Quinlan & Cherrett, 1979). Gongylidia are enriched with transcripts for the pectinolytic enzymes and laccases that pass through the digestive tracts of ants and are present in the fecal droplets that initiate the decomposition of freshly foraged substrate materials via mixing by the ants (De Fine Licht et al., 2013; Schiøtt & Boomsma, 2021; Schiøtt et al., 2010; Weber, 1966). These gongylidia are also enriched for lipids containing linoleic acid, which may be a means of cross-kingdom communication with the ants, as *Atta* ants have different responses to different structures of fatty acids (Khadempour et al., 2021). This process demonstrates the key stages of herbivory mediated by both fungus and ants, which is underscored by specific nutrient limitations that further entangles these mutualistic partners.

As with all organisms relying on plant biomass directly or indirectly, the ant-fungus mutualism is predicted to be nitrogen limited due to the low nitrogen to carbon ratio present in

leaf material. Contrary to this expectation, fungus gardens contain larger proportions of nitrogen than was present in foraged leaf material, indicating a nitrogen source outside of leaf forage material (Bucher et al., 2004; Haines, 1978). This enrichment of nitrogen was shown to be partially attributed to bacteria in the genera *Pantoea* and *Klebsiella* within fungus gardens, which engage in nitrogen fixation and appear responsible for between 45-61% of garden nitrogen in *Atta cephalotes* fungus gardens (Pinto-Tomás et al., 2009). Another nutrient limitation underscoring the obligate nature of the mutualism in fungus-growing ants is arginine. Genomic studies of fungus-growing ants have shown they have lost the capacity to synthesize arginine (Nygaard et al., 2016; Suen et al., 2011), suggesting they solely relying on their fungal mutualists for this nutrient.

In addition to nitrogen-fixing bacteria, other bacteria likely play nutritional roles within this ant-fungus mutualism. Suen and colleagues (2010) conducted the first microbiome study of leaf-cutter ants, showing the presence of a specialized bacterial community occurring within the matrix of leaf-cutter ant fungus gardens and that these bacteria have some lignocellulolytic capacity (Suen et al., 2010). This and other studies demonstrated that bacterial communities in the fungus garden are primarily composed of α-proteobacteria, γ-proteobacteria, δ-proteobacteria, β-proteobacteria, and Actinobacteria, with genera in the family Enterobacteriaceae being highly represented (Jarrod J. Scott et al., 2010; Suen et al., 2010). The composition of bacterial communities associated with *Leucoagaricus* can vary depending on fungus-ant lineages, but there are similar recurrences of genera across all lineages. Several taxa

are commonly identified in fungus-growing ant gardens across multiple lineages of fungus-ant symbiosis, including *Pseudomonas*, *Enterobacter, Pantoea,* and *Klebsiella* (Aylward et al., 2014). The types of substrates ants provide to their nests can also influence the composition of bacterial community members. Specifically, when comparing grass-substrate providing ant species to dicot-leaf-substrate providing ant species, (Khadempour et al., 2020) found that *Pantoea, Pseudomonas, Burkholderia,* and *Enterobacter* bacteria are found in both nest types, whereas *Gluconobacter* bacteria comprised 19% of the community in dicot-leaf substrate nests and are absent in grass-substrate nests. In addition to bacteria, yeasts associated with the fungus garden have been thought to contribute to plant biomass degradation and plant secondary compound degradation, as reviewed by Bizarria and colleagues (Bizarria et al., 2022).

1.3 Symbiotic microbes in a generalist herbivore

Leaf-cutter ants are major ecological players in tropical ecosystems, foraging as much as 10-17% of leaf production within some plant communities, making them one of the most significant herbivores in Neotropical ecosystems (Costa et al., 2008; Herz et al., 2007; Wirth et al., 2002). As previously discussed, through the production of cellulolytic enzymes the fungal mutualist *Leucoagricus* spp. provides access to the energy and nutrients within the foraged plant tissue for both the ants and the fungus. The combination of foraging and pre-treatment of the plant biomass by the ants with the digestion of the material by the fungus makes these mutualists a formidable herbivores for plants to defend against, and has even been likened to an 'unholy alliance' (Cherrett et al., 1989). Most herbivores are limited to a narrow range of plant species

they can feed on, because of the chemical and physical defenses in plants. In contrast, the leaf-cutter ant and *Leucoagaricus* spp. can utilize a high diversity of plant species, with forage estimates between 10-17% of foliar biomass in the American tropics (Costa et al., 2008; Herz et al., 2007). To use such a broad range of plant species in their diet, leafcutter ant and their fungi require specific adaptations to circumvent a range of physical and chemical plant defenses. To overcome physical plant defenses, the leafcutter ants have evolved highly specialized mandibular structures that excel at shearing leaves. These structures contain muscles that constitute 25% of the body mass of the ant and is similar to the flight motor of flying insects (Roces & Lighten, 1995). While the ants aid in overcoming physical plant defenses, the fungal cultivar must combat the chemical defenses present in many plants.

Plants protect themselves from herbivores using chemical defenses. These defenses prevent generalized herbivory through toxicity, however, in the case of leafcutter ants, the ants themselves are not consuming the plants and the fungus is responsible for detoxifying these defensive plant compounds. One means of mediating these defenses could be communication between the fungus and the ants in guiding the selection of foraging substrates to minimize the toxicity of incoming substrates (North et al., 1999). Some species of ants show preferences for newer leaves, because younger leaves that are softer easier to cut (De Vasconcelos, 1990), and leaves with less toxic defense compounds (Howard, 1987, 1990). Several studies have demonstrated with experimental feeding that substrates inoculated with the antifungal agent cycloheximide will initially be given to the fungal cultivar, but after an initial feeding period, the

ants will avoid these substrates in favor of toxin-free substrates (Herz et al., 2008; Ridley et al., 1996; Saverschek et al., 2010). This avoidance of these toxic substrates persists for up to 18 weeks (Saverschek et al., 2010), indicating that the ants receive feedback from the fungal cultivar and preferentially avoid toxic substrates to maintain the health of the fungus garden over time. In addition to ant-fungus feedback, the fungal cultivar produces laccases that degrade defensive plant secondary compounds. These laccases are produced in the fungal cultivar and pass through the digestive tract of the ants, and are then deposited onto freshly foraged leaf material (De Fine Licht et al., 2013). However, mediating the toxicity of more diverse ranges of substrates may be a function delegated to secondary symbiotic microbes.

Recent work indicates that bacterial symbionts within fungus gardens play an important role in plant defense compound detoxification and degradation. For example, in the presence of linalool and **α**-pinene, *Leucoagaricus* isolates reduced linalool but not **α**-pinene, whereas fungus gardens could significantly reduce both molecules. Upon examination of individual fungus garden bacteria isolates, *Enterobacter, Bacillus, and Klebsiella* strains reduced **α**-pinene during exponential growth phases. Additionally, a *Pseudomonas* isolate reduced **β**-caryophyllene, while linalool was reduced by both a *Burkholderia* isolate and a *Pseudomonas* isolate (Francoeur et al., 2020). It appears likely that it is the combination of *Leucoagaricus* and fungus garden bacteria that degrade and detoxify the diversity of plant defensive molecules this mutualist is exposed, and that the community of microbes is greater than the sum of its parts.

Another component of the leaf substrates to consider are fungal endophytes, and how they mediate herbivory in this system. Leaves with a higher abundance of endophytes experience a significant decrease in foraging by leaf-cutter ants (Bittleston et al., 2011; Estrada et al., 2015, 2013; Van Bael et al., 2009; Van Bael, Seid, et al., 2012), because these endophytes change the composition of chemicals released from a wounded leaf (Estrada et al., 2013). Additionally, leaf-cutter ants preferably forage for leaf material containing lower abundances of endophytic fungi (Coblentz & Van Bael, 2013), and colonies that forage leaf material with higher endophyte loads may experience higher mortality at early stages of garden growth (Van Bael, Estrada, et al., 2012). One study found that fungal genera commonly found in rejected leaf materials included *Acremonium, Cylindrocladium, Drechslera, Epicoccum, Fusarium, Trichoderma,* and *Ulocladium*, whereas *Colletrotrichum, Pestalotiopsis, Phomopsis,* and *Xylaria* are genera that escaped foraging preferences (Rocha et al., 2014). Some of these fungi influence the secondary metabolites, toughness, water content, density, and trichome length of leaves, some of which, are factors that may play a role in driving selection preferences in ant foraging behavior (Estrada et al., 2013; Van Bael et al., 2011).

1.4 Specialized fungal garden parasites exploit mutualism

Fungi in the genus *Escovopsis* (Ascomycota: Sordariomycetes: Hypocreales: Hypocreaceae) have evolved to exploit the abundant flow of nutrients within the fungus gardens of attine ants. *Escovopsis* is a specialized parasite of fungus-growing ant gardens and has not been found outside this association. *Escovopsis* specifically parasitizes the fungal cultivar of fungus-growing

ants without competing for substrate forage material (Reynolds & Currie, 2004). Some *Escovopsis* begin degradation of *Leucoagaricus* hyphae through hyphal attachment (Marfetán et al., 2015). Infections from *Escovopsis* are detrimental to the health of the fungus garden, as infected colonies produce fewer worker ants and accumulate less garden mass (Cameron R. Currie, 2001). In addition, under some conditions that are largely unknown, *Escovopsis* can completely overgrow the fungus garden and devastate whole colonies (Cameron R. Currie, Mueller, et al., 1999; Cameron R. Currie & Stuart, 2001). These fungi are known to parasitize all but one ant-fungus lineage in the attine ant consortia, the exception being a lineage of *Cyphomyrmex rimosus* group ants that cultivate fungi as yeasts (Vo et al., 2009). These specialized fungi are evolutionarily related to parasites of basidiomycetes in the family Hypocreaceae. In particular, *Hypomyces* and *Cladobotryum* are parasites to button mushroom agriculture for human consumption and cause wet bubble disease (Rogerson & Samuels, 1994; Tamm & Põldmaa, 2013; Zhang et al., 2017). Like other microbes associated with fungus-growing ants, *Escovopsis* also displays interesting evolutionary patterns across its associations with this mutualism.

Escovopsis presents evolutionary trajectories consistent with both macro- and micro-evolutionary scales. Different species of *Escovopsis* infect different ant-fungus lineages, and display a broad co-phylogenetic pattern that matches their ant-fungus host pairings (Cameron R. Currie et al., 2003). In untangling these relationships, many *Escovopsis* species and potentially genera (Montoya et al., 2021) have been identified. Specifically, certain *Escovopsis* species are associated with different lineages of fungus-growing ants, with many more species likely to be

identified. The *Escovopsis weberi* parasitizes higher attine colonies, along with several other species (*E. moelleri, E. microspora, E. lentecrescens,* and *E. aspergilloides*) (Augustin et al., 2013; Muchovej & Della Lucia, 1990; Seifert et al., 1995). *E. clavatus* and *E. multiformis* are associated with coral-fungus ant agriculture, along with an undescribed morphotype characterized by its yellow spores (Caldera et al., 2019; Montoya et al., 2019). *E. kreiselii, E. trichodermoides,* and at least one more undescribed morphotype characterized by orange spores parasitize lower attine agriculture (Custodio & Rodrigues, 2019; Masiulionis et al., 2015; Meirelles et al., 2015). On the micro-evolutionary scale, some *Escovopsis* strains specialize and have a strict adherence to specific cultivar-ant hosts (Birnbaum & Gerardo, 2016; Gerardo, Mueller, et al., 2006), while some *Escovopsis* strains capable of infecting multiple cultivar-ant hosts within a given lineage of fungus-growing ants, such as the relationships observed amongst *Escovopsis* strains that parasitize *Apterostigma* ant gardens (Gerardo & Caldera, 2007). This flexibility in parasitic host has also been observed in *Escovopsis* that infects leaf-cutter ant gardens (Taerum et al., 2007), and *Cyphomyrmex* ant gardens (Gerardo et al., 2004). While *Escovopsis* is highly specific to individual lineages of fungus-growing ants, it is likely horizontally transmitted between colonies due to it not being isolated from the fungal pellets of fungus-growing ant queens on their inaugural mating flight (Cameron R. Currie, Mueller, et al., 1999; Moreira et al., 2015). The identification of these species and their ecology will help in fully understanding the evolutionary trajectory of this parasite after its introduction into the fungus-growing ant symbiosis.

As expected, given that the fungus garden is largely composed of plant biomass, a diverse collection of common soil fungi have been isolated from the fungus-growing ant symbiosis. These fungi encompass both Ascomycota and Basidiomycota lineages (Bizarria et al., 2022; Pagnocca et al., 2012). Most of these fungi are likely just substrate and soil contaminants, but it does appear that some other fungi in addition to *Escovopsis* are able to exploit this ant-fungus mutualism. Genera isolated from the fungus-garden of multiple types of fungus-ant symbiotic pairings include *Trichosporon chiarellii* sp. found in the gardens of fungus-growing ants in the genus *Myrmicocrypta* and *Atta* (Carreiro et al., 2002; Pagnocca et al., 2010; Pereira et al., 2016), and *Syncephalastrum* in *Atta* fungus gardens (Barcoto et al., 2017; Rodrigues et al., 2009). *Trichoderma* is another genus of fungi that is often found in many lineages fungus-growing ant gardens (Andre Rodrigues et al., 2014; Montoya et al., 2016). In addition to isolations from fungus-gardens, fungi have also been isolated from the exoskeleton or 'integument' of different ants. *Cladosporium* spp. are isolated from the integument of *Atta* ants on their mating flights (Duarte et al., 2014, 2016; Fernando Carlos Pagnocca et al., 2008). Additionally, black yeasts have been isolated from the bodies of diverse ant genera (*Cyphomyrmex, Apterostigma*, *Trachymyrmex,* and *Acromyrmex*) (Ainslie E. F. Little & Cameron R. Currie, 2007). Studies focusing on elucidating the role of other fungal antagonists will help inform on the wealth of fungi that have been identified, as well as any patterns of associations across attine ant lineages. Additionally, the mechanism of how these communities are formed in the garden is unknown,

but has been hypothesized to involve transmission from garden inquilines, predators and potentially foragers (Augustin et al., 2017; Cameron R. Currie, 2001).

1.4 Defensive symbionts guard mutualism resources against parasites

The success of this ant-fungal mutualism depends on the health and stability of the fungus garden that, as previously discussed, is under continuous microbial threat, especially from the specialized parasite *Escovopsis*. Providing conditions that promote strong competitive growth of *Leucoagaricus* within the garden is likely a key to component to suppressing the growth of many potential microbial invaders. Enabling vigorous growth of the fungus and movement of its mycelium around the garden likely leads to competitive exclusion of many soil bacteria and fungi that might otherwise grow (see above for discussion on how *Leucoagaricus* growth is promoted). Some species of fungal cultivar produce antimicrobial molecules that provide generalized inhibition of garden parasites (Gerardo, Jacobs, et al., 2006; Gerardo et al., 2004). Additionally, worker ants in fungus-growing ant nests clean and sanitize the cultivar mycelia to remove parasites (Bonadies et al., 2019; Christopher et al., 2021; Cameron R. Currie & Stuart, 2001; Fernández-Marín et al., 2013). In this fungal grooming, ants remove parasites from the nest by collecting spores and hyphae into their infrabuccal pockets which sterilizes these collections with secretions of phenylacetic acid from ants metapleural glands (Fernández-Marín et al., 2015, 2009). Sterilized pellets are then removed from the nest into external “dump” structures. Lastly, worker ants perform elaborate cleaning behaviors on foraged materials before they are brought to the colony to maintain the fungus (Mangone & Currie, 2007). Cumulatively, these behaviors

provide an effective means for preventing the spoilage of the fungus garden from microbes present in both foraged leaf matter and nearby soil reservoirs that may contact the fungus garden.

While the combined activity of *Leucoagaricus* and the ants suppress most microbes, *Escovopsis* overcomes this inhibition, which is likely a result of the ancient association between *Escovopsis* and the fungus-growing ant cultivar (Gerardo, Jacobs, et al., 2006). To subvert the specialization of *Escovopsis* on *Leucoagaricus*, attine ant associate with Actinobacteria in the genus *Pseudonocardia,* which produces antifungals (Carr et al., 2012; Chevrette et al., 2019; Oh et al., 2009; Van Arnam et al., 2016) that inhibit *Escovopsis* (C. R. Currie et al., 2003; Cameron R. Currie, Mueller, et al., 1999; Cameron R. Currie, Scottt, et al., 1999). *Pseudonocardia* is localized on and in differentiated cuticular structures that evolved across the attine ant tribe (Cameron R. Currie et al., 2006; Li et al., 2018), and is transmitted vertically on founder queens (Cameron R. Currie, Scottt, et al., 1999). Multiple lineages of *Pseudonocardia* are associated with attine ants, with these lineages inhibiting *Escovopsis* more effectively than environmentally isolated strains (Cafaro et al., 2011). This idea is supported by the finding that experimental removal of *Pseudonocardia* from the ant cuticle results in an increased parasitic load of *Escovopsis* in the fungus garden (C. R. Currie et al., 2003). Additionally, strain-level variation in *Pseudonocardia*, along with variability in *Escovopsis* susceptibility was shown to result in differential garden losses in experimental infections to assay *Pseudonocardia*'s protective functionality (Poulsen et al., 2010). *Escovopsis* inhibition has been found to be mediated by antifungal molecules, in particular,

two of the antifungals produced by ant-associated *Pseudonocardia*, dentigerumycin (Oh et al., 2009) and selvamicin (Van Arnam et al., 2016) are potent inhibitors of *Escovopsis.* However, *Pseudonocardia* spp. have high genetic variability in biosynthetic gene clusters responsible for the production of natural products, including antifungal molecules (Mcdonald et al., 2019), which indicates that there may be other mechanisms by which *Pseudonocardia* inhibits *Escovopsis* and other fungal parasites in attine gardens. In addition to *Pseudonocardia,* bacteria in the genius *Amycolatopsis* have been detected on the exoskeletons of some *Trachymyrmex* attine ants (Hansen et al., 2022; Sen et al., 2009), but the extent to which this bacterium either displaces or competes with other exoskeletal residents in unknown. Additionally, *Pseudonocardia* is not present on all attine ants, with losses of the bacterium on ants in the genera *Atta* and *Sericomyrmex* (Li et al., 2018) indicating that there are likely other mechanisms by which fungus-gardens are able to defend against nest parasites.

After the initial discovery of *Pseudonocardia,* investigation into other nest symbionts as potentially defensive symbionts took place. Bacteria in the genus *Burkholderia* are isolated from fungus-gardens and inhibit nest parasites (Francoeur et al., 2021; Santos et al., 2004). These *Burkholderia* are isolated from most attine nests, and isolates from some nests are predicted to contain Pyrrolnitrin and/or Burkholdine BGCs, the presences of which corresponds to strong inhibition of *Escovopsis* (Francoeur et al., 2021). This inhibition of *Escovopsis* was recapitulated with chemical extracts from the strong inhibitor strains, which did not inhibit the growth of the fungal cultivar (Francoeur et al., 2021). These results examining the potency of *Burkholderia*

inhibition, along with the presence of both *Amycolatopsis* and *Pseudonocardia* on attine cuticles demonstrates that there are likely a variety of diverse microbial symbionts that can be recruited to support the function of attine fungus gardens.

1.5 Conclusions

Work over the last several decades on this nutritional mutualism between ants and fungi has revealed the potential complexity of microbes associated with bipartite mutualisms and how these microbes can shape the ecology and evolution of the diverse organisms involved. We discussed barriers, both chemical and physical that this mutualism overcomes to, in some cases, become dominant herbivores in neotropical ecosystems, and that sometimes these barriers are overcome through associations with diverse microbes. These diverse microbes likely play many roles, as has been demonstrated in the fungus-growing ant symbiosis which houses microbes that fix nitrogen and degrade toxic plant compounds. Additionally, we outlined how parasites like *Escovopsis* can take advantage of this mutualism. Ancient parasitic associations like those in the fungus-growing ant symbiosis may drive restructuring of microbial symbioses to incorporate microbes with strong antibiotic capacities. Further studies into the roles of symbiotic fungi and other microbes will be essential for understanding how microbiota shape the evolutionary histories of individual organisms, as well as the mutualism they might be involved in. Additionally, further research into how the differences in community composition impact evolutionary differences of fungus-growing ant gardens will demonstrate the functional importance of these symbionts.

1.6 References

Ainslie E. F. Little, & Cameron R. Currie. (2007). Symbiotic complexity: discovery of a fifth symbiont in the attine ant-microbe symbiosis. *Biology Letters*, *3*(5), 501–504.

Andre Rodrigues, Passarini M.R.Z., Milene Ferro, Nilson S. Nagamoto, Luiz Carlos Forti, Maurício Bacci, Lara Durães Sette, & Fernando Carlos Pagnocca. (2014). Fungal Communities In The Garden Chamber Soils Of Leaf-cutting Ants. *Journal of Basic Microbiology*, *54*(11), 1186–1196.

Augustin, J. O., Groenewald, J. Z., Nascimento, R. J., Mizubuti, E. S. G., Barreto, R. W., Elliot, S. L., & Evans, H. C. (2013). Yet more "weeds" in the garden: Fungal novelties from nests of leaf-cutting ants. *PloS One*, *8*(12), e82265.

Augustin, J. O., Simões, T. G., Dijksterhuis, J., Elliot, S. L., & Evans, H. C. (2017). Putting the waste out: A proposed mechanism for transmission of the mycoparasite Escovopsis between leafcutter ant colonies. *Royal Society Open Science*, *4*(5), 161013.

Aylward, F. O., Burnum-Johnson, K. E., Tringe, S. G., Teiling, C., Tremmel, D. M., Moeller, J. A., Scott, J. J., Barry, K. W., Piehowski, P. D., Nicora, C. D., Malfatti, S. A., Monroe, M. E., Purvine, S. O., Goodwin, L. A., Smith, R. D., Weinstock, G. M., Gerardo, N. M., Suen, G., Lipton, M. S., & Currie, C. R. (2013). *Leucoagaricus gongylophorus* produces diverse enzymes for the degradation of recalcitrant plant polymers in leaf-cutter ant fungus gardens. *Applied and Environmental Microbiology*, *79*(12), 3770–3778.

Aylward, F. O., Suen, G., Biedermann, P. H. W., Adams, A. S., Scott, J. J., Malfatti, S. A., Glavina del Rio, T., Tringe, S. G., Poulsen, M., Raffa, K. F., Klepzig, K. D., & Currie, C. R. (2014). Convergent bacterial microbiotas in the fungal agricultural systems of insects. *MBio*, *5*(6), e02077.

Barcoto, M. O., Pedrosa, F., Bueno, O. C., & Rodrigues, A. (2017). Pathogenic nature of *Syncephalastrum* in *Atta sexdens rubropilosa* fungus gardens. *Pest Management Science*, *73*(5), 999–1009.

Birnbaum, S. S. L., & Gerardo, N. M. (2016). Patterns of specificity of the pathogen *Escovopsis* across the fungus-growing ant symbiosis. *The American Naturalist*, *188*(1), 52–65.

Bittleston, L. S., Brockmann, F., Wcislo, W., & Van Bael, S. A. (2011). Endophytic fungi reduce leaf-cutting ant damage to seedlings. *Biology Letters*, *7*(1), 30–32.

Bizarria, R., Jr, Pagnocca, F. C., & Rodrigues, A. (2022). Yeasts in the attine ant-fungus mutualism: Diversity, functional roles, and putative biotechnological applications. *Yeast* , *39*(1–2), 25–39.

Bolton, B. (n.d.). *AntCat*. An Online Catalog of the Ants of the World. Retrieved September 24, 2022, from https://antcat.org/

Bonadies, E., Wcislo, W. T., Gálvez, D., Hughes, W. O. H., & Fernández-Marín, H. (2019). Hygiene Defense Behaviors Used by a Fungus-Growing Ant Depend on the Fungal Pathogen Stages. *Insects*, *10*(5). https://doi.org/10.3390/insects10050130

Branstetter, M. G., Ješovnik, A., Sosa-Calvo, J., Lloyd, M. W., Faircloth, B. C., Brady, S. G., & Schultz, T. R. (2017). Dry habitats were crucibles of domestication in the evolution of agriculture in ants. *Proceedings of the Royal Society B: Biological Sciences*, *284*(1852), 20170095.

Bucher, E. H., Marchesini, V., & Abril, A. (2004). Herbivory by leaf-cutting ants: Nutrient balance between harvested and refuse material. *Biotropica*, *36*(3), 327–332.

Cafaro, M. J., Poulsen, M., Little, A. E. F., Price, S. L., Gerardo, N. M., Wong, B., Stuart, A. E., Larget, B., Abbot, P., & Currie, C. R. (2011). Specificity in the symbiotic association between fungus-growing ants and protective *Pseudonocardia* bacteria. *Proceedings of the Royal Society B: Biological Sciences*, *278*(1713), 1814–1822.

Caldera, E. J., Chevrette, M. G., McDonald, B. R., & Currie, C. R. (2019). Local adaptation of bacterial symbionts within a geographic mosaic of antibiotic coevolution. *Applied and Environmental Microbiology*, *November*. https://doi.org/10.1128/aem.01580-19

Carr, G., Derbyshire, E. R., Caldera, E., Currie, C. R., & Clardy, J. (2012). Antibiotic and antimalarial quinones from fungus-growing ant-associated *Pseudonocardia* sp. *Journal of Natural Products*, *75*(10), 1806–1809.

Carreiro, S. C., Pagnocca, F. C., Bacci, M., Jr, Bueno, O. C., Hebling, M. J. A., & Middelhoven, W. J. (2002). Occurrence of killer yeasts in leaf-cutting ant nests. *Folia Microbiologica*, *47*(3), 259–262.

Chapela, I. H., Rehner, S. A., Schultz, T. R., & Mueller, U. G. (1994). Evolutionary History of the Symbiosis Between Fungus-Growing Ants and Their Fungi. *Science*, *266*(5191), 1691–1694.

Cherrett, J. M., Powell, R. J., & Stradling, D. J. (1989). 4 - The Mutualism between Leaf-Cutting Ants and their Fungus. In N. Wilding, N. M. Collins, P. M. Hammond, & J. F. Webber (Eds.), *Insect-fungus Interactions* (Vol. 14, pp. 93–120). Academic Press.

Chevrette, M. G., Carlson, C. M., Ortega, H. E., Thomas, C., Ananiev, G. E., Barns, K. J., Book, A. J., Cagnazzo, J., Carlos, C., Flanigan, W., Grubbs, K. J., Horn, H. A., Hoffmann, F. M., Klassen, J. L., Knack, J. J., Lewin, G. R., McDonald, B. R., Muller, L., Melo, W. G. P., … Currie, C. R. (2019). The antimicrobial potential of Streptomyces from insect microbiomes. *Nature Communications*, *10*(1), 516.

Christopher, Y., Wcislo, W. T., Martínez-Luis, S., Hughes, W. O. H., Gerardo, N. M., & Fernández-Marín, H. (2021). Disease management in two sympatric *Apterostigma* fungus-growing ants for controlling the parasitic fungus Escovopsis. *Ecology and Evolution*, *ece3.7379*. https://doi.org/10.1002/ece3.7379

Coblentz, K. E., & Van Bael, S. A. (2013). Field colonies of leaf-cutting ants select plant materials containing low abundances of endophytic fungi. *Ecosphere* , *4*(5), 1–10.

Conlon, B. H., O'Tuama, D., Michelsen, A., Crumière, A. J. J., & Shik, J. Z. (2022). A fungal symbiont converts provisioned cellulose into edible yield for its leafcutter ant farmers. *Biology Letters*, *18*(4), 20220022.

Costa, A. N., Vasconcelos, H. L., Vieira-Neto, E. H. M., & Bruna, E. M. (2008). Do herbivores exert top-down effects in Neotropical savannas? Estimates of biomass consumption by leaf-cutter ants. *Journal of Vegetation Science: Official Organ of the International Association for Vegetation Science*, *19*(6), 849–854.

Currie, C. R., Bot, A. N. M., & Boomsma, J. J. (2003). Experimental evidence of a tripartite mutualism: bacteria protect ant fungus gardens from specialized parasites. *Oikos* , *101*(1), 91–102.

Currie, Cameron R. (2001). Prevalence and impact of a virulent parasite on a tripartite mutualism. *Oecologia*, *128*(1), 99–106.

Currie, Cameron R., Mueller, U. G., & Malloch, D. (1999). The agricultural pathology of ant fungus gardens. *Proceedings of the National Academy of Sciences of the United States of America*, *96*(14), 7998–8002.

Currie, Cameron R., Poulsen, M., Mendenhall, J., Boomsma, J. J., & Billen, J. (2006). Coevolved crypts and exocrine glands support mutualistic bacteria in fungus-growing ants. *Science*, *311*(5757), 81–83.

Currie, Cameron R., Scottt, J. A., Summerbell, R. C., & Malloch, D. (1999). Fungus-growing ants use antibiotic-producing bacteria to control garden parasites. *Nature*, *398*(6729), 701–704.

Currie, Cameron R., & Stuart, A. E. (2001). Weeding and grooming of pathogens in agriculture by ants. *Proceedings of the Royal Society B: Biological Sciences*, *268*(1471), 1033–1039.

Currie, Cameron R., Wong, B., Stuart, A. E., Schultz, T. R., Rehner, S. A., Mueller, U. G., Sung, G. H., Spatafora, J. W., & Straus, N. A. (2003). Ancient tripartite coevolution in the attine ant-microbe symbiosis. *Science*, *299*(5605), 386–388.

Custodio, B. C., & Rodrigues, A. (2019). *Escovopsis kreiselii* specialization to its native hosts in the fungiculture of the lower attine ant *Mycetophylax morschi*. *Antonie van Leeuwenhoek*, *112*(2), 305–317.

De Fine Licht, H. H., Schiøtt, M., Mueller, U. G., & Boomsma, J. J. (2010). Evolutionary transitions in enzyme activity of ant fungus gardens. *Evolution; International Journal of Organic Evolution*, *64*(7), 2055–2069.

De Fine Licht, H. H., Schiøtt, M., Rogowska-Wrzesinska, A., Nygaard, S., Roepstorff, P., & Boomsma, J. J. (2013). Laccase detoxification mediates the nutritional alliance between leaf-cutting ants and fungus-garden symbionts. *Proceedings of the National Academy of Sciences of the United States of America*, *110*(2), 583–587.

De Vasconcelos, H. L. (1990). Foraging activity of two species of leaf-cutting ants (Atta) in a primary forest of the Central Amazon. *Insectes Sociaux*, *37*(2), 131–145.

Duarte, A. P. M., Attili-Angelis, D., Baron, N. C., Forti, L. C., & Pagnocca, F. C. (2014). Leaf-cutting ants: an unexpected microenvironment holding human opportunistic black fungi. *Antonie van Leeuwenhoek*, *106*(3), 465–473.

Duarte, A. P. M., Ferro, M., Rodrigues, A., Bacci, M., Nagamoto, N. S., Forti, L. C., & Pagnocca, F. C. (2016). Prevalence of the genus *Cladosporium* on the integument of leaf-cutting ants characterized by 454 pyrosequencing. *Antonie van Leeuwenhoek, International Journal of General and Molecular Microbiology*, *109*(9), 1235–

1243.

Ehrlich, P. R., & Raven, P. H. (1964). Butterflies and Plants: A Study in Coevolution. *Evolution; International Journal of Organic Evolution*, *18*(4), 586–608.

Estrada, C., Degner, E. C., Rojas, E. I., Wcislo, W. T., & Van Bael, S. A. (2015). The role of endophyte diversity in protecting plants from defoliation by leaf-cutting ants. *Current Science*, *109*(1), 55–61.

Estrada, C., Wcislo, W. T., & Van Bael, S. A. (2013). Symbiotic fungi alter plant chemistry that discourages leaf-cutting ants. *The New Phytologist*, *198*(1), 241–251.

Fernández-Marín, H., Bruner, G., Gomez, E. B., Nash, D. R., Boomsma, J. J., & Wcislo, W. T. (2013). Dynamic disease management in *Trachymyrmex* fungus-growing ants (Attini: Formicidae). *The American Naturalist*, *181*(4), 571–582.

Fernández-Marín, H., Nash, D. R., Higginbotham, S., Estrada, C., van Zweden, J. S., d'Ettorre, P., Wcislo, W. T., & Boomsma, J. J. (2015). Functional role of phenylacetic acid from metapleural gland secretions in controlling fungal pathogens in evolutionarily derived leaf-cutting ants. *Proceedings. Biological Sciences / The Royal Society*, *282*(1807), 20150212.

Fernández-Marín, H., Zimmerman, J. K., Nash, D. R., Boomsma, J. J., & Wcislo, W. T. (2009). Reduced biological control and enhanced chemical pest management in the evolution of fungus farming in ants. *Proceedings of the Royal Society B: Biological Sciences*, *276*(1665), 2263–2269.

Fernando Carlos Pagnocca, Andre Rodrigues, Nilson S. Nagamoto, & Maurício Bacci. (2008). Yeasts and filamentous fungi carried by the gynes of leaf-cutting ants. *Antonie van Leeuwenhoek*, *94*(4), 517–526.

Francoeur, C. B., Khadempour, L., Moreira-Soto, R. D., Gotting, K., Book, A. J., Pinto-Tomás, A. A., Keefover-Ring, K., & Currie, C. R. (2020). Bacteria Contribute to Plant Secondary Compound Degradation in a Generalist Herbivore System. *MBio*, *11*(5). https://doi.org/10.1128/mBio.02146-20

Francoeur, C. B., May, D. S., Thairu, M. W., Hoang, D. Q., Panthofer, O., Bugni, T. S., Pupo, M. T., Clardy, J., Pinto-Tomás, A. A., & Currie, C. R. (2021). *Burkholderia* from Fungus Gardens of Fungus-Growing Ants Produces Antifungals That Inhibit the Specialized Parasite *Escovopsis*. *Applied and Environmental Microbiology*, *87*(14), e0017821.

Gerardo, N. M., & Caldera, E. J. (2007). Labile associations between fungus-growing ant cultivars and their garden pathogens. *The ISME Journal*, *1*(5), 373–384.

Gerardo, N. M., Jacobs, S. R., Currie, C. R., & Mueller, U. G. (2006). Ancient host-pathogen associations maintained by specificity of chemotaxis and antibiosis. *PLoS Biology*, *4*(8), e235.

Gerardo, N. M., Mueller, U. G., & Currie, C. R. (2006). Complex host-pathogen coevolution in the *Apterostigma* fungus-growing ant-microbe symbiosis. *BMC Evolutionary Biology*, *6*(1), 88.

Gerardo, N. M., Mueller, U. G., Price, S. L., & Currie, C. R. (2004). Exploiting a mutualism: Parasite specialization on cultivars within the fungus-growing ant symbiosis. *Proceedings of the Royal Society B: Biological Sciences*, *271*(1550), 1791–1798.

Haines, B. L. (1978). Element and Energy Flows Through Colonies of the Leaf-Cutting Ant, *Atta colombica*, in Panama. *Biotropica*, *10*(4), 270–277.

Hammond, & Lawrence. (1989). Mycophagy in insects: a summary. *Insect–Fungus Interactions*. https://books.google.com/books?hl=en&lr=&id=DwO5_3N7sSAC&oi=fnd&pg=PA275&dq=insect+fungal+associations&ots=12Vw1Qz1Bz&sig=GwzCvTvch8nvbo5I7snCCunwdAE

Hanisch, P. E., Sosa-Calvo, J., & Schultz, T. R. (2022). The Last Piece of the Puzzle? Phylogenetic Position and Natural History of the Monotypic Fungus-Farming Ant Genus *Paramycetophylax* (Formicidae: Attini). *Insect Systematics and Diversity*, *6*(1). https://doi.org/10.1093/isd/ixab029

Hansen, K. A., Kim, R. R., Lawton, E. S., Tran, J., Lewis, S. K., Deol, A. S., & Van Arnam, E. B. (2022). Bacterial Associates of a Desert Specialist Fungus-Growing Ant Antagonize Competitors with a Nocamycin Analog. *ACS Chemical Biology*. https://doi.org/10.1021/acschembio.2c00187

Herz, H., Beyschlag, W., & Hölldobler, B. (2007). Herbivory rate of leaf-cutting ants in a tropical moist forest in Panama at the population and ecosystem scales. *Biotropica*, *39*(4), 482–488.

Herz, H., Hölldobler, B., & Roces, F. (2008). Delayed rejection in a leaf-cutting ant after foraging on plants unsuitable

for the symbiotic fungus. *Behavioral Ecology: Official Journal of the International Society for Behavioral Ecology*, *19*(3), 575–582.

Hölldobler, B., & Wilson, E. O. (2010). *The Leafcutter Ants: Civilization by Instinct*. W. W. Norton & Company.

Howard, J. J. (1987). Leafcutting ant diet selection: The role of nutrients, water, and secondary chemistry. *Ecology*, *68*(3), 503–515.

Howard, J. J. (1990). Infidelity of leafcutting ants to host plants: resource heterogeneity or defense induction? *Oecologia*, *82*(3), 394–401.

Jarrod J. Scott, Kevin J. Budsberg, Garret Suen, Devin L. Wixon, Teri C. Balser, & Cameron R. Currie. (2010). Microbial community structure of leaf-cutter ant fungus gardens and refuse dumps. *PloS One*, *5*(3), e9922.

Khadempour, L., Burnum-Johnson, K. E., Baker, E. S., Nicora, C. D., Webb-Robertson, B.-J. M., White, R. A., 3rd, Monroe, M. E., Huang, E. L., Smith, R. D., & Currie, C. R. (2016). The fungal cultivar of leaf-cutter ants produces specific enzymes in response to different plant substrates. *Molecular Ecology*, *25*(22), 5795–5805.

Khadempour, L., Fan, H., Keefover-Ring, K., Carlos-Shanley, C., Nagamoto, N. S., Dam, M. A., Pupo, M. T., & Currie, C. R. (2020). Metagenomics Reveals Diet-Specific Specialization of Bacterial Communities in Fungus Gardens of Grass- and Dicot-Cutter Ants. *Frontiers in Microbiology*, *11*, 570770.

Khadempour, L., Kyle, J. E., Webb-Robertson, B.-J. M., Nicora, C. D., Smith, F. B., Smith, R. D., Lipton, M. S., Currie, C. R., Baker, E. S., & Burnum-Johnson, K. E. (2021). From Plants to Ants: Fungal Modification of Leaf Lipids for Nutrition and Communication in the Leaf-Cutter Ant Fungal Garden Ecosystem. *MSystems*, *6*(2). https://doi.org/10.1128/mSystems.01307-20

Kooij, P. W., Schiøtt, M., Boomsma, J. J., & De Fine Licht, H. H. (2011). Rapid shifts in *Atta cephalotes* fungus-garden enzyme activity after a change in fungal substrate (Attini, Formicidae). *Insectes Sociaux*, *58*(2), 145–151.

Leal-Dutra, C. A., Grifith, G. W., Neves, M. A., McLaughlin, D. J., Mclaughlin, E. G., Clasen, L. A., & Dentinger, B. T. M. (2020). Reclassification of Pterulaceae Corner (Basidiomycota: Agaricales) introducing the ant-associated genus *Myrmecopterula* gen. nov., *Phaeopterula Henn*. and the corticioid Radulomycetaceae fam. nov. *IMA Fungus*, *11*(2). https://doi.org/10.1186/s43008-019-0022-6

Li, H., Sosa-Calvo, J., Horn, H. A., Pupo, M. T., Clardy, J., Rabeling, C., Schultz, T. R., & Currie, C. R. (2018). Convergent evolution of complex structures for ant-bacterial defensive symbiosis in fungus-farming ants. *Proceedings of the National Academy of Sciences of the United States of America*, *115*(42), 10720–10725.

Li, H., Young, S. E., Poulsen, M., & Currie, C. R. (2021). Symbiont-Mediated Digestion of Plant Biomass in Fungus-Farming Insects. *Annual Review of Entomology*, *66*, 297–316.

Mangone, D. M., & Currie, C. R. (2007). Garden substrate preparation behaviours in fungus-growing ants. *The Canadian Entomologist*, *139*(6), 841–849.

Marfetán, J. A., Romero, A. I., & Folgarait, P. J. (2015). Pathogenic interaction between *Escovopsis weberi* and *Leucoagaricus* sp.: mechanisms involved and virulence levels. *Fungal Ecology*, *17*, 52–61.

Martin. (1992). The evolution of insect-fungus associations: from contact to stable symbiosis. *American Zoologist*. https://academic.oup.com/icb/article-abstract/32/4/593/2056495

Martin, M. M., & Martin, J. S. (1970). The biochemical basis for the symbiosis between the ant, *Atta colombica tonsipes*, and its food fungus. *Journal of Insect Physiology*, *16*(1), 109–119.

Masiulionis, V. E., Cabello, M. N., Seifert, K. A., Rodrigues, A., & Pagnocca, F. C. (2015). *Escovopsis trichodermoides* sp. nov., isolated from a nest of the lower attine ant *Mycocepurus goeldii. Antonie van Leeuwenhoek, International Journal of General and Molecular Microbiology*, *107*(3), 731–740.

Mcdonald, B. R., Chevrette, M. G., Klassen, J. L., Horn, H. A., Caldera, E. J., Wendt-Pienkowski, E., Cafaro, M. J., Ruzzini, A. C., Van Arnam, E. B., Weinstock, G. M., Gerardo, N. M., Poulsen, M., Suen, G., Clardy, J., & Currie, C. R. (2019). *Biogeography and Microscale Diversity Shape the Biosynthetic Potential of Fungus-growing Ant-associated Pseudonocardia*. https://doi.org/10.1101/545640

Meirelles, L. A., Montoya, Q. V., Solomon, S. E., & Rodrigues, A. (2015). New light on the systematics of fungi associated with attine ant gardens and the description of *Escovopsis kreiselii* sp. nov. *PloS One*, *10*(1), e0112067.

Mendgen, K., Hahn, M., & Deising, H. (1996). Morphogenesis and mechanisms of penetration by plant pathogenic

fungi. *Annual Review of Phytopathology*, *34*, 367–386.

Montoya, Q. V., Martiarena, M. J. S., Bizarria, R., Jr, Gerardo, N. M., & Rodrigues, A. (2021). Fungi inhabiting attine ant colonies: reassessment of the genus *Escovopsis* and description of *Luteomyces* and *Sympodiorosea* gens. nov. *IMA Fungus*, *12*(1), 1–18.

Montoya, Q. V., Meirelles, L. A., Chaverri, P., & Rodrigues, A. (2016). Unraveling *Trichoderma* species in the attine ant environment: description of three new taxa. *Antonie van Leeuwenhoek, International Journal of General and Molecular Microbiology*, *109*(5), 633–651.

Montoya, Q. V., Sutta Martiarena, M. J., Polezel, D. A., Kakazu, S., & Rodrigues, A. (2019). More pieces to a huge puzzle: Two new *Escovopsis* species from fungus gardens of attine ants. *MycoKeys*, *46*, 97–118.

Moran, N. A. (2007). Symbiosis as an adaptive process and source of phenotypic complexity. *Proceedings of the National Academy of Sciences*, *104*(Supplement 1), 8627–8633.

Moreira, S. M., Rodrigues, A., Forti, L. C., & Nagamoto, N. S. (2015). Absence of the parasite *Escovopsis* in fungus garden pellets carried by gynes of *Atta sexdens*. *Sociobiology*, *62*(1), 34–38.

Muchovej, J., & Della Lucia, T. (1990). *Escovopsis*, a new genus from leaf cutting ant nests to replace *Phialocladus* nomen invalidum. *Mycotaxon*, *37*, 191–195.

Mueller, U. G., Schultz, T. R., Currie, C. R., Adams, R. M., & Malloch, D. (2001). The origin of the attine ant-fungus mutualism. *The Quarterly Review of Biology*, *76*(2), 169–197.

Mueller, Ulrich G., Rehner, S. A., & Schultz, T. R. (1998). The evolution of agriculture in ants. *Science*, *281*(5385), 2034–2038.

North, R. D., Jackson, C. W., & Howse, P. E. (1999). Communication between the fungus garden and workers of the leaf-cutting ant, *Atta sexdens rubropilosa*, regarding choice of substrate for the fungus. *Physiological Entomology*, *24*(2), 127–133.

Nygaard, S., Hu, H., Li, C., Schiøtt, M., Chen, Z., Yang, Z., Xie, Q., Ma, C., Deng, Y., Dikow, R. B., Rabeling, C., Nash, D. R., Wcislo, W. T., Brady, S. G., Schultz, T. R., Zhang, G., & Boomsma, J. J. (2016). Reciprocal genomic evolution in the ant-fungus agricultural symbiosis. *Nature Communications*, *7*(1), 12233.

Oh, D. C., Poulsen, M., Currie, C. R., & Clardy, J. (2009). Dentigerumycin: A bacterial mediator of an ant-fungus symbiosis. *Nature Chemical Biology*, *5*(6), 391–393.

Pagnocca, F. C., Legaspe, M. F. C., Rodrigues, A., Ruivo, C. C. C., Nagamoto, N. S., Bacci, M., & Forti, L. C. (2010). Yeasts isolated from a fungus-growing ant nest, including the description of *Trichosporon chiarellii* sp. nov., an anamorphic basidiomycetous yeast. *International Journal of Systematic and Evolutionary Microbiology*, *60*(Pt 6), 1454–1459.

Pagnocca, F. C., Masiulionis, V. E., & Rodrigues, A. (2012). Specialized Fungal Parasites and Opportunistic Fungi in Gardens of Attine Ants. *Psyche*, *2012*, 1–9.

Pereira, J. S., Costa, R. R., Nagamoto, N. S., Forti, L. C., Pagnocca, F. C., & Rodrigues, A. (2016). Comparative analysis of fungal communities in colonies of two leaf-cutting ant species with different substratum preferences. *Fungal Ecology*, *21*, 68–75.

Pinto-Tomás, A. A., Anderson, M. A., Suen, G., Stevenson, D. M., Chu, F. S. T., Cleland, W. W., Weimer, P. J., & Currie, C. R. (2009). Symbiotic nitrogen fixation in the fungus gardens of leaf-cutter ants. *Science*, *326*(5956), 1120–1123.

Poulsen, M., Cafaro, M. J., Erhardt, D. P., Little, A. E. F., Gerardo, N. M., Tebbets, B., Klein, B. S., & Currie, C. R. (2010). Variation in *Pseudonocardia* antibiotic defense helps govern parasite-induced morbidity in *Acromyrmex* leaf-cutting ants. *Environmental Microbiology Reports*, *2*(4), 534–540.

Quinlan, R. J., & Cherrett, J. M. (1979). The role of fungus in the diet of the leaf-cutting ant *Atta cephalotes* (L.). *Ecological Entomology*, *4*(2), 151–160.

Reynolds, H. T., & Currie, C. R. (2004). Pathogenicity of *Escovopsis weberi:* The parasite of the attine ant-microbe symbiosis directly consumes the ant-cultivated fungus. *Mycologia*, *96*(5), 955–959.

Ridley, P., Howse, P. E., & Jackson, C. W. (1996). Control of the behavior of leaf-cutting ants by their 'symbiotic' fungus. *Experientia*, *52*(6), 631–635.

Roces, F., & Lighten, J. R. B. (1995). Larger bites of leaf-cutting ants. *Nature*, *373*(6513), 392–392.

Rocha, S. L., Jorge, V. L., Della Lucia, T. M. C., Barreto, R. W., Evans, H. C., & Elliot, S. L. (2014). Quality control by leaf-cutting ants: evidence from communities of endophytic fungi in foraged and rejected vegetation. *Arthropod-Plant Interactions*, *8*(5), 485–493.

Rodrigues, A., Cable, R. N., Mueller, U. G., Bacci, M., Jr, & Pagnocca, F. C. (2009). Antagonistic interactions between garden yeasts and microfungal garden pathogens of leaf-cutting ants. *Antonie van Leeuwenhoek*, *96*(3), 331–342.

Rogerson, C. T., & Samuels, G. J. (1994). Agaricicolous Species of *Hypomyces*. *Mycologia*, *86*(6), 839–866.

Santos, A. V., Dillon, R. J., Dillon, V. M., Reynolds, S. E., & Samuels, R. I. (2004). Occurrence of the antibiotic producing bacterium Burkholderia sp. in colonies of the leaf-cutting ant *Atta sexdens rubropilosa*. *FEMS Microbiology Letters*, *239*(2), 319–323.

Saverschek, N., Herz, H., Wagner, M., & Roces, F. (2010). Avoiding plants unsuitable for the symbiotic fungus: learning and long-term memory in leaf-cutting ants. *Animal Behaviour*, *79*(3), 689–698.

Schiøtt, M., & Boomsma, J. J. (2021). Proteomics reveals synergy between biomass degrading enzymes and inorganic Fenton chemistry in leaf-cutting ant colonies. *ELife*, *10*. https://doi.org/10.7554/eLife.61816

Schiøtt, M., Rogowska-Wrzesinska, A., Roepstorff, P., & Boomsma, J. J. (2010). Leaf-cutting ant fungi produce cell wall degrading pectinase complexes reminiscent of phytopathogenic fungi. *BMC Biology*, *8*, 156.

Schultz, T. R., & Brady, S. G. (2008). Major evolutionary transitions in ant agriculture. *Proceedings of the National Academy of Sciences of the United States of America*, *105*(14), 5435–5440.

Schultz, T. R., Sosa-Calvo, J., Brady, S. G., Lopes, C. T., Mueller, U. G., Bacci, M., & Vasconcelos, H. L. (2015). The most relictual fungus-farming ant species cultivates the most recently evolved and highly domesticated fungal symbiont species. *The American Naturalist*, *185*(5), 693–703.

Seifert, K. A., Samson, R. A., & Chapela, I. H. (1995). *Escovopsis aspergilloides*, a Rediscovered Hyphomycete from Leaf-Cutting Ant Nests. *Mycologia*, *87*(3), 407.

Sen, R., Ishak, H. D., Estrada, D., Dowd, S. E., Hong, E., & Mueller, U. G. (2009). Generalized antifungal activity and 454-screening of *Pseudonocardia* and *Amycolatopsis* bacteria in nests of fungus-growing ants. *Proceedings of the National Academy of Sciences of the United States of America*, *106*(42), 17805–17810.

Somera, A. F., Lima, A. M., Dos Santos-Neto, Á. J., Lanças, F. M., & Bacci, M., Jr. (2015). Leaf-cutter ant fungus gardens are biphasic mixed microbial bioreactors that convert plant biomass to polyols with biotechnological applications. *Applied and Environmental Microbiology*, *81*(13), 4525–4535.

Sosa-Calvo, J., Jesovnik, A., Okonski, E., & Schultz, T. R. (2015). Locating, collecting, and maintaining colonies of fungus-farming ants (Hymenoptera: Myrmicinae: Attini). *Sociobiology*. http://ojs3.uefs.br/index.php/sociobiology/article/view/761

Suen, G., Scott, J. J., Aylward, F. O., Adams, S. M., Tringe, S. G., Pinto-Tomás, A. A., Foster, C. E., Pauly, M., Weimer, P. J., Barry, K. W., Goodwin, L. A., Bouffard, P., Li, L., Osterberger, J., Harkins, T. T., Slater, S. C., Donohue, T. J., & Currie, C. R. (2010). An insect herbivore microbiome with high plant biomass-degrading capacity. *PLoS Genetics*, *6*(9), e1001129.

Suen, G., Teiling, C., Li, L., Holt, C., Abouheif, E., Bornberg-Bauer, E., Bouffard, P., Caldera, E. J., Cash, E., Cavanaugh, A., Denas, O., Elhaik, E., Favé, M. J., Gadau, J., Gibson, J. D., Graur, D., Grubbs, K. J., Hagen, D. E., Harkins, T. T., … Currie, C. R. (2011). The genome sequence of the leaf-cutter ant *Atta cephalotes* reveals insights into its obligate symbiotic lifestyle. *PLoS Genetics*, *7*(2), e1002007.

Taerum, S. J., Cafaro, M. J., Little, A. E. F., Schultz, T. R., & Currie, C. R. (2007). Low host-pathogen specificity in the leaf-cutting ant-microbe symbiosis. *Proceedings of the Royal Society B: Biological Sciences*, *274*(1621), 1971–1978.

Tamm, H., & Põldmaa, K. (2013). Diversity, host associations, and phylogeography of temperate aurofusarin-producing *Hypomyces/Cladobotryum* including causal agents of cobweb disease of cultivated mushrooms. *Fungal Biology*, *117*(5), 348–367.

Van Arnam, E. B., Ruzzini, A. C., Sit, C. S., Horn, H., Pinto-Tomás, A. A., Currie, C. R., Clardy, J., Van Arnam, E. B., Ruzzini, A. C., Sit, C. S., Horn, H., Pinto-Tomás, A. A., Currie, C. R., & Clardy, J. (2016). Selvamicin, an atypical antifungal polyene from two alternative genomic contexts. *Proceedings of the National Academy of Sciences*

of the United States of America, *113*(46), 12940–12945.

Van Bael, S. A., Estrada, C., Rehner, S. A., Santos, J. F., & Wcislo, W. T. (2012). Leaf endophyte load influences fungal garden development in leaf-cutting ants. *BMC Ecology*, *12*, 23.

Van Bael, S. A., Estrada, C., & Wcislo, W. T. (2011). Fungal-Fungal Interactions in Leaf-Cutting Ant Agriculture. *Psyche*, *2011*. https://doi.org/10.1155/2011/617478

Van Bael, S. A., Fernández-Marín, H., Valencia, M. C., Rojas, E. I., Wcislo, W. T., & Herre, E. A. (2009). Two fungal symbioses collide: endophytic fungi are not welcome in leaf-cutting ant gardens. *Proceedings. Biological Sciences / The Royal Society*, *276*(1666), 2419–2426.

Van Bael, S. A., Seid, M. A., & Wcislo, W. T. (2012). Endophytic fungi increase the processing rate of leaves by leaf-cutting ants (Atta). *Ecological Entomology*, *37*(4), 318–321.

Vo, T. L., Mueller, U. G., & Mikheyev, A. S. (2009). Free-living fungal symbionts (Lepiotaceae) of fungus-growing ants (Attini: Formicidae). *Mycologia*, *101*(2), 206–210.

Weber, N. A. (1966). Fungus-Growing Ants. *Science*, *153*(3736), 587–604.

Wirth, R., Herz, H., Ryel, R. J., Beyschlag, W., & Hölldobler, B. (2002). *Herbivory of Leaf-Cutting Ants: A Case Study on Atta colombica in the Tropical Rainforest of Panama*. Springer Berlin Heidelberg.

Zhang, C., Kakishima, M., Xu, J., Wang, Q., & Li, Y. (2017). The effect of *Hypomyces perniciosus* on the mycelia and basidiomes of *Agaricus bisporus*. *Microbiology*, *163*(9), 1273–1281.

Chapter 2: Genomic diversification of the specialized parasite of the fungus-growing ant symbiosis

This chapter is currently in press at The Proceedings of the National Academy of Sciences. Supplemental materials can be found in Appendix 1.

Kirsten Gotting[1,2], Daniel S. May[1], Jeffrey Sosa-Calvo[3], Lily Khadempour[4], Charlotte B. Francoeur[1], Aileen Berasategui[5], Margaret W. Thairu[1], Shelby Sandstrom[1], Caitlin M. Carlson[1], Marc G. Chevrette[6,7], Monica T. Pupo[8], Tim S. Bugni[9], Ted R. Schultz[3], J. Spencer Johnston[10], Nicole M. Gerardo[5], Cameron R. Currie[1,11].

Affiliations:
[1]Department of Bacteriology, University of Wisconsin-Madison, Madison, 53706, WI, USA
[2]Laboratory of Genetics, University of Wisconsin-Madison, Madison, 53706, WI, USA
[3]Department of Entomology, National Museum of Natural History, Smithsonian Institution, Washington, DC 20560, USA
[4]Department of Earth and Environmental Sciences, Rutgers University, Newark, NJ 08854
[5]Department of Biology, Emory University, Atlanta, GA 30322
[6]Wisconsin Institute for Discovery, University of Wisconsin-Madison, Madison, 53705, WI, USA
[7]Department of Plant Pathology, University of Wisconsin-Madison, Madison, 53705, WI, USA
[8]School of Pharmaceutical Sciences of Ribeirão Preto, University of São Paulo, Ribeirão Preto, 14040-903, SP, Brazil
[9]Pharmaceutical Sciences Division, School of Pharmacy, University of Wisconsin-Madison, Madison, 53705, WI, USA
[10]Department of Entomology, Texas A&M University, College Station, TX, 77843, USA
[11]McMaster University, Department of Biochemistry and Biomedical Sciences, Hamilton, Ontario

Author Contributions:
K.G., D.S.M., J.S.C., L.K., A.B.L., M.G.C., A.R., M.T.P., T.S.B., T.R.S., N.M.G., C.R.C. designed research; K.G., D.S.M, J.S.C., L.K., M.W.T., S.S., C.M.C., J.S.J. performed research; K.G., D.S.M., J.S.C., J.S.J. analyzed data; K.G., C.F., T.R.S., C.R.C. wrote the paper.

2.1 Abstract

Fungi shape the diversity of life. Characterizing the evolution of fungi is critical to understanding symbiotic associations across kingdoms. In this study, we investigate the genomic and metabolomic diversity of the genus *Escovopsis*, a specialized parasite of fungus-growing ant gardens. Based on 25 high-quality draft genomes, we show that *Escovopsis* forms a monophyletic group arising from a mycoparasitic fungal ancestor 61.82 million years ago (Mya). Across the evolutionary history of fungus-growing ants, the dates of origin of most clades of *Escovopsis* correspond to the dates of origin of the fungus-growing ants whose gardens they parasitize. We reveal that genome reduction, determined by both genomic sequencing and flow cytometry, is a consistent feature across the genus *Escovopsis,* largely occurring in coding regions, specifically in the form of gene loss and reductions in copy numbers of genes. All functional gene categories have reduced copy numbers, but resistance and virulence genes maintain functional diversity. Biosynthetic gene clusters (BGCs) contribute to phylogenetic differences among *Escovopsis* spp., and sister taxa in the Hypocreaceae. The phylogenetic patterns of co-diversification among BGCs are similarly exhibited across mass spectrometry analyses of the metabolomes of *Escovopsis* and their sister taxa. Taken together, our results indicate that *Escovopsis* spp. evolved unique genomic repertoires to specialize on the fungus-growing ant-microbe symbiosis.

2.2 Significance Statement

Fungi represent a kingdom of organisms with diverse interspecies associations and broad variability in genome content. The fungal genus *Escovopsis* is a parasite of the multipartite

fungus-growing ant symbiosis. We present this genus as a eukaryotic model of genomic reduction and diversification over the 60-million-year-old history of the fungus-growing ant symbiosis. This genomic evolution represents an example of a eukaryotic genus evolving a reduced genomic toolkit while maintaining ancient host associations.

2.3 Introduction

Fungi engage in complex interspecific interactions that have helped shape the biocomplexity and biodiversity of life on earth (Blackwell & Vega, 2018). In terrestrial ecosystems, fungi play critical roles as beneficial and antagonistic symbionts. Fungi occupied the terrestrial environment prior to the first land plants and animals (Gan et al., 2021; Taylor & Berbee, 2006; D. Y. Wang et al., 1999), and played a key role in species radiations (Lutzoni et al., 2018) in the other two kingdoms. Interactions between fungi and other organisms are mediated by small molecules, including those encoded by groupings of genes known as biosynthetic gene clusters (Keller, 2015; Robey et al., 2021). These molecules are often targets of evolution due to their mediation of symbiotic interactions, and frequently facilitate symbiotic specialization (Noda-Garcia & Tawfik, 2020; Stahl & Bishop, 2000). While a number of studies focusing on plant-fungal symbioses have provided key insights into the macroevolutionary dynamics of fungi (Clay & Holah, 1999; Hoeksema et al., 2018; Lutzoni et al., 2018; van der Heijden et al., 2016), exploring the evolution of animal-fungal and fungal-fungal associations within ancient clades of fungal symbionts is necessary for understanding the processes underlying major transitions in these associations over time, and how these transitions impact genomic evolution.

The genus *Escovopsis* (Ascomycota, Pezizomycotina: Hypocreales: Hypocreaceae), a specialized mycoparasite of the fungi cultivated by fungus-growing ants, is part of an emerging model system for the study of fungal symbiosis. Fungus-growing ants (Formicidae: Myrmicinae: Attini: Attina) participate in a >60-million-year-old obligate nutritional symbiosis with specialized fungi (Basidomycota: Agaricomycetes: Agaricales: Agaricaceae or Pterulaceae), which they farm for food. Lineages of these ant-fungus mutualists have evolved diverse methods of fungal cultivation across a broad geographic range in the American tropics, with ants and fungal cultivars exhibiting high levels of symbiont fidelity (Branstetter et al., 2017; Schultz et al., 2015). *Escovopsis* has only been observed within the structural matrix of the gardens (Fig. 1A) where the ants maintain their fungal cultivar (Currie, Mueller, et al., 1999) and in the refuse piles where ants discard old garden material (Bot et al., 2001; Currie, Mueller, et al., 1999; Currie & Stuart, 2001). No free-living form of *Escovopsis* has been identified and *Escovopsis* is likely horizontally transmitted between gardens (Currie, Mueller, et al., 1999). *Escovopsis* gets energy from necrotrophically degrading (Reynolds & Currie, 2004) and consuming the fungus growing ants' cultivar (Steffan et al., 2015), functioning as a mycoparasite. *Escovopsis* can destabilize ant colonies by completely overwhelming the fungus-growing ant gardens (Fig. 1A-B) and producing insecticidal molecules that disrupt ant behaviors (Dhodary et al., 2018; Heine et al., 2018). To defend against *Escovopsis,* fungus-growing ants weed and groom out hyphae and conidia (Currie, 2001; Currie & Stuart, 2001). Additionally, many fungus-growing ants associate with *Pseudonocardia* (Actinobacteria) that produces antifungal molecules that inhibit *Escovopsis*

growth (Currie, Scottt, et al., 1999; Oh et al., 2009; Van Arnam et al., 2016). Despite these defenses, *Escovopsis* parasitizes the gardens of the majority of fungus-growing ant lineages (Currie, Mueller, et al., 1999; Currie, Scott, et al., 1999; Currie et al., 2003).

The fungus-growing ant symbiosis is characterized by phylogenetically concordant associations between the ants, their cultivars, and the specialized fungal parasites of the symbiosis in the genus *Escovopsis* (Currie et al., 2003). In total, nine species of *Escovopsis* have been described to associate with fungus-growing ant lineages across four of the five different ant agricultural strategies, and many more species, and possibly genera, are likely yet to be described (Montoya et al., 2021). These strategies are based on the macroevolutionary ant-cultivar relationships described by Schultz and Brady (Schultz & Brady, 2008) as follows. 'Lower agriculture' encompasses the mutualism between the broadest range of attine ants and agaricaceous fungi in the genera *Leucocoprinus* and *Leucoagaricus* cultivated in filamentous forms. The *Escovopsis* species that associate with lower agriculture ant lineages are *E. trichodermoides* and *E. kreiselii* (Masiulionis et al., 2015; Meirelles et al., 2015). Yeast agriculture is practiced by species within the *Cyphomyrmex rimosus* group that cultivate agaricaceous fungi in an atypical yeast-like form and is not known to be parasitized by any *Escovopsis* species (Currie, 2001). 'Coral-fungus agriculture' is practiced by a subset of ants in the genus *Apterostigma* (the *pilosum* species group) that cultivate pterulaceous fungi in the genus *Myrmecopterula* (Leal-Dutra et al., 2020). *Escovopsis clavatus* and *E. multiformis* associate with coral-fungus ant agriculture (Caldera et al., 2019; Christopher et al., 2021; Montoya et al., 2019). 'Higher

agriculture' is practiced by attine ants that cultivate a distinct clade of agaricaceous fungi derived from lower-agriculture fungi that are parasitized by *E. moelleri, E. microspora, E. lentecrescens, E. weberi,* and *E. aspergilloides* (Augustin et al., 2013; Muchovej & Della Lucia, 1990; Seifert et al., 1995). Within higher agriculture, there are three ant genera, *Amoimyrmex*, *Acromyrmex,* and *Atta,* known as leaf-cutter ants, most of which cultivate the single, highly derived fungal species *Leucoagaricus gongylophorus*. In summary, specific species of *Escovopsis* associate with specific ant-cultivar hosts.

Comparative genomic studies of fungi have provided valuable insights into macroevolutionary patterns in diverse fungal symbionts (Stajich, 2017), such as those of plants (Bittleston et al., 2016; Kohler et al., 2015; Ohm et al., 2012; Riley et al., 2014; Wolfe et al., 2012) and lichens (Nelsen et al., 2020). Comparative genomic and metabolomic studies could likewise provide valuable insights into the coevolutionary dynamics of *Escovopsis*. A study of the *E. weberi* draft genome sequence revealed a genome that contained primary metabolism genes and exhibited reductions in several carbohydrate active enzyme (CAZyme) gene families and genes associated with sexual reproduction (de Man et al., 2016). These gene family reductions are consistent with the obligate parasitic life history of *E. weberi*. In addition, the *E. weberi* genome revealed unique suites of BGCs, some of which are expressed during parasitic growth towards the cultivar (de Man et al., 2016). Further, *E. weberi* was shown to produce melinacidins capable of inhibiting *Pseudonocardia in vitro,* as well as shearinines capable of influencing ant behavior *in vivo* (Dhodary et al., 2018; Heine et al., 2018). We hypothesize that the pattern of genome

reduction exemplified in the *E. weberi* genome was inherited by all species of *Escovopsis* from their shared common ancestor, which originated more or less coincident with the origin of ant agriculture. Additionally, we hypothesize that *Escovopsis* lineages will exhibit genomic diversification and specialization across the different fungus-growing ant lineages practicing different agricultural strategies. Overall, we expect that *Escovopsis* genomes will share a similar suite of core genes that facilitate parasitism of fungus-growing ant gardens and that they will also possess unique subsets of non-core accessory genes that evolved subsequent to the evolutionary divergences of the fungus-growing ant lineages.

Here, we investigate the macroevolutionary history of *Escovopsis* mycoparasites, within the iconic fungus-growing ant symbiosis. Specifically, we sequenced and assembled 18 high quality draft genomes from *Escovopsis,* which, combined with the seven publicly available genomes, represent strains isolated across the phylogenetic diversity of fungus-growing ants. We use maximum-likelihood and coalescent-based phylogenomic inference to construct a species tree of *Escovopsis* to ascertain its phylogenetic position within the Hypocreales. We date the origin of species lineages across *Escovopsis* spp. using the MCMCTREE (Ziheng Yang, 2007) phylogenetic dating analysis and estimate genome sizes across all species using k-mer estimation and propidium iodide flow cytometry. We then estimate the effect of genome reduction on lineage-specific functional gene diversity and determine how this relates to BGCs underlying the production of small molecules. Finally, we use high-resolution electrospray ionization-Mass spectrometry (HRESI-LC-MS) to conduct untargeted metabolomic characterization of *Escovopsis*

across representative strains to determine variation and diversification of small molecule production. Taken together, our results reconstruct the evolutionary histories of different species of *Escovopsis* and their diversification across associated fungus-growing ant lineages from genomes to metabolomes. We observe gene loss across the monophyletic group of *Escovopsis* species that has implications for niche specialization parallel to major evolutionary events following the origin of the fungus-growing ant symbiosis.

2.4 Results and Discussion

2.4.1 Macroevolutionary dynamics of *Escovopsis.*

To examine the macroevolutionary dynamics of the garden pathogen *Escovopsis*, we sequenced, assembled, and annotated 18 draft genomes of *Escovopsis* species. The 18 strains, together with seven previously sequenced and publicly available *Escovopsis* genomes, span the phylogenetic diversity of fungus-growing ants, including four representatives from lower-attine agriculture, six from *Apterostigma* coral agriculture, seven from higher-attine agriculture, and eight from leaf-cutter ant agriculture (Dataset S1). The 25 *Escovopsis* genomes have an average Benchmarking Universal Single-Copy Orthologs (BUSCO) completeness of 97.8% for the ascomycete lineage dataset, an average N50 of 1.04 Mbp, and an average assembly length of 29.7 Mbp. Using the alignment-independent k-mer method in GenomeScope (Vurture et al., 2017) we estimated the average genome size to be 24.7 Mbp, with an average of 6,665 protein-coding genes (Dataset S1).

Next, we reconstructed the phylogeny of the 25 *Escovopsis* genomes together with 77 publicly available genomes of outgroup fungal species from the order Hypocreales. In total, we aligned 1706 single-copy orthologs from the BUSCO ascomycete lineage data set, resulting in a concatenated alignment composed of 2,882,422 base pairs. Our by-gene partitioned maximum-likelihood (ML) analyses resulted in strong statistical bootstrap support for the phylogeny, with most nodes exceeding 95% bootstrap support (Fig. S1A). Additionally, we constructed a coalescent-based species tree using gene trees from the same 1706 single-copy orthologs with most nodes on the primary topology exceeding a quartet score of 0.9 (Dataset S2, Fig. S1B).

Our phylogenomic analyses show that the strains of *Escovopsis* used in our study all form a monophyletic group, which is supported by both ML and coalescent-based analyses (Fig. S1). Further, we find that the evolutionary placement of the genus *Escovopsis* is within the family Hypocreaceae (Fig. 1), and that the sister clade is composed of *Cladobotryum protrusum* (GCA_004303015.1) and *Hypomyces rosellus* (GCA_011799845.1), two mycoparasites of agaricaceous fungi. *Escovopsis* forms a monophyletic group of five clades: (i) one clade (the sister of all the rest) parasitizing lower agriculture, (ii) two clades parasitizing coral-fungus agriculture, (iii) one clade parasitizing non-leaf-cutting higher agriculture, and, in the most apical clade, (iv) two sister clades, one parasitizing non-leaf-cutting higher agriculture and one parasitizing leaf-cutter agriculture (Fig. 2, colored boxes). One clade of *Escovopsis* parasitizing lower agriculture (quartet support 0.99) is composed of four strains: two from a currently undescribed *Escovopsis* species (ICBG2046 and ICBG2048), isolated from a *Cyphomyrmex muelleri* ant garden from

Panama and a *Mycetophylax* cf. *faunulus* ant garden from Guyana, respectively, and two strains of *E. kreiselii* (ICBG2047 and ICBG2049), both isolated from *Myrmicocrypta ednaella* ant gardens from Panama. Of the two clades of *Escovopsis* coral-fungus agriculture parasites, the first clade (quartet support 0.99) consists of two strains of an undescribed *Escovopsis* species (ICBG712 and ICBG721) that were isolated from *Apterostigma urichii* ant host gardens from Brazil and the second (quartet support 0.93) consists of *E. multiformis* strains (ICBG1065 and ICBG1075) isolated from *Apterostigma bruchi* gardens from Brazil and *E. clavatus* strains (ICBG1054 and ICBG726) isolated from *Apterostigma urichii* gardens from Brazil. Of the two clades of higher-agriculture-parasitizing *Escovopsis*, the first (quartet support 0.84) consists of three *E. aspergilloides* strains (ICBG730, ICBG710, and NIGD00000000) and the second (quartet support 0.99) consists of three *E. moelleri* strains (ICBG751, ICBG1096, and ICBG733). All of the higher agriculture-associated *Escovopsis* strains were isolated from *Paratrachymyrmex diversus* gardens from Brazil except for NIGD00000000, which was isolated from a *Paratrachymyrmex cornetzi* fungus garden from Panama. The clade of *Escovopsis weberi* leaf-cutter parasites (quartet support 0.82) consists of nine strains (ICBG731, ICBG736, ICBG742, LGSR00000000, NIGB00000000, NIGC00000000, NQYQ00000000, NQYR00000000, NQYS00000000). Leaf-cutter-associated strains were isolated from *Acromyrmex hystrix* from Brazil (ICBG742), *Acromyrmex echinatior* from Panama (NIGC00000000, NQYQ00000000, NQYR00000000), *Atta cephalotes* from Panama (LGSR00000000), *Atta colombica* from Panama (NQYS00000000), and

Paratrachymyrmex diversus from Brazil (ICBG736), with two strains that do not have host identifications (ICBG731 and NIGB00000000) from Brazil and Panama.

The temporal sequence of evolutionary divergences in *Escovopsis* revealed by our ML analyses mirrors the evolutionary history of fungus-growing ants. The most early-diverging *Escovopsis* lineage (Fig. 2, left) contains species associated with lower agriculture, whereas the next two diverging lineages contain parasites of coral-fungus agriculture. *Escovopsis* spp. associated with higher and leaf-cutter agriculture are the most derived in the genus (Fig. 2). Our coalescent-based gene tree supports most of these major evolutionary transitions; however, it is fundamentally conflicted about the position of the coral-fungus-parasitizing clade containing ICBG712 and ICBG721. The primary topology, supported by 719 genes, reconstructs ICBG712 and ICBG721 as the most early-diverging *Escovopsis* clade, whereas the secondary topology, supported by 706 genes, is consistent with our ML tree (i.e., with the lower-agriculture clade as the sister to the remainder of the genus) (Fig. S1A-B, Dataset S2). As an independent topology test, we reconstructed the phylogeny of the mitochondrial genome. All major nodes of the mitochondrial genome tree are supported by greater than 98% bootstrap support and support the same major topology as that of the primary coalescent-based gene tree by placing the clade consisting of ICBG712 and ICBG721 (coral agriculture) as the most early-diverging *Escovopsis* clade (Fig. S1B-C). The clade consisting of ICBG712 and ICBG721 positioned as the most early-diverging *Escovopsis* clade is also supported by the elongation factor 1-alpha gene tree (Fig. S1D), and the mitochondrial genome tree (Fig. S1C).

The divergence dates resulting from our genome-scale *Escovopsis,* and fungus-growing ant divergence-dating analyses reveal that the dates of origin of the majority of *Escovopsis* clades coincide with the dates of origin of their fungus-growing ant hosts. For example, *Escovopsis* likely originated from 72.69 (stem; 47.74-97.99 Mya highest posterior density (HPD)) to 61.82 (crown; 40.45-83.81 Mya HPD) Mya, whereas fungus-growing ants likely originated from 72.89 (stem; 63.68-81.92 Mya HPD) to 68.04 (crown; 59.35-76.93 Mya HPD) Mya. The ancestral fungus-growing ant practiced lower agriculture (Branstetter et al., 2017; Schultz & Brady, 2008) and the earliest-diverging lineage of *Escovopsis* parasitizes lower agriculture, suggesting that most or all *Escovopsis* species are descended from a parasite of lower agriculture. *Escovopsis* parasites of higher ant agriculture arose from 40.85 (stem; 26.06-55.82 Mya HPD) Mya, to 30.75 (crown; 19.47-42.83 HPD) Mya, which closely corresponds to the origins of higher ant agriculture from 34.78 (stem; 29.08-40.57 Mya HPD) to 28.71 (crown; 24.13-33.37 Mya HPD) Mya. Most recently, *Escovopsis* parasites of leaf-cutting ants arose 17.83 (stem; 10.72-25.52 HPD) to 11.9 (crown; 6.85-17.2 HPD) Mya, whereas leaf-cutting ants arose from 20.0 (stem; 16.49-23.61 Mya HPD) to 18.94 (crown; 15.47-22.39 Mya HPD) Mya. Correspondence between the dates of origin of coral fungus-cultivating ants and their *Escovopsis* parasites is more complex. The clade of coral-fungus-cultivating *Apterostigma* ant species originated from 24.95 (stem; 20.08-29.97 Mya) to 18.67 (crown; 14.76-22.66 Mya HPD) Mya. The younger of the two clades of coral-fungus-parasitizing *Escovopsis*, containing *E. multiformis* and *E. clavatus*, originated from 40.85 (stem; 26.06-55.82 Mya HPD) to 25.96 (crown; 15.1-37.62 Mya HPD) Mya, coinciding with the HPD ant stem age.

However, the older clade of coral-fungus-parasitizing *Escovopsis,* containing ICBG712 and ICBG721 originated from 54.13 (stem; 34.99-73.53 Mya HPD) to 1.01 (crown; 0.48-1.62 Mya HPD) Mya, suggesting that, paradoxically, it originated prior to the origin of coral-fungus agriculture. An alternative and arguably more likely hypothesis, however, is that the ancestor of the coral-fungus-associated clade (ICBG712 and ICBG721) (Fig. 2) originated as a parasite of lower ant agriculture but that, coincident with or following the origin of coral-fungus agriculture 20-30 Mya, its descendant lineage host-switched to become a parasite of coral-fungus agriculture. This hypothesis of host-switching from lower to coral-fungus agriculture is also consistent with the alternative topologies produced by the coalescent, mitochondrial genome, and single-gene elongation factor 1-alpha analyses discussed above (Fig. S1).

These results indicate that *Escovopsis* is a monophyletic group within the family Hypocreaceae. The species in the sister group of *Escovopsis*, represented in our phylogeny by *Hypomyces rosellus* and *Cladobotryum protrusum*, are, like *Escovopsis*, mycoparasites of agaricaceous fungi, as is *Hypomyces perniciosus*, an early-diverging member of the sister clade of *H. rosellus, C. protrusum,* and *Escovopsis* (Figs. 1 and 2). The molecular dating analysis indicates that *Escovopsis* parasitism of agaricaceous fungi may have coincided with the inception of the fungus-growing ant-microbe symbiosis, and subsequently differentiated in concordance with diversification of the symbiosis after the K-Pg extinction event. The origin of the main clades of *Escovopsis* correspond to the origins of the major ant agricultural systems. This temporal correspondence of evolutionary histories supports significant co-diversification and coevolution

in the fungus-growing ant agricultural symbiosis. Future studies integrating more fossil evidence and more *Escovopsis* genomes will further resolve the evolutionary history of *Escovopsis* and its correlations with fungus-growing ant evolution. Additional sampling of *Hypomyces* and *Cladobotryum* genomes is necessary to better resolve the phylogenetic position of the *Escovopsis* clade consisting of ICBG712 and ICBG721, which is currently confounded by gene tree discordance.

2.4.2 Genome Reduction in *Escovopsis.*

To test the hypothesis that a reduced genome is an ancestral feature of *Escovopsis* genomes, we estimated genome sizes using k-mer based methods and assembly lengths, as well as examined the relative contributions of coding sequence (CDS), introns, and repeat content to genome sizes (Dataset S1). *Escovopsis* genome sizes, as estimated with k-mer based methods, range from 19 Mbp to 28.8 Mbp, which is substantially smaller than the genome size estimates for *Cladobotryum protrusum* (39.6 Mbp), *Hypomyces perniciosus* (44.6 Mbp), and *Hypomyces rosellus* (39 Mbp). Further, k-mer estimates of *Trichoderma* spp. genome sizes range from 31.28 Mbp to 39.18 Mbp (Fig. S2A). *Escovopsis* genomes exhibit substantial reductions in CDS DNA, ranging between 9.4 Mbp to 10.9 Mbp. In comparison, *Hypomyces perniciosus*, *Hypomyces rosellus*, and *Cladobotryum protrusum* genomes have 13.6 Mbp, 15.2 Mbp, and 15.2 Mbp, respectively, while *Trichoderma* spp. range from 13.5 Mbp to 17.5 Mbp (Fig. S2C). Additionally, *Escovopsis* spp. have between 10,734 to 13,420 introns in CDS regions (Fig. S2E), while *Hypomyces perniciosus, Hypomyces rosellus*, and *Cladobotryum protrusum* have 17,690, 16,633,

and 18,581 introns in CDS regions, respectively. Comparatively, *Trichoderma* spp. have between 15,546 and 23,690 introns in CDS regions. While *Escovopsis* genomic features are smaller for both metrics, mean CDS lengths of *Escovopsis* genes are on average 1,561 base pairs, which is only 3% smaller than *Hypomyces perniciosus, Hypomyces rosellus*, and *Cladobotryum protrusum*, and is larger than *Trichoderma* spp. whose genes are on average 1,427 base pairs (Fig. S2D). Repeat content as estimated with k-mer frequency spectra across genome assemblies for *Escovopsis* genomes is highly variable (Fig. S2F) ranging from 0.6 Mbp to 6.5 Mbp, like the variability among *Hypomyces rosellus* (0.98 Mbp), *Cladobotryum protrusum* (1.5 Mbp), and *Hypomyces perniciosus* (11.5 Mbp). The distributions of these estimates are broader than the distributions of repeat content in *Trichoderma* genomes (1.3 Mbp), which is also smaller than the average for *Escovopsis* (1.5 Mbp). Additionally, we estimated repeat content with k-mer frequency spectra across Illumina reads. Estimates for *Escovopsis* ranged from 0.38 Mbp to 1.68 Mbp, which is smaller than the range estimated across genomic reads from *Trichoderma* which ranged from 0.9 Mbp to 3.8 Mbp (Fig. S2G). The differences in repeat content as estimated from assemblies and sequenced reads could reflect technical variation in genome assembly, with the estimates from the Illumina reads likely reflecting values closer to biological reality.

To further establish genome reduction in *Escovopsis* genomes, we conducted propidium iodide flow cytometry. We estimate genome sizes of 31.71 Mbp for ICBG2048, a strain of *Escovopsis* from lower agriculture, 21.94 Mbp for ICBG1065 and 26.52 for ICBG1075, strains of *Escovopsis multiformis*, 19.7 Mbp for ICBG1054, a strain of *Escovopsis clavatus,* 30.34 Mbp for

ICBG730, a strain of *Escovopsis* from *Paratrachymyrmex diversus* higher agriculture, and 24.43 Mbp for ICBG736, a strain of *Escovopsis weberi* isolated from leaf-cutter agriculture. This range of genome sizes from 19.7 Mbp to 31.71 Mbp is like our k-mer based predictions, which ranged from 19 Mbp to 28.8 Mbp. In particular, the genome size for ICBG1065 predicted with both methods varied by only 2.95 Mbp at 18.99 Mbp with k-mers and 21.94 Mbp with flow cytometry.

To understand how *Escovopsis* genomes differ across lineages, we examined shared orthologues and gene loss between *Escovopsis* and three outgroup genera, *Cladobotryum*, *Hypomyces*, and *Trichoderma*, using clade-specific pangenomes. Genes were included if they were present in all *Hypomyces* and *Cladobotryum* genomes and in at least 95% of all genomes for *Escovopsis* and *Trichoderma* genomes. In total, 8,783 orthologous genes were considered in this analysis (Fig. 3A). 1,943 genes are completely lost in *Escovopsis* (Figure S3A). We tested these genes for enrichment of gene ontology (GO) terms to determine if there were specific molecular functions, cellular components, or biological processes that predominated across these lost genes. These genes were enriched for GO terms such as 'regulation of transcription, DNA-templated', 'transmembrane transport', 'regulation of metabolic process', 'RNA biosynthetic process', 'transcription, DNA-templated', and 'oxidation-reduction process' (Fig. S3B). Within *Escovopsis* genomes, 6,849 orthologues are shared, of which 6,573 are also shared with at least one of the outgroup taxa (Fig. S3A). There are 729 orthologues that are shared between *Trichoderma, Hypomyces,* and *Cladobotryum* genomes that are not present in *Escovopsis*. Additionally, there are 605 orthologues that are only present in the genus *Trichoderma* and 600

only present in *Hypomyces* and *Cladobotryum*. Finally, *Escovopsis* shares 486 genes with *Hypomyces* and *Cladobotryum* and 133 genes with *Trichoderma* (Fig. S3A).

While sequencing-dependent genome size estimates tend to underestimate genome sizes, the genome size differences are uneven across the genus *Escovopsis*, with some species exhibiting larger, lineage-specific reductions. This result may be partially due to changes in gene size. When considering all annotated genes, *Escovopsis* genes are on average longer and have fewer introns compared to other fungi in the Hypocreaceae. Longer genes may be a result of loss of intergenic regions and gene fusion. In addition to structural changes in gene sizes, certain genes were lost in *Escovopsis*, which GO enrichment tests indicated were metabolism and membrane transport genes, as well as genes related to transcription. The reduction in genes related to transmembrane transport could be a result of specialization of this parasite, resulting in the loss of genes related to generalized interspecies signaling. Additionally, many transcription factors are multi-copy genes, where a loss of some copies may not sacrifice the function (Fig. S3B). Overall, the patterns of gene loss suggest non-uniform reductive evolution of *Escovopsis* lineages (Fig. S3A).

While many of the *Escovopsis* genomes share high levels of sequence similarity, as measured by average nucleotide identity (Fig. 3A, upper right corner), the highest sequence similarity is found among species of *Escovopsis* parasitizing the same ant agricultural system. 276 genes are unique to *Escovopsis* and have different patterns of distribution corresponding with host association, i.e., with the parasitized ant agricultural systems. The distribution of these 276

orthologues across ant agriculture show the distinct trajectories that lineages of *Escovopsis* have taken during their evolution (Figure 3B). We observe that *Escovopsis* from lower, coral, higher, and leaf-cutter fungal agriculture have 31, 4, 15, and 79 lineage-specific orthologous genes, respectively. None of these groups of genes were enriched for any GO terms but do have functional domain annotations, as noted in the outer rings of Figure 3A. Taken together, these data suggest that the selective pressures unique to different ant agricultural systems have played a role in shaping the genomic diversity seen in extant lineages of *Escovopsis*.

To determine the influence of reduced genome size on protein-coding gene families, we analyzed orthologous genes among and within species of *Escovopsis* by comparing the mean number of gene copies in each orthologous group in *Escovopsis* against the number in other fungal outgroups in the Hypocreaceae. We examined genes characterized as fungal virulence factors from the database of fungal virulence factors: DFVF (Lu et al., 2012), lipase encoding genes from the Lipase Engineering Database: LED (Fischer & Pleiss, 2003), peptidases from the MEROPS peptidase database (Rawlings et al., 2016), carbohydrate-active enzymes (CAZymes) from dbCAN2 for automated CAZyme annotation (Zhang et al., 2018), antimicrobial resistance genes from the Comprehensive Antibiotic Resistance Database: CARD (Jia et al., 2017), and BGCs using antiSMASH (Blin et al., 2017) with transmembrane domains or extracellular locations (see methods for more detail on these designations). This analysis shows that *Escovopsis* spp. genomes are reduced in gene copies of 1,479 orthologues, whereas, in contrast, gains of gene copies occur in only 56 orthologues. CAZymes and resistance genes have the highest loss-to-gain

ratios, 6.60 and 6.63 respectively, followed by peptidase genes (2.94), lipase genes (1.99), and virulence genes (1.72) (Fig. 4A). *Escovopsis* spp. also have a reduction in BGCs, with a loss-to-gain ratio of 4.62 and with eight clusters gained and 37 lost.

To examine how this observed reduction of copy number impacts the diversity of gene functions present in *Escovopsis*, we calculated entropy for the same protein coding gene families. We hypothesize that a uniform reduction in copy number would uniformly reduce the amount of diversity, as measured by entropy, observed in different gene classes. We expect that the overall gene number will be reduced in every category, while the evenness of different functions may be increased or decreased based on whether there is selection on those functions. As a control, we used annotated BUSCOs, which have similar diversity levels across all genomes (Fig. S2 F). Lipase genes, peptidase genes, CAZyme genes, and BGCs supported our hypothesis of uniform diversity reduction, but resistance and virulence genes increased entropy relative to the outgroup taxa (Fig. 4B, Fig. S4). We looked at whether the diversity increases in select gene categories and genomes were due to increased genetic evenness or richness and determined that virulence and resistance genes have increased evenness relative to the outgroup taxa (Fig. S4 A, E). CAZymes had increased evenness, but the overall decrease in gene richness resulted in lower entropy values (Fig. S4 D, G). Lipases and peptidase decreased both in richness and evenness of genes (Fig. S4 B, C). BGCs were the only group of loci examined that exhibited decreased richness but not evenness of annotated clusters (Fig. S4 G).

Our results regarding copy number reduction and diversity support the hypothesis that *Escovopsis* genomes likely initially evolved a reduced suite of genes, which subsequently diversified across ant agriculture as different *Escovopsis* lineages specialized on the differing ecologies of the ant-cultivar agricultural strategies. This genomic diversification is exhibited through signaling molecules encoded by BGCs, as well as CAZymes, lipases, and peptidases for breaking down host material, resistance genes for confronting antibiotic pressure from ant-fungus-garden bacterial symbionts, and virulence genes for detecting and interacting with hosts. The case for reductive evolution followed by diversification is further supported by differing patterns of functional diversity for categories of protein-coding genes. The increase in entropy in protein-coding genes for resistance and virulence gene categories indicates that, although these categories exhibit gene copy reduction categories in *Escovopsis* genomes, functional genetic diversity has been maintained. Range restriction of *Escovopsis* to the fungus-growing ant-microbe symbiosis likely relaxed constraint on genes required for a generalist lifestyle, resulting in purifying selection and genome-wide reduction. While this reduction occurred in all classes of genes, certain virulence and resistance genes that likely confer pathogenic advantages to *Escovopsis* maintained functional diversity.

2.4.3 Lineage-specific differences among *Escovopsis* spp. are characterized by genome reduction and gene content diversification.

To identify evolutionary changes associated with the origin, life history, and diversification differentiating the garden pathogen *Escovopsis* from closely related Hypocreaceae, we examined the genomic-predicted putative secretome composition as characterized by fungal virulence

factors, lipase encoding genes, peptidases, carbohydrate-active enzymes, and antimicrobial resistance genes with either transmembrane domains or extracellular locations (see methods for more detail on these designations), as well as BGCs. We then chemically characterized the metabolome for a subset of strains using HRESI-LC-MS. This suite of secreted proteins, secondary metabolites, and molecules likely mediates host interactions in symbiosis. Figure 5A shows broad patterns of representation of secretome annotations across the genomes, with a broad swath shared, lost, and specific to *Escovopsis*. Additionally, we found a diversity of chemical potential across all *Escovopsis* lineages, and we found that molecules stratify *Escovopsis* lineages similarly to BGCs when analyzed with PCA (Fig. 5B-C). With this in mind, we consider these groups of annotations and molecules with respect to genome reduction, genome retention, and genome diversification in comparison to outgroup taxa from *Trichoderma, Hypomyces,* and *Cladobotryum*. With respect to genome reduction, we identified 72 secretome annotations across 90% of *Escovopsis* species, which is smaller than the predicted secretomes in *Trichoderma* (129 across 90% of *Trichoderma* species), *Hypomyces* (169 across *Hypomyces* genomes), and *Cladobotryum protrusum* (272*)*. Eighty-one annotations are lost across all *Escovopsis* genomes but are present in genomes of *Trichoderma, Hypomyces,* and *Cladobotryum*. Of note are sixteen CAZymes annotated as GH1, GH27, GH13_1, GH5_15, GH5_31, AA12, GH37, GH105, GH24, GH39, GH43_14, GH32, GH43_34, AA14, PL20, and PL8_4. With respect to our metabolomics analysis, five molecular families are present in *Cladobotryum protrusum*, *Hypomyces perniciosus,* and *Hypomyces rosellus* that are not present in *Escovopsis* (Dataset S4).

Next, we examined gene annotations and molecules that are shared and retained in *Escovopsis* from the ancestral state. Among the secretome 37 annotations are retained across all genomes surveyed (Fig. 4A). Seventeen of these are CAZymes, 16 are lipases, 11 are virulence genes, and 1 is a resistance gene (Dataset S4). Several are predicted to be involved in chitin degradation (ids: GH16, GH18, Q8J1Y3_BEABA, O59928_HYPVI, AA11, AA7). Additionally, two (ids: abH36, CE5) are predicted to degrade cutin. All *Escovopsis* genomes share a putative Type one PKS BGC. Additionally, four BGCs are present in the majority of *Escovopsis* genomes and are putatively characterized as "NRPS", "Terpene", or "Other KS" (Fig. S5A). Our metabolomic analyses identified 79 molecular families present across all *Escovopsis* metabolomes, none of which have natural product representatives in the Global Natural Product Social Molecular Networking Database (GNPS) (Nothias et al., 2020; M. Wang et al., 2016). Additionally, known Epipolythiodiketopiperazines are present in all *Escovopsis* strains except for ICBG1075, as well as in *Cladobotryum protrusum*, *Hypomyces perniciosus,* and *Hypomyces rosellus*.

Lastly, we considered genomic diversification among compared genera. We observe 148 secretome annotations that are lineage-specific to *Escovopsis*, defined as less than 10% presence in *Trichoderma* genomes, and a greater than 30% presence in at least one *Escovopsis* agricultural lineage (Dataset S4). Four of these proteins are predicted to be involved in resistance to tetracycline antibiotics and are present in all but coral agriculture-associated *Escovopsis*. Additionally, there are three CAZymes, two lipases, 82 peptidases, and 56 virulence factors that fall into this category. Eight of these proteins are predicted to be involved in degrading plant

tissue (ids: Q9C1R1_FUSOX, Q00350_COCCA, PLYB_COLGL, MER0000339, MER0019139, MER0011060, CUTI2_FUSSO). Additionally, several are annotated as subtilisin-like serine protease, which play a role in fungal virulence (ids: SUB4A_COCP7, SUB7A_COCP7, SUB6_ARTOC, MER1073654). There are 82 BGCs across ant agriculture, with only three matching clusters present in the MIBiG (Kautsar et al., 2020) repository. The known clusters are identified as follows. BGC0001583 is an emodin BGC from *Escovopsis weberi* and is present in all higher and leaf-cutter agriculture *Escovopsis*. BGC0001777 is a shearinine D BGC and is present in all but two strains (ICBG751 and NIGD00000000) of higher and leaf-cutter agriculture *Escovopsis* as well as in coral agriculture (ICBG1065). Our metabolomics results additionally confirmed the presence of shearinines in all higher and leaf-cutter strains surveyed, as well as in ICBG1054 and ICBG726 from coral agriculture *Escovopsis*. Lastly, among identified BGCs, BGC0001585: melinacidin IV BGC is present in all but two strains of leaf-cutter agriculture (NIGB0000000 and NQYS00000000) as well as in all strains of higher agriculture except for the clade formed by ICBG730, ICBG710, and NIGD00000000. Eleven other unidentified clusters have mixed lineage specificity across agricultural types (Fig. S5A). Twenty-four BGCs are only found in *Escovopsis* strains ICBG712 and ICBG721. Fourteen BGCs are only found among lower-agriculture-associated *Escovopsis* strains. Six BGCs are only found in *Escovopsis* strains ICBG726 and ICBG1054 and three BGCs are only found in *Escovopsis* strains ICBG1065 and ICBG1075. The remaining clusters from the original 82 have mixed patterns of lineage specificity (Fig. S5A). Our metabolomics results identified eight molecular families specific to leaf-cutter agriculture *Escovopsis*, fifteen molecular families specific

to higher-agriculture *Escovopsis,* 62 molecular families specific to coral-agriculture *Escovopsis*, and 49 molecular families specific to lower-agriculture *Escovopsis*. Fifteen molecular families are shared between leaf-cutter, higher, and coral agriculture *Escovopsis* (including shearinines), 12 molecular families are shared between higher, coral, and lower agriculture *Escovopsis*, 11 molecular families are shared across higher and coral agriculture *Escovopsis*, and 25 molecular families are shared between coral and lower *Escovopsis*.

The secretome, BGCs, and metabolomics highlight the ancient evolutionary history of these organisms, originating from a free-living common ancestor, and the genetic basis of a range of life history strategies. The reduced genomes of these specialized fungus-garden mycoparasites likely highlight the need to preserve chitin-degrading genes in the core secretome, whereas the functional capacity for degradation of plant tissue has been reduced across all lineages of *Escovopsis* with the loss of GH1, GH13_1, GH5_15, GH105, GH39, GH5_31, GH43_14, GH32, AA14, and GH43_34, which play roles in the degradation of xylan, cellulose, amylose, and fructose. One exception to this trend is proteins involved in cutin degradation, which could indicate that *Escovopsis* encounters these polymers, a key component of plant cuticles, during their life cycle. While most *Escovopsis* species had similar evolutionary patterns in their genomes and metabolomes, ICBG712 and ICBG721, isolated from the *Apterostigma* coral-fungus symbiosis, had notable differences in all functional suites of genes as well as metabolites, which is notable given that these *Escovopsis* are associated with gardens containing cultivars distantly related to those of the other agricultural systems. These results indicate that these genes likely

persist in *Escovopsis* lineages as part of a co-evolutionary dynamic involving fungus-growing ant-microbe behavioral and antimicrobial defenses. Additionally, the trend toward greater across-lineage functional diversity in virulence and resistance genes is underscored by the presence of tetracycline resistance genes in all but one clade of *Escovopsis* and the presence of subtilisin-like serine proteases that have unorganized specificity across lineages. Lastly, the evolutionary origin of shearinines and melinacidin IV, two BGCs that are not found in *Hypomyces*, *Cladobotryum,* or *Trichoderma* or in lower attine associated *Escovopsis,* represent genomic diversification known to have negative consequences for both leaf-cutter ants and their associated *Pseudonocardia* bacteria (Heine et al., 2018). Taken together, these data suggest that *Escovopsis* spp. evolved a diverse and streamlined molecular toolkit to adapt to the unique selective pressures applied by the fungus-growing ant niche. Additionally, these results demonstrate that *Escovopsis* has diversified along with its ant-cultivar hosts. Future research will unveil how these genes are causative for various traits that facilitate the parasitism of *Escovopsis*.

2.4.4 Conclusions

Our study reveals the distinct trajectories that *Escovopsis* spp. have undergone in their evolutionary histories, resulting in small genomes that encode diverse metabolites. These differences across species correspond to differences in fungus-growing ant agriculture. Our co-phylogenetic results suggest a significant "coevolutionary arms race" dynamic between *Escovopsis* and the ant fungal cultivars, in which fungal cultivars continually diversify (resulting in the major ant-cultivar agricultural systems), perhaps to avoid parasitism, and in which *Escovopsis*

continually adapts and evolves to parasitize these new systems. Additionally, the observed gene loss across *Escovopsis* species serves as further evidence that this genus likely originated as mycoparasites of agaricaceous cultivar ancestors that then diversified alongside the evolutionary history of ant-cultivar agriculture. This genomic diversification likely resulted in directional selection on niche-maintenance genes and in relaxed selection on genes ancillary to the ant-cultivar symbiotic ecology. Future research will aim to disentangle the relationship between species of *Escovopsis* and transitions to different agricultural strategies employed by the ants as well as different cultivar types.

2.5 Materials and Methods

2.5.1 Sample Collection, Isolation, DNA extraction, and Genome Assembly

We collected samples from Brazil in 2017, and from Panama in 1999 (Dataset S1). Research and collection of biological samples in Brazil were authorized by SISBIO (46555-6) and CNPq (010936/2014-9). Strains were isolated and maintained on potato dextrose agar as in Currie *et al* (Currie, Mueller, et al., 1999). For genomic DNA preparation strains were grown up on OXOID malt extract agar (CM59) 8.33 grams, agar 7.5 grams, 500 mL distilled water with a cellophane overlay. Tissue was scraped off the plates with a scalpel and stored at -80C. DNA was prepared by grinding fungal tissue in liquid nitrogen and isolating with a CTAB-based protocol. Genomic DNA was sequenced at the University of Wisconsin-Madison Biotechnology Center in July of 2017 and January of 2019 with 2X300 base pair Illumina MiSeq. Raw Illumina genomic reads were

filtered for bacterial and mitochondrial contamination by aligning to contaminant genomes using bwa mem (H. Li & Durbin, 2009) and discarding aligned reads using pysam (Developers, 2018; Heger et al., 2014). Reads were corrected using Musket (Liu et al., 2013) with default settings. Paired-end reads were then merged using FLASh (Magoč & Salzberg, 2011) with default settings. Merged and unmerged reads from FLASh were used as input for genome assembly with SPAdes v3.11.1 (Bankevich et al., 2012) with default settings. Genomes that were particularly fragmented were scaffolded using RagOO (Alonge et al., 2019) with a closely related (defined as greater than or equal to 95% average nucleotide identity) genome as a reference. Mitochondrial genomes were assembled using NOVOplasty (Dierckxsens et al., 2017), or downloaded from the NCBI from the following accessions: *Hypomyces aurantius* *Trichoderma atroviride* (MN125601.1), *Trichoderma gamsii* (KU687109.1), *Trichoderma asperellum* (NC_037075.1), *Trichoderma hamatum* (NC_036144.1), *Trichoderma lixii* (MT495248.1), *Trichoderma reesei* (AF447590.1). Species of *Escovopsis* were identified using a phylogenetic species concept by grouping species based on similarity to sequences of elongation factor 1-alpha of published species Fig. S1D).

2.5.2 Genome Size Estimation

Reads used for genome assembly were quality and adapter trimmed using fastp (Chen et al., 2018) using default parameters for single end reads, and the '--detect_adapter_for_pe' flag for paired end reads. Remaining reads were k-mer-counted using jellyfish (Marcais & Kingsford, 2012) and a k-mer size of 31. These counts were made into a histogram with KAT “kat hist” (Mapleson et al., 2017). Genome sizes were estimated using genomescope2 (Ranallo-Benavidez

et al., 2020), using the mean read length as reported by fastp, the k-mer size of 31, and the k-mer frequency spectra as produced by jellyfish. Genome sizes were only reported for genomes that had sufficient reads to meet 25X coverage of the genome. Furthermore, the k-mer frequency spectra for any genome with at least 25X coverage was manually inspected for an approximate Poisson distribution shape. If the spectra did not fit a Poisson distribution, the estimated genome size from genomescope2 was not reported. The computer program "agat_sp_statistics.pl" to tabulate genomic features shown in Supplementary Figure 2 (Dainat, n.d.). KAT "kat sect" with options -E and -F was used to estimate repetitive content in genome assemblies. As a second measure of nuclear genome size estimation, we performed propidium iodide flow cytometry after Bennett et al. (2003) (Bennett et al., 2003). Chopping tissue with a fresh razor blade in Galbraith buffer supplemented with agarose was used to release nuclei from fungi. *Drosophila melanogaster* (1C = 175 Mbp) was used as an external standard to anchor the estimates. After filtration through 40 um nylon the DNA in the nuclei of sample and standard were stained with 1mg/ml concentration of Propidium Iodide for 2 hours in the cold and dark, with red PI fluorescence scored using a CytoFLEX (BeckmanCoulter) flow cytometer. The 1C amount of DNA in each sample was estimated as the ratio (mean 2C red PI fluorescence of the sample/mean red PI fluorescence of the standard) times 175 Mbp.

2.5.3 Gene prediction and protein annotation

The Trinity-v2.6.5 *de novo* transcriptome (Haas et al., 2013) assembler with default parameters was used to assemble an initial transcriptome from RNA-seq data for *Escovopsis* (Bioproject:

PRJNA253870). Augustus-v3.3 (Stanke et al., 2006) was used to train and optimize initial gene models for Escovopsis based on the first genome annotation (de Man et al., 2016) and the assembled Trinity transcriptome. Repeat families were predicted for each genome using RepeatModeler-v1.0.11 (A. F. A. Smit et al., 2015; Arian F. A. Smit & Hubley, 2008). Genes were predicted for each genome using MAKER-v2.31.9 (Holt & Yandell, 2011), with EST evidence from the assembled transcriptome, proteomes for publicly available *Trichoderma* assemblies, and the SWISS-PROT (Boeckmann et al., 2003) database of curated proteins. After an initial run with MAKER, BUSCO- v4.1.1 (Manni et al., 2021; Simão et al., 2015; Waterhouse et al., 2018) was used to assess the completeness and quality of the annotation. Then, hmm-assembler.pl from SNAP (Korf, 2004) was used to retrain on high confidence genome models used as input for a second run with MAKER. This process was repeated iteratively until the annotation reached greater than or equal to 90% completeness, or the quality of the annotation as measured by BUSCO degraded. InterProScan (Jones et al., 2014) was used to annotate proteins with Pfam, TMHMM, SignalP, and GO terms. CAZymes (carbohydate active enzymes) were annotated to protein sequences using dbcan (Zhang et al., 2018). Lipases, peptidases, and virulence factors were annotated by aligning protein sequences with DIAMOND to the LED (Fischer & Pleiss, 2003), MEROPS (Rawlings et al., 2016), and DFVF (Lu et al., 2012), respectively, and taking the top hit for each protein according to bitscore. Resistance genes were annotated using the RGI software distributed by CARD (Jia et al., 2017). Subcellular locations of proteins were annotated using TargetP and WoLF PSORT

(Horton et al., 2007, 2005). Orthologous protein families were annotated with OrthoFinder (Emms & Kelly, 2019).

To annotate biosynthetic gene clusters, antiSMASH (Blin et al., 2017) was run twice using the options "--taxon fungi --full-hmmer --smcogs --subclusterblast --knownclusterblast" for both runs, in addition to the following. The first run used just the genome FASTA file as input, and the second run used the genome FASTA file, and the maker annotated gene models as an input with the "--gff3" option. BiG-SCAPE (Navarro-Muñoz et al., 2020) with the option "--include_singletons --mix --mibig" was used to find clusters of similar BGCs among genomes and clusters from the MIBiG repository (Kautsar et al., 2020).

2.5.4 Secretome Annotation

To define the secretome of each genome we annotated the presence of lipases, proteinases, carbohydrate-active enzymes, resistance genes and fungal virulence genes among the protein-coding genes for each genome. These annotated proteins were considered part of the secretome if they contain either a signal peptide as annotated with SignalP via InterProScan, one transmembrane domain as annotated with TMHMM via InterproScan, or a subcellular location outside of the cell as annotated with TargetP and WolF PSORT.

2.5.5 Phylogenetic Reconstruction

Representative RefSeq genomes of Hypocreales fungi were used to reconstruct phylogenetic relationships, along with *Saccharomyces cerevisiae*, *Candida albicans,* and *Saitoella complicata* as outgroups (Dataset S3). BUSCOv4.1.1 ran with the ascomycota_odb10 lineage database

generated single copy orthologues from each genome. The 1706 shared single copy orthologs were used as input for building the species tree. Sequences were aligned individually using MAFFT v7.475 (Katoh et al., 2002; Katoh & Standley, 2013) with default parameters, then trimmed using trimAL v1.2rev59 (Capella-Gutiérrez et al., 2009) with the '-automated1' flag. Output alignments from trimAL were used as input to IQ-TREE2 (Hoang et al., 2018; Kalyaanamoorthy et al., 2017; Minh et al., 2020) with parameters "-bb 1000 -alrt 1000" to construct individual gene trees, using ModelFinder to select the best evolutionary model for each gene (Kalyaanamoorthy et al., 2017). These alignments and evolutionary models were used to reconstruct the species tree with concatenation-based methods, whereas the individual gene trees were used to reconstruct the species tree with coalescent based methods. Methods for both approaches are as follows. The concatenation-based tree was constructed from the set of 1706 BUSCO gene alignments from MAFFT and trimAL. The alignment was partitioned by gene, using the best evolutionary model as predicted with ModelFinder. We reconstructed the tree using IQ-TREE2 (Chernomor et al., 2016; Hoang et al., 2018; Kalyaanamoorthy et al., 2017; Minh et al., 2020) with parameters "-bb 1000 -alrt 1000". The resulting tree was rooted to *Saccharomyces cerevisiae* and *Candida albicans* in FigTree (*FigTree*, n.d.). The multi-allele coalescent species tree was constructed from the 1706 gene trees which were used as input for ASTRAL v5.7.7 (Rabiee et al., 2019; Sayyari & Mirarab, 2016) with option "-t 32". Mitochondrial genome trees were reconstructed similarly to the individual gene trees using full genome alignments.

Ant phylogenomic analysis used ultraconserved elements (UCEs) markers and are based on a modified version of the alignments of Li et al. (2018) (Hongjie Li et al., 2018) and Hanisch et al. (2022) (Hanisch et al., 2022). The dataset consisted of 133 taxa (57 outgroup Myrmicinae taxa and 76 fungus-growing ant taxa), 558,222 nucleotide characters, representing 942 UCE loci. We employed the Sliding Window Site Characteristics based in Entropy (Tagliacollo & Lanfear, 2018) approach to first split the UCE loci into its three regions (a core and two flanking regions). The subsets identified by the SWSC-EN algorithm were then used as input to identify the best partitioning scheme using ModelFinder (Kalyaanamoorthy et al., 2017) as implemented in IQ-TREE multicore v2.0.6 (Minh et al., 2020). For the merging step, we used the -m MF+MERGE command, the fast relaxed -rcluster algorithm (Lanfear et al., 2016), and compared the top 10% of the resulting partition schemes using the corrected Akaike Information Criterion (AICc). The evaluated models were restricted to those implemented in RaxML by using the command -mset raxml. The best-fit partitioning scheme consisted of 853 subsets. Maximum Likelihood (ML) analysis were performed in IQ-TREE multicore v2.0.6 with ultrafast bootstrap (Hoang et al., 2018) and SH-like approximation likelihood ratio test (Guindon et al., 2010) set at 1000 replicates, with other settings set at default values.

2.5.6 Divergence Dating

We inferred divergence dates of *Escovopsis* and the fungus-growing ants using the Bayesian program MCMCTREE (Z. Yang & Rannala, 1997) implemented as part of the package PAML (Ziheng Yang, 2007) which uses the approximate-likelihood approach of (Thorne et al., 1998). For

both analyses, we input the alignments and the ML topologies generated for each dataset (see above). For *Escovopsis,* three calibrations nodes were used for phylogenetic dating analyses that were retrieved from the TimeTree database (Kumar et al., 2017) and previously published dates across the Ascomycota (Shen et al., 2020). The calibration nodes used were the origin of the Saccharomycotina (304 Mya to 590 Mya), the divergence between *Cordyceps tenuipes* (GCA_003025305.1) and *Torrubiella hemipterigena* (GCA_000825705.1) 50.2 Mya, and the *Trichoderma* root 20 Mya. The calibrations were employed as follows: (i) the root was modeled as the uniform distribution B(3.04, 5.09), i.e., of 304 Mya to 509 Mya; (ii) the most recent common ancestor (MRCA) of GCA_007896495_1 and GCA003012105_1 was modeled as the Cauchy distribution L(0.20, 0.1, 1.0, 0.025), and (iii) the MRCA of GCA_003025305_1 and GCA_000825705_1 was modeled as the Cauchy distribution L(0.502, 0.1, 1.0, 0.025). For the fungus-growing ants, we employed information available from two fossils as well as from two published studies (secondary calibrations) to calibrate our analysis. The two fossils were: (i) A *Pheidole* species from Florissant Formation (34 Ma) (Carpenter, 1930; Ward et al., 2015) used to calibrate the crown node of the genus *Pheidole* and modeled as the Cauchy distribution L(0.34, 0.05, 0.085, 1e-300) and (ii) the species *Mycetomoellerius primaevus* from Dominican Amber (15 Ma) (Baroni Urbani, 1980) used to calibrate the MRCA of *Mycetomoellerius* and *Acromyrmex* (i.e., the higher Attina), and modeled as the uniform distribution B(0.15, 0.35), i.e., of 15 Mya to 35 Mya. The two secondary calibrations were: (i) the root (or crown age of the subfamily Myrmicinae) (95% CI 110.1 Mya to 87.1 Mya, median 98.6 Mya; (Branstetter et al., 2017; Ward

et al., 2015)), modeled as the skew-normal distribution SN(0.986, 0.06, 0). (ii) The crown age of the tribe Crematogastrini (95% CI 93.704 Mya to 66.132 Mya, median 78.55 Mya; (Blaimer et al., 2018) modeled as the skew-normal distribution SN(0.7855, 0.08, 0).

MCMCTREE analyses of both *Escovopsis* and fungus-growing ants used the independent-rates clock model and the GTR+G4 substitution model. For *Escovopsis*, we conducted six independent MCMCTREE runs, each consisting of 210 million generations, and each with the following settings: sampfreq = 3,000, nsample = 70,000, and burnin = 21,000,000. For the fungus-growing ants, we conducted four independent MCMCTREE runs, each consisting of 50 million generations, and each with the following settings: sampfreq = 1,000, nsample = 50,000, and burnin = 5,000,000. We assessed run convergence and stationarity by examining the resulting mcmc.txt files in Tracer v1.7.1 (Rambaut et al., 2018) using the criterion of ESS values higher than 500. Analyses were conducted on the Smithsonian High Performance Cluster (SI/HPC), Smithsonian Institution (https://doi.org/10.25572/SIHPC).

2.5.7 Genomic Comparisons

Lists of genes were tested for GO term enrichment using topGO. Significantly enriched, defined as having a Benjamini-Hochberg adjusted p value less than or equal to 0.01 GO terms were then tested for semantic similarity using REVIGO with the options ‘similarity: Medium (0.7), numbers associated with GO terms: p-values, database with GO term sizes: whole UniProt, semantic similarity measure: SimRel’. We annotated orthologous genes with OrthoFinder (Emms & Kelly, 2019) and used these to define the presence and copy number of genes across genomes and

agriculture as visualized with UpSetR (Gehlenborg, 2019; Lex et al., 2014). Orthogroups were considered in our analysis if they were present in the pan-genome of each phylogenetic grouping, i.e., in 95% of genomes for groups with more than four representative genomes, and in all genomes for groups with four or fewer representative genomes. To characterize differences in functional genomic content, we calculated the Shannon entropy of genes for functional gene classes using the R package vegan (Oksanen et al., 2019). We made plots using ggplot2, cowplot, and pheatmap (Kolde, 2019; Suzuki et al., 2019; Wickham, 2016; Wilke, 2019) and made extensive use of the tidyverse suite of R packages for data analysis (Wickham et al., 2019). Lastly, Anvi'o interactive was used to visualize orthologous genes among genomes and the functional annotations of the orthologues (Eren et al., 2015).

2.5.8 Metabolomics

Escovopsis strains were grown on potato dextrose agar for 3 weeks. The agar plates were cut into pieces and frozen at -80° C for 6 hours. The cell material and agar were then extracted with ethyl acetate with excess anhydrous sodium sulfate to remove water overnight. The ethyl acetate was filtered and dried *in vacuo*. The cell material and agar were extracted a second time with methanol overnight and subsequently filtered and dried *in vacuo*. The two extracts were combined and analyzed by HRESI-LC-MS for the detection of small molecules. *Escovopsis* extracts were analyzed on a ThermoScientific Q-Exactive quadrupole orbitrap mass spectrometer coupled to a Dionex UPLC system. The UPLC method was 5% methanol for 0.5 minutes followed by a gradient from 5% methanol to 97% methanol over 16 minutes. 97% methanol was held for a two-

minute wash before switching back to 5% methanol over 0.5 minutes and re-equilibrating at 5% methanol for 1 minute. The flow rate was kept consistent at 0.35 mL/min. The method was run on a Phenomenex Kinetex XB-C18 column with dimensions 2.1 x 100 mm and 2.6-micron particle size. The mass spectrometer scanned from 200 to 2000 m/z in positive mode and ion fragmentation was achieved using normalized collision energy of 30, 35, and 40%. The profile data was manually inspected and filtered using MzMINE2 (Pluskal et al., 2010). Additionally, an aligned feature table and quantification table were created for feature based molecular networking using MzMINE2. Feature based molecular networking was performed through GNPS (Nothias et al., 2020; M. Wang et al., 2016) with a precursor ion mass tolerance of 0.05 Da, a fragment ion mass tolerance of 0.05 Da, a minimum cosine score of 0.7, and a minimum matched fragment ions of 6. The GNPS spectral libraries were searched for matches to submitted MS/MS spectra with a cosine score threshold of 0.7 and minimum of 6 matched peaks to the library spectra. The resulting network file was visualized and analyzed using Cytoscape v3.8.0 (Shannon et al., 2003).

2.6 Acknowledgments

We are grateful to Reed Stubbendieck and Donny Hoang for comments on the manuscript. We thank Heidi Horn, Camila Carlos, Weilan Gomes de Paixão Melo, and Quimi Vidaurre Montoya for their work on the ICBG collections. We acknowledge the Programming for Biology course at Cold Spring Harbor and the course instructors Sofia M. Robb and Simon Prochnik, as well as Eric J. Ross and Jessen V. Bredeson for bioinformatic advice. This material is based on work supported

in part by National Institutes of Health grant U19 TW009872, National Institutes of Health grant U19 AI142720, and National Science Foundation grant DEB-1927155, and São Paulo Research Foundation (FAPESP) grant # 2013/50954-0. TRS and JSC were supported by National Science Foundation award DEB 1927161. AB was supported by the German Research Foundation by Germany's Excellence Strategy - EXC2124 - 390838134, projects 09.030 and BE 6922/1-1.

2.7 Data, Materials, and Software Availability

Raw sequences associated with this paper have been deposited with links to can be found in NCBI Bioproject (accession number: PRJNA719863) in the NCBI BioProject database (https://www.ncbi.nlm.nih.gov/bioproject/), specifically, raw reads are available under the following SRA ids: SRR14176643, SRR14176642, SRR14176633, SRR14176632, SRR14176631, SRR14176630, SRR14176629, SRR14176628, SRR14176627, SRR14176626, SRR14176641, SRR14176640, SRR14176639, SRR14176638, SRR14176637, SRR14176636, SRR14176635, SRR14176634. All code is available at through GitHub (https://github.com/kirstengott/EscoEvoGenomics) and Figshare at https://doi.org/10.6084/m9.figshare.21624261, with datasets available through FigShare for antiSMASH annotation (10.6084/m9.figshare.16985137), BiG-SCAPE (10.6084/m9.figshare.16985092), anvi'o (10.6084/m9.figshare.16985119), k-mer-based genome size estimates, (10.6084/m9.figshare.16985122), and phylogenetic tree analyses (10.6084/m9.figshare.16985125).

2.8 References

Alonge, M., Soyk, S., Ramakrishnan, S., Wang, X., Goodwin, S., Sedlazeck, F. J., Lippman, Z. B., & Schatz, M. C. (2019). RaGOO: fast and accurate reference-guided scaffolding of draft genomes. *Genome Biology*, *20*(1), 224. https://doi.org/10.1186/s13059-019-1829-6

Augustin, J. O., Groenewald, J. Z., Nascimento, R. J., Mizubuti, E. S. G., Barreto, R. W., Elliot, S. L., & Evans, H. C. (2013). Yet more "weeds" in the garden: Fungal novelties from nests of leaf-cutting ants. *PloS One*, *8*(12), e82265. https://doi.org/10.1371/journal.pone.0082265

Bankevich, A., Nurk, S., Antipov, D., Gurevich, A. A., Dvorkin, M., Kulikov, A. S., Lesin, V. M., Nikolenko, S. I., Pham, S., Prjibelski, A. D., Pyshkin, A. V., Sirotkin, A. V., Vyahhi, N., Tesler, G., Alekseyev, M. A., & Pevzner, P. A. (2012). SPAdes: a new genome assembly algorithm and its applications to single-cell sequencing. *Journal of Computational Biology: A Journal of Computational Molecular Cell Biology*, *19*(5), 455–477. https://doi.org/10.1089/cmb.2012.0021

Baroni Urbani, C. (1980). First description of fossil gardening ants (Amber Collection Stuttgart and Natural History Museum Basel; Hymenoptera: Formicidae. I: Attini). *Stuttgarter Beiträge Zur Naturkunde B: Geologie Und Paläontologie.*, *54*, 1–13. https://antcat.s3.amazonaws.com/169/6326.pdf?X-Amz-Algorithm=AWS4-HMAC-SHA256&X-Amz-Credential=AKIAJJR3DGROFMVL2FBQ%2F20210825%2Fus-east-1%2Fs3%2Faws4_request&X-Amz-Date=20210825T195714Z&X-Amz-Expires=86400&X-Amz-SignedHeaders=host&X-Amz-Signature=bd3ee21371120db6641366eb215dbf7b8aa6bb9c8d3fe19b60d4f9f13cebcfbb

Bennett, M. D., Leitch, I. J., Price, H. J., & Johnston, J. S. (2003). Comparisons with *Caenorhabditis* (approximately 100 Mb) and *Drosophila* (approximately 175 Mb) using flow cytometry show genome size in Arabidopsis to be approximately 157 Mb and thus approximately 25% larger than the *Arabidopsis* genome initiative estimate of approximately 125 Mb. *Annals of Botany*, *91*(5), 547–557. https://doi.org/10.1093/aob/mcg057

Bittleston, L. S., Pierce, N. E., Ellison, A. M., & Pringle, A. (2016). Convergence in Multispecies Interactions. *Trends in Ecology & Evolution*, *31*(4), 269–280. https://doi.org/10.1016/j.tree.2016.01.006

Blackwell, M., & Vega, F. E. (2018). Lives within lives: Hidden fungal biodiversity and the importance of conservation. *Fungal Ecology*, *35*, 127–134. https://doi.org/10.1016/j.funeco.2018.05.011

Blaimer, B. B., Ward, P. S., Schultz, T. R., Fisher, B. L., & Brady, S. G. (2018). Paleotropical Diversification Dominates the Evolution of the Hyperdiverse Ant Tribe Crematogastrini (Hymenoptera: Formicidae). *Insect Systematics and Diversity*, *2*(5), 1–14. https://doi.org/10.1093/isd/ixy013

Blin, K., Wolf, T., Chevrette, M. G., Lu, X., Schwalen, C. J., Kautsar, S. A., Suarez Duran, H. G., De Los Santos, E. L. C., Kim, H. U., Nave, M., Dickschat, J. S., Mitchell, D. A., Shelest, E., Breitling, R., Takano, E., Lee, S. Y., Weber, T., & Medema, M. H. (2017). AntiSMASH 4.0 - improvements in chemistry prediction and gene cluster boundary identification. *Nucleic Acids Research*, *45*(W1), W36–W41. https://doi.org/10.1093/nar/gkx319

Boeckmann, B., Bairoch, A., Apweiler, R., Blatter, M.-C., Estreicher, A., Gasteiger, E., Martin, M. J., Michoud, K., O'Donovan, C., Phan, I., Pilbout, S., & Schneider, M. (2003). The SWISS-PROT protein knowledgebase and its supplement TrEMBL in 2003. *Nucleic Acids Research*, *31*(1), 365–370. https://doi.org/10.1093/nar/gkg095

Bot, A. N. M., Currie, C. R., Hart, A. G., & Boomsma, J. J. (2001). Waste management in leaf-cutting ants. *Ethology Ecology & Evolution*, *13*(3), 225–237. https://doi.org/10.1080/08927014.2001.9522772

Branstetter, M. G., Ješovnik, A., Sosa-Calvo, J., Lloyd, M. W., Faircloth, B. C., Brady, S. G., & Schultz, T. R. (2017). Dry habitats were crucibles of domestication in the evolution of agriculture in ants. *Proceedings of the Royal Society B: Biological Sciences*, *284*(1852), 20170095. https://doi.org/10.1098/rspb.2017.0095

Caldera, E. J., Chevrette, M. G., McDonald, B. R., & Currie, C. R. (2019). Local adaptation of bacterial symbionts within a geographic mosaic of antibiotic coevolution. *Applied and Environmental Microbiology*, *November*. https://doi.org/10.1128/aem.01580-19

Capella-Gutiérrez, S., Silla-Martínez, J. M., & Gabaldón, T. (2009). trimAl: a tool for automated alignment trimming in large-scale phylogenetic analyses. *Bioinformatics* , *25*(15), 1972–1973. https://doi.org/10.1093/bioinformatics/btp348

Carpenter, F. M. (1930). The fossil ants of North America. *Bulletin of the Museum of Comparative Zoology*, *70*, 1–66. https://www.antwiki.org/wiki/images/7/73/Carpenter_1930.pdf

Chen, S., Zhou, Y., Chen, Y., & Gu, J. (2018). fastp: an ultra-fast all-in-one FASTQ preprocessor. *Bioinformatics* , *34*(17), i884–i890. https://doi.org/10.1093/bioinformatics/bty560

Chernomor, O., von Haeseler, A., & Minh, B. Q. (2016). Terrace Aware Data Structure for Phylogenomic Inference from Supermatrices. *Systematic Biology*, *65*(6), 997–1008. https://doi.org/10.1093/sysbio/syw037

Christopher, Y., Wcislo, W. T., Martínez-Luis, S., Hughes, W. O. H., Gerardo, N. M., & Fernández-Marín, H. (2021). Disease management in two sympatric Apterostigma fungus-growing ants for controlling the parasitic fungus Escovopsis. *Ecology and Evolution*, *ece3.7379*. https://doi.org/10.1002/ece3.7379

Clay, K., & Holah, J. (1999). Fungal endophyte symbiosis and plant diversity in successional fields. *Science*, *285*(5434), 1742–1745. https://doi.org/10.1126/science.285.5434.1742

Currie, C. R. (2001). A Community of Ants, Fungi, and Bacteria: A Multilateral Approach to Studying Symbiosis. *Annual Review of Microbiology*, *55*(1), 357–380. https://doi.org/10.1146/annurev.micro.55.1.357

Currie, C. R., Mueller, U. G., & Malloch, D. (1999). The agricultural pathology of ant fungus gardens. *Proceedings of the National Academy of Sciences of the United States of America*, *96*(14), 7998–8002. https://doi.org/10.1073/pnas.96.14.7998

Currie, C. R., Scottt, J. A., Summerbell, R. C., & Malloch, D. (1999). Fungus-growing ants use antibiotic-producing bacteria to control garden parasites. *Nature*, *398*(6729), 701–704. https://doi.org/10.1038/19519

Currie, C. R., & Stuart, A. E. (2001). Weeding and grooming of pathogens in agriculture by ants. *Proceedings of the Royal Society B: Biological Sciences*, *268*(1471), 1033–1039. https://doi.org/10.1098/rspb.2001.1605

Currie, C. R., Wong, B., Stuart, A. E., Schultz, T. R., Rehner, S. A., Mueller, U. G., Sung, G. H., Spatafora, J. W., & Straus, N. A. (2003). Ancient tripartite coevolution in the attine ant-microbe symbiosis. *Science*, *299*(5605), 386–388. https://doi.org/10.1126/science.1078155

Dainat, J. (n.d.). *Another Gff Analysis Toolkit to handle annotation in any GTF/GFF format* (Version v0.2.3) [Computer software]. https://www.doi.org/10.5281/zenodo.3552717

de Man, T. J. B., Stajich, J. E., Kubicek, C. P., Teiling, C., Chenthamara, K., Atanasova, L., Druzhinina, I. S., Levenkova, N., Birnbaum, S. S. L. L., Barribeau, S. M., Bozick, B. A., Suen, G., Currie, C. R., Gerardo, N. M., De Mana, T. J. B., Stajich, J. E., Kubicek, C. P., Teiling, C., Chenthamara, K., … Gerardo, N. M. (2016). Small genome of the fungus Escovopsis weberi, a specialized disease agent of ant agriculture. *Proceedings of the National Academy of Sciences of the United States of America*, *113*(13), 3567–3572. https://doi.org/10.1073/pnas.1518501113

Developers, P. (2018). *Pysam: a python module for reading and manipulating files in the sam/bam format*.

Dhodary, B., Schilg, M., Wirth, R., & Spiteller, D. (2018). Secondary Metabolites from *Escovopsis weberi* and Their Role in Attacking the Garden Fungus of Leaf-Cutting Ants. *Chemistry - A European Journal*, *24*(17), 4445–4452. https://doi.org/10.1002/chem.201706071

Dierckxsens, N., Mardulyn, P., & Smits, G. (2017). NOVOPlasty: de novo assembly of organelle genomes from whole genome data. *Nucleic Acids Research*, *45*(4), e18. https://doi.org/10.1093/nar/gkw955

Emms, D. M., & Kelly, S. (2019). OrthoFinder: phylogenetic orthology inference for comparative genomics. *Genome Biology*, *20*(1), 238. https://doi.org/10.1186/s13059-019-1832-y

Eren, A. M., Esen, Ö. C., Quince, C., Vineis, J. H., Morrison, H. G., Sogin, M. L., & Delmont, T. O. (2015). Anvi'o: an advanced analysis and visualization platform for 'omics data. *PeerJ*, *3*, e1319. https://doi.org/10.7717/peerj.1319

FigTree. (n.d.). Retrieved August 25, 2021, from http://tree.bio.ed.ac.uk/software/figtree/

Fischer, M., & Pleiss, J. (2003). The Lipase Engineering Database: a navigation and analysis tool for protein families. *Nucleic Acids Research*, *31*(1), 319–321. https://doi.org/10.1093/nar/gkg015

Gan, T., Luo, T., Pang, K., Zhou, C., Zhou, G., Wan, B., Li, G., Yi, Q., Czaja, A. D., & Xiao, S. (2021). Cryptic terrestrial fungus-like fossils of the early Ediacaran Period. *Nature Communications*, *12*(1), 641. https://doi.org/10.1038/s41467-021-20975-1

Gehlenborg, N. (2019). *UpSetR: A More Scalable Alternative to Venn and Euler Diagrams for Visualizing Intersecting Sets* (1.4.0) [Computer software]. https://CRAN.R-project.org/package=UpSetR

Guindon, S., Dufayard, J.-F., Lefort, V., Anisimova, M., Hordijk, W., & Gascuel, O. (2010). New algorithms and methods to estimate maximum-likelihood phylogenies: assessing the performance of PhyML 3.0. *Systematic Biology*, *59*(3), 307–321. https://doi.org/10.1093/sysbio/syq010

Haas, B. J., Papanicolaou, A., Yassour, M., Grabherr, M., Blood, P. D., Bowden, J., Couger, M. B., Eccles, D., Li, B., Lieber, M., MacManes, M. D., Ott, M., Orvis, J., Pochet, N., Strozzi, F., Weeks, N., Westerman, R., William, T., Dewey, C. N., … Regev, A. (2013). De novo transcript sequence reconstruction from RNA-seq using the Trinity platform for reference generation and analysis. *Nature Protocols*, *8*(8), 1494–1512. https://doi.org/10.1038/nprot.2013.084

Hanisch, P. E., Sosa-Calvo, J., & Schultz, T. R. (2022). The Last Piece of the Puzzle? Phylogenetic Position and Natural History of the Monotypic Fungus-Farming Ant Genus *Paramycetophylax* (Formicidae: Attini). *Insect Systematics and Diversity*, *6*(1). https://doi.org/10.1093/isd/ixab029

Heger, A., Belgrad, T. G., Goodson, M., & Jacobs, K. (2014). pysam: Python interface for the SAM. *BAM Sequence Alignment and Mapping Format*.

Heine, D., Holmes, N. A., Worsley, S. F., Santos, A. C. A., Innocent, T. M., Scherlach, K., Patrick, E. H., Yu, D. W., Colin Murrell, J., Vieria, P. C., Boomsma, J. J., Hertweck, C., Hutchings, M. I., & Wilkinson, B. (2018). Chemical warfare between leafcutter ant symbionts and a co-evolved pathogen. *Nature Communications*, *9*(1), 1–11. https://doi.org/10.1038/s41467-018-04520-1

Hoang, D. T., Chernomor, O., von Haeseler, A., Minh, B. Q., & Vinh, L. S. (2018). UFBoot2: Improving the Ultrafast Bootstrap Approximation. *Molecular Biology and Evolution*, *35*(2), 518–522. https://doi.org/10.1093/molbev/msx281

Hoeksema, J. D., Bever, J. D., Chakraborty, S., Chaudhary, V. B., Gardes, M., Gehring, C. A., Hart, M. M., Housworth, E. A., Kaonongbua, W., Klironomos, J. N., Lajeunesse, M. J., Meadow, J., Milligan, B. G., Piculell, B. J., Pringle, A., Rúa, M. A., Umbanhowar, J., Viechtbauer, W., Wang, Y.-W., … Zee, P. C. (2018). Evolutionary history of plant hosts and fungal symbionts predicts the strength of mycorrhizal mutualism. *Communications Biology*, *1*, 116. https://doi.org/10.1038/s42003-018-0120-9

Holt, C., & Yandell, M. (2011). MAKER2: an annotation pipeline and genome-database management tool for second-generation genome projects. *BMC Bioinformatics*, *12*(1), 1–14. https://doi.org/10.1186/1471-2105-12-491

Horton, P., Park, K.-J., Obayashi, T., Fujita, N., Harada, H., Adams-Collier, C. J., & Nakai, K. (2007). WoLF PSORT: protein localization predictor. *Nucleic Acids Research*, *35*(Web Server issue), W585-7. https://doi.org/10.1093/nar/gkm259

Horton, P., Park, K.-J., Obayashi, T., & Nakai, K. (2005). PROTEIN SUBCELLULAR LOCALIZATION PREDICTION WITH WOLF PSORT. In *Proceedings of the 4th Asia-Pacific Bioinformatics Conference* (Vol. 3, pp. 39–48). PUBLISHED BY IMPERIAL COLLEGE PRESS AND DISTRIBUTED BY WORLD SCIENTIFIC PUBLISHING CO. https://doi.org/10.1142/9781860947292_0007

Jia, B., Raphenya, A. R., Alcock, B., Waglechner, N., Guo, P., Tsang, K. K., Lago, B. A., Dave, B. M., Pereira, S., Sharma, A. N., Doshi, S., Courtot, M., Lo, R., Williams, L. E., Frye, J. G., Elsayegh, T., Sardar, D., Westman, E. L., Pawlowski, A. C., … McArthur, A. G. (2017). CARD 2017: Expansion and model-centric curation of the comprehensive antibiotic resistance database. *Nucleic Acids Research*, *45*(D1), D566–D573. https://doi.org/10.1093/nar/gkw1004

Jones, P., Binns, D., Chang, H.-Y., Fraser, M., Li, W., McAnulla, C., McWilliam, H., Maslen, J., Mitchell, A., Nuka, G., Pesseat, S., Quinn, A. F., Sangrador-Vegas, A., Scheremetjew, M., Yong, S.-Y., Lopez, R., & Hunter, S. (2014). InterProScan 5: genome-scale protein function classification. *Bioinformatics* , *30*(9), 1236–1240. https://doi.org/10.1093/bioinformatics/btu031

Kalyaanamoorthy, S., Minh, B. Q., Wong, T. K. F., von Haeseler, A., & Jermiin, L. S. (2017). ModelFinder: fast model selection for accurate phylogenetic estimates. *Nature Methods*, *14*(6), 587–589. https://doi.org/10.1038/nmeth.4285

Katoh, K., Misawa, K., Kuma, K.-I., & Miyata, T. (2002). MAFFT: a novel method for rapid multiple sequence alignment based on fast Fourier transform. *Nucleic Acids Research*, *30*(14), 3059–3066. https://doi.org/10.1093/nar/gkf436

Katoh, K., & Standley, D. M. (2013). MAFFT multiple sequence alignment software version 7: improvements in performance and usability. *Molecular Biology and Evolution*, *30*(4), 772–780. https://doi.org/10.1093/molbev/mst010

Kautsar, S. A., Blin, K., Shaw, S., Navarro-Muñoz, J. C., Terlouw, B. R., van der Hooft, J. J. J., van Santen, J. A., Tracanna, V., Suarez Duran, H. G., Pascal Andreu, V., Selem-Mojica, N., Alanjary, M., Robinson, S. L., Lund, G., Epstein, S. C., Sisto, A. C., Charkoudian, L. K., Collemare, J., Linington, R. G., … Medema, M. H. (2020). MIBiG 2.0: a repository for biosynthetic gene clusters of known function. *Nucleic Acids Research*, *48*(D1), D454–D458. https://doi.org/10.1093/nar/gkz882

Keller, N. P. (2015). Translating biosynthetic gene clusters into fungal armor and weaponry. *Nature Chemical Biology*, *11*(9), 671–677. https://doi.org/10.1038/nchembio.1897

Kohler, A., Kuo, A., Nagy, L. G., Morin, E., Barry, K. W., Buscot, F., Canbäck, B., Choi, C., Cichocki, N., Clum, A., Colpaert, J., Copeland, A., Costa, M. D., Doré, J., Floudas, D., Gay, G., Girlanda, M., Henrissat, B., Herrmann, S., … Martin, F. (2015). Convergent losses of decay mechanisms and rapid turnover of symbiosis genes in mycorrhizal mutualists. *Nature Genetics*, *47*(4), 410–415. https://doi.org/10.1038/ng.3223

Kolde, R. (2019). *pheatmap: Pretty Heatmaps*. https://CRAN.R-project.org/package=pheatmap

Korf, I. (2004). Gene finding in novel genomes. *BMC Bioinformatics*, *5*, 59. https://doi.org/10.1186/1471-2105-5-59

Kumar, S., Stecher, G., Suleski, M., & Hedges, S. B. (2017). TimeTree: A Resource for Timelines, Timetrees, and Divergence Times. *Molecular Biology and Evolution*, *34*(7), 1812–1819. https://doi.org/10.1093/molbev/msx116

Lanfear, R., Frandsen, P. B., Wright, A. M., Senfeld, T., & Calcott, B. (2016). PartitionFinder 2: New Methods for Selecting Partitioned Models of Evolution for Molecular and Morphological Phylogenetic Analyses. *Molecular Biology and Evolution*, *34*(3), 772–773. https://doi.org/10.1093/molbev/msw260

Leal-Dutra, C. A., Grifith, G. W., Neves, M. A., McLaughlin, D. J., Mclaughlin, E. G., Clasen, L. A., & Dentinger, B. T. M. (2020). Reclassification of Pterulaceae Corner (Basidiomycota: Agaricales) introducing the ant-associated genus *Myrmecopterula* gen. nov., *Phaeopterula* Henn. and the corticioid Radulomycetaceae fam. nov. *IMA Fungus*, *11*(2). https://doi.org/10.1186/s43008-019-0022-6

Lex, A., Gehlenborg, N., Strobelt, H., Vuillemot, R., & Pfister, H. (2014). UpSet: Visualization of Intersecting Sets. *IEEE Transactions on Visualization and Computer Graphics*, *20*(12), 1983–1992. https://doi.org/10.1109/TVCG.2014.2346248

Li, H., & Durbin, R. (2009). Fast and accurate short read alignment with Burrows-Wheeler transform. *Bioinformatics* , *25*(14), 1754–1760. https://doi.org/10.1093/bioinformatics/btp324

Li, Hongjie, Sosa-Calvo, J., Horn, H. A., Pupo, M. T., Clardy, J., Rabeling, C., Schultz, T. R., & Currie, C. R. (2018). Convergent evolution of complex structures for ant-bacterial defensive symbiosis in fungus-farming ants. *Proceedings of the National Academy of Sciences of the United States of America*, *115*(42), 10720–10725. https://doi.org/10.1073/pnas.1809332115

Liu, Y., Schröder, J., & Schmidt, B. (2013). Musket: A multistage k-mer spectrum-based error corrector for Illumina sequence data. *Bioinformatics* , *29*(3), 308–315. https://doi.org/10.1093/bioinformatics/bts690

Lu, T., Yao, B., & Zhang, C. (2012). DFVF: database of fungal virulence factors. *Database*, *2012*(0), bas032–bas032. https://doi.org/10.1093/database/bas032

Lutzoni, F., Nowak, M. D., Alfaro, M. E., Reeb, V., Miadlikowska, J., Krug, M., Arnold, A. E., Lewis, L. A., Swofford, D. L., Hibbett, D., Hilu, K., James, T. Y., Quandt, D., & Magallón, S. (2018). Contemporaneous radiations of fungi and plants linked to symbiosis. *Nature Communications*, *9*(1), 5451. https://doi.org/10.1038/s41467-018-07849-9

Magoč, T., & Salzberg, S. L. (2011). FLASH: Fast length adjustment of short reads to improve genome assemblies. *Bioinformatics* , *27*(21), 2957–2963. https://doi.org/10.1093/bioinformatics/btr507

Manni, M., Berkeley, M. R., Seppey, M., Simão, F. A., & Zdobnov, E. M. (2021). BUSCO update: Novel and streamlined workflows along with broader and deeper phylogenetic coverage for scoring of eukaryotic, prokaryotic, and viral genomes. *Molecular Biology and Evolution*, *38*(10), 4647–4654. https://doi.org/10.1093/molbev/msab199

Mapleson, D., Garcia Accinelli, G., Kettleborough, G., Wright, J., & Clavijo, B. J. (2017). KAT: a K-mer analysis toolkit to quality control NGS datasets and genome assemblies. *Bioinformatics* , *33*(4), 574–576. https://doi.org/10.1093/bioinformatics/btw663

Marcais, G., & Kingsford, C. (2012). *Jellyfish: A fast k-mer counter*. https://eagle.fish.washington.edu/whale/fish546/Trinity_r2013-08-14_analysis1-2014-02-08-20-44-13.233/bin/trinityrnaseq_r2013_08_14/trinity-plugins/jellyfish/doc/jellyfish.pdf

Masiulionis, V. E., Cabello, M. N., Seifert, K. A., Rodrigues, A., & Pagnocca, F. C. (2015). *Escovopsis trichodermoides* sp. nov., isolated from a nest of the lower attine ant *Mycocepurus goeldii*. *Antonie van Leeuwenhoek, International Journal of General and Molecular Microbiology*, *107*(3), 731–740. https://doi.org/10.1007/s10482-014-0367-1

Meirelles, L. A., Montoya, Q. V., Solomon, S. E., & Rodrigues, A. (2015). New light on the systematics of fungi associated with attine ant gardens and the description of *Escovopsis kreiselii* sp. nov. *PloS One*, *10*(1), e0112067. https://doi.org/10.1371/journal.pone.0112067

Minh, B. Q., Schmidt, H. A., Chernomor, O., Schrempf, D., Woodhams, M. D., von Haeseler, A., & Lanfear, R. (2020). IQ-TREE 2: New Models and Efficient Methods for Phylogenetic Inference in the Genomic Era. *Molecular Biology and Evolution*, *37*(5), 1530–1534. https://doi.org/10.1093/molbev/msaa015

Montoya, Q. V., Martiarena, M. J. S., Bizarria, R., Jr, Gerardo, N. M., & Rodrigues, A. (2021). Fungi inhabiting attine ant colonies: reassessment of the genus *Escovopsis* and description of *Luteomyces* and *Sympodiorosea* gens. nov. *IMA Fungus*, *12*(1), 1–18. https://doi.org/10.1186/s43008-021-00078-8

Montoya, Q. V., Sutta Martiarena, M. J., Polezel, D. A., Kakazu, S., & Rodrigues, A. (2019). More pieces to a huge puzzle: Two new *Escovopsis* species from fungus gardens of attine ants. *MycoKeys*, *46*, 97–118. https://doi.org/10.3897/mycokeys.46.30951

Muchovej, J., & Della Lucia, T. (1990). *Escovopsis*, a new genus from leaf cutting ant nests to replace *Phialocladus* nomen invalidum. *Mycotaxon*, *37*, 191–195.

Navarro-Muñoz, J. C., Selem-Mojica, N., Mullowney, M. W., Kautsar, S. A., Tryon, J. H., Parkinson, E. I., De Los Santos, E. L. C., Yeong, M., Cruz-Morales, P., Abubucker, S., Roeters, A., Lokhorst, W., Fernandez-Guerra, A., Cappelini, L. T. D., Goering, A. W., Thomson, R. J., Metcalf, W. W., Kelleher, N. L., Barona-Gomez, F., & Medema, M. H. (2020). A computational framework to explore large-scale biosynthetic diversity. *Nature Chemical Biology*, *16*(1), 60–68. https://doi.org/10.1038/s41589-019-0400-9

Nelsen, M. P., Lücking, R., Kevin Boyce, C., Thorsten Lumbsch, H., & Ree, R. H. (2020). The macroevolutionary dynamics of symbiotic and phenotypic diversification in lichens. *Proceedings of the National Academy of Sciences*. https://doi.org/10.1073/pnas.2001913117

Noda-Garcia, L., & Tawfik, D. S. (2020). Enzyme evolution in natural products biosynthesis: target- or diversity-oriented? *Current Opinion in Chemical Biology*, *59*, 147–154. https://doi.org/10.1016/j.cbpa.2020.05.011

Nothias, L.-F., Petras, D., Schmid, R., Dührkop, K., Rainer, J., Sarvepalli, A., Protsyuk, I., Ernst, M., Tsugawa, H., Fleischauer, M., Aicheler, F., Aksenov, A. A., Alka, O., Allard, P.-M., Barsch, A., Cachet, X., Caraballo-Rodriguez, A. M., Da Silva, R. R., Dang, T., … Dorrestein, P. C. (2020). Feature-based molecular networking in the GNPS analysis environment. *Nature Methods*, *17*(9), 905–908. https://doi.org/10.1038/s41592-020-0933-6

Oh, D. C., Poulsen, M., Currie, C. R., & Clardy, J. (2009). Dentigerumycin: A bacterial mediator of an ant-fungus symbiosis. *Nature Chemical Biology*, *5*(6), 391–393. https://doi.org/10.1038/nchembio.159

Ohm, R. A., Feau, N., Henrissat, B., Schoch, C. L., Horwitz, B. A., Barry, K. W., Condon, B. J., Copeland, A. C., Dhillon, B., Glaser, F., Hesse, C. N., Kosti, I., LaButti, K., Lindquist, E. A., Lucas, S., Salamov, A. A., Bradshaw, R. E.,

Ciuffetti, L., Hamelin, R. C., … Grigoriev, I. V. (2012). Diverse Lifestyles and Strategies of Plant Pathogenesis Encoded in the Genomes of Eighteen Dothideomycetes Fungi. *PLoS Pathogens*, *8*(12), e1003037. https://doi.org/10.1371/journal.ppat.1003037

Oksanen, J., Blanchet, F. G., Friendly, M., Kindt, R., Legendre, P., McGlinn, D., Minchin, P. R., O'Hara, R. B., Simpson, G. L., Solymos, P., Stevens, M. H. H., Szoecs, E., & Wagner, H. (2019). *vegan: Community Ecology Package*. https://CRAN.R-project.org/package=vegan

Pluskal, T., Castillo, S., Villar-Briones, A., & Oresic, M. (2010). MZmine 2: modular framework for processing, visualizing, and analyzing mass spectrometry-based molecular profile data. *BMC Bioinformatics*, *11*, 395. https://doi.org/10.1186/1471-2105-11-395

Rabiee, M., Sayyari, E., & Mirarab, S. (2019). Multi-allele species reconstruction using ASTRAL. *Molecular Phylogenetics and Evolution*, *130*, 286–296. https://doi.org/10.1016/j.ympev.2018.10.033

Rambaut, A., Drummond, A. J., Xie, D., Baele, G., & Suchard, M. A. (2018). Posterior Summarization in Bayesian Phylogenetics Using Tracer 1.7. *Systematic Biology*, *67*(5), 901–904. https://doi.org/10.1093/sysbio/syy032

Ranallo-Benavidez, T. R., Jaron, K. S., & Schatz, M. C. (2020). GenomeScope 2.0 and Smudgeplot for reference-free profiling of polyploid genomes. *Nature Communications*, *11*(1), 1432. https://doi.org/10.1038/s41467-020-14998-3

Rawlings, N. D., Barrett, A. J., & Finn, R. (2016). Twenty years of the MEROPS database of proteolytic enzymes, their substrates and inhibitors. *Nucleic Acids Research*, *44*(D1), D343-50. https://doi.org/10.1093/nar/gkv1118

Reynolds, H. T., & Currie, C. R. (2004). Pathogenicity of Escovopsis weberi: The parasite of the attine ant-microbe symbiosis directly consumes the ant-cultivated fungus. *Mycologia*, *96*(5), 955–959. https://doi.org/10.1080/15572536.2005.11832895

Riley, R., Salamov, A. A., Brown, D. W., Nagy, L. G., Floudas, D., Held, B. W., Levasseur, A., Lombard, V., Morin, E., Otillar, R., Lindquist, E. A., Sun, H., LaButti, K. M., Schmutz, J., Jabbour, D., Luo, H., Baker, S. E., Pisabarro, A. G., Walton, J. D., … Grigoriev, I. V. (2014). Extensive sampling of basidiomycete genomes demonstrates inadequacy of the white-rot/brown-rot paradigm for wood decay fungi. *Proceedings of the National Academy of Sciences of the United States of America*, *111*(27), 9923–9928. https://doi.org/10.1073/pnas.1400592111

Robey, M. T., Caesar, L. K., Drott, M. T., Keller, N. P., & Kelleher, N. L. (2021). An interpreted atlas of biosynthetic gene clusters from 1,000 fungal genomes. *Proceedings of the National Academy of Sciences of the United States of America*, *118*(19). https://doi.org/10.1073/pnas.2020230118

Sayyari, E., & Mirarab, S. (2016). Fast Coalescent-Based Computation of Local Branch Support from Quartet Frequencies. *Molecular Biology and Evolution*, *33*(7), 1654–1668. https://doi.org/10.1093/molbev/msw079

Schultz, T. R., & Brady, S. G. (2008). Major evolutionary transitions in ant agriculture. *Proceedings of the National Academy of Sciences of the United States of America*, *105*(14), 5435–5440. https://doi.org/10.1073/pnas.0711024105

Schultz, T. R., Sosa-Calvo, J., Brady, S. G., Lopes, C. T., Mueller, U. G., Bacci, M., & Vasconcelos, H. L. (2015). The most relictual fungus-farming ant species cultivates the most recently evolved and highly domesticated fungal symbiont species. *The American Naturalist*, *185*(5), 693–703. https://doi.org/10.1086/680501

Seifert, K. A., Samson, R. A., & Chapela, I. H. (1995). *Escovopsis aspergilloides*, a Rediscovered Hyphomycete from Leaf-Cutting Ant Nests. *Mycologia*, *87*(3), 407. https://doi.org/10.2307/3760838

Shannon, P., Markiel, A., Ozier, O., Baliga, N. S., Wang, J. T., Ramage, D., Amin, N., Schwikowski, B., & Ideker, T. (2003). Cytoscape: a software environment for integrated models of biomolecular interaction networks. *Genome Research*, *13*(11), 2498–2504. https://doi.org/10.1101/gr.1239303

Shen, X.-X., Steenwyk, J. L., LaBella, A. L., Opulente, D. A., Zhou, X., Kominek, J., Li, Y., Groenewald, M., Hittinger, C. T., & Rokas, A. (2020). Genome-scale phylogeny and contrasting modes of genome evolution in the fungal phylum Ascomycota. In *bioRxiv* (p. 2020.05.11.088658). https://doi.org/10.1101/2020.05.11.088658

Simão, F. A., Waterhouse, R. M., Ioannidis, P., Kriventseva, E. V., & Zdobnov, E. M. (2015). BUSCO: Assessing genome assembly and annotation completeness with single-copy orthologs. *Bioinformatics* , *31*(19), 3210–3212. https://doi.org/10.1093/bioinformatics/btv351

Smit, A. F. A., Hubley, R., & Green, P. (2015). RepeatModeler Open-1.0. 2008--2015. *Seattle, USA: Institute for Systems Biology. Available from: Httpwww. Repeatmasker. Org, Last Accessed May*, *1*, 2018.

Smit, Arian F. A., & Hubley, R. (2008). RepeatModeler Open-1.0. *Available Fom Http://Www. Repeatmasker. Org*.

Stahl, E. A., & Bishop, J. G. (2000). Plant-pathogen arms races at the molecular level. *Current Opinion in Plant Biology*, *3*(4), 299–304. https://doi.org/10.1016/s1369-5266(00)00083-2

Stajich, J. E. (2017). Fungal Genomes and Insights into the Evolution of the Kingdom. *Microbiology Spectrum*, *5*(4), 1–25. https://doi.org/10.1002/cncr.27633.Percutaneous

Stanke, M., Tzvetkova, A., & Morgenstern, B. (2006). AUGUSTUS at EGASP: using EST, protein and genomic alignments for improved gene prediction in the human genome. *Genome Biology*, *7 Suppl 1*, S11.1-8. https://doi.org/10.1186/gb-2006-7-s1-s11

Steffan, S. A., Chikaraishi, Y., Currie, C. R., Horn, H., Gaines-Day, H. R., Pauli, J. N., Zalapa, J. E., & Ohkouchi, N. (2015). Microbes are trophic analogs of animals. *Proceedings of the National Academy of Sciences of the United States of America*, *112*(49), 15119–15124. https://doi.org/10.1073/pnas.1508782112

Suzuki, R., Terada, Y., & Shimodaira, H. (2019). *pvclust: Hierarchical Clustering with P-Values via Multiscale Bootstrap Resampling*. https://CRAN.R-project.org/package=pvclust

Tagliacollo, V. A., & Lanfear, R. (2018). Estimating Improved Partitioning Schemes for Ultraconserved Elements. *Molecular Biology and Evolution*, *35*(7), 1798–1811. https://doi.org/10.1093/molbev/msy069

Taylor, J. W., & Berbee, M. L. (2006). Dating divergences in the Fungal Tree of Life: review and new analyses. *Mycologia*, *98*(6), 838–849. https://doi.org/10.3852/mycologia.98.6.838

Thorne, J. L., Kishino, H., & Painter, I. S. (1998). Estimating the rate of evolution of the rate of molecular evolution. *Molecular Biology and Evolution*, *15*(12), 1647–1657. https://doi.org/10.1093/oxfordjournals.molbev.a025892

Van Arnam, E. B., Ruzzini, A. C., Sit, C. S., Horn, H., Pinto-Tomás, A. A., Currie, C. R., Clardy, J., Van Arnam, E. B., Ruzzini, A. C., Sit, C. S., Horn, H., Pinto-Tomás, A. A., Currie, C. R., & Clardy, J. (2016). Selvamicin, an atypical antifungal polyene from two alternative genomic contexts. *Proceedings of the National Academy of Sciences of the United States of America*, *113*(46), 12940–12945. https://doi.org/10.1073/pnas.1613285113

van der Heijden, M. G. A., Bruin, S. de, Luckerhoff, L., van Logtestijn, R. S. P., & Schlaeppi, K. (2016). A widespread plant-fungal-bacterial symbiosis promotes plant biodiversity, plant nutrition and seedling recruitment. *The ISME Journal*, *10*(2), 389–399. https://doi.org/10.1038/ismej.2015.120

Vurture, G. W., Sedlazeck, F. J., Nattestad, M., Underwood, C. J., Fang, H., Gurtowski, J., & Schatz, M. C. (2017). GenomeScope: fast reference-free genome profiling from short reads. *Bioinformatics* , *33*(14), 2202–2204. https://doi.org/10.1093/bioinformatics/btx153

Wang, D. Y., Kumar, S., & Hedges, S. B. (1999). Divergence time estimates for the early history of animal phyla and the origin of plants, animals and fungi. *Proceedings. Biological Sciences / The Royal Society*, *266*(1415), 163–171. https://doi.org/10.1098/rspb.1999.0617

Wang, M., Carver, J. J., Phelan, V. V., Sanchez, L. M., Garg, N., Peng, Y., Nguyen, D. D., Watrous, J., Kapono, C. A., Luzzatto-Knaan, T., Porto, C., Bouslimani, A., Melnik, A. V., Meehan, M. J., Liu, W.-T., Crüsemann, M., Boudreau, P. D., Esquenazi, E., Sandoval-Calderón, M., … Bandeira, N. (2016). Sharing and community curation of mass spectrometry data with Global Natural Products Social Molecular Networking. *Nature Biotechnology*, *34*(8), 828–837. https://doi.org/10.1038/nbt.3597

Ward, P. S., Brady, S. G., Fisher, B. L., & Schultz, T. R. (2015). The evolution of myrmicine ants: phylogeny and biogeography of a hyperdiverse ant clade (Hymenoptera: Formicidae). *Systematic Entomology*, *40*(1), 61–81. https://doi.org/10.1111/syen.12090

Waterhouse, R. M., Seppey, M., Simao, F. A., Manni, M., Ioannidis, P., Klioutchnikov, G., Kriventseva, E. V., & Zdobnov, E. M. (2018). BUSCO applications from quality assessments to gene prediction and phylogenomics. *Molecular Biology and Evolution*, *35*(3), 543–548. https://doi.org/10.1093/molbev/msx319

Wickham, H. (2016). *ggplot2: Elegant Graphics for Data Analysis*. Springer-Verlag New York. https://ggplot2.tidyverse.org

Wickham, H., Averick, M., Bryan, J., Chang, W., McGowan, L. D., François, R., Grolemund, G., Hayes, A., Henry, L., Hester, J., Kuhn, M., Pedersen, T. L., Miller, E., Bache, S. M., Müller, K., Ooms, J., Robinson, D., Seidel, D. P., Spinu, V., … Yutani, H. (2019). Welcome to the tidyverse. In *Journal of Open Source Software* (Vol. 4, Issue 43, p. 1686). https://doi.org/10.21105/joss.01686

Wilke, C. O. (2019). *cowplot: Streamlined Plot Theme and Plot Annotations for "ggplot2."* https://CRAN.R-project.org/package=cowplot

Wolfe, B. E., Tulloss, R. E., & Pringle, A. (2012). The irreversible loss of a decomposition pathway marks the single origin of an ectomycorrhizal symbiosis. *PloS One*, *7*(7), e39597. https://doi.org/10.1371/journal.pone.0039597

Yang, Z., & Rannala, B. (1997). Bayesian phylogenetic inference using DNA sequences: a Markov Chain Monte Carlo Method. *Molecular Biology and Evolution*, *14*(7), 717–724. https://doi.org/10.1093/oxfordjournals.molbev.a025811

Yang, Ziheng. (2007). PAML 4: Phylogenetic analysis by maximum likelihood. *Molecular Biology and Evolution*, *24*(8), 1586–1591. https://doi.org/10.1093/molbev/msm088

Zhang, H., Yohe, T., Huang, L., Entwistle, S., Wu, P., Yang, Z., Busk, P. K., Xu, Y., & Yin, Y. (2018). dbCAN2: a meta server for automated carbohydrate-active enzyme annotation. *Nucleic Acids Research*, *46*(W1), W95–W101. https://doi.org/10.1093/nar/gky418

2.9 Figures

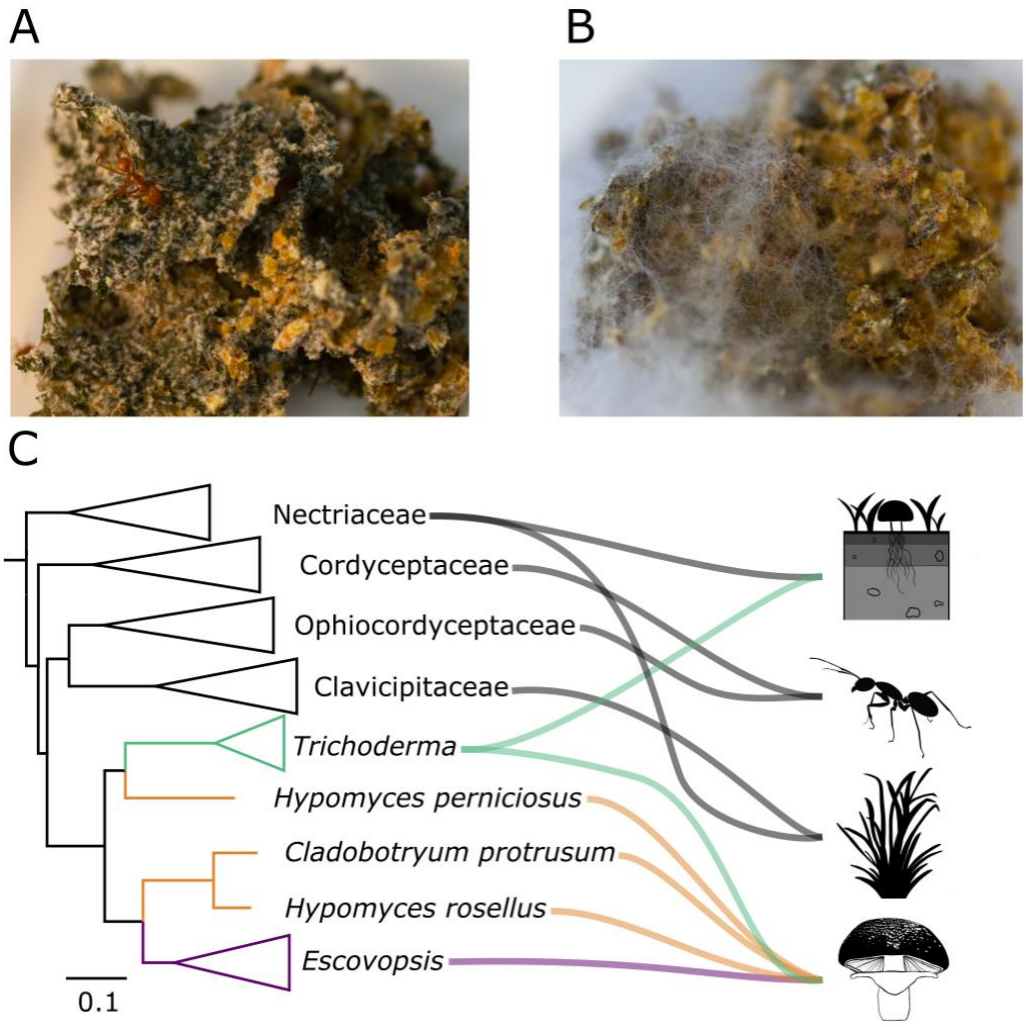

Figure 1. *Escovopsis* parasites are descended from parasites of mushroom-forming fungi. A. *Atta* fungus-growing ant with basidiomycete (Agaricales: Agaricaceae) fungus garden. Photo credit: Caitlin Carlson. B. Fungus Garden overgrown by *Escovopsis* parasite after experimental inoculation. Photo credit: Caitlin Carlson. C. The phylogenetic placement of *Escovopsis* within hypocrealean fungi and rooted to *Saccharomyces cerevisiae*. Common host associations are indicated by the lines connected to the illustrations; in order from top to bottom: free-living, insects, plants, and mushroom-forming fungi. The colors indicate groupings of fungi used in this paper: green – *Trichoderma*, orange – *Hypomyces* and *Cladobotryum*, purple – *Escovopsis*. Illustrations by Kirsten Gotting

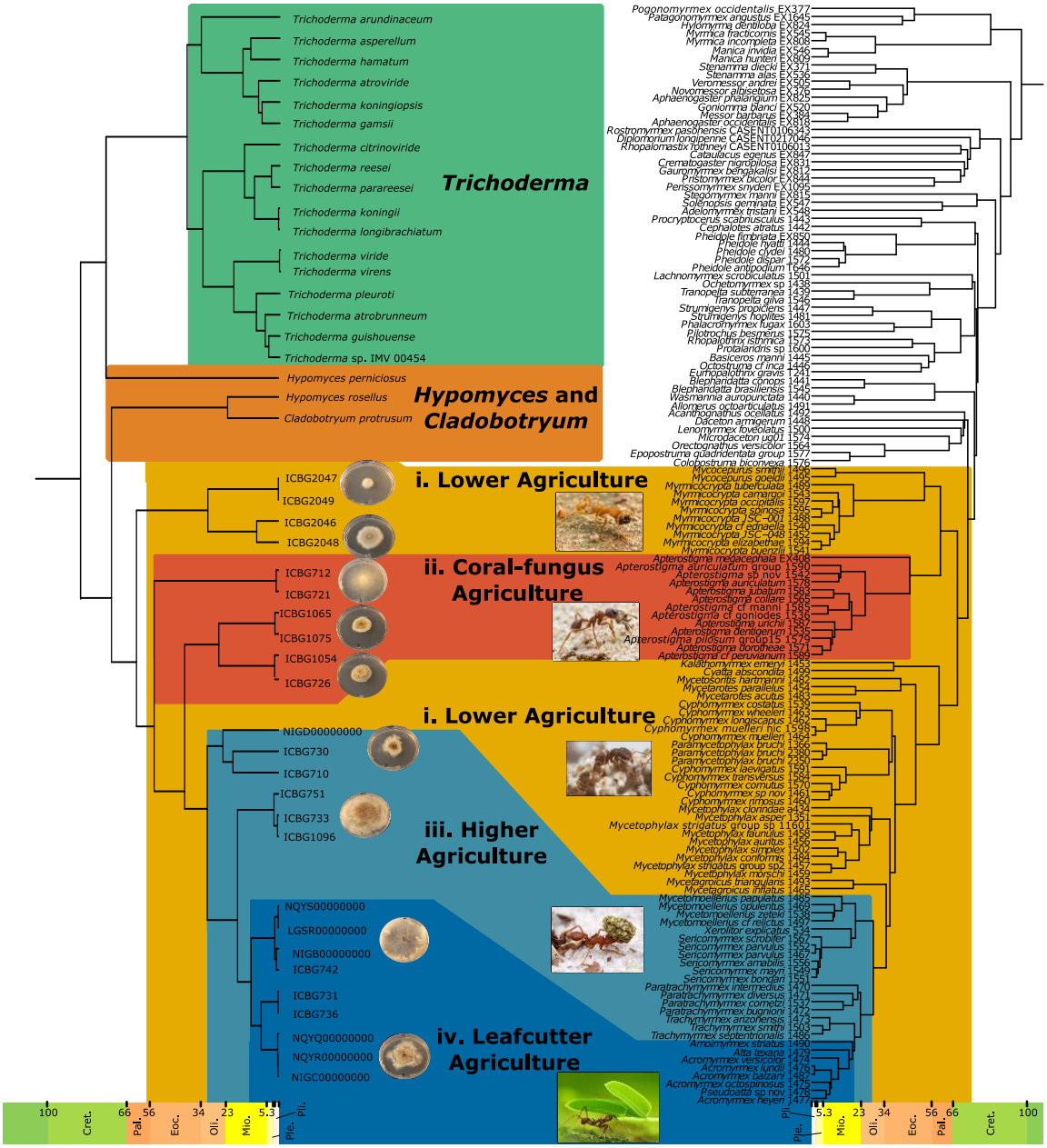

Figure 2. *Escovopsis* originated simultaneously with the origin of fungus-growing ants and specialized parasitic lineages of *Escovopsis* correspond to specialized host lineages of fungus-growing ants. The phylogenetic relationships and the divergence dating analysis of *Escovopsis* genomes are consistent with the dating of the ant agricultural systems they parasitize. Left: Time tree of hypocrealean fungi, including *Escovopsis* (i. lower: yellow, ii. coral-fungus: red, and iii. higher, iv. leafcutter: blue boxes), its sister clade (orange box), and *Trichoderma* (green box). Right: Time tree of fungus-growing ants and non-fungus-farming ant outgroups. Center left: Culture plates of *Escovopsis* strains after seven days of growth on potato dextrose agar. Center

right: Images of ants corresponding to selected ant agricultural systems. The dashed gray lines connecting *Escovopsis* fungal strains to ant images indicate parasite-host associations. Vertical gray bars indicate bins across the time scale. Photographs of *Escovopsis* by Kirsten Gotting, photographs of ants by Alex Wild.

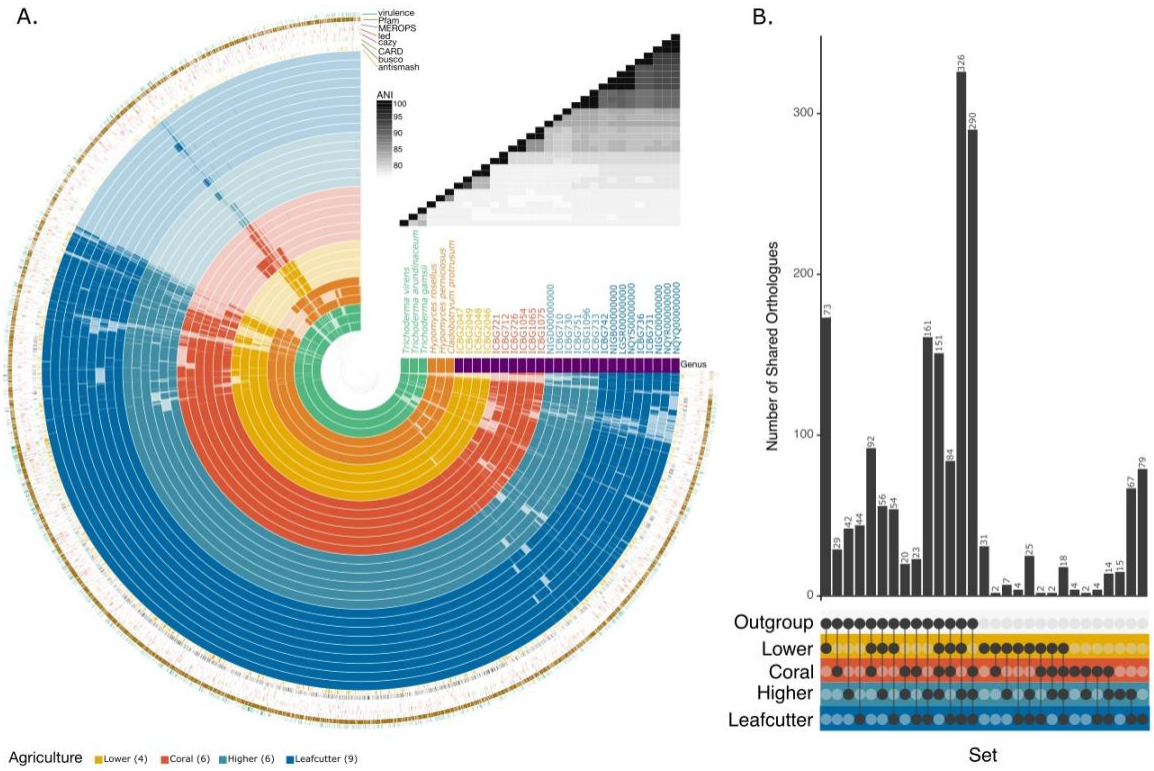

Figure 3. A. Anvi'o interactive visualization of presence-absence matrix of 8783 orthologues among depicted genomes, with the rows along the radial axis indicating each genome and the columns indicating the presence (saturated) or absence (unsaturated) of each ortholog. Functional and informative annotations of orthologs are placed in the outer rings, in order from the outermost ring, number of genomes with each orthologue, presence in figure 3B, orthologs with a PFAM annotation, orthologs with a virulence annotation, orthologs with a MEROPS annotation, orthologs with a LED annotation, orthologs with a CAZyme annotation, orthologs with a CARD annotation, orthologs in an antiSMASH annotated BGC. The legend annotates the colors associated with each genome, indicating the genus each genome originates from and, for *Escovopsis* spp. the fungus-growing ant agriculture origin. The upper right-hand corner indicates pairwise average nucleotide identity (ANI) between genomes for this set of 8783 orthologues. B. UpSet (Gehlenborg, 2019; Lex et al., 2014) plot of shared orthologues content between sets that have greater than or equal to 40 orthologues. Shared orthologues among *Escovopsis* genomes show distinct evolutionary trajectories. These genes are not enriched for any specific GO term, but are annotated to various functional categories as shown in B.

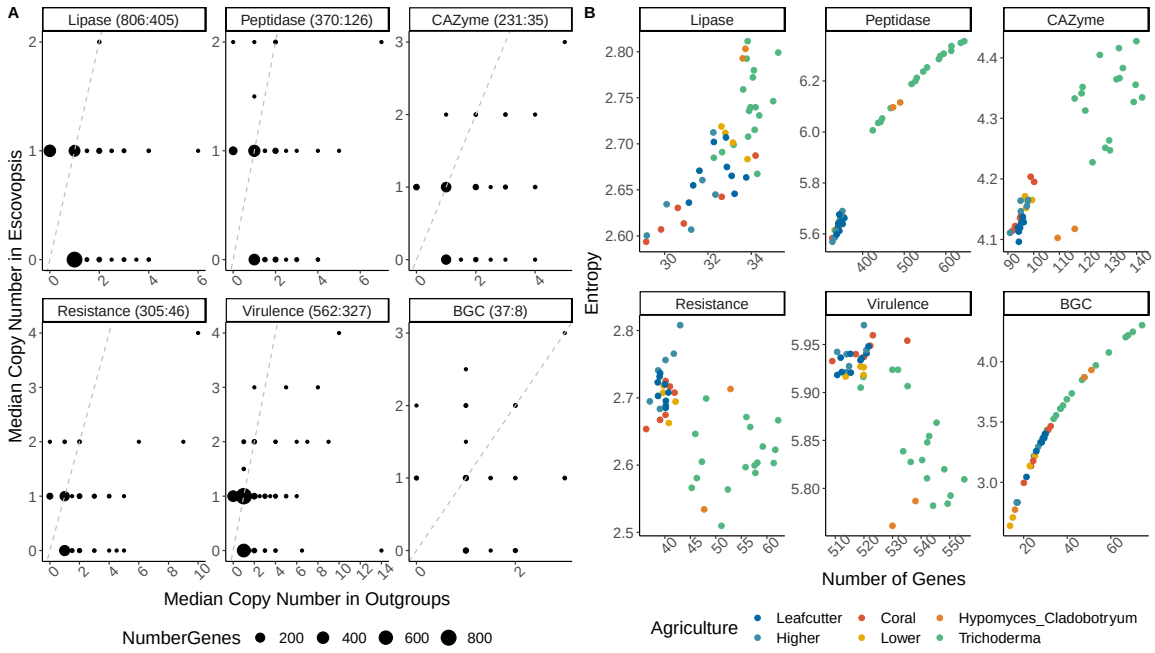

Figure 4. *Escovopsis* spp. exhibit reduced copy numbers in all functions, while maintaining diversity in resistance and virulence gene functions. A. For lipase genes, peptidase genes, CAZyme genes, resistance genes, virulence genes and BGCs identified as similar by BiG-SCAPE, the mean copy number of each gene in *Escovopsis* (y-axis) is compared to the mean copy number in the outgroups (x-axis). The dotted gray line indicates a 1:1 copy ratio, with the size of the circle indicating the number of genes with a given ratio. The numbers in title parenthesis indicate the total number of gene copies per functional group that are lost and gained. B. The same gene categories as in (A) are analyzed for functional diversity of genes as measured by entropy on the y-axis versus the number of genes for each category in each genome on the x-axis. Colors indicate the grouping of the genome either as a part of ant-agriculture or genus level groupings.

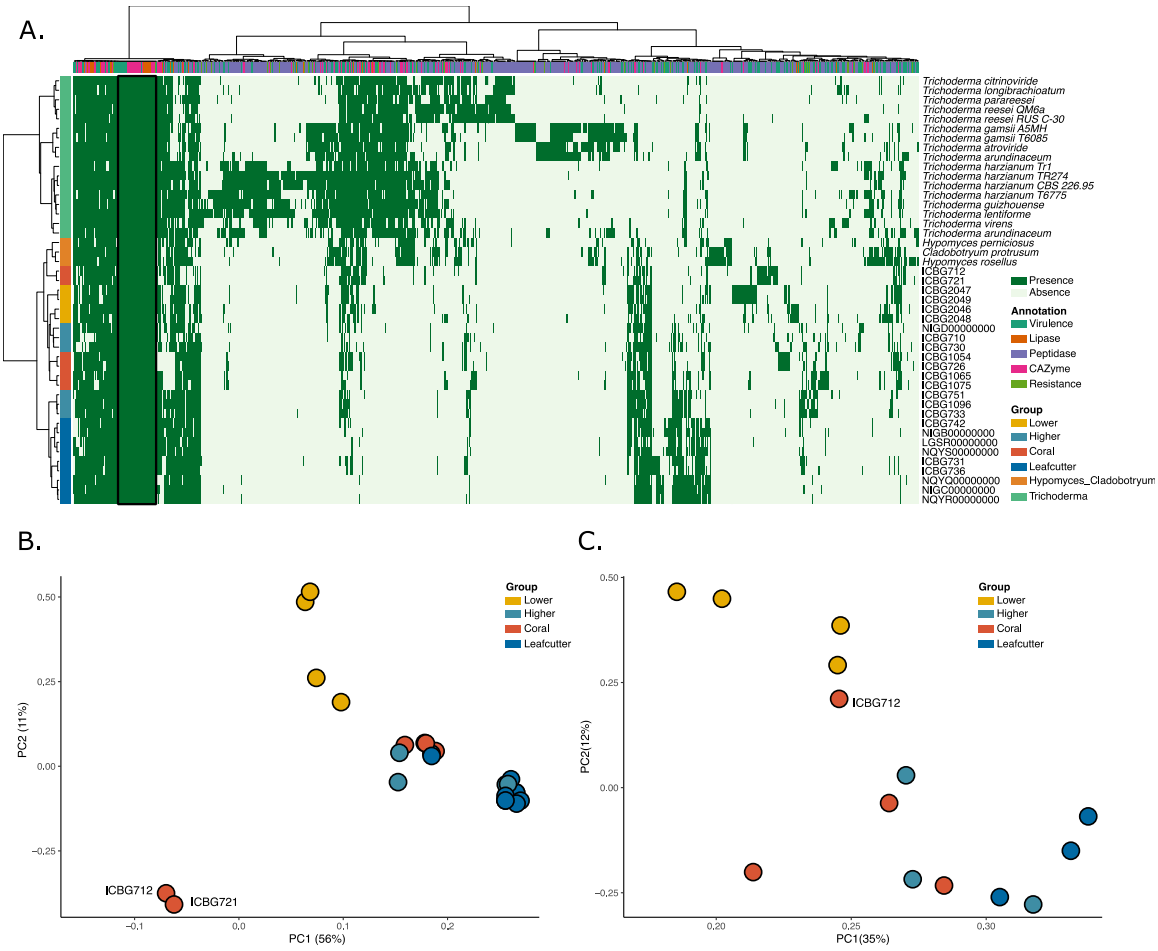

Figure 5. Garden pathogen genomes have specialized genes related to host-signaling and specialized metabolites. A. Heatmap of the secretome genes present in *Escovopsis* and outgroups. The columns represent individual genes and their presence (dark green) and absence (light green) across genomes in the rows. The black box on the left side indicates genes present in all genomes analyzed. B. PCA of BGC presence/absence as defined by BiG-SCAPE clustering per strain across ant agriculture. C. PCA of the presence/absence of molecular networking subclusters as identified with GNPS.

Chapter 3: Metagenomic insights into fungal associates of fungus-growing ants

Kirsten Gotting[1] (gotting@wisc.edu)
Cameron Currie[1,2] (curric7@mcmaster.ca, currie@bact.wisc.edu)

This chapter is in preparation for submission for publication, pending minor changes.
Supplemental material for this chapter can be found in Appendix 2 of this dissertation, with supplemental dataset S1 available through FigShare: 10.6084/m9.figshare.21652094.

Affiliations:
[1]University of Wisconsin Madison, Department of Bacteriology, Madison, Wisconsin
[2]McMaster University, Department of Biochemistry and Biomedical Sciences, Hamilton, Ontario

Author Contributions:
K.G., and C.R.C. designed research; K.G. performed research; K.G., and C.R.C. wrote the paper.

3.1 Abstract

Microbes live and associate with many diverse organisms, forming speciose communities on a microscopic scale. These microbes may have different functions within these associations. Some may play roles in gathering nutrients, while others may detoxify molecules, and some may be parasitic to others in the same community. One way of measuring these microbes is using metagenomic sequencing, which aims to gain insight into these microbial communities by unveiling the DNA present in the community. While metagenomics is a great tool for gaining insight into these communities on broad scales, it isn't as clear how well this tool can recapitulate insights gained through culture-dependent methodologies. Here, using the fungus-growing ant-microbe model symbiosis we aim to determine how well metagenomics recapitulates extensive

efforts in culture-based microbial studies. We show that on broad scales, metagenomics identifies key players known to the fungus-growing ant symbiosis. However, microbes with identified ecological roles are often missed by metagenomic detection. These results indicate that while metagenomics can be useful for gaining insight on broad scales, it may miss ecologically important symbionts. While this may skew some interpretations of the community function, metagenomic sequencing yields valuable information about microbes that may be more difficult to assay or isolate with culture-based methods.

3.2 Introduction

The living world is full of complex interactions between organisms. Symbiosis is an interaction between two organisms that have close physical proximity. These symbioses can take many forms, with one ubiquitous example being the symbiosis between microbes and their hosts. These microbial consortia can range from simple to complex, parasitic to mutualistic in nature. Some well-studied symbionts provide specific benefits to their hosts, ranging from mediating toxicity or availability of nutrient resources to defense of common goods from pathogens. Key questions for the study of symbiosis involve both the identification of partners in symbiosis, as well as their ecological roles in the symbiosis.

The fungus-growing ant microbe symbiosis is one such symbiotic consortia with well-studied partners with defined ecological roles. This symbiosis is structured by a nutritional mutualism between ants and fungi. The ants forage for a diversity of substrates to return to their fungus, which then decomposes those substrates and returns some of nutrients to the ants,

serving as the ant's primary source of food. These substrates are composed of recalcitrant plant polymers which the ants do not have the capacity to digest on their own but are broken down by the diverse suite of enzymes produced by the fungus. In addition, these 'fungus gardens' also house nitrogen fixing bacteria in the genera *Pantoea* and *Klebsiella* (Pinto-Tomás et al., 2009), and many other bacteria and fungi that may have diverse roles within the symbiosis. Fungus-growing ant colonies can take many forms or so called 'agricultures', ranging from the charismatic 'leaf-cutter' ant agricultures that have large colonies with thousands of chambers, and whose substrates are from freshly cut leaves, to 'lower' ant agricultures whose colonies are smaller and primarily subsist on insect frass and dead leaf material.

Fungus-growing ants and their cultivars have been studied since the late 19th century, because both the ants, the fungal cultivar and their interactions are visible without the use of microscopy (Möller, 1893). These studies were built upon with culture-based methods, experimental manipulations, microscopy, and comparative phylogenetic approaches to tease apart more of the microbial complexity in this symbiosis. These approaches led to the discovry of more partners associated with this symbiosis. One example was the discovery of the specialized fungal parasite *Escovopsis*, which is isolated from nearly all mature fungus-growing ant colonies and has detrimental effects to the fungus garden. This fungus can overgrow the fungus garden in the absence of the ants and can result in the loss of large sections of fungus garden (Currie et al., 1999). The ants of fungus-growing ant colonies implement weeding and grooming behaviors to dull the impact of this parasite, as well as associate with diverse bacteria that produce

antifungals, such as *Pseudonocardia* and *Burkholderia* that inhibit the growth of *Escovopsis*. Additionally, many other garden guests have been documented.

Black yeasts have been isolated from fungus-growing ant nests (Carreiro et al., 1997), and have been identified to be within the genera *Phialophora* (Eurotiomycetes: Chaetothyriales) (Moreno et al., 2015; Vasse et al., 2017). These cuticular black yeasts have been shown to be detrimental to the effectiveness of *Pseudonocardia* antibiotic production (Little & Currie, 2008). Another genus of black yeasts isolated from the cuticle of ants is *Cladosporium* fungi (Duarte et al., 2014, 2016; Fernando Carlos Pagnocca et al., 2008). Another fungus, *Syncephalastrum racemosum* (Mucoromycota: Mucorales) is often isolated from leafcutter ant nests (Rodrigues et al., 2009), and additionally has been shown to be a pathogen to the fungus-garden (Barcoto et al., 2017).

Further examination of these fungus gardens using metagenomic sequencing recovered many more bacterial genera putatively associated with these gardens that were subsequently recovered with strain isolations including *Enterobacter, Asaia, Klebsiella*, *Pseudomonas*, *Burkholderia, Gluconobacter, Dysgonomonas, Serratia, Pantoea*, *Parabacteroides, Bacillus, Acinetobacter,* and *Erwinia* (Aylward et al., 2014; Barcoto et al., 2020; Francoeur et al., 2020; Khadempour et al., 2020; Kopac et al., 2018). While these studies used different methodologies to recover these bacterial genera, several of them are consistently recovered through both strain isolation and metagenomic identification. Namely, three of these studies used a differential centrifugation procedure to enrich bacteria in the sample for metagenomic sequencing (Aylward

et al., 2014; Barcoto et al., 2020; Khadempour et al., 2020). Additionally, one study used metatranscriptomics without an enrichment procedure (Francoeur et al., 2020). While these studies have provided information about the bacteria associated with these fungus gardens, they have not described whether there are non-cultivar garden fungi present in these collections of sequences.

In this study, we used publicly available metagenomes from the fungus-growing ant symbiosis to determine 1) what bacterial, fungal, protist, viral, and plant taxa are detected, 2) what similarities exist amongst the samples in these studies, 3) if non-bacterial genera isolated in fungus-gardens are also found in metagenomic sequencing, and 4) the relative contribution of assembled vs. unassembled reads to identifying taxa, 5) how difference amongst 1,2,3 and 4 influence functional comparisons between samples. We approached these questions by first identifying key microbes that have been isolated repeatedly and are reported in the literature as being associated with fungus-growing ant fungus gardens. We then used sourmash (Irber et al., 2022; Titus Brown & Irber, 2016), a k-mer based searching tool with high accuracy to assess metagenomic assemblies and identify taxa in metagenomic sequencing. As a second tool for confirming our taxonomic detection, we also identified genera using marker genes for bacterial and fungal sequences. These tools enabled us to find consistent genera across metagenomes using multiple methodologies.

3.3 Results

3.3.1 Taxonomic composition of fungus-growing ant microbial communities

To determine broad taxonomic differences between samples, we used sourmash to identify taxa. Relative proportions of sequences that mapped to plant, archaea, protist, bacterial, viral and fungal genomes differed across sequencing methods, and sample types. Metagenomes enriched for bacterial sequences via differential centrifugation contained a median of 6% fungal sequences, 12.8% plant sequences, and 74% bacterial sequences. Protist sequences made up 1.5% of the sequences, with viruses and archaeal sequences occupying less than 1% of the total sequences identified (Fig. 1b). Metatranscriptomes contained a median of 79% fungal sequences, 14% plant sequences, and 3% bacterial sequences. The proportion of sequences identified for virus, archaea and protist references was less than 1%. The difference in proportion of bacteria and fungi amongst metagenomes and metatranscriptomes is due to the differential centrifugation procedure that enriched for a bacterial fraction.

3.3.2 Nucleotide congruency between reads and assemblies

To ensure that these metagenomes and metatranscriptomes are reasonably similar to eachother and suitable for comparison, we examined them with using average nucleotide identities (ANI). In addition to differences of taxonomic origin for many sequences, differences in sample preparation and assemblies exhibit differences in sequence signatures across samples. In examining the differences between assemblies and sequenced reads using ANI, samples isolated

from fungus-growing ant colonies shared higher levels of identity than samples from other habitats. Within fungus-growing ant samples, the mean ANI was 88%, whereas when compared to external samples, the mean ANI was 75%. In some cases, reads and assemblies did not share high levels of ANI (Fig. 2), as seen with sample *Atta_cephalotes*_RNA1, where the reads share higher ANI with samples from different sequencing batches, whereas the *Atta_cephalotes*_RNA1 assembly more closely matches the *Atta_cephalotes*_RNA2 and *Atta_colombica*_RNA assemblies from the same sequencing and assembly batch.

3.3.3 Detection of genera amongst fungus-growing ant metagenomes

Of the focal genera examined in this study (Dataset 2), several genera of fungi were detected across samples. Focal fungi from Saccharomycetes, Tremellomycetes and other fungal classes were identified across some samples, but not others (Fig. 3a). The fungal cultivar, represented by both *Leucoagaricus* and *Leucocoprinus* sequences, were identified in 18/26 samples, for a sum of 653.6 mb and 56.6 mb uniquely intersecting megabases, respectively, but were not present in samples from lower attines. The second most identified fungus was *Aureobasidium*, which was present in 17/26 samples for a sum of 2.2 mb of uniquely intersecting base pairs and spanned both lower and leafcutter attine samples. *Phialophora* was present in 16/26 samples and 1.5 uniquely intersecting megabases. *Saccharomyces* was present in 16/26 samples and 5.5 uniquely intersecting megabases. *Saitozyma* was present in eight samples 0.4 uniquely intersecting megabases. *Trichoderma* was present in ten samples and 0.39 uniquely intersecting megabases. *Escovopsis* and *Candida* were detected in three samples, with 0.45 and 0.23 uniquely intersecting

megabases, and *Calivispora* was detected in two samples (Fig. 3a) with 7.3 uniquely intersecting megabases. Undetected fungal genera that are commonly isolated from fungus gardens were *Hannaella, Apiotrichum, Cutaneotrichosporon, Debaryomyces,* and *Trichomonascus*.

Among bacterial classes, Gammaproteobacteria were frequently identified across all samples (Fig. 3a). Bacteroidia were rarely identified (Fig. 3a). Actinomycetia were frequently identified in the reads of metagenomic samples but were not as frequently identified in the assemblies (Fig. 3a). Several genera of bacteria that are consistently found in fungal gardens were found across more than 90% of samples (20 samples) including *Pseudomonas*, *Klebsiella*, *Pantoea*, *Acinetobacter*, and *Enterobacter* at 311.7, 118.8, 650.5, 42, and 220.7 uniquely intersecting megabases, respectively (Fig. 3a). Additionally, *Burkholderia* and *Serratia* are found in over 80% of samples at 118.7, 64.5 uniquely intersecting megabases, respectively. Only one candidate bacterial genus was not identified: *Weisella* (Dataset 2). We note that many of these genera were primarily identified in samples with deeper sequencing (Fig. 3a), and that deeper sequencing resulted in increased richness and diversity amongst identified (Fig. S1).

We also identified several genera that are not commonly isolated from fungus growing ant fungus gardens from fungal, bacterial and protist databases. To minimize false positives, we list here genera that are present in at least two samples, at least three sequencing batches, and are represented in both reads and assemblies. Fungi that were detected that are not commonly isolated were *Podosphaera, Puccinia, Fusarium, Microbotryum, Tubarium, Astraeus, Beauveria, Rhizopus, Colletotrichum, Clavaria, Cantharellus, Calonectria,* and *Corynespora* (Dataset S1).

There was also evidence in both reads and assemblies for the presence of six genera of protists: *Acytostelium, Dinobryon, Physarum, Entamoeba, Phytophthora,* and *Spumella* (Dataset S1). One bacterial genus also matched this criterion: *Citrobacter* (Dataset S1).

As a second methodology for detecting these genera, we annotated marker genes (16S for bacteria; 18S, 28S, and ITS for fungi) using the NCBI RefSeq Targeted Loci Project. In examining these marker genes for fungi and bacteria, many of the genera found through whole genome kmer matching were also identified. All bacteria identified in 16S sequences were also identified with kmer signature matching. The same was not true for fungal genera. Fungal genera identified by mapping reads to marker genes that were not identified through matching kmer signatures were *Hannaella* (18S), *Apiotrichum* (18S), *Cutaneotrichosporon* (18S, 28S), and *Debaryomyces* (28S) (Fig. 3B). Fewer fungal genera were identified with ITS sequences as compared to 18S sequences and 28S sequences, which is likely not due to the size of the databases (ITS: 15,080, 28S: 9,090, 18S: 3299, 16S: 22089).

3.3.4 Detection amongst assembled contigs and raw reads

Overall, metagenomic reads recovered higher numbers of genera than assemblies. The following statistics refer to data aggregated from all fungus-growing ant samples. Seventeen archaea genera were recovered in reads, whereas assemblies recovered two. 625 bacterial genera were recovered in reads, whereas assemblies recovered 169. 183 fungal genera were recovered in reads, whereas assemblies recovered 72. 70 protist genera were recovered in reads, whereas assemblies recovered 33. 716 plant genera were recovered in reads, whereas assemblies

recovered 269. Viruses were the only taxonomic grouping where reads and assemblies both recovered five genera.

Several genera of interest were identified only in DNA reads of samples, including for fungi: *Candida*, *Escovopsis*, *Meyerozyma*, *Papiliotrema*, *Pichia*, *Rhodoturula*, *Syncephalastrum*, and *Trichosporon*, and bacteria: *Chitinophaga*, *Moraxella*, and *Rahnella* (Fig. 3). Two bacterial genera were exclusively found in assemblies: *Dysgonomonas*, and *Parabacterioides* (Fig. 3). The bacterial genera *Pantoea*, *Enterobacter*, and *Pseudomonas* were recovered in more assemblies than reads, whereas *Erwinia*, *Acinetobacter*, *Gluconobacter*, *Serratia*, *Burkholderia*, *Nocardioides*, *Amycolatopsis*, *Pseudonocardia*, *Streptomyces*, *Bacillus*, *Paraburkholderia*, and *Mycobacterium* were recovered in more reads than assemblies. Additionally, fungal genera recovered more frequently in reads were *Aureobasidium*, *Clavispora*, *Saccharomyces*, and *Saitozyma*. All focal genera identified in metatranscriptomic data were also recovered in metagenomic data (Dataset S1, Fig. 3).

3.3.5 Functional dynamics across fungus-growing ant communities

To gain insight about functional processes that may differ amongst these samples, we annotated resistance genes with the Comprehensive Antibiotic Resistance Database (CARD), as well as pathways and functions with the Clusters of Orthologous Genes (COG) database using both reads and protein sequences from metagenome assemblies. In comparing these annotations, reads and assemblies have different numbers of resistance genes detected, with annotations with reads detecting fewer numbers of resistance genes across all categories and samples (Fig. S2).

Additionally, non-ant metagenomic samples had larger numbers of uniquely annotated resistance genes pertaining to “antibiotic inactivation” (Fig. S2).

In examining detection resistance gene annotations across all metagenomes, most categories of resistance mechanisms have higher numbers of resistance genes annotated in non-ant associated samples than ant-associated samples. For example, for antibiotic efflux, ant samples have a median count of 196.3 genes, whereas non-ant samples have a median count of 209.5. This was also true for “antibiotic inactivation” (ant-associated: 153.5 median gene count, non-ant-associated 298.7 median gene count) and “antibiotic target alteration” (ant-associated: 138.5 median gene count, non-ant-associated 172.7 median gene count), There are no categories where ant samples have higher numbers of resistance genes, but some categories where ant samples are within 5 genes. These categories are “antibiotic target protection” (ant-associated: 42.3 median gene count, non-ant-associated 53.3 median gene count), “target alteration; antibiotic efflux” (ant-associated: 12.7 median gene count, non-ant-associated 13.7 median gene count), “target alteration; antibiotic efflux; reduced permeability to antibiotic” (ant-associated: 1.8 median gene count, non-ant-associated 1.5 median gene count), “target alteration; antibiotic target replacement” (ant-associated: 4.4 median gene count, non-ant-associated 5 median gene count), “reduced permeability to antibiotic” (ant-associated: 2.7 median gene count, non-ant-associated 1.7 median gene count), “antibiotic target replacement” (ant-associated: 11.2 median gene count, non-ant-associated 16 median gene count), and “efflux; reduced permeability to antibiotic” (ant-associated: 1.9 median gene count, non-ant-associated 2 median gene count).

Supplemental figure S3 shows the distribution of presence and absence of these genes, along with the numbers of copies of these genes across all samples for select resistance mechanisms.

In examining COG annotations, most categories of annotations had within ten COGs separating the number of annotations for ant and non-ant samples. These categories are "Carbohydrate transport and metabolism", "Cell motility", "Cell wall/membrane/envelope biogenesis", "Chromatin structure and dynamics", "Coenzyme transport and metabolism", "Cytoskeleton", "Defense mechanisms", "Extracellular structures", "Inorganic ion transport and metabolism", "Intracellular trafficking, secretion, and vesicular transport", "Lipid transport and metabolism", "Nucleotide transport and metabolism", "Post-translational modification, protein turnover, chaperones", "Replication, recombination and repair", "RNA processing and modification", "Secondary metabolites biosynthesis, transport and catabolism", "Signal transduction mechanisms", and "Transcription". Categories where non-ant samples have greater than 10 COGs more than ant samples are "Amino acid transport and metabolism" with a median of 13 more COGs, "Cell cycle control, cell division, chromosome partitioning" with a median of 60 more COGs, "Mobilome: prophages, transposons" with a median of 16 more COGs. Categories where ant-samples have greater than 10 COGs more than non-ant samples are "Energy production and conversion" with a median of 42 more COGs, and "Translation, ribosomal structure and biogenesis" with a median of 16 more COGs (Fig. 4a). Figure 4b demonstrates that gene categories with higher richness (more genes) are also more diverse in functional capacity within a category. Next, to demonstrate how metagenomic annotations represent known functional

capacities in fungus-growing ant gardens, COGs associated with functions pertaining to plant biomass degradation, arginine biosynthesis, nitrogen processing, chitin processing, and 16S as a positive control were curated. The COGs were nearly universally present in all ant metagenomes, notably, with the arginine biosynthesis pathway fully represented in each metagenome. These same functional categories were also present in the metatranscriptomic sequencing, but to a lesser degree. (Fig. 4c)

3.4 Discussion

In this study, we aimed to determine how well metagenomic sequencing approaches recapitulate the identification of organisms in a community, using the model microbial community present in fungus-growing ant gardens. Our analysis demonstrates that k-mer based approaches for metagenomic detection of taxa yield similar results to traditional approaches. We find similar proportions of taxonomic classes as were reported in the original publications for each dataset (Fig. 1b). Additionally, we identify similar organisms as previously reported. These results demonstrate that while k-mer based approaches like sourmash may sacrifice breadth, for well-sequenced communities like fungus-growing ant gardens, they recapitulate identifications for key ecological players in this community.

In examining similarities amongst the samples in these studies, we find that metagenomes and metatranscriptomes from ant samples more closely resemble each other than those from other habitats (Fig. 2). Additionally, genus, and to a lesser degree, species predicts patterns of clustering and similarity amongst sampled metagenomes. This finding lends itself to the idea that

fungus-growing ant gardens have a similar community structure likely defined by the function of plant-biomass degradation.

In determining if non-bacterial genera isolated in fungus-gardens are also found in metagenomic sequencing we find that metagenomics can often recapitulate the identification of microbes in a community that are found through traditional microbial culturing techniques. For example, despite bacterial enrichments in many samples, we detect many fungi across all samples. Additionally, we detect cultivar sequences in all samples, while other fungi that we know to be present and key ecological players in this symbiosis were only detected in some samples, such as *Escovopsis* and *Syncephalastrum*. This result could likely be due to two things: 1) some of these fungi are known pathogens to the system and may not be present in every garden sample, and 2) the abundance of these pathogens in any given sample of garden may be below the level that would be picked up through a genomic DNA extraction. Additionally, somewhat unexpectedly, many strains from Bacteroidia which are commonly found with culturing methodology were not found often in metagenomes. These results underscore the importance of isolations in determining key microbes with underlying ecological roles that drive the functioning of a community.

We find that the relative contribution of assembled vs. unassembled reads to identifying taxa depends on the taxon. Bacteria and fungi, such as Gammaproteobacteria and *Leucoagaricus*, that we might expect to have high abundances in the garden were frequently found in both reads and assemblies. Other fungi and actinobacteria identified with culture-dependent techniques were

frequently found in the reads of deeply sequenced metagenomes, but not as frequently in the assemblies of our metagenomes, or in metagenomes with lower sequencing depth. This indicates that metagenomic sequencing may be able to detect a diverse microbial consortium, but the capacity for comparative functional metagenomics is more limited. For representation of taxa such as *Escovopsis*, with well-defined ecological roles in the symbiosis, it would be of utility to be able to detect more sequences. Future studies could examine metagenomes of artificial infections with Escovopsis, or other microbes, to determine how the fungus-garden functionally responds to these parasites and microbes.

One key result from this study is that methodological replication at the sample isolation and nucleic acid preparation steps account for most variability amongst samples. This result was present in both clustering distances between metagenomes (Fig. 2), as well as finer-scale taxonomic identifications (Fig. 3). However, these were less apparent in analyzing functions shared amongst these samples, across broad (Fig. 4a) and narrow (Fig. 4b) scales.

Lastly, arginine biosynthesis, a function lost in fungus-growing ants, is a function commonly found in plants, bacteria, and fungi. The genes required to biosynthesize arginine are present in the metagenomic community and metatranscriptomes of the fungus-gardens (Fig. 4c). Additionally, while fixation of nitrogen is an activity of some bacteria in fungus-growing ant gardens, there is a lack of some COGs relating to nitrogen. This could indicate that fungus-growing ant gardens have a reduced set of genes for this function that are still sufficient for the activity (Fig. 4c).

3.5 Methods

3.5.1 Genomic Data Processing and Annotation

We downloaded data for metagenomic assemblies and annotations for fungus-growing ant associated samples, as well as control-group soil samples from the JGI Genomes Portal between April 12th, 2022, and April 20th, 2022 (Grigoriev et al., 2012; Nordberg et al., 2014). See Dataset 2 for accessions and associated metadata. Data types used in this study were: metagenomic assemblies, metagenomic raw reads, and predicted amino acid sequences.

3.5.2 Marker Gene Identification

Marker genes were annotated in two ways. First: the NCBI RefSeq Targeted Loci Project (Accession: PRJNA224725, https://www.ncbi.nlm.nih.gov/refseq/targetedloci/) was used to identify putative matches to loci for fungal ITS, 28S, and 18S, as well as bacterial 16S sequences. Raw reads were aligned to these databases using BWA-MEM (Li & Durbin, 2009) with default settings. Mapped reads were sorted, indexed, and counted against the references using SAMtools v1.7 (Danecek et al., 2021) programs ‘view’, ‘sort’, ‘index’, and ‘idxstats’. A marker gene was considered ‘detected’ if there were greater than or equal to 10 reads mapping to the gene. Second: RNA families from the Rfam database (Kalvari et al., 2018, 2021) were annotated with infernal v1.1.2 (Nawrocki & Eddy, 2013). These were then blasted to the NCBI RefSeq Targeted Loci, with a marker being detected if one putative infernal sequence matched with a top hit.

3.5.3 Metagenomic Comparisons

Metagenomic assemblies and reads were compared using several utilities from the sourmash v. 4.5 codebase (Titus Brown & Irber, 2016) with a kmer size of 31. The program “sourmash sketch dna” with options “-p k=21,k=31,k=51,scaled=1000,abund” was used to create kmer profiles for reads and assemblies. The program “sourmash compare” was used to create distance metrics between assemblies and reads, with the option “--ani”.

3.5.4 Taxonomic Identifications

Metagenomic assemblies and reads were taxonomically classified using several utilities from the sourmash v. 4.3.0 codebase (Titus Brown & Irber, 2016) with a kmer size of 31.The program “sourmash gather” with option “threshold-bp 10000” was used to taxonomically classify assemblies and reads with pre-compiled databases for Genbank genomes as of March 2022 (https://sourmash.readthedocs.io/en/latest/databases.html) for viral, archael, protist, and bacterial sequences. A custom database for plant sequences was generated from Genbank sequences downloaded with ncbi-genome-download.py v0.3.1 (https://github.com/kblin/ncbi-genome-download) on August 22, 2022, with the program “sourmash sketch dna” with options “-p k=21,k=31,k=51,scaled=1000,abund” to create kmer signatures. This database was also used to taxonomically classify assemblies with “sourmash gather” as before. Genera reported as common reagent and laboratory contaminants (Salter et al., 2014) were excluded from the analysis unless these genera had been reported to be manually isolated from a fungus garden,

specifically, the genera *Burkholderia*, *Acinetobacter*, *Enterobacter*, *Pseudomonas*, *Firmicutes*, and *Bacillus*.

3.5.5 Functional Protein Annotation

Predicted protein sequences were functionally annotated to both the COG database (Galperin et al., 2021) and the CARD database (Alcock et al., 2020). COGs were annotated by diamond blastp (Buchfink et al., 2021) to the cog-20 protein sequences and parsing for the best match according to bitscore. CARDs were annotated using rgi v. 5.1.1 against predicted protein sequences.

3.6 Acknowledgments

We are grateful to Donny Hoang for comments on the manuscript. We thank Lily Khadempour, Frank O. Aylward, Garret Suen, Charlotte B. Francoeur, and Mariana O. Barcoto for generating and publishing the data that this study was based on. This material is based on work supported in part by National Institutes of Health grant U19 TW009872, National Institutes of Health grant U19 AI142720, and National Science Foundation grant DEB-1927155, and São Paulo Research Foundation (FAPESP) grant # 2013/50954-0. Additional support was granted to K.G. through the Big Ten Academic Alliance Smithsonian Fellowship through the Smithsonian Tropical Research Institute.

3.7 Figures

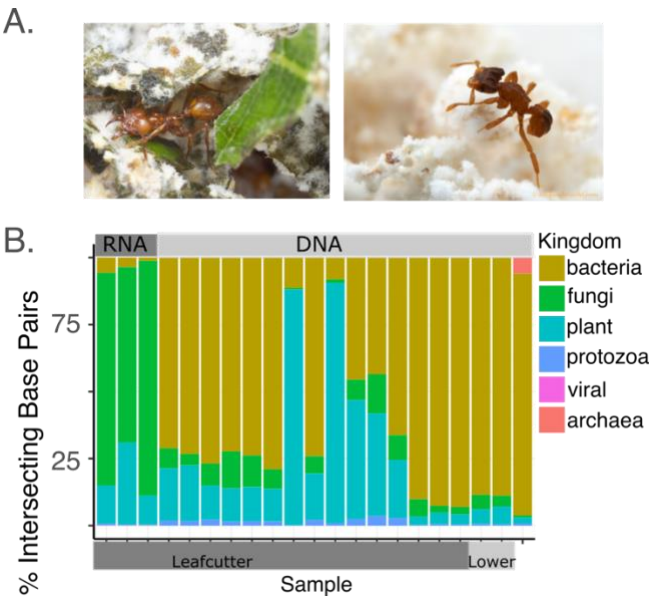

Figure 1. (A) Two genera of fungus growing ants with gardens sampled in this study, left: *Atta,* right: *Cyphomyrmex* from leafcutter and lower agriculture, respectively. (B). Kingdom level detection of bacteria, archaea, plantae, fungi, protist, and viruses across metagenomic samples, indicated by 'DNA' or metatranscriptomic samples, indicated by 'RNA'. Additionally, columns are annotated as coming from either 'leafcutter' or 'lower' ant agriculture. The y-axis is the percentage of intersecting base pairs that indicates the fraction of base pairs that intersect with sequences in a given database. The legend color-codes each database used as a reference.

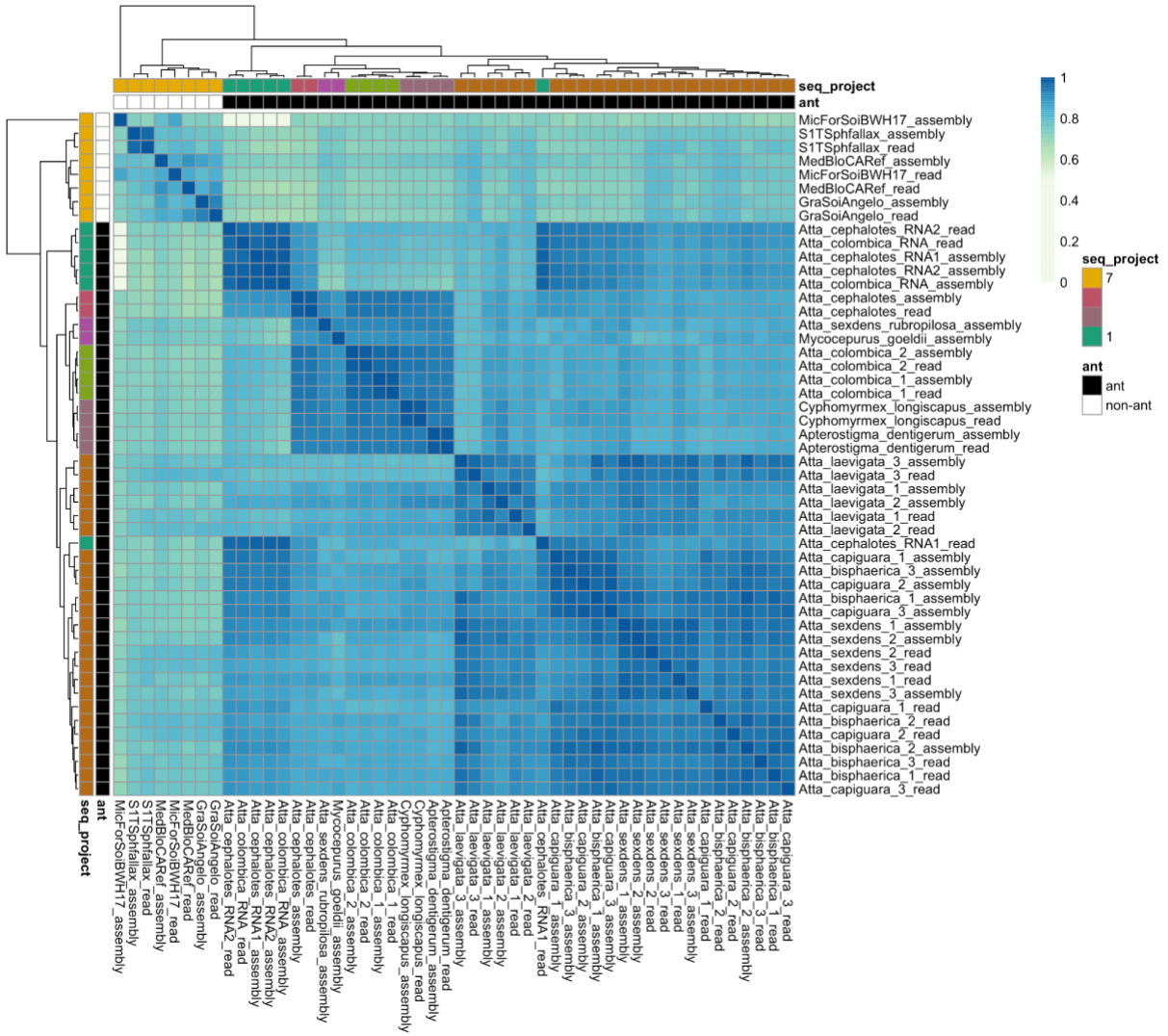

Figure 2. Assemblies and reads both indicate a unique community pertaining to fungus-growing ant fungus gardens. Average nucleotide identities are indicated by the heatmap color scale. Either axis indicates samples compared, including whether these samples came from metatranscriptomic sequencing, indicated with “RNA” in the name, and additionally, whether assemblies are reads were used for the comparison. Outer annotations of rows and columns indicate both the sequencing batch for each sample, as well as whether the sample was from a fungus-growing ant garden (black) or not (white).

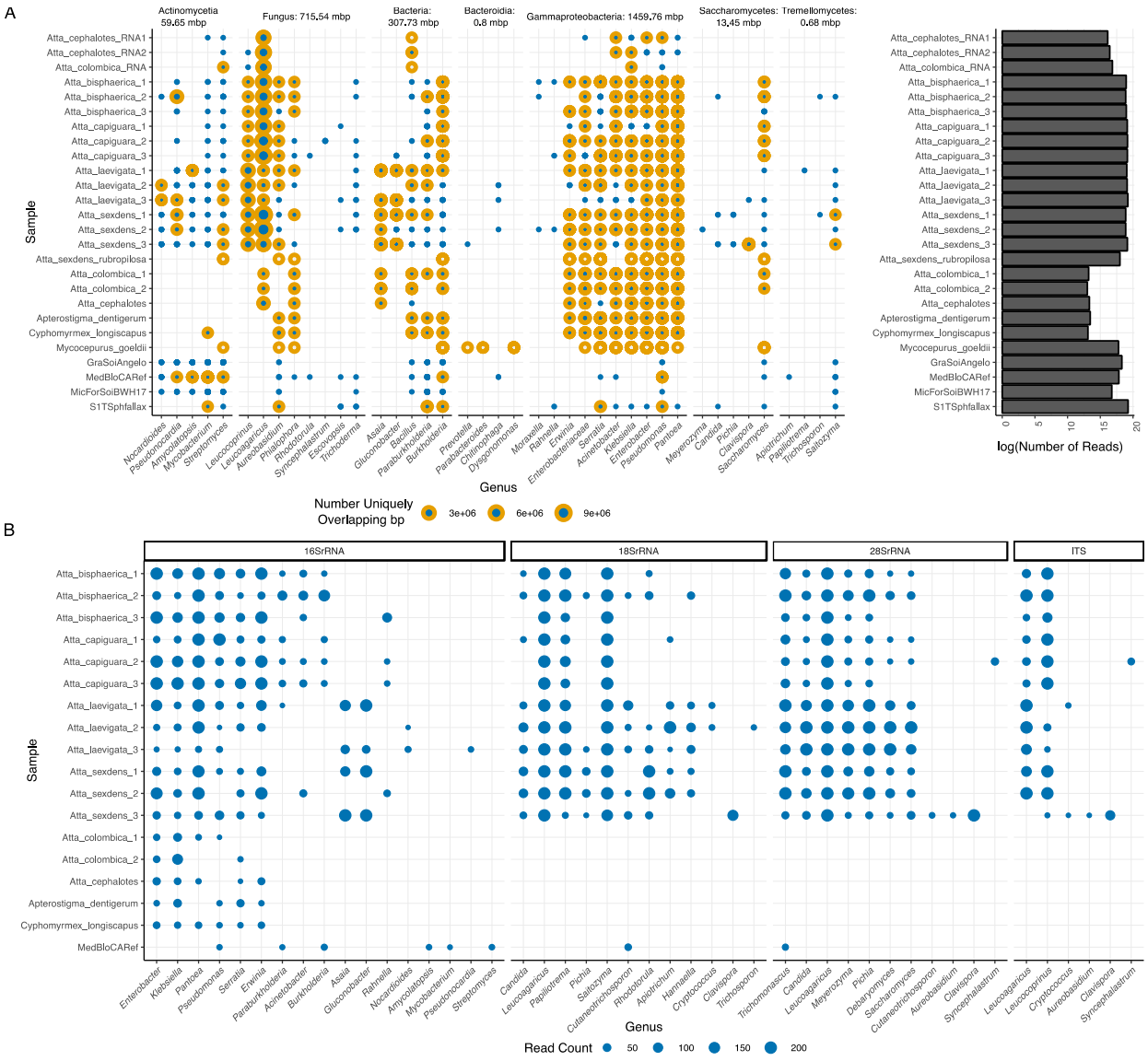

Figure 3. (A) Both bacterial and fungal genera commonly identified in fungus gardens are also identified in both reads (blue points) and assemblies (yellow outlines). Read depth across samples are on marginal bar plot. Facet labels indicate the number of mega base-pairs (mbp) intersecting with a given taxonomic class. (B) Marker genes present in sequencing data recapitulate similar genera identifications as whole genome databases.

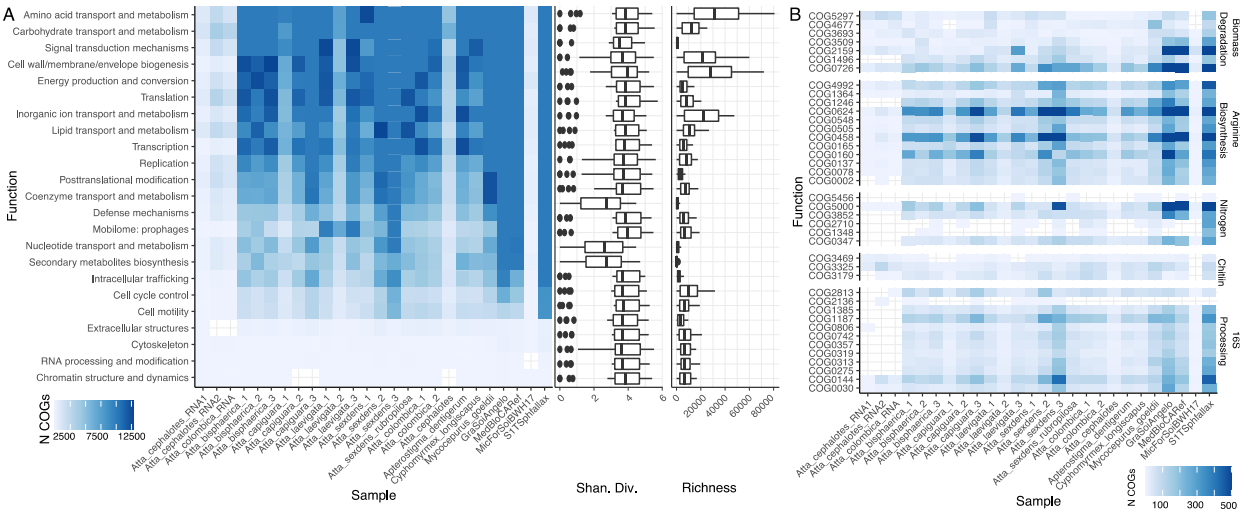

Figure 4. A. All metagenomic annotations share similar levels of representation of COGs, with the exception of metatranscriptomic annotations. The heatmap color scale indicates the number of COGs in each category in A and C. B. Shannon diversity and richness of functions demonstrate that the number of unique genes mapping to a given COG determines the amount of diversity amongst those gene groups. C. Known functions encoded in fungus-growing ant microbes are annotated in the metagenomes.

3.8 Datasets

3.8.1 Dataset 1

Metadata of samples used in this study.

Group	ID	assembly_lengt	n_proteins	IMG ID	Host Metadata	Enrichment Procedure	Sequencing Type	Fungus Garden Sa	Geographic Location	Study
experimental	AptfungaCombined	97571324	220188	2029527003	Apterostigma dentigerum	Bacteria enrichment via differential ce	Metagenome	garden	Gamboa, Panama	Aylward et al., 2014
experimental	AttbisABBM1_FD	389484451	607042	3300013023	Atta bisphaerica	Bacteria enrichment via differential ce	Metagenome	garden center	Botucatu, State of Sao Paulo Brazil	Khadempour et al. 2020
experimental	AttbisABBM2_FD	627226396	358547	3300013025	Atta bisphaerica	Bacteria enrichment via differential ce	Metagenome	garden center	Botucatu, State of Sao Paulo Brazil	Khadempour et al. 2020
experimental	AttbisABBM3_FD	185710356	910609	3300013022	Atta bisphaerica	Bacteria enrichment via differential ce	Metagenome	garden center	Botucatu, State of Sao Paulo Brazil	Khadempour et al. 2020
experimental	AttcapACBM1_FD	148286676	272096	3300012994	Atta capiguara	Bacteria enrichment via differential ce	Metagenome	garden center	Botucatu, State of Sao Paulo Brazil	Khadempour et al. 2020
experimental	AttcapACBM2_FD	260748832	456916	3300012996	Atta capiguara	Bacteria enrichment via differential ce	Metagenome	garden center	Botucatu, State of Sao Paulo Brazil	Khadempour et al. 2020
experimental	AttcapACBM3_FD	358973568	644865	3300012997	Atta capiguara	Bacteria enrichment via differential ce	Metagenome	garden center	Botucatu, State of Sao Paulo Brazil	Khadempour et al. 2020
experimental	AttcepgaCombined	40623338	73881	2029527004	Atta cephalotes	Bacteria enrichment via differential ce	Metagenome	garden center	Gamboa, Panama	Aylward et al., 2014
experimental	AttcolfgardenTop	100904834	240966	2029527005	Atta colombica	Bacteria enrichment via differential ce	Metagenome	garden top	Gamboa, Panama	Aylward et al., 2012
experimental	AttcolgardBottom	83167033	199019	2029527006	Atta colombica	Bacteria enrichment via differential ce	Metagenome	garden bottom	Gamboa, Panama	Suen et al., 2010
experimental	AttlaeALBM1_FD	513701281	871330	3300013000	Atta laevigata	Bacteria enrichment via differential ce	Metagenome	garden center	Ribeiro Preto, State of Sao Paulo, Brazil	Khadempour et al. 2020
experimental	AttlaeALBM2_FD	187167002	332737	3300012995	Atta laevigata	Bacteria enrichment via differential ce	Metagenome	garden center	Ribeiro Preto, State of Sao Paulo, Brazil	Khadempour et al. 2020
experimental	AttlaeALBM3_FD	543363875	722718	3300012998	Atta laevigata	Bacteria enrichment via differential ce	Metagenome	garden center	Ribeiro Preto, State of Sao Paulo, Brazil	Khadempour et al. 2020
experimental	AttsexASBM1_FD	702519501	822403	3300012999	Atta sexdens	Bacteria enrichment via differential ce	Metagenome	garden center	Botucatu, State of Sao Paulo Brazil	Khadempour et al. 2020
experimental	AttsexASBM2_FD	806785955	1086719	3300013002	Atta sexdens	Bacteria enrichment via differential ce	Metagenome	garden center	Botucatu, State of Sao Paulo Brazil	Khadempour et al. 2020
experimental	AttsexASBM3_FD	559676975	1029784	3300013001	Atta sexdens	Bacteria enrichment via differential ce	Metagenome	garden center	Ribeiro Preto, State of Sao Paulo, Brazil	Khadempour et al. 2020
experimental	AttsexdGarden	228694198	269449	3300009944	Atta sexdens rubropilosa	Bacteria enrichment via differential ce	Metagenome	garden center	Botucatu, State of Sao Paulo Brazil	Barcoto et al., 2020
experimental	CypfungaCombined	88331577	190064	2030936005	Cyphomyrmex longiscapus	Bacteria enrichment via differential ce	Metagenome	garden	Gamboa, Panama	Aylward et al., 2014
experimental	FG1	28232203	22995	NA	Atta cephalotes	None	Metatranscriptome	garden top	La Selva, Costa Rica	Francoeur et al. 2020
experimental	FG2	147105201	100503	NA	Atta cephalotes	None	Metatranscriptome	garden top	La Selva, Costa Rica	Francoeur et al. 2020
experimental	FG3	82246742	54683	NA	Atta colombica	None	Metatranscriptome	garden top	La Selva, Costa Rica	Francoeur et al. 2020
control	GraSoiAngelo_129_FD	633321502	1083369	3300026328	Grasslands soil	NA	Metagenome	NA	Angelo Coastal Reserve, California, USA	Diamond et al. 2019
control	MedBloCARef_M1_FD	333334921	788687	3300027633	Forest Soil	NA	Metagenome	NA	El Dorado National Forest, Georgetown, California, USA	
control	MicForSoilBWH17_O_FD	12727925	13705	3300001609	Temperate Forest soil	NA	Metagenome	NA	Harvard Forest LTER, Petersham, MA, USA	
experimental	MycgoeldiiGarden	320980619	395806	3300009856	Mycocepurus goeldii	Bacteria enrichment via differential ce	Metagenome	garden	Botucatu, State of Sao Paulo Brazil	Barcoto et al., 2020
control	S1TSphfallax_3_FD	1346775198	2119103	3300027807	Alpine/subalpine bogs - Sphagnum f	NA	Metagenome	NA	Minnesota, USA	

3.8.2 Dataset 2

Focal genera examined in this study.

genus	type	taxonomy
Aureobasidium	fungus	Dothideomycetes
Candida	fungus	Saccharomycetes
Cryptococcus	fungus	Tremellomycetes
Haglerozyma	fungus	Tremellomycetes
Hannaella	fungus	Tremellomycetes
Meyerozyma	fungus	Saccharomycetes
Rhodotorula	fungus	Microbotryomycetes
Saitozyma	fungus	Tremellomycetes
Leucoagaricus	fungus	Agaricomycetes

Leucocoprinus	fungus	Agaricomycetes
Enterobacter	bacteria	Gammaproteobacteria
Pseudomonas	bacteria	Gammaproteobacteria
Moraxella	bacteria	Gammaproteobacteria
Rahnella	bacteria	Gammaproteobacteria
Burkholderia	bacteria	Betaproteobacteria
Pseudonocardia	bacteria	Actinomycetia
Escovopsis	fungus	Sordariomycetes
Gluconobacter	bacteria	Alphaproteobacteria
Dysgonomonas	bacteria	Bacteroidia
Comamonas	bacteria	Betaproteobacteria
Parabacteroides	bacteria	Bacteroidia
Prevotella	bacteria	Bacteroidia
Erwinia	bacteria	Gammaproteobacteria
Rhizobium	bacteria	Alphaproteobacteria
Weisella	bacteria	Bacillota
Klebsiella	bacteria	Gammaproteobacteria
Pantoea	bacteria	Gammaproteobacteria
Syncephalastrum	fungus	Mucoromycetes
Clavispora	fungus	Saccharomycetes
Acinetobacter	bacteria	Gammaproteobacteria
Bacillus	bacteria	Bacilli
Asaia	bacteria	Alphaproteobacteria
Chitinophaga	bacteria	Bacteroidia
Chryseobacterium	bacteria	Bacteroidia

Paraburkholderia	bacteria	Betaproteobacteria
Trichosporon	fungus	Tremellomycetes
Pichia	fungus	Saccharomycetes
Rhodosporidium	fungus	Microbotryomycetes
Apiotrichum	fungus	Tremellomycetes
Cutaneotrichosporon	fungus	Tremellomycetes
Debaryomyces	fungus	Saccharomycetes
Papiliotrema	fungus	Tremellomycetes
Rhodotorula	fungus	Microbotryomycetes
Trichomonascus	fungus	Saccharomycetes
Serratia	bacteria	Gammaproteobacteria
Enterobacteriaceae	bacteria	Gammaproteobacteria
Saccharomyces	fungus	Saccharomycetes
Streptomyces	bacteria	Actinomycetia
Amycolatopsis	bacteria	Actinomycetia
Kribella	bacteria	Actinomycetia
Tsukamurella	bacteria	Actinomycetia
Nocardioides	bacteria	Actinomycetia
Mycobacterium	bacteria	Actinomycetia
Microbacterium	bacteria	Actinomycetia

3.9 References

Alcock, B. P., Raphenya, A. R., Lau, T. T. Y., Tsang, K. K., Bouchard, M., Edalatmand, A., Huynh, W., Nguyen, A.-L. V., Cheng, A. A., Liu, S., Min, S. Y., Miroshnichenko, A., Tran, H.-K., Werfalli, R. E., Nasir, J. A., Oloni, M., Speicher, D. J., Florescu, A., Singh, B., … McArthur, A. G. (2020). CARD 2020: antibiotic resistome surveillance with the comprehensive antibiotic resistance database. *Nucleic Acids Research*, *48*(D1), D517–D525.

Aylward, F. O., Suen, G., Biedermann, P. H. W., Adams, A. S., Scott, J. J., Malfatti, S. A., Glavina del Rio, T., Tringe, S. G., Poulsen, M., Raffa, K. F., Klepzig, K. D., & Currie, C. R. (2014). Convergent bacterial microbiotas in the fungal agricultural systems of insects. *MBio*, *5*(6), e02077.

Barcoto, M. O., Carlos-Shanley, C., Fan, H., Ferro, M., Nagamoto, N. S., Bacci, M., Jr, Currie, C. R., & Rodrigues, A. (2020). Fungus-growing insects host a distinctive microbiota apparently adapted to the fungiculture environment. *Scientific Reports*, *10*(1), 12384.

Barcoto, M. O., Pedrosa, F., Bueno, O. C., & Rodrigues, A. (2017). Pathogenic nature of *Syncephalastrum* in *Atta sexdens rubropilosa* fungus gardens. *Pest Management Science*, *73*(5), 999–1009.

Buchfink, B., Reuter, K., & Drost, H.-G. (2021). Sensitive protein alignments at tree-of-life scale using DIAMOND. *Nature Methods*, *18*(4), 366–368.

Carreiro, S. C., Pagnocca, F. C., Bueno, O. C., Júnior, M. B., Hebling, M. J. A., & da Silva, O. A. (1997). Yeasts associated with nests of the leaf-cutting ant *Atta sexdens rubropilosa Forel*, 1908. *Antonie van Leeuwenhoek*, *71*(3), 243–248.

Currie, C. R., Mueller, U. G., & Malloch, D. (1999). The agricultural pathology of ant fungus gardens. *Proceedings of the National Academy of Sciences of the United States of America*, *96*(14), 7998–8002.

Danecek, P., Bonfield, J. K., Liddle, J., Marshall, J., Ohan, V., Pollard, M. O., Whitwham, A., Keane, T., McCarthy, S. A., Davies, R. M., & Li, H. (2021). Twelve years of SAMtools and BCFtools. *GigaScience*, *10*(2). https://doi.org/10.1093/gigascience/giab008

Duarte, A. P. M., Attili-Angelis, D., Baron, N. C., Forti, L. C., & Pagnocca, F. C. (2014). Leaf-cutting ants: an unexpected microenvironment holding human opportunistic black fungi. *Antonie van Leeuwenhoek*, *106*(3), 465–473.

Duarte, A. P. M., Ferro, M., Rodrigues, A., Bacci, M., Nagamoto, N. S., Forti, L. C., & Pagnocca, F. C. (2016). Prevalence of the genus *Cladosporium* on the integument of leaf-cutting ants characterized by 454 pyrosequencing. *Antonie van Leeuwenhoek, International Journal of General and Molecular Microbiology*, *109*(9), 1235–1243.

Fernando Carlos Pagnocca, Andre Rodrigues, Nilson S. Nagamoto, & Maurício Bacci. (2008). Yeasts and filamentous fungi carried by the gynes of leaf-cutting ants. *Antonie van Leeuwenhoek*, *94*(4), 517–526.

Francoeur, C. B., Khadempour, L., Moreira-Soto, R. D., Gotting, K., Book, A. J., Pinto-Tomás, A. A., Keefover-Ring, K., & Currie, C. R. (2020). Bacteria Contribute to Plant Secondary Compound Degradation in a Generalist Herbivore System. *MBio*, *11*(5).

https://doi.org/10.1128/mBio.02146-20

Galperin, M. Y., Wolf, Y. I., Makarova, K. S., Vera Alvarez, R., Landsman, D., & Koonin, E. V. (2021). COG database update: focus on microbial diversity, model organisms, and widespread pathogens. *Nucleic Acids Research*, *49*(D1), D274–D281.

Grigoriev, I. V., Nordberg, H., Shabalov, I., Aerts, A., Cantor, M., Goodstein, D., Kuo, A., Minovitsky, S., Nikitin, R., Ohm, R. A., Otillar, R., Poliakov, A., Ratnere, I., Riley, R., Smirnova, T., Rokhsar, D., & Dubchak, I. (2012). The genome portal of the Department of Energy Joint Genome Institute. *Nucleic Acids Research*, *40*(Database issue), D26-32.

Irber, L., Brooks, P. T., Reiter, T., Tessa Pierce-Ward, N., Hera, M. R., Koslicki, D., & Titus Brown, C. (2022). Lightweight compositional analysis of metagenomes with FracMinHash and minimum metagenome covers. In *bioRxiv* (p. 2022.01.11.475838). https://doi.org/10.1101/2022.01.11.475838

Kalvari, I., Nawrocki, E. P., Argasinska, J., Quinones-Olvera, N., Finn, R. D., Bateman, A., & Petrov, A. I. (2018). Non-Coding RNA Analysis Using the Rfam Database. *Current Protocols in Bioinformatics / Editoral Board, Andreas D. Baxevanis ... [et Al.]*, *62*(1), e51.

Kalvari, I., Nawrocki, E. P., Ontiveros-Palacios, N., Argasinska, J., Lamkiewicz, K., Marz, M., Griffiths-Jones, S., Toffano-Nioche, C., Gautheret, D., Weinberg, Z., Rivas, E., Eddy, S. R., Finn, R. D., Bateman, A., & Petrov, A. I. (2021). Rfam 14: expanded coverage of metagenomic, viral and microRNA families. *Nucleic Acids Research*, *49*(D1), D192–D200.

Khadempour, L., Fan, H., Keefover-Ring, K., Carlos-Shanley, C., Nagamoto, N. S., Dam, M. A., Pupo, M. T., & Currie, C. R. (2020). Metagenomics Reveals Diet-Specific Specialization of Bacterial Communities in Fungus Gardens of Grass- and Dicot-Cutter Ants. *Frontiers in Microbiology*, *11*, 570770.

Kopac, S., Beatty, H., Gialopsos, P., Huntemann, M., Clum, A., Spunde, A., Pillay, M., Palaniappan, K., Varghese, N., Mikhailova, N., Stamatis, D., Reddy, T. B. K., Daum, C., Ng, V., Ivanova, N., Kyrpides, N., Woyke, T., & Klassen, J. L. (2018). High-Quality Draft Genome Sequences of Eight Bacteria Isolated from Fungus Gardens Grown by *Trachymyrmex septentrionalis* Ants. *Microbiology Resource Announcements*, *7*(2). https://doi.org/10.1128/MRA.00871-18

Li, H., & Durbin, R. (2009). Fast and accurate short read alignment with Burrows-Wheeler transform. *Bioinformatics* , *25*(14), 1754–1760.

Little, A. E. F., & Currie, C. R. (2008). Black yeast symbionts compromise the efficiency of antibiotic defenses in fungus-growing ants. *Ecology*, *89*(5), 1216–1222.

Möller, A. (1893). *Die Pilzgärten einiger südamerikanischer Ameisen*. Fischer.

Moreno, L. F., Stielow, J. B., de Vries, M., Weiss, V. A., Vicente, V. A., & de Hoog, S. (2015). Draft Genome Sequence of the Ant-Associated Fungus Phialophora attae (CBS 131958). *Genome Announcements*, *3*(6). https://doi.org/10.1128/genomeA.01099-15

Nawrocki, E. P., & Eddy, S. R. (2013). Infernal 1.1: 100-fold faster RNA homology searches. *Bioinformatics* , *29*(22), 2933–2935.

Nordberg, H., Cantor, M., Dusheyko, S., Hua, S., Poliakov, A., Shabalov, I., Smirnova, T., Grigoriev,

I. V., & Dubchak, I. (2014). The genome portal of the Department of Energy Joint Genome Institute: 2014 updates. *Nucleic Acids Research*, *42*(Database issue), D26-31.

Pinto-Tomás, A. A., Anderson, M. A., Suen, G., Stevenson, D. M., Chu, F. S. T., Cleland, W. W., Weimer, P. J., & Currie, C. R. (2009). Symbiotic nitrogen fixation in the fungus gardens of leaf-cutter ants. *Science*, *326*(5956), 1120–1123.

Rodrigues, A., Cable, R. N., Mueller, U. G., Bacci, M., Jr, & Pagnocca, F. C. (2009). Antagonistic interactions between garden yeasts and microfungal garden pathogens of leaf-cutting ants. *Antonie van Leeuwenhoek*, *96*(3), 331–342.

Salter, S. J., Cox, M. J., Turek, E. M., Calus, S. T., Cookson, W. O., Moffatt, M. F., Turner, P., Parkhill, J., Loman, N. J., & Walker, A. W. (2014). Reagent and laboratory contamination can critically impact sequence-based microbiome analyses. *BMC Biology*, *12*, 87.

Titus Brown, C., & Irber, L. (2016). sourmash: a library for MinHash sketching of DNA. *Journal of Open Source Software*, *1*(5), 27.

Vasse, M., Voglmayr, H., Mayer, V., Gueidan, C., Nepel, M., Moreno, L., de Hoog, S., Selosse, M.-A., McKey, D., & Blatrix, R. (2017). A phylogenetic perspective on the association between ants (Hymenoptera: Formicidae) and black yeasts (Ascomycota: Chaetothyriales). *Proceedings. Biological Sciences / The Royal Society*, *284*(1850). https://doi.org/10.1098/rspb.2016.2519

Chapter 4: *Candida* yeasts in the *Azteca-Cecropia* mutualism

Kirsten Gotting[1,2] and Bunyaporn Zeng[1], Taise T. H. Fukuda[3], Camila F. Pereira[3], Weilan G. P. Melo[3], Monica Tallarico Pupo[3], Chris T. Hittinger[2], Cameron R. Currie[1,4]

This chapter is in preparation for submission for publication, pending minor changes.
Supplemental material for this chapter can be found in Appendix 3 of this dissertation. Dataset S1 can be found on FigShare (10.6084/m9.figshare.21652325).

Affiliations:
[1]Department of Bacteriology, University of Wisconsin-Madison, Madison, 53706, WI, USA
[2]Laboratory of Genetics, University of Wisconsin-Madison, Madison, 53706, WI, USA
[3]School of Pharmaceutical Sciences of Ribeirão Preto, University of São Paulo, Ribeirão Preto, 14040-903, SP, Brazil
[4]McMaster University, Department of Biochemistry and Biomedical Sciences, Hamilton, Ontario

Author Contributions:
K.G., B.Z., M.T.P., C.T.H, C.R.C. designed research; K.G., B.Z., T.T.H.F., C.F.P., W.G.P.M. performed research; K.G., B.Z., analyzed data; K.G., B.Z., C.R.C. wrote the paper.

4.1 Abstract

Interactions between microbes and insect hosts are widespread in nature. The presence of microorganisms in insect host has been reported to play key roles in nutrient acquisition and detoxifications. While many studies have examined these associations in bacterial-insect interactions, fewer studies have looked at interactions between fungal symbionts and their hosts. Symbiotic fungi involved in the myrmecophytic mutualistic relationship between *Azteca* ants and *Cecropia* plants has been reported. We performed fieldwork to examine microbes associated with this symbiosis and assayed them for bioactivity. Here, we show that *Candida* isolated from the *Azteca*/*Cecropia* mutualism have bioactivity against other yeast fungi. We sequenced the genomes of these yeasts and found that they form two clades within the CUG-Ser1 clade of

yeasts. We report two BGCs found in these *Candida*, one most like a squalane synthase inhibitor, and one most like a metallophore. These molecules may be modalities by which these *Candida* maintain a competitive presence amongst the microbial communities in the fungal cartons formed by *Azteca* ants. Our results demonstrate how fungal associates of insects may contain different types of BGCs as compared to evolutionarily similar yeasts.

4.2 Introduction

Organisms exist in communities that are mediated by diverse ways of interactions. Microbes use specialized molecules that have various impacts on neighboring microbes. These molecules are encoded in the genome by clustered gene modules called biosynthetic gene clusters (BGCs), and likely play a role in how microbial communities are structured and how they function (Chevrette et al., 2022). Many microbes associate with insects. These associations take on many forms and are often beneficial to both partners, particularly in nutrient acquisition and detoxification. For example, the pea aphid *Acyrthosiphon pisum* and endosymbiont *Buchnera* for synthesizing amino acids (Munson et al., 1991). Other insects rely on fungi for a food source, such as seen in relationships between fungus-growing ants and termites, as well as ambrosia beetles (Li et al., 2021). Finally, detoxification of plant toxins are exemplified in yeasts and the cigarette beetle *Ladioderma serricorne* (Dowd & Shen, 1990) as well as the gut microbes in the pine weevil, *Hylobius abietis* (Berasategui et al., 2017). These relationships underscore how microbes often drive adaptations in insects and can be a strong framework for understanding interactions between organisms in communities.

Azteca ants live in an ancient association with the neotropical trees of the genus *Cecropia* (Cecropiaceae). In this myrmecophytic mutualistic relationship both species receive protection and exchange nutrients. The ants protect the trees from predators (Marting et al., 2018; Wcislo et al., 2021), while the trees provide the ants with food and shelter (Bischof et al., 2013). This relationship is beneficial to plant growth (Oliveira et al., 2015; Schupp, 1986). Inside of the trees where the ants live, there are suites of diverse microbes in 'fungal patches'. These microbial communities are vertically transmitted between colonies by new founder ant queens (Mayer et al., 2018), and are primarily composed of Proteobacteria, Gemmatimonadetes, Ascomycetes, and Basidiomycetes (Lucas et al., 2019). Several of these taxa have been studied more deeply, for example, *Azteca* ants are associated with specific strains of Chaetothyriales fungi (Nepel et al., 2016; Vasse et al., 2017), these fungi alter the volatile chemistry with *Cecropia* trees (Mayer et al., 2021). Additionally, bacteria in the genera *Pantoea*, *Rhizobium*, *Methylobacterium*, *Pseudomonas*, and *Streptomyces* are frequently isolated from these fungal patches (Fukuda et al., 2021).

Here, we used an interdisciplinary approach with field work, microbiology, and genomics to examine microbial associates in the *Azteca/ Cecropia* symbiosis. We collected fungal patches from *Cecropia* trees in Brazil. From these fungal patches, we isolated *Candida* strains from different *Cecropia* host trees and assayed these strains for bioactivity. We then conduct genome sequencing and explore if there could be loci associated with detected bioactivity. We reconstruct their phylogenetic relationships amongst other yeasts, characterize the BGCs in these

strains, and compare their BGCs to other phylogenetically diverse yeasts. We expect that given the vertical transmission by founder queens, these *Candida* will form a monophyletic clade and will likely contain a similar set of BGCs.

4.3 Results

4.3.1 Presence and bioactivity of *Candida*

Fieldwork to explore microbes potentially associated with the *Azteca-Cecropia* symbiosis was performed in 2017 in Brazil. We isolated strains from fungal patches of four *Cecropia* hosts collected in Brazil. Fungal strains ICBGSID1880 and ICBGSID1889 were isolated from fungal patches in *Cecropia pachystachya Trécul* hosts in Itatiaia Nacional Park, while strains ICBGSID1896 and ICBGSID1897 were isolated from fungal patches in *Cecropia latifolia Miq* hosts in Anavilhanas national park. To determine if these strains have antifungal activity, we tested strains using a bioassay pipeline to screen for inhibitory activity against several fungal and bacterial pathogens. Four strains that had strong antifungal activity towards yeasts were selected for genome sequencing (Fig. S1, S2). These strains had a score of 2/3 for inhibition of two *Candida* strains, and a score of one against *Cryptococcus neoformans*. ICBGSID1880 also had a score of one against a strain of *Trichoderma*. LSU sequencing of these strains indicated them to be likely related to *Candida pseudointermedia* (ICBGSID1896), *Candida blattae* (ICBGSID1889), *Candida picinguabensis* (ICBGSID1880), and *Candida intermedia* (ICBGSID1897).

4.3.2 Genome statistics

Four genomes from *Candida* yeasts were sequenced at an average of 1,005,252,233 base pairs per isolate. The genomes assembled to an average length of 12.5 megabases, have an average of 964 contigs, with an average of 27 contigs greater than 10 kilobases in length. The mean N50 for these genomes is 1.02 megabases, with mean GC content of 45%. These genomes were also assessed for completeness using benchmarked universal single-copy orthologs from BUSCO, and on average were 95.2% complete (Dataset 1).

4.3.3 Phylogenetic analysis of yeast genomes.

We conducted phylogenomic analyses for the four strains in this study with 305 yeast genomes previously used to study genome evolution across the budding yeast subphylum (Shen et al., 2018). 112 BUSCO genes were aligned with mafft resulting in 465016 base-pairs aligned, and individual gene trees were constructed with iqtree2. The resulting 112 trees were used as input for the coalescent tree builder ASTRAL. Our astral phylogeny indicates that the four yeast strains isolated from Azteca ants fall within the CUG-Ser1 clade, which contains fungal pathogens *Candida auris* and *Candida albicans*. Three azteca-associated yeasts clade together with a genome from *Candida blattae*, a species found in association with other insects (Nguyen et al., 2007), and additionally, *Candida fructus* and *Clavispora lusitaniae*. The fourth azteca-ant-associated strain genome is phylogenetically basal within another clade composed of *Candida wancherniae*, *Candida golubevii*, *Metschnikowia bicuspidata*, *Candida hawaiiana*, *Metschnikowia kipukae*, as well as several other *Metschnikowia* species (Fig. 2).

4.3.4 Identification of biosynthetic gene clusters

1184 yeast genomes from the budding yeast class Saccharomycetes were surveyed for BGCs, including the four genomes from this study. Of these genomes, 995 contained at least one BGC. Of these, 349 genomes contained one BGC, 405 genomes contained 2 BGCs, 181 genomes contained 3 BGCs, 57 genomes contained four BGCs, and three genomes contained five or more BGCs but no more than eight BGCs. Network analysis of these BGCs indicates that these genomes largely contain two BGC classes. The two BGC classes represented were Terpenes with 878 annotated BGCs, and NRPSs with 742 annotated BGCs. Among 742 annotated NRPSs, 176 are annotated singletons, while 355 cluster into eleven families containing ten or more BGCs. Among the 878 annotated Terpenes, 199 are singletons, while 442 cluster into 14 families containing ten or more BGCs (Fig. 3, Dataset 2). None of the annotated BGCs have similarity to BGCs in the MIBiG database (Dataset 2).

All four genomes in this study contained two annotated BGCs, one annotated as an NRPS and one annotated as a Terpene classification. Each NRPS is most similar (score of either 0.21, or 0.2) to MIBIG BGC0001900.1, which encodes a metallophore called fragin from *Burkholderia*. Each terpene is most similar (score: 0.38) to MIBIG BGC0001839.1, which encodes squalestatin S1 from *Aspergillus*, which inhibits squalane synthase, a step in the cholesterol and ergosterol biosynthesis pathways. In analyzing these BGCs with a network, they cluster together into one clan and five families; three families primarily classified as terpenes, with two families primarily

classified as NRPSs. The NRPS BGC in each genome contains three domains: an AMP binding domain (PF00501), a phosphopantetheine binding domain (PF00550) predicted to be inactive, and an NAD binding domain (PF07993). These three domains compose the NRPS module. The Terpene BGC in each genome contains four domains across all genomes: an aldo/keto reductase (PF00248), a squalene/phytoene synthase (PF00494), a ras domain (PF00071), and a calcineurin-like phosphoesterase (PF00149) (Fig. 4).

4.3.5 Similarity of biosynthetic gene clusters in other yeasts

Our network analysis shows that the NRPS BGCs form three families. FAM_02537 contains the NRPS from ICBGSID1889, which is most similar to an NRPS from *Candida blattae* (Fig. 5). This family also contains a BGC from phylogenetically close (Fig. 3) yeasts *Candida oregonensis*, *Candida blattae*, and *Candida hawaiiana*. However, in the 'mixed' network analysis the BGC's from *Candida blattae* and *Candida hawaiiana* end up in a separate clan, indicating a difference in BGC structure (Fig. S4). FAM_02440 contains the NRPS from ICBGSID1880, which is most similar to several NRPS' from *Candida thailandica*, *Candida heveicola*, *Candida duobushaemulonis*, and two NRPS' from *Candida pseudohaemulonis* strains. This family also contains BGCs from *Danielozyma ontarioensis*, and other more distantly related fungi (Fig. S3, S4). FAM_02392 contains NRPS' from ICBGSID1897 and ICBGSID1896 which are most similar to NRPS' from *Clavispora* sp. NYNU 161120 and *Clavispora fructus*. This family also contains BGCs from *Hyphopichia burtonii*, *Candida gotoi*, and *Hyphopichia heimii*, which are evolutionarily close

to azteca-associated yeast strains (Fig. S3, S4). In examining the families formed for terpene BGCs, three families are formed. FAM_03865 contains the terpene from ICBGSID1889 and a terpene from *Candida blattae*. FAM_03863 contains the terpene from ICBGSID1880. FAM_03866 contains the terpenes from ICBBSID1896 and ICBGSID1897 (Fig. 5, Fig. S4).

4.4 Discussion

In this study, we isolated four strains of *Candida* from *Azteca-Cecropia* fungal patches. These strains had bioactivity against other fungi. *Candida* generally have broad ecological representation, and can be commensal or sometimes pathogenic (Odds, 1984). Yeasts are predicted to play various roles in their relationships with insects, including being a food source to various insects (Madden et al., 2018). The *Candida* in the *Azteca-Cecropia* fungal patches could potentially be a food source for *Azteca* ants or could have roles associated with the growth of these fungal patches, given that they inhibit the growth of other fungi.

Additionally, we present the first genomes and analysis of *Candida* associated with the *Azteca-Cecropia* mutualism. These genomes are on average 12.5 mb, which is similar to the average genomes size seen in other yeasts (Shen et al., 2018). These genomes demonstrate that these *Candida* are similar to other *Candida blattae*, which were originally identified in association with other insects (Nguyen et al., 2007) (Fig. 2).

We identified two BGCs in each of these genomes, which have similarity to NRPS and terpene BGCs found in other yeast genomes. While terpenes amongst the yeasts in this study are relatively divergent, with many families containing only two BGCs, the terpene in particular is

divergent compared to terpenes in other yeasts (Fig. 3), with the only non-azteca yeast containing a similar terpene is from insect-associated *Candida blattae*. The NRPS on the other hand, had higher levels of similarity amongst other yeast NRPSs. This result could indicate that the NRPS may be foundational to the biology of certain yeasts, while the terpenes may be more specific to finer levels of ecology.

While these BGCs have similarity to other BGCs on a broad scale, they are not as similar on a finer scale, with the patterns of similarity not recapitulating the phylogenetic patterns of these genomes (Fig. 5). This has also been seen in other analyses of these loci, which show that evolution of these BGCs can vary on a geographic scale and may not be consistent with the evolutionary patterns across the rest of the genome (Mcdonald et al., 2019).

While other microbes have been studied and isolated from this mutualism, the role of *Candida* yeasts has not yet been explored. The *Candida* isolated in this study was most like other *Candida* associated with insects, which could indicate an underlying genotype of yeasts that associate with insects. These yeasts could have many roles, including chemical detoxification, or defensives against pathogens, or nutrient acquisition. Overall, more studies into these yeasts will be necessary for understanding their role in the *Azteca-Cecropia* symbiosis.

4.5 Methods

4.5.1 Sample collection and strain isolation

We collected samples from Brazil in 2017. Isolates were maintained in 30% (v/v) glycerol stocks at -80°C. For DNA extraction and co-culture inhibition bioassays, frozen glycerol isolate stocks were plated onto Petri dishes containing ISP Medium 2 (Difco) and incubated at 28°C for 5 days in June 2022.

4.5.2 Co-culture Inhibition Bioassay

Pairwise interactions against diverse fungi (*Candida albicans, Candida* sp., *Metarhizium* sp., *Trichoderma* sp., *Rhizopus oryzae,* and *Aspergillus flavus)* were carried out using previously described methods (Chevrette et al., 2019; Temkin et al., 2019). Briefly, isolates were inoculated onto each well containing 3mL of yeast peptone mannitol (YPM) agar (2g yeast extract, 2g peptone, 4g mannitol, 15g agar, 1L H_2O) and incubated at 28°C for 5 days prior to the addition of tested fungi. Yeast fungi (*Candida albicans* and *Candida* sp) were inoculated in 3mL of yeast peptone dextrose (YPD) and shaken overnight at 28°C and diluted 1:10. For tested filamentous fungi (*Metarhizium* sp., *Trichoderma* sp., *Rhizopus oryzae,* and *Aspergillus flavus)*, spore stocks of each fungal strains were diluted 1:10. 3µL of diluted cultures were used to inoculate in the center of the well, and plates were maintained at 28°C for 7 days. Inhibition were scored based on the level of inhibition (0—no inhibition, 1—slight inhibition, 2—presence of a zone of inhibition, 3—complete inhibition).Results were plotted with pheatmap (Kolde, 2019).

4.5.3 DNA Extraction, Library prep and Sequencing

Genomic DNA was extracted from isolates using the MasterPure Yeast DNA Purification Kit according to manufacturer's specifications (Lucigen). Genomes were sequenced at the Microbial Genomes Sequencing Center in June, 2022. Libraries were prepared with the Illumina DNA Prep kit abd UDT 10bp UDI indices. These libraries were sequenced with the Illumina NextSeq 2000 machine, with 2X151bp reads. Reads were demultiplexed, quality controlled, and adapter trimmed with bcl-convert v3.9.3 (Illumina, 2021). LSU sequences were aligned the 'nt' database using NCBI BLASTn (Altschul et al., 1990; Camacho et al., 2009) to determine initial species predictions.

4.5.4 Genome assembly and BGC annotation

Raw reads were trimmed using fastp v.0.19.5 with the options "--detect_adapter_for_pe --trim_poly_g --trim_poly_x -p" (Chen et al., 2018). Trimmed reads were used for genome assembly with SPAdes v3.15.4 with option "--isolate" (Bankevich et al., 2012). Genomes were assessed for completeness using BUSCO v5.4.3 against the ascomycota_odb10 database (Manni et al., 2021). BGCs were annotated with antiSMASH v.6.1 (Blin et al., 2021), and assessed for similarity with BiG-SCAPE v.1.1.2 (Navarro-Muñoz et al., 2020). Families were defined at a distance cutoff of 0.3, and clans were defined using a distance cutoff of 0.7.

4.5.5 Phylogenetic analysis

Genes identified with BUSCO (Manni et al., 2021) were aligned for all genomes using MAFFT v7.475 (Katoh et al., 2002; Katoh & Standley, 2013) and trimmed with trimAL v.1.2 (Capella-Gutiérrez et al., 2009). IQtree2 v. 2.1.2 (Minh et al., 2020) was used to construct individual gene trees, which were then used for constructing a coalescent based phylogeny with Astral v.5.7.7 (Rabiee et al., 2019; Sayyari & Mirarab, 2016). The resulting phylogenetic tree was visualized using FigTree (*FigTree*, n.d.).

4.6 Acknowledgements

This material is based on work supported in part by National Institutes of Health grant U19 TW009872, National Institutes of Health grant U19 AI142720, and National Science Foundation grant DEB-1927155, and São Paulo Research Foundation (FAPESP) grant # 2013/50954-0. Additional support was granted to K.G. through the Big Ten Academic Alliance Smithsonian Fellowship through the Smithsonian Tropical Research Institute.

4.7 Figures

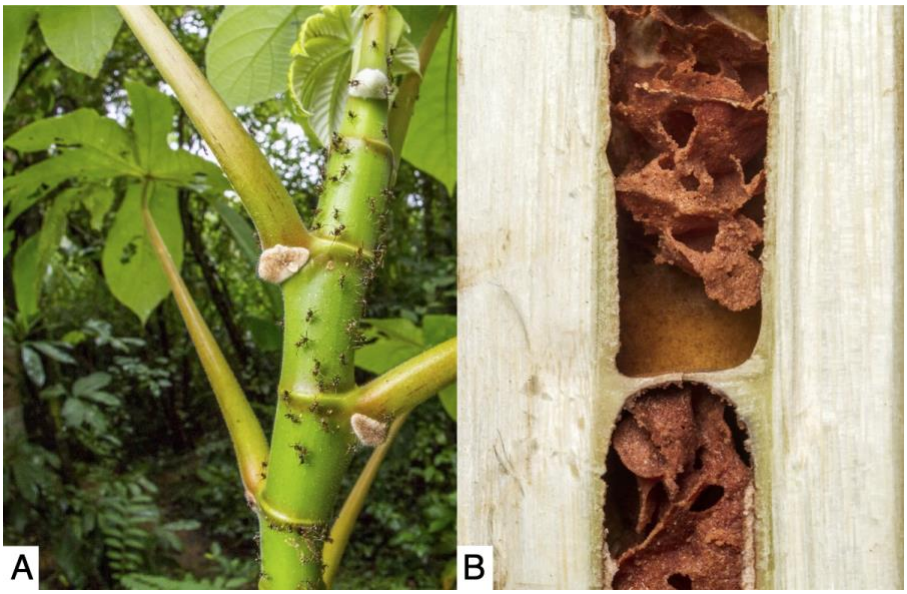

Figure 1. A) Azteca ants live in an ancient association with cecropia trees. B) The azteca ants build cartons inside of the trees, which serve as their home. Photos by Alex Wild.

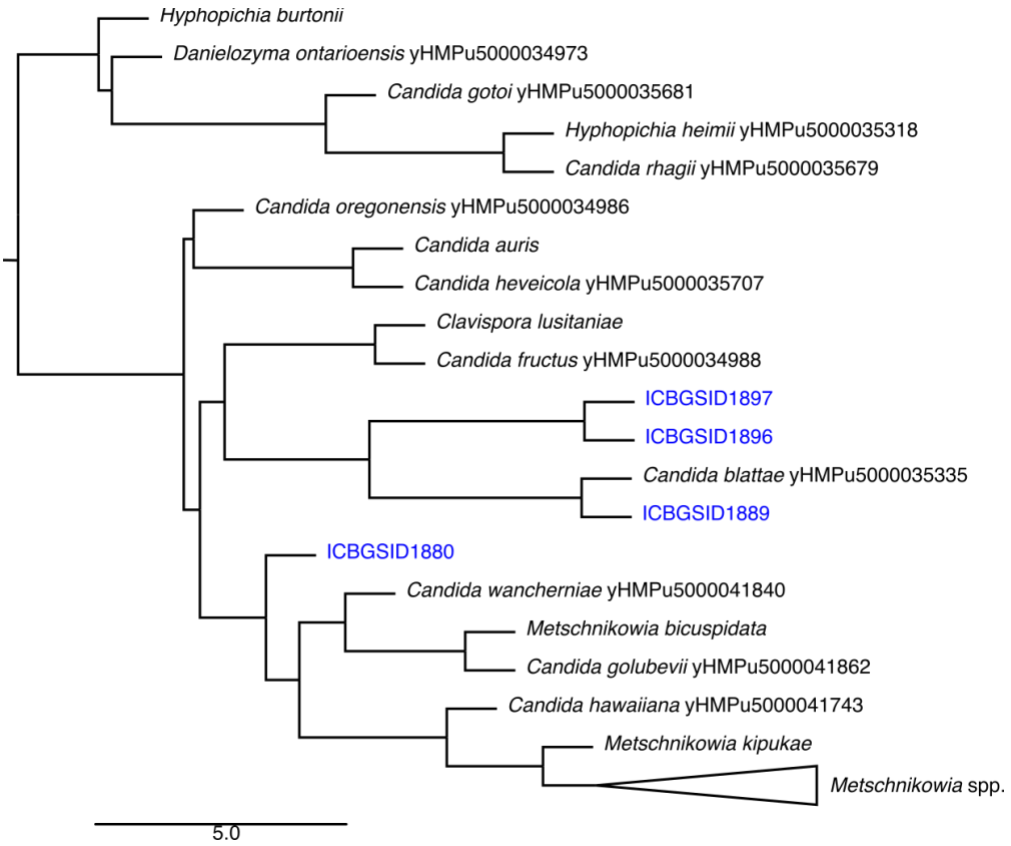

Figure 2. Phylogeny of azteca-associated yeasts amongst other yeast genomes. Azteca-associate yeasts are highlighted in blue.

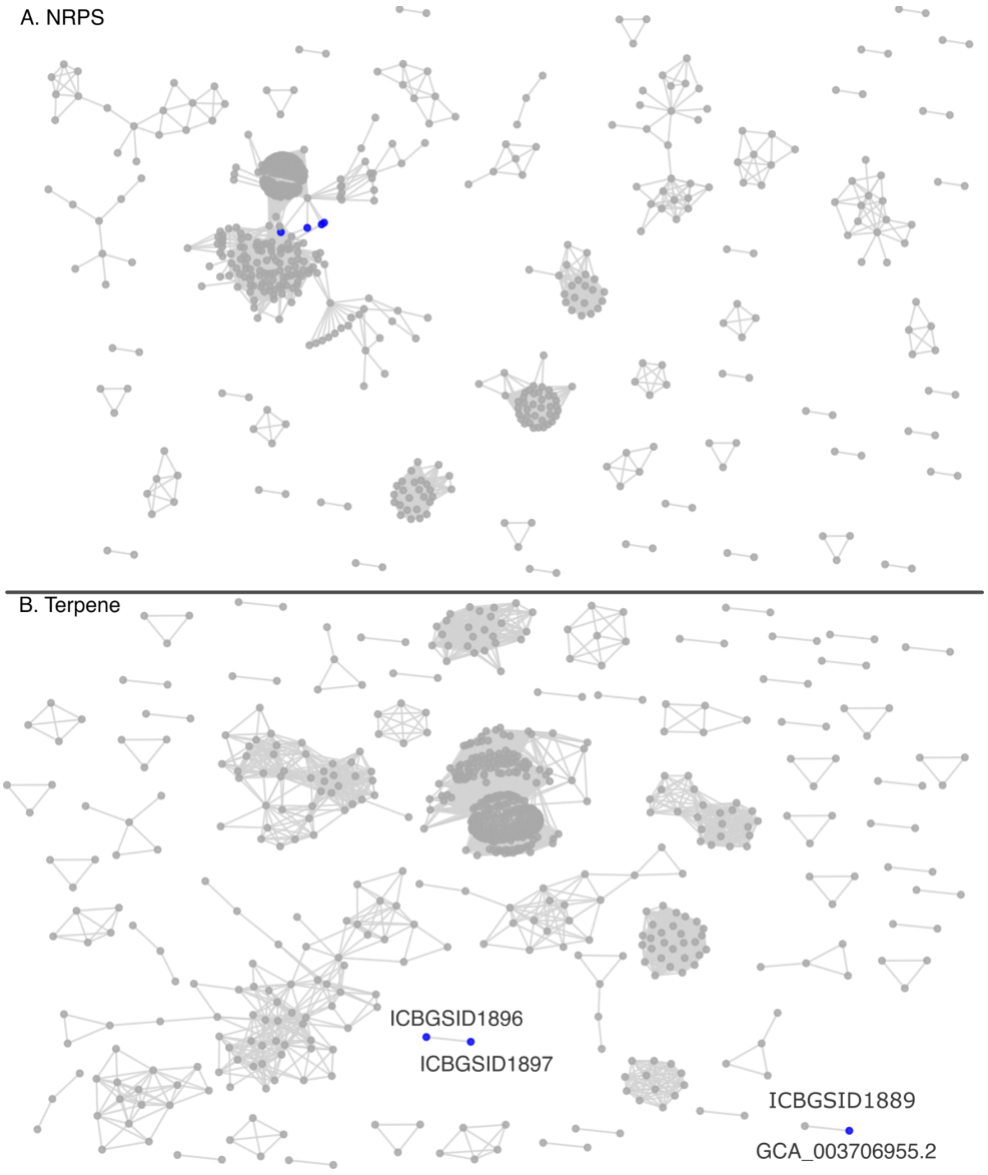

Figure 3. Network analysis of BGCs in 1188 yeast genomes. Gray dots indicate one BGC, and connections represent the similarity within a distance of 0.3 similarity. A) Subnetwork of NRPS BGCs. BGCs from yeasts associated with azteca ants are highlighted in blue. B) Subnetwork of terpene BGCs. BGCs in families with BGCs from yeasts associated with azteca ants are highlighted in blue and labeled.

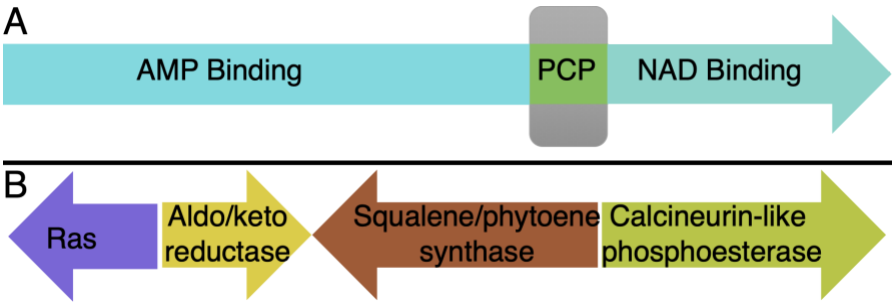

Figure 4. Domain structures for A) NRPS BGCs and B) Terpene BGCs found in yeast genomes associated with azteca ants. Colors represent different active domains. Arrows indicate if the domains are on the same or different genes in a region. The gray box around the PCP domain indicates that this domain is predicted to be inactive.

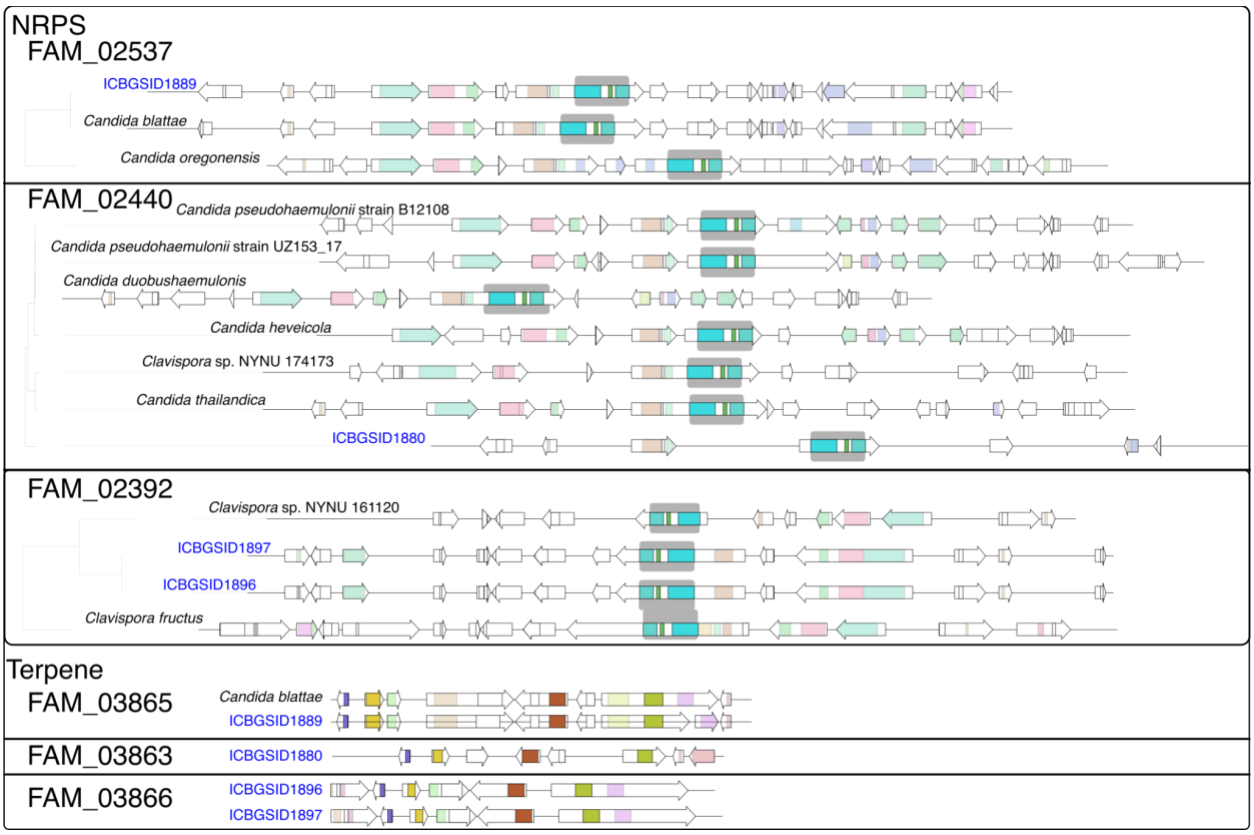

Figure 5. NRPS and terpene BGC families with similarities to BGCs from other yeast genomes. Saturated colors indicate the active domains presented in figure 4. Unsaturated colors indicate other biosynthetic domains. The gray box indicates the core biosynthetic module.

4.8 Dataset 1

Metadata for *Candida* yeast collections and genomes

Candida Strain Collection Details					
Strain ID	Host ID	Collection Site	GPS	Host	Collection Date
ICBGSID1880	ICBGHID2940	Itatiaia Nacional Park	S 22o26'706" W 44o36'573"	*Cecropia pachystachya Trécul.*	2017
ICBGSID1889	ICBGHID2938	Itatiaia Nacional Park	S 22o27'050" W 44o36'833"	*Cecropia pachystachya Trécul.*	2017
ICBGSID1896	ICBGHID2941	Parque Nacional de Anavilhanas	S02o36'37.7" W60o52'31.3"	*Cecropia latifolia Miq.*	2017
ICBGSID1897	ICBGHID2942	Parque Nacional de Anavilhanas	S 02o36'36.7" W 60o52'31.3"	*Cecropia latifolia Miq.*	2017

Candida genomes metadata							
Strain ID	Contigs	Contigs >= 10kb	Length	GC %	N50	Total Bases Sequenced	BUSCO stats
ICBGSID1880	1141	36	11984926	44.15	678792	825069780	C:93.1%[S:93.0%,D:0.1%],F:0.8%,M:6.1%,n:1706
ICBGSID1889	548	23	12001125	49.86	1136382	902157053	C:95.7%[S:95.6%,D:0.1%],F:0.5%,M:3.8%,n:1706
ICBGSID1896	1031	26	13172210	43.47	1019514	1506196929	C:96.1%[S:96.0%,D:0.1%],F:0.5%,M:3.4%,n:1706
ICBGSID1897	1137	26	13103613	43.49	1271339	787585168	C:96.0%[S:95.9%,D:0.1%],F:0.5%,M:3.5%,n:1706

4.9 References

Altschul, S. F., Gish, W., Miller, W., Myers, E. W., & Lipman, D. J. (1990). Basic local alignment search tool. *Journal of Molecular Biology*, *215*(3), 403–410.

Bankevich, A., Nurk, S., Antipov, D., Gurevich, A. A., Dvorkin, M., Kulikov, A. S., Lesin, V. M., Nikolenko, S. I., Pham, S., Prjibelski, A. D., Pyshkin, A. V., Sirotkin, A. V., Vyahhi, N., Tesler, G., Alekseyev, M. A., & Pevzner, P. A. (2012). SPAdes: a new genome assembly algorithm and its applications to single-cell sequencing. *Journal of Computational Biology: A Journal of Computational Molecular Cell Biology*, *19*(5), 455–477.

Berasategui, A., Salem, H., Paetz, C., Santoro, M., Gershenzon, J., Kaltenpoth, M., & Schmidt, A. (2017). Gut microbiota of the pine weevil degrades conifer diterpenes and increases insect fitness. *Molecular Ecology*, *26*(15), 4099–4110.

Bischof, S., Umhang, M., Eicke, S., Streb, S., Qi, W., & Zeeman, S. C. (2013). *Cecropia peltata* accumulates starch or soluble glycogen by differentially regulating starch biosynthetic genes. *The Plant Cell*, *25*(4), 1400–1415.

Blin, K., Shaw, S., Kloosterman, A. M., Charlop-Powers, Z., van Wezel, G. P., Medema, M. H., & Weber, T. (2021). antiSMASH 6.0: improving cluster detection and comparison capabilities. *Nucleic Acids Research*, *49*(W1), W29–W35.

Camacho, C., Coulouris, G., Avagyan, V., Ma, N., Papadopoulos, J., Bealer, K., & Madden, T. L. (2009). BLAST+: architecture and applications. *BMC Bioinformatics*, *10*(1), 421.

Capella-Gutiérrez, S., Silla-Martínez, J. M., & Gabaldón, T. (2009). trimAl: a tool for automated alignment trimming in large-scale phylogenetic analyses. *Bioinformatics* , *25*(15), 1972–1973.

Chen, S., Zhou, Y., Chen, Y., & Gu, J. (2018). fastp: an ultra-fast all-in-one FASTQ preprocessor. *Bioinformatics* , *34*(17), i884–i890.

Chevrette, M. G., Carlson, C. M., Ortega, H. E., Thomas, C., Ananiev, G. E., Barns, K. J., Book, A. J., Cagnazzo, J., Carlos, C., Flanigan, W., Grubbs, K. J., Horn, H. A., Hoffmann, F. M., Klassen, J. L., Knack, J. J., Lewin, G. R., McDonald, B. R., Muller, L., Melo, W. G. P., … Currie, C. R. (2019). The antimicrobial potential of *Streptomyces* from insect microbiomes. *Nature Communications*, *10*(1), 516.

Chevrette, M. G., Thomas, C. S., Hurley, A., Rosario-Meléndez, N., Sankaran, K., Tu, Y., Hall, A., Magesh, S., & Handelsman, J. (2022). Microbiome composition modulates secondary metabolism in a multispecies bacterial community. *Proceedings of the National Academy of Sciences*, *119*(42), e2212930119.

Dowd, P. F., & Shen, S. K. (1990). The contribution of symbiotic yeast to toxin resistance of the cigarette beetle (Lasioderma serricorne). *Entomologia Experimentalis et Applicata*, *56*(3), 241–248.

FigTree. (n.d.). Retrieved August 25, 2021, from http://tree.bio.ed.ac.uk/software/figtree/

Fukuda, T. T. H., Pereira, C. F., Melo, W. G. P., Menegatti, C., Andrade, P. H. M., Groppo, M., Lacava, P. T., Currie, C. R., & Pupo, M. T. (2021). Insights Into the Ecological Role of *Pseudomonas* spp. in an Ant-plant Symbiosis. *Frontiers in Microbiology*, *12*, 621274.

Illumina. (2021). *BCL Convert: a proprietary Illumina software for the conversion of BCL files to basecalls*.

Katoh, K., Misawa, K., Kuma, K.-I., & Miyata, T. (2002). MAFFT: a novel method for rapid multiple sequence alignment based on fast Fourier transform. *Nucleic Acids Research*, *30*(14), 3059–3066.

Katoh, K., & Standley, D. M. (2013). MAFFT multiple sequence alignment software version 7: improvements in performance and usability. *Molecular Biology and Evolution*, *30*(4), 772–780.

Kolde, R. (2019). *pheatmap: Pretty Heatmaps*. https://CRAN.R-project.org/package=pheatmap

Li, H., Young, S. E., Poulsen, M., & Currie, C. R. (2021). Symbiont-Mediated Digestion of Plant Biomass in Fungus-Farming Insects. *Annual Review of Entomology*, *66*, 297–316.

Lucas, J. M., Madden, A. A., Penick, C. A., Epps, M. J., Marting, P. R., Stevens, J. L., Fergus, D. J., Dunn, R. R., & Meineke, E. K. (2019). *Azteca* ants maintain unique microbiomes across functionally distinct nest chambers. *Proceedings. Biological Sciences / The Royal Society*, *286*(1908), 20191026.

Madden, A. A., Epps, M. J., Fukami, T., Irwin, R. E., Sheppard, J., Sorger, D. M., & Dunn, R. R. (2018). The ecology of insect-yeast relationships and its relevance to human industry. *Proceedings. Biological Sciences / The Royal Society*, *285*(1875). https://doi.org/10.1098/rspb.2017.2733

Manni, M., Berkeley, M. R., Seppey, M., Simão, F. A., & Zdobnov, E. M. (2021). BUSCO update: Novel and streamlined workflows along with broader and deeper phylogenetic coverage for scoring of eukaryotic, prokaryotic, and viral genomes. *Molecular Biology and Evolution*, *38*(10), 4647–4654.

Marting, P. R., Wcislo, W. T., & Pratt, S. C. (2018). Colony personality and plant health in the Azteca-Cecropia mutualism. *Behavioral Ecology: Official Journal of the International Society for Behavioral Ecology*, *29*(1), 264–271.

Mayer, V. E., de Hoog, S., Cristescu, S. M., Vera, L., & Prenafeta-Boldú, F. X. (2021). Volatile Organic Compounds in the Azteca/Cecropia Ant-Plant Symbiosis and the Role of Black Fungi. *Journal of Fungi (Basel, Switzerland)*, *7*(10). https://doi.org/10.3390/jof7100836

Mayer, V. E., Nepel, M., Blatrix, R., Oberhauser, F. B., Fiedler, K., Schönenberger, J., & Voglmayr, H. (2018). Transmission of fungal partners to incipient *Cecropia*-tree ant colonies. *PloS One*, *13*(2), e0192207.

Mcdonald, B. R., Chevrette, M. G., Klassen, J. L., Horn, H. A., Caldera, E. J., Wendt-Pienkowski, E., Cafaro, M. J., Ruzzini, A. C., Van Arnam, E. B., Weinstock, G. M., Gerardo, N. M., Poulsen, M., Suen, G., Clardy, J., & Currie, C. R. (2019). *Biogeography and Microscale Diversity Shape the Biosynthetic Potential of Fungus-growing Ant-associated Pseudonocardia*. https://doi.org/10.1101/545640

Minh, B. Q., Schmidt, H. A., Chernomor, O., Schrempf, D., Woodhams, M. D., von Haeseler, A., & Lanfear, R. (2020). IQ-TREE 2: New Models and Efficient Methods for Phylogenetic Inference in the Genomic Era. *Molecular Biology and Evolution*, *37*(5), 1530–1534.

Munson, M. A., Baumann, P., Clark, M. A., Baumann, L., Moran, N. A., Voegtlin, D. J., & Campbell, B. C. (1991). Evidence for the establishment of aphid-eubacterium endosymbiosis in an ancestor of four aphid families. *Journal of Bacteriology*, *173*(20), 6321–6324.

Navarro-Muñoz, J. C., Selem-Mojica, N., Mullowney, M. W., Kautsar, S. A., Tryon, J. H., Parkinson, E. I., De Los Santos, E. L. C., Yeong, M., Cruz-Morales, P., Abubucker, S., Roeters, A., Lokhorst, W., Fernandez-Guerra, A., Cappelini, L. T. D., Goering, A. W., Thomson, R. J., Metcalf, W. W., Kelleher, N. L., Barona-Gomez, F., & Medema, M. H. (2020). A computational framework to explore large-scale biosynthetic diversity. *Nature Chemical Biology*, *16*(1), 60–68.

Nepel, M., Voglmayr, H., Blatrix, R., Longino, J. T., Fiedler, K., Schönenberger, J., & Mayer, V. E. (2016). Ant-cultivated Chaetothyriales in hollow stems of myrmecophytic *Cecropia* sp. trees – diversity and patterns. *Fungal Ecology*, *23*, 131–140.

Nguyen, N. H., Suh, S.-O., & Blackwell, M. (2007). Five novel *Candida* species in insect-associated yeast clades isolated from Neuroptera and other insects. *Mycologia*, *99*(6), 842–858.

Odds, F. C. (1984). Ecology and epidemiology of *Candida* species. *Zentralblatt Fur Bakteriologie, Mikrobiologie, Und Hygiene. Series A, Medical Microbiology, Infectious Diseases, Virology, Parasitology*, *257*(2), 207–212.

Oliveira, K. N., Coley, P. D., Kursar, T. A., Kaminski, L. A., Moreira, M. Z., & Campos, R. I. (2015). The effect of symbiotic ant colonies on plant growth: a test using an *Azteca-Cecropia* system. *PloS One*, *10*(3), e0120351.

Rabiee, M., Sayyari, E., & Mirarab, S. (2019). Multi-allele species reconstruction using ASTRAL. *Molecular Phylogenetics and Evolution*, *130*, 286–296.

Sayyari, E., & Mirarab, S. (2016). Fast Coalescent-Based Computation of Local Branch Support from Quartet Frequencies. *Molecular Biology and Evolution*, *33*(7), 1654–1668.

Schupp, E. W. (1986). Azteca protection of *Cecropia*: ant occupation benefits juvenile trees. *Oecologia*, *70*(3), 379–385.

Shen, X.-X., Opulente, D. A., Kominek, J., Zhou, X., Steenwyk, J. L., Buh, K. V., Haase, M. A. B., Wisecaver, J. H., Wang, M., Doering, D. T., Boudouris, J. T., Schneider, R. M., Langdon, Q. K., Ohkuma, M., Endoh, R., Takashima, M., Manabe, R.-I., Čadež, N., Libkind, D., … Rokas, A. (2018). Tempo and Mode of Genome Evolution in the Budding Yeast Subphylum. *Cell*, *175*(6), 1533-1545.e20.

Temkin, M. I., Carlson, C. M., Stubbendieck, A. L., Currie, C. R., & Stubbendieck, R. M. (2019). High Throughput Co-culture Assays for the Investigation of Microbial Interactions. *Journal of Visualized Experiments: JoVE*, *152*. https://doi.org/10.3791/60275

Vasse, M., Voglmayr, H., Mayer, V., Gueidan, C., Nepel, M., Moreno, L., de Hoog, S., Selosse, M.-A., McKey, D., & Blatrix, R. (2017). A phylogenetic perspective on the association between ants (Hymenoptera: Formicidae) and black yeasts (Ascomycota: Chaetothyriales). *Proceedings. Biological Sciences / The Royal Society*, *284*(1850). https://doi.org/10.1098/rspb.2016.2519

Wcislo, A., Graham, X., Stevens, S., Toppe, J. E., Wcislo, L., & Wcislo, W. T. (2021). *Azteca* ants repair damage to their *Cecropia* host plants. *Journal of Hymenoptera Research*, *88*, 61–70.

Chapter 5: Conclusions and Future Directions

In this dissertation I explored the relationships of fungi in the fungus-growing ant and *Azteca* ant mutualisms. These mutualisms are model systems for studying symbiosis. This works contributes to this foundation by deeply diving into the evolutionary history of fungal symbionts associated with this mutualism, as well as assaying the ecology of fungal symbionts and guests. Many new directions for researching complex symbioses can be informed by the long-standing history of study on fungus-growing ants. The addition of new symbionts, and the further characterization of phylogenetic relationships amongst symbionts simultaneously creates more structure and more disorder to the complexity of these communities.

In chapter two, I characterized the genomes of the parasite *Escovopsis* across the phylogenetic diversity of fungus-growing ants. Many future directions exist from this chapter, in particular, the role the genome scale phylogeny can contribute to defining species of *Escovopsis*. Additionally, all species of *Escovopsis* contain BGCs with no known functions, so characterizing them deeply will inform more on the ecology of this organism. Additionally, the natural history of *Escovopsis* has yet to be determined, specifically, how is *Escovopsis* transmitted between colonies, does it have alternative hosts, and how much micro-scale diversity exists in the genus? Additionally, further characterization of the sister taxa, *Hypomyces* and *Cladobotryum* will aid in further refining the dates of origin of *Escovopsis* clades, as well as reconstructing the ancestral state of these genera, and the ecology of fungi the parasitize other fungi.

In chapter three, I explore how metagenomes adds to a deep history of microbial identification. As was discussed in chapter two, many isolations from fungus-gardens and their ants have repeatedly found novel microbes, and metagenomics further characterizes more putative residents and guests of this symbiosis. However, the distribution of these microbes across the phylogenetic diversity of the symbiosis often isn't characterized. To demonstrate that these microbes are resident, and possibly coevolved with the symbiosis future work will prioritize targeted isolations from a diversity of ants ranging from lower to leafcutter agriculture. Additionally, these isolates must by phylogenetically characterized along with free-living organisms to determine if these taxa form clades specific to the fungus-growing ant niche. Further, how these communities assemble and shift across the structure of the fungus-garden will be key to understanding how individual microbes impact the symbiosis. For example, the finding that certain microbes play a role in nitrogen-fixation demonstrated the important functional capacity of symbiotic microbes. While many microbes have been characterized, learning their functional capacities and how that influences their distribution amongst the fungus garden will unveil how these microbes shape each other's ecology and evolution.

In chapter four, I look at four *Candida* yeast genomes isolated from the *Azteca*/*Cecropia* symbiosis. These genomes showed that there are similar genotypes of *Candida* that associate with *Azteca* ants, and that these, like other yeasts contain two BGCs. This chapter opens a lot of interesting questions about deeply characterizing yeast BGCs, specifically, looking at NRPSs that are shared amongst many yeasts, as well as the various terpenes that are only apparent in a few

yeast genomes. More information about these molecules can reveal more about the ecology of different types of yeasts, and the utility of these BGCs in shaping it.

The field of fungal biology is an exciting place to do research with a seemingly endless number of questions to ask. With relatively little known about the diversity, ecology, and evolution of these organisms, every research project adds foundational knowledge. With the multitude of important roles fungi play, and services they provide we need to know more about fungi to protect them. These organisms are beautiful, wondrous, and are in partnership with nearly all other living beings in some context. The study of them will always leave room for more questions and will always satisfy the most curious researchers.

Appendix 1: Supplemental Material for Chapter 2

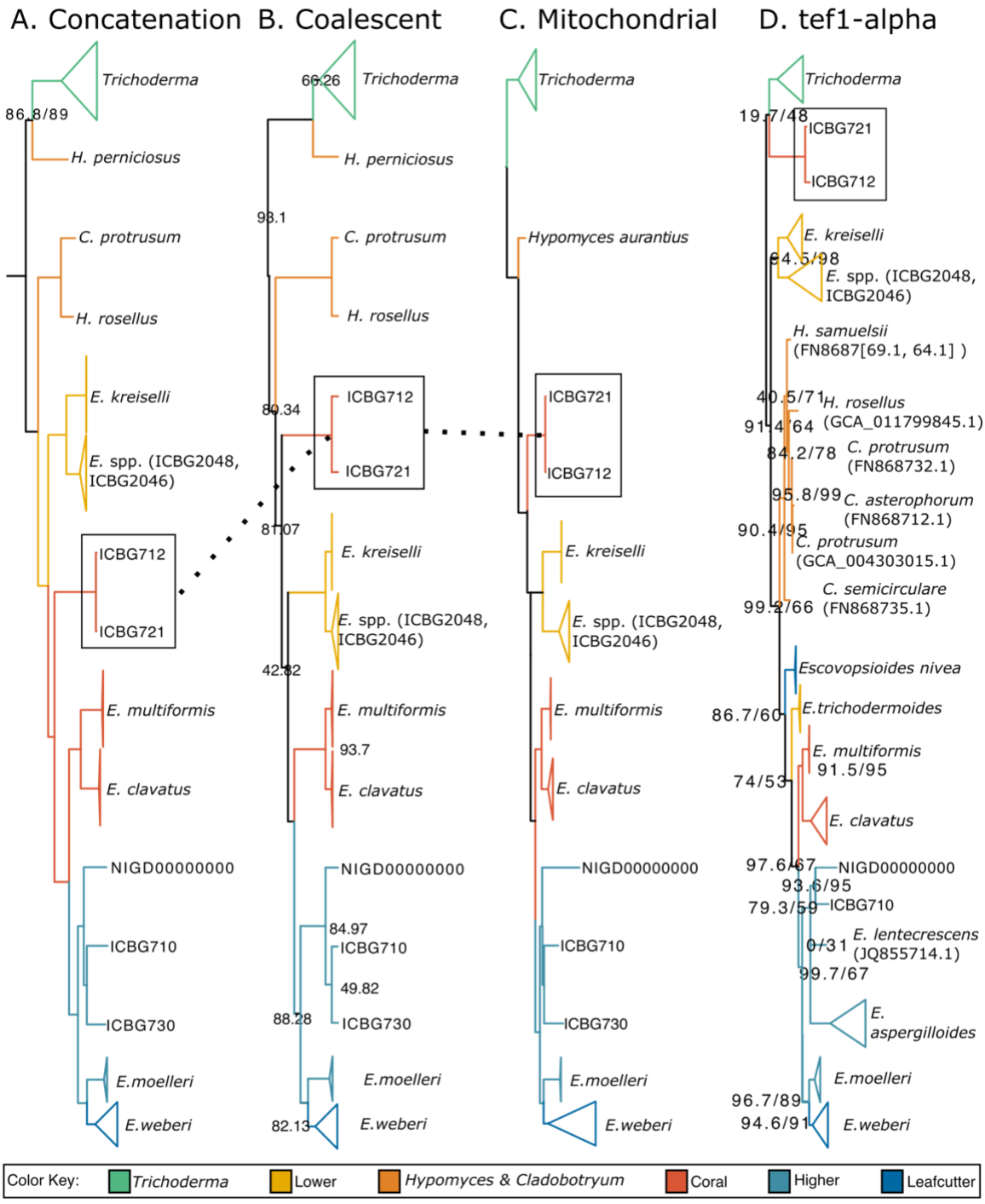

Fig. S1. Phylogenetic topologies derived from (A) concatenation and (B) coalescent approaches for 1706 BUSCO CDS sequences. Nodes without scores have a confidence greater than or equal to 95. C. Phylogenetic topology based on mitochondrial genomic DNA. The squares indicate the alternative topologies and positioning of the early diverging clade consisting of ICBG712 and ICBG721. D. Phylogenetic topology based on elongation factor one alpha (tef1-alpha) gene sequences.

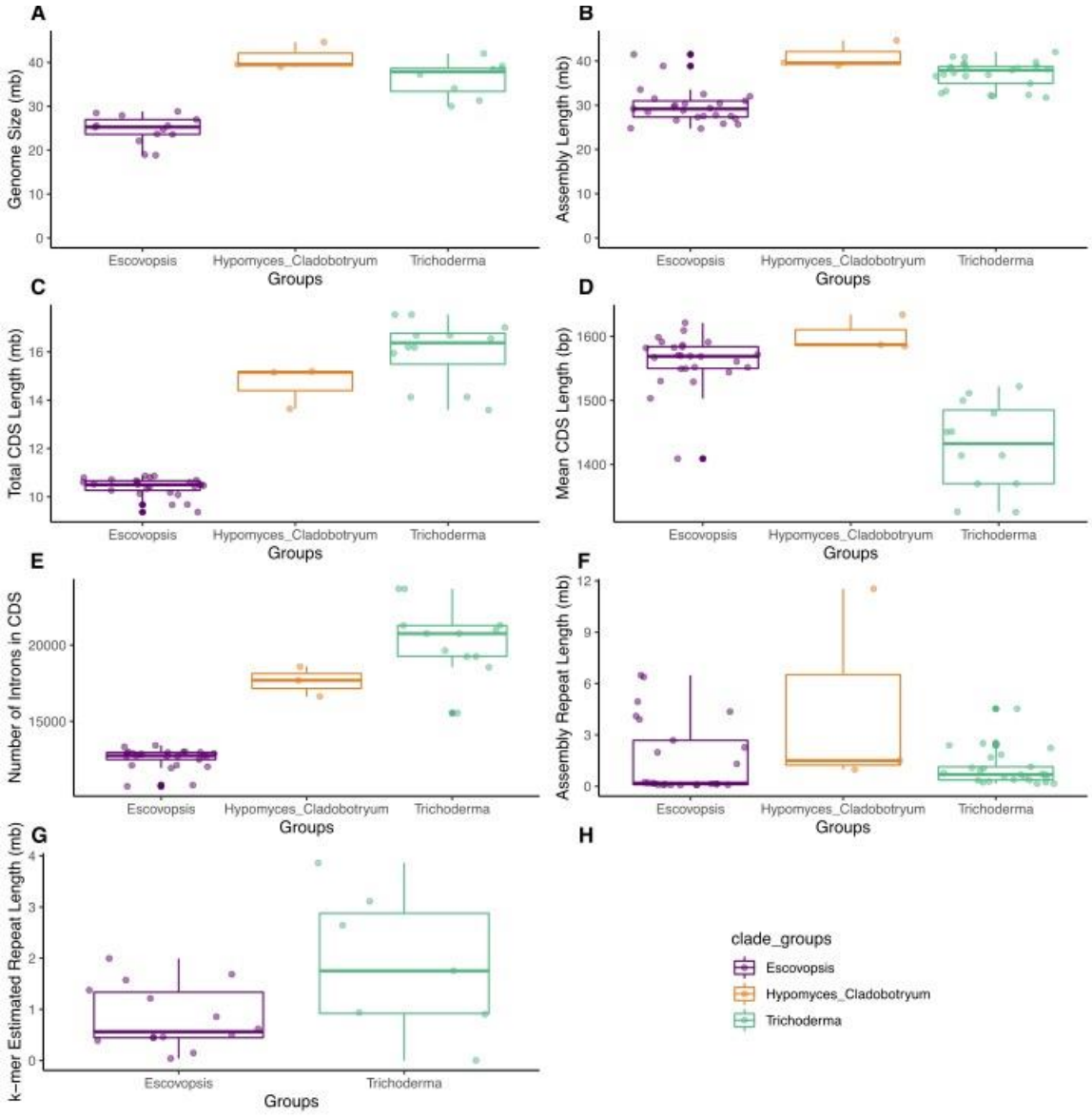

Fig. S2. A. Length distributions of genome size based on three strategies (k-mer or PacBio assembly length (*Hypomyces* and *Cladobotryum*), as well as measurements of assembly length (B), total CDS length (C), mean CDS length (D), number of introns in CDS regions (E), estimated repetitive DNA length from assemblies (F), estimated repetitive DNA length from k-mer based estimations on Illumina reads (G), legend for colors used (H).

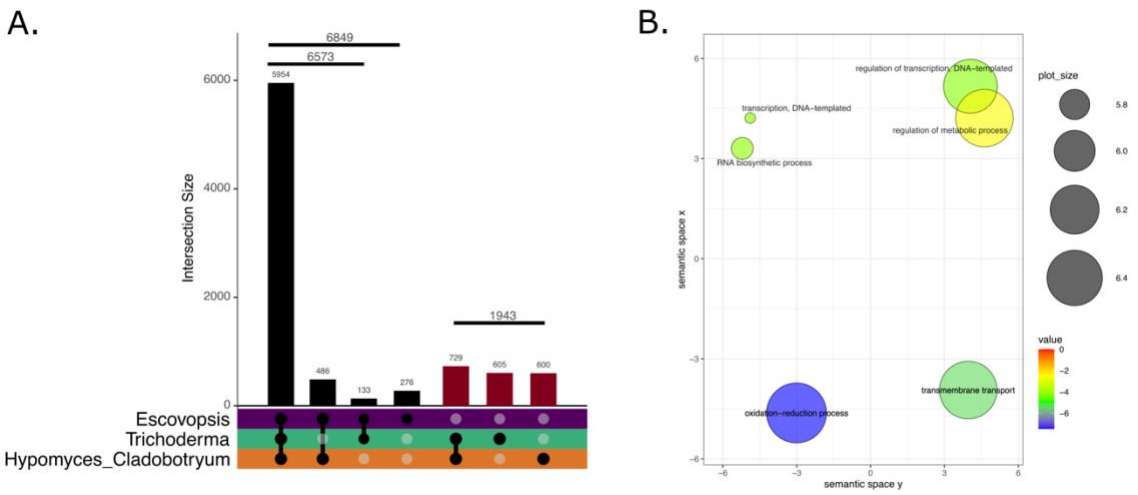

Fig. S3. A. UpSet plot distribution of orthologues amongst *Escovopsis* (purple), *Hypomyces* and *Cladobotryum* (orange), and *Trichoderma* (green) shows evidence for ancestral gene loss and gain with 1943 gene losses (annotated in red) in *Escovopsis*. B. REVIGO semantic similarity of enriched Gene Ontology terms for 1943 genes.

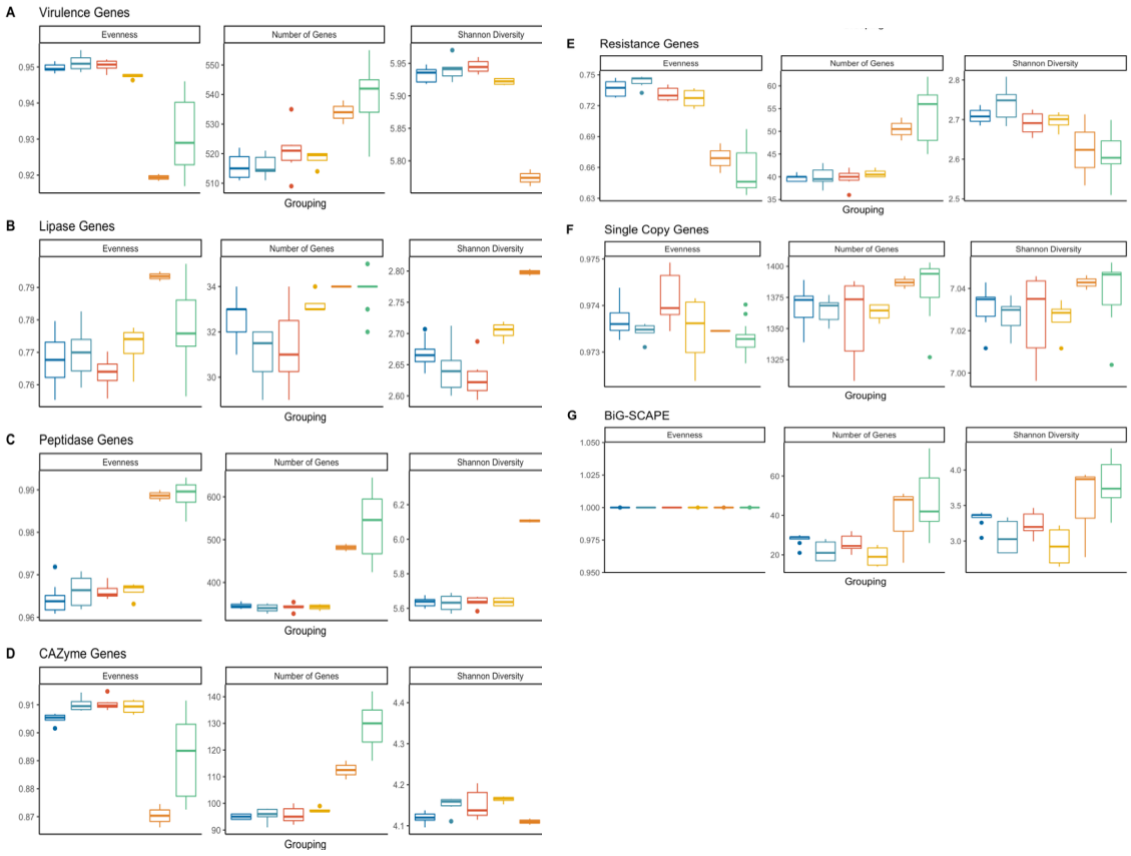

Fig. S4. Evenness, numbers of genes, and Shannon diversity distributions are shown for various functional gene categories (A-G). The x-axis and color-codings indicate comparison groupings as follows: Dark blue: leaf-cutter agriculture-associated *Escovopsis*, light blue: higher agriculture-associated *Escovopsis*, red: coral agriculture-associated *Escovopsis,* yellow: lower agriculture-associated *Escovopsis,* orange: *Hypomyces* and *Cladobotryum*, green: *Trichoderma*.

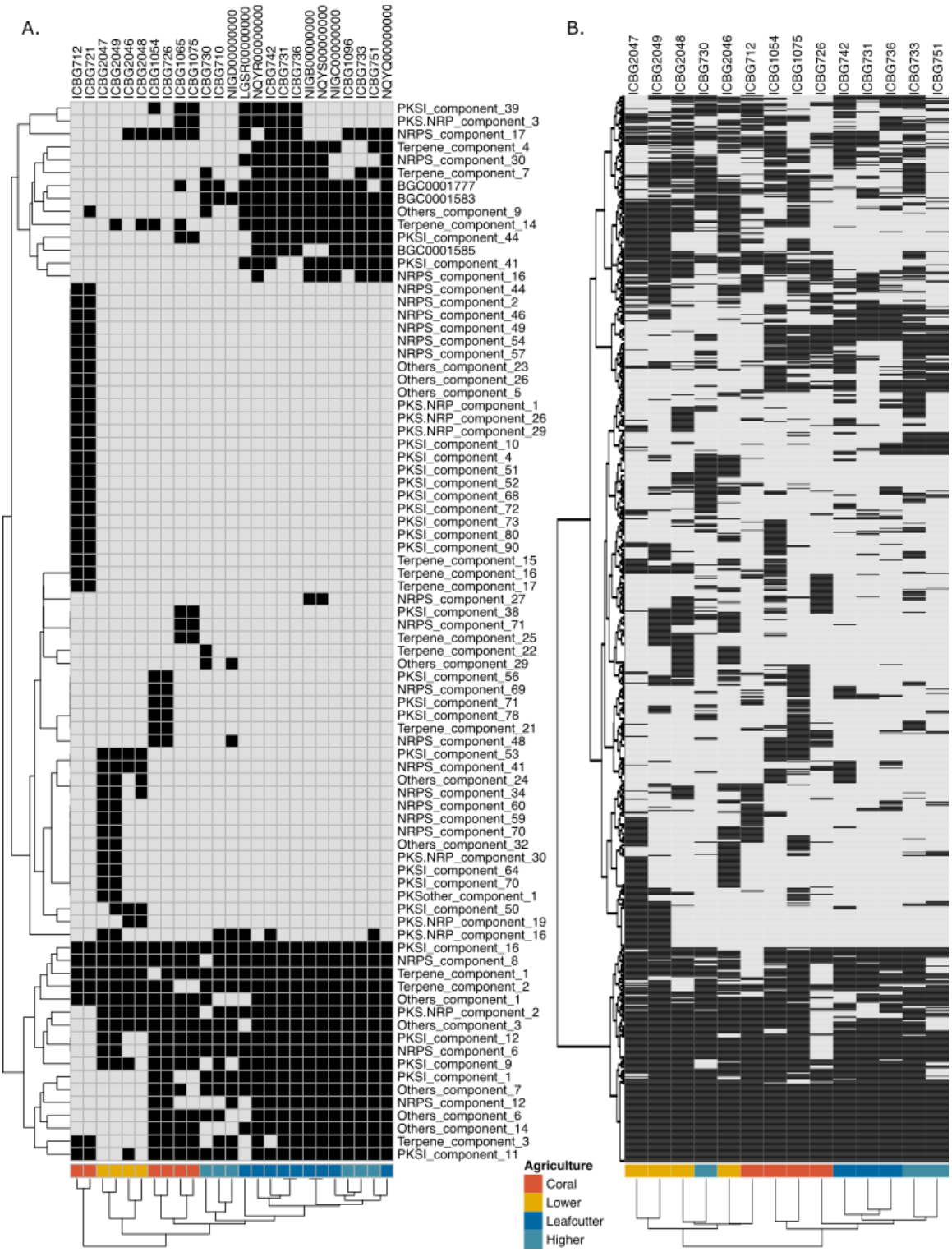
A.
ICBG712
ICBG721
ICBG2047
ICBG2049
ICBG2046
ICBG2048
ICBG1064
ICBG726
ICBG1065
ICBG1075
ICBG730
ICBG710
NIGD00000000
LGSR00000000
NQYR00000000
ICBG742
ICBG731
ICBG736
NIGB00000000
NQYS00000000
NIGC00000000
ICBG1096
ICBG733
ICBG751
NQYQ00000000
PKSI_component_39
PKS.NRP_component_3
NRPS_component_17
Terpene_component_4
NRPS_component_30
Terpene_component_7
BGC0001777
BGC0001583
Others_component_9
Terpene_component_14
PKSI_component_44
BGC0001585
PKSI_component_41
NRPS_component_16
NRPS_component_44
NRPS_component_2
NRPS_component_46
NRPS_component_49
NRPS_component_54
NRPS_component_57
Others_component_23
Others_component_26
Others_component_5
PKS.NRP_component_1
PKS.NRP_component_26
PKS.NRP_component_29
PKSI_component_10
PKSI_component_4
PKSI_component_51
PKSI_component_52
PKSI_component_68
PKSI_component_72
PKSI_component_73
PKSI_component_80
PKSI_component_90
Terpene_component_15
Terpene_component_16
Terpene_component_17
NRPS_component_27
PKSI_component_38
NRPS_component_71
Terpene_component_25
Terpene_component_22
Others_component_29
PKSI_component_56
NRPS_component_69
PKSI_component_71
PKSI_component_78
Terpene_component_21
NRPS_component_48
PKSI_component_53
NRPS_component_41
Others_component_24
NRPS_component_34
NRPS_component_60
NRPS_component_59
NRPS_component_70
Others_component_32
PKS.NRP_component_30
PKSI_component_64
PKSI_component_70
PKSother_component_1
PKSI_component_50
PKS.NRP_component_19
PKS.NRP_component_16
PKSI_component_16
NRPS_component_8
Terpene_component_1
Terpene_component_2
Others_component_1
PKS.NRP_component_2
Others_component_3
PKSI_component_12
NRPS_component_6
PKSI_component_9
PKSI_component_1
Others_component_7
NRPS_component_12
Others_component_6
Others_component_14
Terpene_component_3
PKSI_component_11
Agriculture
Coral
Lower
Leafcutter
Higher
B.
ICBG2047
ICBG2049
ICBG2048
ICBG730
ICBG2046
ICBG712
ICBG1054
ICBG1075
ICBG726
ICBG742
ICBG731
ICBG736
ICBG733
ICBG751

Fig. S5. A. Presence/absence matrix of BGC content (rows) across *Escovopsis* genomes (columns) as annotated by antiSMASH and grouped by similarity with BiG-SCAPE. Black indicates presence, and grey indicates absence. B. Presence/absence matrix of molecular networking subclusters from LC-MS/MS (rows) across *Escovopsis* strains (columns), black indicates presence, grey indicates absence.

Dataset S1. Metadata for genomes used in this article, including: attine ant host species, accessions, collection information, morphotypes of *Escovopsis* and genome statistics.

acc	family	GenomeSizeEstimation	genus	kmer_repe	kmer_repe	genus_species	HostSpecies	Country	Area	species	date_collect
ICBG1054	Hypocreaceae	failed genomescope qc	Escovopsis		1982233	ICBG1054	Apterostigma urichii	Brazil	Anavilhanas	clavata	2017-01-21
ICBG1065	Hypocreaceae	kmer	Escovopsis	457,752	4,360,718	ICBG1065	Apterostigma bruchi	Brazil	Itatiaia	multiformis	2017-01-14
ICBG1075	Hypocreaceae	failed genomescope qc	Escovopsis		6488806	ICBG1075	Apterostigma bruchi	Brazil	Itatiaia	multiformis	2017-01-15
ICBG1096	Hypocreaceae	failed genomescope qc	Escovopsis		196149	ICBG1096	Paratrachymyrmex diversus	Brazil	Anavilhanas	moelleri	2017-01-24
ICBG2046	Hypocreaceae	kmer	Escovopsis	439,951	4,107,675	ICBG2046	Cyphomyrmex muelleri	Panama	Gamboa	morphotype: pink	1996-04-10
ICBG2047	Hypocreaceae	kmer	Escovopsis	1,214,777	3,913,116	ICBG2047	Myrmicocrypta ednaella	Panama	Gamboa	kreiselii	1996-04-15
ICBG2048	Hypocreaceae	failed genomescope qc	Escovopsis		2,274,552	ICBG2048	Mycetophylax cf. faunulus		Guyana	morphotype: pink	1997-05-09
ICBG2049	Hypocreaceae	failed genomescope qc	Escovopsis		1308890	ICBG2049	Myrmicocrypta ednaella	Panama	Gamboa	kreiselii	1996-04-15
ICBG710	Hypocreaceae	failed genomescope qc	Escovopsis		110865	ICBG710	Paratrachymyrmex diversus	Brazil	Anavilhanas	lentecrescens	2017-01-24
ICBG712	Hypocreaceae	kmer	Escovopsis	618,953	4,945,846	ICBG712	Apterostigma urichii	Brazil	Anavilhanas	morphotype: yellow	2017-01-20
ICBG721	Hypocreaceae	kmer	Escovopsis	1,994,786	6,384,234	ICBG721	Apterostigma urichii	Brazil	Ducke	morphotype: yellow	2017-01-28
ICBG726	Hypocreaceae	kmer	Escovopsis	146,462	2,681,763	ICBG726	Apterostigma urichii	Brazil	Anavilhanas	clavata	2017-01-20
ICBG730	Hypocreaceae	failed genomescope qc	Escovopsis		78053	ICBG730	Paratrachymyrmex diversus	Brazil	Ducke	aspergilloides	2017
ICBG731	Hypocreaceae	kmer	Escovopsis	38,569	93,453	ICBG731	Attini	Brazil	Ducke	weberi	2017
ICBG733	Hypocreaceae	failed genomescope qc	Escovopsis	387,565	98746	ICBG733	Paratrachymyrmex diversus	Brazil	Ducke	moelleri	2017-01-28
ICBG736	Hypocreaceae	kmer	Escovopsis	459,072	66,259	ICBG736	Paratrachymyrmex diversus	Brazil	Anavilhanas	weberi	2017-01-20
ICBG742	Hypocreaceae	failed genomescope qc	Escovopsis		230221	ICBG742	Acromyrmex hystrix	Brazil	Anavilhanas	weberi	2017-01-21
ICBG751	Hypocreaceae	failed genomescope qc	Escovopsis		83805	ICBG751	Paratrachymyrmex diversus	Brazil	Anavilhanas	moelleri	2017-01-20
LGSR00000000	Hypocreaceae	kmer	Escovopsis	855,175	83,299	LGSR00000000	Atta cephalotes	Panama	Gamboa		
NIGB00000000	Hypocreaceae	kmer	Escovopsis	506,089	179,354	NIGB00000000	Attini	Colombia			
NIGC00000000	Hypocreaceae	kmer	Escovopsis	1,683,659	141,870	NIGC00000000	Acromyrmex echinatior	Panama	Gamboa		
NIGD00000000	Hypocreaceae	failed genomescope qc	Escovopsis		123,938	NIGD00000000	Paratrachymyrmex cornetzi	Panama	Gamboa		
NQYQ00000000	Hypocreaceae	kmer	Escovopsis	1,375,123	154,009	NQYQ00000000	Acromyrmex echinatior	Panama	Gamboa		
NQYR00000000	Hypocreaceae	kmer	Escovopsis	1,572,806	167,164	NQYR00000000	Acromyrmex echinatior	Panama	Gamboa		
NQYS00000000	Hypocreaceae	failed genomescope qc	Escovopsis		85115	NQYS00000000	Atta colombica	Panama	Gamboa		
GCA_004303015.1	Hypocreaceae	pacbio	Cladobotryum		1496974	Cladobotryum protrusum					
GCA_008477525.1	Hypocreaceae	pacbio	Hypomyces		11536407	Hypomyces perniciosus					
GCA_011799845.1	Hypocreaceae	pacbio	Hypomyces		980620	Hypomyces rosellus					
GCA_000170995.2	Hypocreaceae	failed genomescope qc	Trichoderma		507,390	Trichoderma virens					
GCA_000171015.2	Hypocreaceae	kmer	Trichoderma	3,862,372	284,730	Trichoderma atroviride					
GCA_000331835.2	Hypocreaceae	no public reads	Trichoderma		496584	Trichoderma hamatum					
GCA_000332775.1	Hypocreaceae	failed genomescope qc	Trichoderma		558827	Trichoderma longibrachiatum					
GCA_000513815.1	Hypocreaceae	kmer	Trichoderma	936,577	363038	Trichoderma reesei RUT C-30					
GCA_000988865.1	Hypocreaceae	no public reads	Trichoderma		1139416	Trichoderma harzianum T6776					
GCA_001050175.1	Hypocreaceae	no public reads	Trichoderma		226820	Trichoderma parareesei					
GCA_001481775.2	Hypocreaceae	kmer	Trichoderma	1,753,550	679,183	Trichoderma gamsii					
GCA_001721665.1	Hypocreaceae	no public reads	Trichoderma		1848563	Trichoderma pleuroti					
GCA_001931985.1	Hypocreaceae	no public reads	Trichoderma		4530103	Trichoderma sp. IMV 00454					
GCA_001950475.1	Hypocreaceae	kmer	Trichoderma	2,645,757	761,675	Trichoderma koningii					
GCA_002006585.1	Hypocreaceae	failed genomescope qc	Trichoderma		2237669	Trichoderma reesei					
GCA_002022785.1	Hypocreaceae	no public reads	Trichoderma		148765	Trichoderma guizhouense					
GCA_002246955.1	Hypocreaceae	no public reads	Trichoderma		686617	Trichoderma koningiopsis					
GCA_002838845.1	Hypocreaceae	no public reads	Trichoderma		2389597	Trichoderma harzianum TR274					
GCA_002894145.1	Hypocreaceae	no public reads	Trichoderma		944692	Trichoderma harzianum Tr1					
GCA_002894205.1	Hypocreaceae	failed genomescope qc	Trichoderma		1043313	Trichoderma gamsii A5MH					
GCA_003012105.1	Hypocreaceae	no public reads	Trichoderma		347561	Trichoderma arundinaceum					
GCA_003025095.1	Hypocreaceae	kmer	Trichoderma	3,112,115	2510150	Trichoderma harzianum CBS 226.95					
GCA_003025105.1	Hypocreaceae	kmer	Trichoderma		1690983	Trichoderma asperellum					
GCA_003025115.1	Hypocreaceae	no public reads	Trichoderma		1084032	Trichoderma citrinoviride					
GCA_003025155.1	Hypocreaceae	failed genomescope qc	Trichoderma		719773	Trichoderma longibrachioatum ATCC 18648					
GCA_003439915.1	Hypocreaceae	no public reads	Trichoderma		389784	Trichoderma atrobrunneum					
GCA_007896495.1	Hypocreaceae	kmer	Trichoderma	902,100	240,757	Trichoderma viride					
GCA_011066345.1	Hypocreaceae	no public reads	Trichoderma		151892	Trichoderma lentiforme CFAM-422					

acc	Genom	mean	Agriculture	cult	assembly_	n_prot	Numbe	Total_cds_	N50	N_Se	clade_groups	coordinates	BUSC	BUSCO Full Results
ICBG1054	NA	1591	Coral	G2	24790039	6546	12032	10415229	96241	593	Escovopsis	-2.508908, -60.82772	98.2	C:98.2%[S:98.2%,D:0.0%],F:0.2%,M:1.6%,n:1706
ICBG1065	18.99	1582	Coral	G4	26620154	6488	10743	10266954	35690	2289	Escovopsis	-22.369772, -44.628362	97.7	C:97.7%[S:97.6%,D:0.1%],F:0.4%,M:1.9%,n:1706
ICBG1075	NA	1609	Coral	G4	28477262	6008	10820	9668892	638213	248	Escovopsis	-22.369772, -44.628362	98.5	C:98.5%[S:98.5%,D:0.0%],F:0.2%,M:1.3%,n:1706
ICBG1096	NA	1584	Higher	G1	24707161	6811	12976	10791234	87673	953	Escovopsis	-2.508908, -60.82775	97.8	C:97.8%[S:97.7%,D:0.1%],F:0.3%,M:1.9%,n:1706
ICBG2046	23.69	1529	Lower	G3	29171929	6627	12900	10133775	160205	1507	Escovopsis	9.115856, -79.69698	98.7	C:98.7%[S:98.7%,D:0.0%],F:0.1%,M:1.2%,n:1706
ICBG2047	24.72	1552	Lower	G3	28809826	6997	12858	10865019	55110	1785	Escovopsis	9.115856, -79.69698	97.5	C:97.5%[S:97.5%,D:0.0%],F:0.5%,M:2.0%,n:1706
ICBG2048	NA	1544	Lower	G3	27317560	6853	12757	10583301	23068	3179	Escovopsis		98.3	C:98.3%[S:97.9%,D:0.4%],F:0.4%,M:1.3%,n:1706
ICBG2049	NA	1550	Lower	G3	25699474	6836	12492	10602123	54529	1290	Escovopsis	9.115856, -79.69698	98.6	C:98.6%[S:98.4%,D:0.2%],F:0.1%,M:1.3%,n:1706
ICBG710	NA	1583	Higher	G1	41491680	6425	12751	10172625	150232	868	Escovopsis	-2.508908, -60.82776	98.8	C:98.8%[S:98.5%,D:0.3%],F:0.1%,M:1.1%,n:1706
ICBG712	23.6	1570	Coral	G2	29354113	6760	12706	10617873	304748	967	Escovopsis	-2.508908, -60.82773	98.8	C:98.8%[S:98.6%,D:0.2%],F:0.0%,M:1.2%,n:1706
ICBG721	26.98	1503	Coral	G2	30984735	6230	12120	9365742	361630	2997	Escovopsis	-2.963333, -59.922951	98.7	C:98.7%[S:98.1%,D:0.6%],F:0.1%,M:1.2%,n:1706
ICBG726	18.86	1599	Coral	G2	25818384	6521	12114	10433448	141428	371	Escovopsis	-2.508908, -60.82774	96.4	C:96.4%[S:96.0%,D:0.4%],F:0.5%,M:3.1%,n:1706
ICBG730	NA	1530	Higher	G1	33534959	6589	12709	10085052	37940	3062	Escovopsis	-2.963333, -59.922951	98.3	C:98.3%[S:98.1%,D:0.2%],F:0.4%,M:1.3%,n:1706
ICBG731	22.13	1571	Leafcutter	G1	29579511	6913	12909	10861212	154167	619	Escovopsis	-2.963333, -59.922951	98.7	C:98.7%[S:98.2%,D:0.5%],F:0.1%,M:1.2%,n:1706
ICBG733	NA	1591	Higher	G1	32506954	6730	12709	10713027	79253	1793	Escovopsis	-2.963333, -59.922951	97.7	C:97.7%[S:97.3%,D:0.4%],F:0.8%,M:1.5%,n:1706
ICBG736	25.59	1561	Leafcutter	G1	30002316	6723	12961	10500540	153758	562	Escovopsis	-2.508908, -60.82770	98.5	C:98.5%[S:98.3%,D:0.2%],F:0.2%,M:1.3%,n:1706
ICBG742	NA	1552	Leafcutter	G1	26974256	6964	12983	10813374	17919	2694	Escovopsis	-2.508908, -60.82771	98.7	C:98.7%[S:98.4%,D:0.3%],F:0.1%,M:1.2%,n:1706
ICBG751	NA	1586	Higher	G1	31502876	6737	12733	10686975	296376	243	Escovopsis	-2.508908, -60.82777	99.1	C:99.1%[S:98.9%,D:0.2%],F:0.1%,M:0.8%,n:1706
LGSR00000000	25.26	1409	Leafcutter	G1	27540933	6870	11939	9681356	2575554	29	Escovopsis	9.115856, -79.69701	99	C:99.0%[S:98.8%,D:0.2%],F:0.1%,M:0.9%,n:1706
NIGB00000000	25.55	1572	Leafcutter	G1	27769974	6782	13420	10661571	3930483	13	Escovopsis	3.420094, -73.012106	98.9	C:98.9%[S:98.7%,D:0.2%],F:0.0%,M:1.1%,n:1706
NIGC00000000	27.92	1569	Leafcutter	G1	30341680	6690	12913	10503180	3264004	17	Escovopsis	9.115856, -79.69700	97	C:97.0%[S:96.5%,D:0.5%],F:0.3%,M:2.7%,n:1706
NIGD00000000	NA	1621	Higher	G1	38867474	6470	12974	10491306	6115915	19	Escovopsis	9.115856, -79.69698	94.7	C:94.7%[S:94.4%,D:0.3%],F:1.9%,M:3.4%,n:1706
NQYQ00000000	28.81	1569	Leafcutter	G1	32007231	6590	12837	10344192	790282	234	Escovopsis	9.115856, -79.69699	96	C:96.0%[S:95.4%,D:0.6%],F:1.4%,M:2.6%,n:1706
NQYR00000000	28.47	1567	Leafcutter	G1	30405957	6713	13016	10521114	2264659	25	Escovopsis	9.115856, -79.69696	98.7	C:98.7%[S:96.1%,D:2.6%],F:0.1%,M:1.2%,n:1706
NQYS00000000	NA	1549	Leafcutter	G1	27522798	6753	13328	10465536	4280189	13	Escovopsis	9.115856, -79.69697	99	C:99.0%[S:98.6%,D:0.4%],F:0.0%,M:1.0%,n:1706
GCA_004303015.1	39.57	1587	Hypomyces_Cladobotryum	NA	39575829	9548	18581	15153546			Hypomyces_Cladobotryum		98.4	C:98.4%[S:98.2%,D:0.2%],F:0.2%,M:1.4%,n:1706
GCA_008477525.1	44.64	1585	Hypomyces_Cladobotryum	NA	44635166	8605	16633	13641489			Hypomyces_Cladobotryum		97.5	C:97.5%[S:97.5%,D:0.0%],F:0.9%,M:1.6%,n:1706
GCA_011799845.1	39.02	1634	Hypomyces_Cladobotryum	NA	39024775	9299	17690	15196830			Hypomyces_Cladobotryum		96.9	C:96.9%[S:96.9%,D:0.0%],F:1.1%,M:2.0%,n:1706
GCA_000170995.2	NA				39510495	12405	23690	17542937			Trichoderma		98.8	C:98.8%[S:98.4%,D:0.4%],F:0.2%,M:1.0%,n:1706
GCA_000171015.2	39.18				36595476	11809	21294	16200578			Trichoderma		98.5	C:98.5%[S:98.5%,D:0.0%],F:0.1%,M:1.4%,n:1706
GCA_000331835.2	NA				38431721	NA	NA	NA			Trichoderma		98.6	C:98.6%[S:98.5%,D:0.1%],F:0.2%,M:1.2%,n:1706
GCA_000332775.1	NA				31743061	NA	NA	NA			Trichoderma		98.6	C:98.6%[S:98.6%,D:0.0%],F:0.1%,M:1.3%,n:1706
GCA_000513815.1	34.1				32681481	9849	18396	13865063			Trichoderma		99.1	C:99.1%[S:98.9%,D:0.2%],F:0.0%,M:0.9%,n:1706
GCA_000988865.1	NA				39721542	11498	21348	17439922			Trichoderma		98.3	C:98.3%[S:97.9%,D:0.4%],F:0.2%,M:1.5%,n:1706
GCA_001050175.1	NA				32070663	9062	15546	13596111			Trichoderma		97.9	C:97.9%[S:97.9%,D:0.0%],F:0.7%,M:1.4%,n:1706
GCA_001481775.2	38.4				37908251	11179	19638	16552763			Trichoderma		97.5	C:97.5%[S:97.0%,D:0.5%],F:0.9%,M:1.6%,n:1706
GCA_001721665.1	NA				38137656	NA	NA	NA			Trichoderma		97.8	C:97.8%[S:97.8%,D:0.0%],F:0.4%,M:1.8%,n:1706
GCA_001931985.1	NA				42030438	NA	NA	NA			Trichoderma		97.8	C:97.8%[S:97.6%,D:0.2%],F:0.6%,M:1.6%,n:1706
GCA_001950475.1	38.46				32322684	NA	NA	NA			Trichoderma		94.7	C:94.7%[S:94.7%,D:0.0%],F:2.1%,M:3.2%,n:1706
GCA_002006585.1	NA				34922528	NA	NA	NA			Trichoderma		97.6	C:97.6%[S:96.5%,D:1.1%],F:0.4%,M:2.0%,n:1706
GCA_002022785.1	NA				38329450	11255	21000	17013570			Trichoderma		98.1	C:98.1%[S:98.1%,D:0.0%],F:0.4%,M:1.5%,n:1706
GCA_002246955.1	NA				36580823	NA	NA	NA			Trichoderma		98.3	C:98.3%[S:98.0%,D:0.3%],F:0.1%,M:1.6%,n:1706
GCA_002838845.1	NA				40865014	13925	24515	18509004			Trichoderma		98.7	C:98.7%[S:98.3%,D:0.4%],F:0.2%,M:1.1%,n:1706
GCA_002894145.1	42				38779109	11264	17525	16010289			Trichoderma		98.7	C:98.7%[S:98.5%,D:0.2%],F:0.1%,M:1.2%,n:1706
GCA_002894205.1	NA				38490345	10994	16717	15433963			Trichoderma		98.9	C:98.9%[S:98.7%,D:0.2%],F:0.0%,M:1.1%,n:1706
GCA_003012105.1	NA				36872412	10473	18549	15946872			Trichoderma		97.8	C:97.8%[S:97.7%,D:0.1%],F:0.3%,M:1.9%,n:1706
GCA_003025095.1	30				40980648	14090	23473	18624559			Trichoderma		98.7	C:98.7%[S:98.2%,D:0.5%],F:0.1%,M:1.2%,n:1706
GCA_003025105.1	31.28				37333967	12556	20757	16689377			Trichoderma		95.6	C:95.6%[S:95.5%,D:0.1%],F:0.5%,M:3.9%,n:1706
GCA_003025115.1	NA				33215161	9734	19256	14127903			Trichoderma		98.5	C:98.5%[S:98.4%,D:0.1%],F:0.4%,M:1.1%,n:1706
GCA_003025155.1	NA				32238325	10934	18195	14052123			Trichoderma		89.6	C:89.6%[S:89.4%,D:0.2%],F:3.5%,M:6.9%,n:1706
GCA_003439915.1	NA				39149368	NA	NA	NA			Trichoderma		98.1	C:98.1%[S:98.1%,D:0.0%],F:0.4%,M:1.5%,n:1706
GCA_007896495.1	37.32				36986606	NA	NA	NA			Trichoderma		97.8	C:97.8%[S:97.8%,D:0.0%],F:0.6%,M:1.6%,n:1706
GCA_011066345.1	NA				38315448	12978	23047	19054509			Trichoderma		98.5	C:98.5%[S:97.9%,D:0.6%],F:0.1%,M:1.4%,n:1706

Dataset S2. Results from ASTRAL coalescent species tree analysis.

node	topology	normalized_quartet_score	n_genes_support	n_useful_genes
N0	t1	0.6329588014981273	225.33333333333331	356.0
N0	t2	0.19007490636704122	67.66666666666667	356.0
N0	t3	0.17696629213483148	63.00000000000001	356.0
N1	t1	0.8227232305734442	1326.229847684392	1612.0
N1	t2	0.10595495889574254	170.79939373993696	1612.0
N1	t3	0.07132181053081303	114.97075857567062	1612.0
N2	t1	0.8503254957385755	1385.1802325581396	1629.0
N2	t2	0.07539580567333362	122.81976744186046	1629.0
N2	t3	0.07427869858809086	121.0	1629.0
N3	t1	0.9982806511987167	1639.1768292682927	1642.0
N3	t2	9.411650145734102E-4	1.5453929539295395	1642.0
N3	t3	7.781837867099742E-4	1.2777777777777777	1642.0
N4	t1	0.997522466532004	1599.0285138508025	1603.0
N4	t2	0.0024064813694939045	3.8575896352987287	1603.0
N4	t3	7.105209850189362E-5	0.11389651389853547	1603.0
N5	t1	0.8450608810704272	1378.2942970258669	1631.0
N5	t2	0.07432400771948652	121.22245659048252	1631.0
N5	t3	0.08061511121008565	131.48324638364969	1631.0
N6	t1	0.8097051307242026	1307.6737861195872	1615.0
N6	t2	0.11340508511761016	183.1492124649404	1615.0
N6	t3	0.07688978415818726	124.17700141547242	1615.0

N7	t1	0.8344527667587528	1355.1512932162145	1624.0
N7	t2	0.07444898204435964	120.90514684004006	1624.0
N7	t3	0.09109825119688761	147.94355994374547	1624.0
N8	t1	0.9776802465114972	1599.4848832928094	1636.0
N8	t2	0.008264401701518553	13.520561183684352	1636.0
N8	t3	0.014055351786984397	22.994555523506474	1636.0
N9	t1	0.9759793507976186	1599.630155957297	1639.0
N9	t2	0.01210866723758327	19.846105602398982	1639.0
N9	t3	0.011911981964798026	19.523738440303966	1639.0
N10	t1	0.9527339423857976	1562.483665512708	1640.0
N10	t2	0.04060869020928756	66.5982519432316	1640.0
N10	t3	0.00665736740491472	10.918082544060141	1640.0
N11	t1	0.962588692757178	1596.9346412841583	1659.0
N11	t2	0.02691535728688253	44.65257773893811	1659.0
N11	t3	0.010495949955939492	17.412780976903615	1659.0
N12	t1	0.9984702792068447	1619.5187928735022	1622.0
N12	t2	4.776657259443423E-4	0.7747738074817232	1622.0
N12	t3	0.0010520550672111994	1.7064333190165655	1622.0
N13	t1	0.8344989411808635	191.9347564715986	230.0
N13	t2	0.056822742474916386	13.069230769230769	230.0
N13	t3	0.10867831634422023	24.996012759170654	230.0
N14	t1	0.9890420407674352	1327.294418709898	1342.0
N14	t2	0.004061064360346894	5.449948371585532	1342.0
N14	t3	0.006896894872217744	9.255632918516213	1342.0

N15	t1	0.603472446885413	818.9121104235054	1357.0
N15	t2	0.12712740107822254	172.51188326314798	1357.0
N15	t3	0.2694001520363645	365.5760063133466	1357.0
N16	t1	0.6127261928274457	990.1655276091522	1616.0
N16	t2	0.10488015121585713	169.48632436482512	1616.0
N16	t3	0.2823936559566979	456.3481480260238	1616.0
N17	t1	0.5792815949127783	942.4911549230902	1627.0
N17	t2	0.2960684782314773	481.70341408261356	1627.0
N17	t3	0.12464992685574448	202.80543099429627	1627.0
N18	t1	0.5113714724228157	846.8311583321828	1656.0
N18	t2	0.19446202793630374	322.029118262519	1656.0
N18	t3	0.2941664996408802	487.1397234052976	1656.0
N19	t1	0.8386924776858938	1301.6507253685072	1552.0
N19	t2	0.03918757456350431	60.81911572255869	1552.0
N19	t3	0.12211994775060217	189.53015890893457	1552.0
N20	t1	0.694116897457707	1132.7987766509777	1632.0
N20	t2	0.08147245636312012	132.96304878461203	1632.0
N20	t3	0.2244106461791728	366.23817456441003	1632.0
N21	t1	0.3967894333816673	652.321828479461	1644.0
N21	t2	0.3051971563904339	501.74412510587325	1644.0
N21	t3	0.29801341022789873	489.9340464146655	1644.0
N22	t1	0.9903779823332618	1635.1140488322153	1651.0
N22	t2	0.004030400927799129	6.654191931796362	1651.0
N22	t3	0.005591616738938696	9.231759235987786	1651.0

N23	t1	0.5073066105811357	855.3189454397947	1686.0
N23	t2	0.32823588712955176	553.4057057004243	1686.0
N23	t3	0.1644575022893124	277.2753488597807	1686.0
N24	t1	0.8786618431970671	1486.6958386894376	1692.0
N24	t2	0.04837618038369988	81.8524972092202	1692.0
N24	t3	0.07296197641923212	123.45166410134075	1692.0
N25	t1	0.9869935528314256	1630.513349277515	1652.0
N25	t2	0.008460361184579563	13.976516676925439	1652.0
N25	t3	0.004546085983995036	7.510134045559799	1652.0
N26	t1	0.9950245302430428	1006.9648246059594	1012.0
N26	t2	0.0019791385472622395	2.0028882098293863	1012.0
N26	t3	0.0029963312096948982	3.032287184211237	1012.0
N27	t1	0.7801672179781963	1269.3320636505255	1627.0
N27	t2	0.13869652819940942	225.65925138043914	1627.0
N27	t3	0.08113625382239441	132.0086849690357	1627.0
N28	t1	0.9796615028698632	1596.848249677877	1630.0
N28	t2	0.006706866290224809	10.932192053066439	1630.0
N28	t3	0.013631630839911944	22.21955826905647	1630.0
N29	t1	0.5626713851899816	934.5971708005595	1661.0
N29	t2	0.23356357070508646	387.9490909411486	1661.0
N29	t3	0.20376504410493182	338.45373825829176	1661.0
N30	t1	0.4287171926241856	712.9566913340207	1663.0
N30	t2	0.3819177448504278	635.1292096862614	1663.0
N30	t3	0.18936506252538637	314.91409897971755	1663.0

N31	t1	0.9612035688160607	1607.1323670604536	1672.0
N31	t2	0.021591653093625787	36.10124397254231	1672.0
N31	t3	0.01720477809031347	28.766388967004122	1672.0
N32	t1	0.9903989034830183	1633.167791843497	1649.0
N32	t2	0.0032747970819318813	5.400140388105672	1649.0
N32	t3	0.006362994350498 21	10.432067768397156	1649.0
N33	t1	0.6894754706417974	1139.0134775002493	1652.0
N33	t2	0.08427722816598468	139.2259809302067	1652.0
N33	t3	0.22624730119221678	373.7605415695421	1652.0
N34	t1	0.9964453430038142	748.3304525958645	751.0
N34	t2	0.0022021296573094483	1.6537993726393956	751.0
N34	t3	0.001352527338876249	1.015748031496063	751.0
N35	t1	0.5592162749976868	876.8511191963728	1568.0
N35	t2	0.21036044010324972	329.84517008189556	1568.0
N35	t3	0.23042328489906352	361.3037107217316	1568.0
N36	t1	0.8978789950953191	1386.3251684271727	1544.0
N36	t2	0.048592183288512246	75.0263309974629	1544.0
N36	t3	0.05352882161616871	82.6485005753645	1544.0
N37	t1	0.9499840085395341	1509.5245895693197	1589.0
N37	t2	0.03557967320339207	56.53610072019	1589.0
N37	t3	0.014436318257073652	22.939309710490033	1589.0
N38	t1	0.9653608757736569	1607.3258581631387	1665.0
N38	t2	0.011034095384989668	18.371768816007798	1665.0
N38	t3	0.02360502884135371	39.30237302085393	1665.0

N39	t1	0.5103546250475641	856.8854154548602	1679.0
N39	t2	0.472229659542582	792.8735983719952	1679.0
N39	t3	0.017415715409853736	29.24098617314442	1679.0
N40	t1	0.9798043477379244	1624.5156085494787	1658.0
N40	t2	0.015603420855254912	25.870471778012643	1658.0
N40	t3	0.004592231406820728	7.613919672508766	1658.0
N41	t1	0.6605142086770548	1098.4351290299421	1663.0
N41	t2	0.06752355598991043	112.29167361122104	1663.0
N41	t3	0.27196223533303365	452.2731973588349	1663.0
N42	t1	0.9962783038593861	1653.821984406581	1660.0
N42	t2	0.0013539363593266433	2.247534356482228	1660.0
N42	t3	0.002367759781287331	3.930481236936969	1660.0
N43	t1	1.0	114.0	114.0
N43	t2	0.0	0.0	114.0
N43	t3	0.0	0.0	114.0
N44	t1	0.9913200637452289	1609.9037835222516	1624.0
N44	t2	0.0037116858237547894	6.027777777777778	1624.0
N44	t3	0.004968250431016294	8.068438699970462	1624.0
N45	t1	0.9905960028670473	1650.332940776501	1666.0
N45	t2	0.004598108051377514	7.660448013594938	1666.0
N45	t3	0.004805889081575052	8.006611209904037	1666.0
N46	t1	0.999875557704305	1566.804998922646	1567.0
N46	t2	0.0	0.0	1567.0
N46	t3	1.2444229569497035E-4	0.19500107735401853	1567.0

N47	t1	1.0	1633.0	1633.0
N47	t2	0.0	0.0	1633.0
N47	t3	0.0	0.0	1633.0
N48	t1	1.0	1602.0	1602.0
N48	t2	0.0	0.0	1602.0
N48	t3	0.0	0.0	1602.0
N49	t1	0.9313597441556059	1552.576693507395	1667.0
N49	t2	0.026701942734516076	44.5121385384383	1667.0
N49	t3	0.04193831310987847	69.91116795416741	1667.0
N50	t1	0.498919166384389	803.7587770452507	1611.0
N50	t2	0.21010732805988927	338.4829055044816	1611.0
N50	t3	0.29097350555572155	468.75831745026744	1611.0
N51	t1	0.8415095458540416	1390.1737697508768	1652.0
N51	t2	0.08184039421734107	135.20033124704744	1652.0
N51	t3	0.07665005992861744	126.62589900207601	1652.0
N52	t1	0.9406481128478841	1011.1967213114754	1075.0
N52	t2	0.03443410852713178	37.016666666666666	1075.0
N52	t3	0.024917778624984115	26.786612021857923	1075.0
N53	t1	0.9988655140282596	1639.138308520374	1641.0
N53	t2	2.0253814545611275E-4	0.332365096693481	1641.0
N53	t3	9.319478262842517E-4	1.529326382932457	1641.0
N54	t1	0.7903057917618835	1217.0709193133007	1540.0
N54	t2	0.12465986999792888	191.97619979681048	1540.0
N54	t3	0.08503433824018751	130.95288088988877	1540.0

N55	t1	0.9820846905537459	603.0	614.0
N55	t2	0.003257328990228013	2.0	614.0
N55	t3	0.014657980456026058	9.0	614.0
N56	t1	0.9938826231502934	1653.8206849220883	1664.0
N56	t2	0.0035021767186799815	5.827622059883489	1664.0
N56	t3	0.002615200131026442	4.351693018028	1664.0
N57	t1	0.9937961224204891	477.02213876183475	480.0
N57	t2	0.0027972721551889246	1.3426906344906837	480.0
N57	t3	0.0034066054243219596	1.6351706036745406	480.0
N58	t1	0.40417551963048504	175.008	433.0
N58	t2	0.3071593533487298	133.0	433.0
N58	t3	0.28866512702078523	124.992	433.0
N59	t1	0.9958905519451877	1092.491935483871	1097.0
N59	t2	0.002058399741229747	2.2580645161290325	1097.0
N59	t3	0.002051048313582498	2.25	1097.0
N60	t1	0.8783466721564891	1466.8389425013368	1670.0
N60	t2	0.0977114537839364	163.1781278191738	1670.0
N60	t3	0.02394187405957421	39.982929679488926	1670.0
N61	t1	0.8172255821051063	1371.3045267723685	1678.0
N61	t2	0.07589360512740928	127.34946940379277	1678.0
N61	t3	0.10688081276748457	179.3460038238391	1678.0
N62	t1	0.9548342875761041	1605.076437415431	1681.0
N62	t2	0.018346138031242555	30.839858030518737	1681.0
N62	t3	0.026819574392653374	45.08370455405032	1681.0

N63	t1	0.8899812326037315	1494.2784895416653	1679.0
N63	t2	0.05592790335224575	93.90294972842061	1679.0
N63	t3	0.05409086404402309	90.81856072991478	1679.0
N64	t1	0.9242291478803734	1542.538447812343	1669.0
N64	t2	0.027914516078941805	46.58932733575387	1669.0
N64	t3	0.047856336040684753	79.87222485190286	1669.0
N65	t1	0.4202406565895829	702.6423778177825	1672.0
N65	t2	0.41884267401206	700.3049509481643	1672.0
N65	t3	0.16091666939835697	269.05267123405287	1672.0
N66	t1	0.7303792450111711	1226.3067523737564	1679.0
N66	t2	0.017213993208862827	28.902294597680687	1679.0
N66	t3	0.252406761779966	423.7909530285629	1679.0
N67	t1	0.8051604987616301	1353.4747984183002	1681.0
N67	t2	0.018796272507275703	31.596534084730457	1681.0
N67	t3	0.17604322873109468	295.92866749697015	1681.0
N68	t1	0.9310094577488397	1578.0610308842834	1695.0
N68	t2	0.033400651636374	56.61410452365393	1695.0
N68	t3	0.03558989061478733	60.32486459206452	1695.0
N69	t1	0.7679401748221985	1272.4768696803828	1657.0
N69	t2	0.13001215630505475	215.43014299747574	1657.0
N69	t3	0.1020476688727467	169.09298732214128	1657.0
N70	t1	0.9932740357980162	1339.9266742915238	1349.0
N70	t2	0.005189028910303929	7.0	1349.0
N70	t3	0.0015369352916799848	2.0733257084762995	1349.0

N71	t1	0.8374011823220121	1396.7851721131162	1668.0
N71	t2	0.1025783831124513	171.10074303156875	1668.0
N71	t3	0.06002043456553639	100.1140848553147	1668.0
N72	t1	0.9964276732434214	1617.202113674073	1623.0
N72	t2	0.0018135478994809014	2.943388240857503	1623.0
N72	t3	0.001758778857097619	2.8544980850694355	1623.0
N73	t1	0.4050818436373248	667.169796470674	1647.0
N73	t2	0.252537413576192	415.92912015998826	1647.0
N73	t3	0.34238074278648317	563.9010833693378	1647.0
N74	t1	0.57573379712313	959.1725060071346	1666.0
N74	t2	0.16627146223140113	277.00825607751426	1666.0
N74	t3	0.2579947406454682	429.81923791534996	1666.0
N75	t1	0.9902392947103275	1572.5	1588.0
N75	t2	0.0053526448362720405	8.5	1588.0
N75	t3	0.004408060453400504	7.0	1588.0
N76	t1	0.992129698354977	1622.1320568103874	1635.0
N76	t2	0.00303044593105201	4.954779097270036	1635.0
N76	t3	0.0048398557139710755	7.913164092342708	1635.0
N77	t1	0.7462391299592884	1238.0107166024595	1659.0
N77	t2	0.08739726551661452	144.9920634920635	1659.0
N77	t3	0.1663636045240969	275.99721990547675	1659.0
N78	t1	0.9978625560861003	1664.4347435516154	1668.0
N78	t2	3.624105840370312E-4	0.6045008541737681	1668.0
N78	t3	0.0017750333298624445	2.9607555942105575	1668.0

N79	t1	0.5487086872509693	919.6357598326247	1676.0
N79	t2	0.289153751195281	484.6216870032909	1676.0
N79	t3	0.16213756155375	271.742553164085	1676.0
N80	t1	0.7404233408471593	1237.2474025556032	1671.0
N80	t2	0.0825037181170123	137.86371297352756	1671.0
N80	t3	0.1770729410358289	295.8888844708701	1671.0
N81	t1	0.9944623626516396	1652.7964467270249	1662.0
N81	t2	0.0019103567033790004	3.175012841015899	1662.0
N81	t3	0.0036272806449818007	6.028540431959753	1662.0
N82	t1	0.7218142220202615	1208.3170076619176	1674.0
N82	t2	0.08656998703645483	144.91815829902538	1674.0
N82	t3	0.19161579094328413	320.76483403905763	1674.0
N83	t1	0.8462726763092224	1429.3545502862767	1689.0
N83	t2	0.07186537734329819	121.38062233283064	1689.0
N83	t3	0.08186194634747929	138.2648273808925	1689.0
N84	t1	0.9991034942873821	1140.9761904761904	1142.0
N84	t2	8.756567425569177E-4	1.0	1142.0
N84	t3	2.084897006087899E-5	0.023809523809523808	1142.0
N85	t1	0.9741638520701407	1193.3507187859223	1225.0
N85	t2	0.011431096984708998	14.003093806268524	1225.0
N85	t3	0.01440505094515045	17.6461874078093	1225.0
N86	t1	0.7562058721016954	338.78023070155956	448.0
N86	t2	0.08228259041068957	36.86260050398893	448.0
N86	t3	0.16151153748761532	72.35716879445167	448.0

N87	t1	0.3943802842224133	257.9247058814583	654.0
N87	t2	0.3277004685412738	214.3161064259931	654.0
N87	t3	0.2779192472363127	181.75918769254852	654.0
N88	t1	0.5463303700241178	352.92941903558005	646.0
N88	t2	0.27755003616475377	179.29732336243094	646.0
N88	t3	0.1761195938111286	113.77325760198907	646.0
N89	t1	0.8867226432275744	637.553580480626	719.0
N89	t2	0.048604097811928815	34.94634632677682	719.0
N89	t3	0.06467325896049662	46.50007319259707	719.0
N90	t1	0.7561193063105771	468.7939699125578	620.0
N90	t2	0.136139725190842	84.40662961832204	620.0
N90	t3	0.10774096849858084	66.79940046912012	620.0
N91	t1	0.6654511842398929	194.31174579804872	292.0
N91	t2	0.18753033267515118	54.75885714114415	292.0
N91	t3	0.14701848308495577	42.929397060807084	292.0
N92	t1	0.7469547849669035	345.0931106547094	462.0
N92	t2	0.10065788924749981	46.503944832344914	462.0
N92	t3	0.15238732578559674	70.4029445129457	462.0
N93	t1	0.8922495533851096	734.3213824359452	823.0
N93	t2	0.05703145750461106	46.936889526294905	823.0
N93	t3	0.05071898911027952	41.74172803776005	823.0
N94	t1	0.9830176119966603	947.6289779647805	964.0
N94	t2	0.007937129881439247	7.651393205707434	964.0
N94	t3	0.00904525812190044	8.719628829512024	964.0

N95	t1	0.45353839884178687	506.6023915062759	1117.0
N95	t2	0.26456808491202294	295.52255084672964	1117.0
N95	t3	0.2818935162461902	314.87505764699443	1117.0
N96	t1	0.9532160512590854	1472.718799195287	1545.0
N96	t2	0.025724850241948212	39.744893623809986	1545.0
N96	t3	0.021059098498966665	32.5363071809035	1545.0
N97	t1	0.9987236692976097	1643.8991596638655	1646.0
N97	t2	2.5526614047806244E-5	0.04201680672268908	1646.0
N97	t3	0.0012508040883425057	2.0588235294117645	1646.0
N98	t1	0.9915670467964984	1577.583171453229	1591.0
N98	t2	0.0024068527692886095	3.8293027559381776	1591.0
N98	t3	0.006026100434212876	9.587525790832686	1591.0
N99	t1	0.8434320962727228	1362.1428354804473	1615.0
N99	t2	0.07241024879528339	116.94255180438267	1615.0
N99	t3	0.08415765493199327	135.91461271516914	1615.0
N100	t1	0.9964055970980605	1641.0800184205057	1647.0
N100	t2	0.002012566023423299	3.3146962405781735	1647.0
N100	t3	0.0015818368785162462	2.6052853389162576	1647.0
N101	t1	0.9992240726722179	1319.975	1321.0
N101	t2	1.8925056775170325E-5	0.025	1321.0
N101	t3	7.57002271006813E-4	1.0	1321.0
N102	t1	0.9949746808745948	1578.0298438671075	1586.0
N102	t2	0.0029722915725602745	4.714054434080595	1586.0
N102	t3	0.0020530275528449523	3.256101698812094	1586.0

N103	t1	0.9965846819677588	1656.323741430415	1662.0
N103	t2	0.0026616402544724625	4.423646102933232	1662.0
N103	t3	7.536777777689097E-4	1.252612466651928	1662.0
N104	t1	0.8045957377881575	1329.9967545638244	1653.0
N104	t2	0.0865443841157661	143.05786694336135	1653.0
N104	t3	0.10885987809607607	179.94537849281375	1653.0
N105	t1	0.5565697548303248	925.0189325279997	1662.0
N105	t2	0.18045394444307156	299.91445566438495	1662.0
N105	t3	0.26297630072660333	437.0666118076148	1662.0
N106	t1	0.7020786883508292	1171.769330857534	1669.0
N106	t2	0.1057410670526852	176.4818409109316	1669.0
N106	t3	0.1921802445964858	320.7488282315348	1669.0
N107	t1	0.5046591750756637	845.3041182517367	1675.0
N107	t2	0.22819011967866726	382.21845046176765	1675.0
N107	t3	0.2671507052456694	447.47743128649626	1675.0
N108	t1	0.9999291558924588	258.98165137614683	259.0
N108	t2	0.0	0.0	259.0
N108	t3	7.084410754135526E-5	0.01834862385321101	259.0
N109	t1	0.9930734202613453	1622.681968707038	1634.0
N109	t2	0.002714907360118401	4.436158626433468	1634.0
N109	t3	0.004211672378536482	6.881872666528611	1634.0
N110	t1	0.9252569631722296	1526.6739892341789	1650.0
N110	t2	0.035863327267752	59.17448999179081	1650.0
N110	t3	0.03887970956001835	64.15152077403027	1650.0

N111	t1	0.9928429732577313	1652.090707500865	1664.0
N111	t2	0.005429432816397795	9.034576206485932	1664.0
N111	t3	0.0017275939258707348	2.8747162926489027	1664.0
N112	t1	0.9971481039239408	1665.2373335529812	1670.0
N112	t2	0.001793289863747545	2.9947940724584003	1670.0
N112	t3	0.0010586062123118703	1.7678723745608234	1670.0
N113	t1	0.45505598367960876	760.8536047123058	1672.0
N113	t2	0.3207733099079954	536.3329741661684	1672.0
N113	t3	0.22417070641239553	374.8134211215253	1672.0
N114	t1	0.9974715549936789	1578.0	1582.0
N114	t2	0.0012642225031605564	2.0	1582.0
N114	t3	0.0012642225031605564	2.0	1582.0
N115	t1	0.5230597779908265	853.6335576810288	1632.0
N115	t2	0.24338535843449488	397.20490496509564	1632.0
N115	t3	0.2335548635746787	381.16153735387564	1632.0
N116	t1	0.964964527058182	1596.0513277542332	1654.0
N116	t2	0.021120093214711876	34.932634177133444	1654.0
N116	t3	0.013915379727105971	23.016038068633275	1654.0
N117	t1	0.959998367765071	1585.9173035478973	1652.0
N117	t2	0.023586561109277055	38.9649989525257	1652.0
N117	t3	0.016415071125651843	27.117697499576842	1652.0
N118	t1	0.9291154783025248	1546.9772713737038	1665.0
N118	t2	0.02922197941440677	48.654595724987274	1665.0
N118	t3	0.041662542283068676	69.36813290130935	1665.0

N119	t1	0.9428292165894148	1545.2970859900508	1639.0
N119	t2	0.03344702172758049	54.81966861150442	1639.0
N119	t3	0.02372376168300462	38.88324539844457	1639.0
N120	t1	0.9373386903215734	1543.7968229596313	1647.0
N120	t2	0.034015337355651404	56.02326062475786	1647.0
N120	t3	0.028645972322775118	47.17991641561062	1647.0
N121	t1	0.966942953455899	1596.4228161556891	1651.0
N121	t2	0.024812560827280086	40.96553792583942	1651.0
N121	t3	0.008244485716821019	13.6116459184715	1651.0
N122	t1	0.9844349571190284	1602.6601101897782	1628.0
N122	t2	0.0061443520436766305	10.003005127105554	1628.0
N122	t3	0.009420690837294965	15.336884683116203	1628.0
N123	t1	0.5600324370732321	907.2525480586361	1620.0
N123	t2	0.263533382228118	426.92407920955117	1620.0
N123	t3	0.17643418069865016	285.82337273181327	1620.0
N124	t1	0.7067224674548946	1175.9861858449447	1664.0
N124	t2	0.2173709606124129	361.7052784590551	1664.0
N124	t3	0.07590657193269315	126.3085356960014	1664.0
N125	t1	0.8884773828523748	1497.972867489104	1686.0
N125	t2	0.06543528830605252	110.32389608400456	1686.0
N125	t3	0.04608732884157179	77.70323642689003	1686.0
N126	t1	0.6348494571356327	1065.2773890735916	1678.0
N126	t2	0.20616171831642632	345.9393633349634	1678.0
N126	t3	0.15898882454794255	266.7832475914476	1678.0

N127	t1	0.5285305707508579	876.8322168756731	1659.0
N127	t2	0.26776809385397743	444.22726770374857	1659.0
N127	t3	0.2037013353951643	337.9405154205776	1659.0
N128	t1	0.8979358455214782	1498.654926175347	1669.0
N128	t2	0.05044058499922462	84.1853363637059	1669.0
N128	t3	0.051623569479298054	86.15973746094845	1669.0
N129	t1	0.4132699876899922	696.7731992453269	1686.0
N129	t2	0.3348452231854386	564.5490462906495	1686.0
N129	t3	0.2518847891245687	424.67775446402277	1686.0
N130	t1	0.4352534768314605	730.7905876000221	1679.0
N130	t2	0.35902746933119306	602.8071210070732	1679.0
N130	t3	0.20571905383734646	345.4022913929047	1679.0
N131	t1	0.4471427711065908	755.2241403990319	1689.0
N131	t2	0.23906556381684071	403.781737286644	1689.0
N131	t3	0.31379166507656964	529.9941223143261	1689.0
N132	t1	0.39190660630768315	664.6736042978306	1696.0
N132	t2	0.31483197558480625	533.9550305918314	1696.0
N132	t3	0.29326141810751083	497.37136511033833	1696.0
N133	t1	0.7124398360688985	1208.297961972852	1696.0
N133	t2	0.1420743816739598	240.9581513190358	1696.0
N133	t3	0.14548578225714195	246.74388670811274	1696.0
N134	t1	0.9827116042736737	1658.8171880139612	1688.0
N134	t2	0.008882674349344925	14.993954301694233	1688.0
N134	t3	0.008405721376981812	14.188857684345297	1688.0

N135	t1	0.6087060441789928	1023.8435663090659	1682.0
N135	t2	0.2660555016637749	447.5053537984694	1682.0
N135	t3	0.12523845415723298	210.65107989246584	1682.0
N136	t1	0.34811254656083984	574.3857018253857	1650.0
N136	t2	0.3004598121994995	495.7586901291742	1650.0
N136	t3	0.35142764123966064	579.85560804544	1650.0
N137	t1	0.9489612163073866	1567.6839293398027	1652.0
N137	t2	0.017604056769236782	29.081901782779163	1652.0
N137	t3	0.033434726923377	55.234168877418796	1652.0
N138	t1	0.6696042402507146	1122.9263109004485	1677.0
N138	t2	0.028355567953514325	47.55228745804352	1677.0
N138	t3	0.30204019179577074	506.5214016415075	1677.0
N139	t1	0.8479257689403455	1374.4876714523002	1621.0
N139	t2	0.02556467157682429	41.44033262603217	1621.0
N139	t3	0.12650955948282996	205.0719959216674	1621.0
N140	t1	0.9110822848630106	1485.9752066115702	1631.0
N140	t2	0.045370938074800735	74.0	1631.0
N140	t3	0.04354677706218869	71.02479338842974	1631.0
N141	t1	0.999965182743224	1629.943247871455	1630.0
N141	t2	1.9479833463133434E-5	0.0317521285449075	1630.0
N141	t3	1.5337423312883436E-5	0.025	1630.0
N142	t1	0.8129641494004803	1309.6852446841738	1611.0
N142	t2	0.07554299636842247	121.69976714952861	1611.0
N142	t3	0.11149285423109691	179.6149881662971	1611.0

N143	t1	0.5016377040348297	798.6072248234489	1592.0
N143	t2	0.2152840521011612	342.7322109450486	1592.0
N143	t3	0.2830782438640093	450.6605642315028	1592.0

Dataset S3. Accessions and species names for genomes used in *Escovopsis* phylogenetic tree dating.

Accession	Genus	Species	
GCA_000222935.2	Aciculosporium	take	
GCA_000769265.1	Acremonium	chrysogenum	
GCA_001636795.1	Akanthomyces	lecanii	
GCA_003415625.1	Aquanectria	penicillioides	
GCA_001008035.1	Atkinsonella	texensis	
GCA_000709145.1	Balansia	obtecta	
GCA_000280675.1	Beauveria	bassiana	
GCA_001636735.1	Beauveria	brongniartii	
GCA_002179835.1	Calonectria	leucothoes	
GCA_000149445.2	Candida	albicans	Outgroup
GCA_004303015.1	Cladobotryum	protrusum	
GCA_000223175.2	Claviceps	paspali	
GCA_000347355.1	Claviceps	purpurea	
GCA_003693555.1	Coccinonectria	pachysandricola	
GCA_003025305.1	Cordyceps	tenuipes	
GCA_006981975.1	Cordyceps	javanica	
GCA_003385255.1	Corinectria	fuckeliana	
GCA_000935225.1	Dactylonectria	macrodidyma	
GCA_011426265.1	Dactylonectria	torresensis	

GCA_001625195.1	Drechmeria	coniospora	
GCA_000222955.2	Epichloe	typhina	
GCA_001043855.1	Epichloe	uncinata	
GCA_900079805.1	Fusarium	fujikuroi	
GCA_900188565.1	Geosmithia	flava	
GCA_900188575.1	Geosmithia	putterillii	
GCA_001599755.1	Gliomastix	tumulicola	
GCA_000472125.2	Hirsutella	thompsonii	
GCA_000956045.1	Hirsutella	minnesotensis	
GCA_000731825.1	Hypocrella	siamensis	
GCA_008477525.1	Hypomyces	perniciosus	
GCA_011799845.1	Hypomyces	rosellus	
GCA_002796755.1	Lecanicillium	psalliotae	
GCA_001599555.1	Memnoniella	echinata	
GCA_000426965.1	Metarhizium	anisopliae	
GCA_000804445.1	Metarhizium	album	
GCA_001636675.1	Moelleriella	libera	
GCA_002682825.1	Nectria	sp.	
GCA_003385265.1	Neonectria	hederae	
GCA_000448365.1	Ophiocordyceps	sinensis	
GCA_900080695.1	Ophiocordyceps	bispora	
GCA_001455915.2	Paecilomyces	hepiali	
GCA_003012165.1	Paramyrothecium	roridum	
GCA_000222875.2	Periglandula	ipomoeae	

GCA_001653235.2	Pochonia	chlamydosporia	
GCA_002911195.1	Pseudonectria	foliicola	
GCA_003693515.1	Pseudonectria	buxi	
GCA_001653205.1	Purpureocillium	lilacinum	
GCA_000151485.1	Saccharomyces	cerevisiae	Outgroup
GCA_001661265.1	Saitoella	complicata	Outgroup
GCA_001972265.1	Sarocladium	oryzae	
GCA_008271525.1	Sarocladium	brachiariae	
GCA_012273805.1	Simplicillium	aogashimaense	
GCA_000730325.1	Stachybotrys	chartarum	
GCA_000732775.1	Stachybotrys	chlorohalonata	
GCA_013420875.1	Thelonectria	rubi	
GCA_000421905.1	Tolypocladium	inflatum	
GCA_002901185.1	Tolypocladium	capitatum	
GCA_000825705.1	Torrubiella	hemipterigena	
GCA_000170995.2	Trichoderma	virens	
GCA_000171015.2	Trichoderma	atroviride	
GCA_000331835.2	Trichoderma	hamatum	
GCA_000332775.1	Trichoderma	longibrachiatum	
GCA_001050175.1	Trichoderma	parareesei	
GCA_001481775.2	Trichoderma	gamsii	
GCA_001721665.1	Trichoderma	pleuroti	
GCA_001931985.1	Trichoderma	sp.	
GCA_001950475.1	Trichoderma	koningii	

GCA_002006585.1	Trichoderma	reesei	
GCA_002022785.1	Trichoderma	guizhouense	
GCA_002246955.1	Trichoderma	koningiopsis	
GCA_003012105.1	Trichoderma	arundinaceum	
GCA_003025105.1	Trichoderma	asperellum	
GCA_003025115.1	Trichoderma	citrinoviride	
GCA_003439915.1	Trichoderma	atrobrunneum	
GCA_007896495.1	Trichoderma	viride	
GCA_003012095.1	Trichothecium	roseum	
GCA_003012115.1	Trichothecium	sympodiale	
GCA_000687475.1	Ustilaginoidea	virens	
GCA_012184525.1	Xenoacremonium	recifei	

Dataset S4. Annotation data of secretome genes across *Escovopsis*.

id	type	all	Coral	Higher	Hypo_Clado	Leafcutter	Lower	Trichoderma
GT24	CAZYME	0.82	0.67	0.83	1.00	0.67	1.00	0.88
AA9	CAZYME	0.82	0.83	0.83	0.67	0.89	NA	1.00
GH30_3	NA	0.82	0.83	0.83	1.00	0.56	0.50	1.00
GH65	CAZYME	0.84	0.83	0.50	1.00	0.89	0.50	1.00
abH32	LED	0.91	0.83	0.83	1.00	0.78	1.00	1.00
MER0064741	MEROPS	0.87	1.00	0.67	1.00	0.89	1.00	0.82
GH75	CAZYME	0.93	1.00	0.50	1.00	1.00	1.00	1.00
abH13	LED	0.93	1.00	0.67	1.00	0.89	1.00	1.00
GH5_5	NA	0.96	1.00	0.67	1.00	1.00	1.00	1.00
CE10	CAZYME	0.93	1.00	0.83	1.00	1.00	0.50	1.00
abH04	LED	0.98	1.00	0.83	1.00	1.00	1.00	1.00
abH03	LED	0.98	1.00	0.83	1.00	1.00	1.00	1.00
abH01	LED	0.98	1.00	0.83	1.00	1.00	1.00	1.00
abH02	LED	0.98	1.00	0.83	1.00	1.00	1.00	1.00
GH36	CAZYME	0.89	0.67	1.00	0.67	1.00	1.00	0.88
GH12	CAZYME	0.91	0.83	0.83	0.67	0.89	1.00	1.00
abH22	LED	0.93	1.00	1.00	1.00	0.89	0.50	1.00
GH64	CAZYME	0.96	1.00	1.00	1.00	1.00	0.50	1.00

GH95	CAZYME	0.98	1.00	1.00	1.00	1.00	0.75	1.00
GH63	CAZYME	0.89	0.67	0.83	1.00	0.89	0.75	1.00
AA1_2	NA	0.93	0.83	1.00	1.00	0.78	1.00	1.00
GH89	CAZYME	0.93	1.00	1.00	1.00	1.00	0.75	0.88
GH31	CAZYME	0.96	1.00	1.00	1.00	1.00	1.00	0.88
abH16	LED	0.98	1.00	1.00	1.00	1.00	0.75	1.00
abH19	LED	0.96	1.00	0.83	1.00	1.00	0.75	1.00
GH132	CAZYME	0.93	0.83	0.83	1.00	1.00	1.00	0.94
3003392	CARD	0.98	1.00	1.00	1.00	1.00	1.00	0.94
3003942	CARD	1.00	1.00	1.00	1.00	1.00	1.00	1.00
GH92	CAZYME	1.00	1.00	1.00	1.00	1.00	1.00	1.00
GH76	CAZYME	1.00	1.00	1.00	1.00	1.00	1.00	1.00
GH72	CAZYME	1.00	1.00	1.00	1.00	1.00	1.00	1.00
GH55	CAZYME	1.00	1.00	1.00	1.00	1.00	1.00	1.00
GH47	CAZYME	1.00	1.00	1.00	1.00	1.00	1.00	1.00
GH3	CAZYME	1.00	1.00	1.00	1.00	1.00	1.00	1.00
GH28	CAZYME	1.00	1.00	1.00	1.00	1.00	1.00	1.00
GH20	CAZYME	1.00	1.00	1.00	1.00	1.00	1.00	1.00
GH2	CAZYME	1.00	1.00	1.00	1.00	1.00	1.00	1.00
GH18	CAZYME	1.00	1.00	1.00	1.00	1.00	1.00	1.00

GH16	CAZYME	1.00	1.00	1.00	1.00	1.00	1.00	1.00
GH128	CAZYME	1.00	1.00	1.00	1.00	1.00	1.00	1.00
GH125	CAZYME	1.00	1.00	1.00	1.00	1.00	1.00	1.00
CE5	CAZYME	1.00	1.00	1.00	1.00	1.00	1.00	1.00
AA7	CAZYME	1.00	1.00	1.00	1.00	1.00	1.00	1.00
AA2	CAZYME	1.00	1.00	1.00	1.00	1.00	1.00	1.00
AA11	CAZYME	1.00	1.00	1.00	1.00	1.00	1.00	1.00
abH36	LED	1.00	1.00	1.00	1.00	1.00	1.00	1.00
abH34	LED	1.00	1.00	1.00	1.00	1.00	1.00	1.00
abH27	LED	1.00	1.00	1.00	1.00	1.00	1.00	1.00
abH23	LED	1.00	1.00	1.00	1.00	1.00	1.00	1.00
abH11	LED	1.00	1.00	1.00	1.00	1.00	1.00	1.00
abH09	LED	1.00	1.00	1.00	1.00	1.00	1.00	1.00
abH08	LED	1.00	1.00	1.00	1.00	1.00	1.00	1.00
abH07	LED	1.00	1.00	1.00	1.00	1.00	1.00	1.00
GH35	CAZYME	0.80	0.67	0.83	NA	0.78	0.75	1.00
PL7_4	NA	0.84	0.33	0.67	1.00	0.89	1.00	1.00
GH71	CAZYME	0.89	0.50	1.00	1.00	0.78	1.00	1.00
GH79	CAZYME	0.87	0.50	1.00	1.00	0.67	1.00	1.00
GH15	CAZYME	0.56	0.33	0.67	NA	0.67	NA	0.76

abH12	LED	0.60	0.33	NA	0.33	0.44	0.75	1.00
GH7	CAZYME	0.64	0.33	0.50	NA	0.67	0.25	1.00
MER0032555	MEROPS	0.67	NA	0.67	1.00	0.78	NA	0.94
abH20	LED	0.71	0.33	0.67	0.67	1.00	0.75	0.71
abH06	LED	0.60	0.33	1.00	0.33	0.89	0.50	0.47
MER0014006	MEROPS	0.58	NA	0.83	0.67	1.00	1.00	0.35
MER0080921	MEROPS	0.80	1.00	1.00	1.00	0.89	1.00	0.53
MER0080922	MEROPS	0.73	1.00	0.83	1.00	1.00	0.75	0.41
MER0625340	MEROPS	0.78	1.00	0.67	1.00	1.00	1.00	0.53
MER0209434	MEROPS	0.87	1.00	0.83	1.00	1.00	1.00	0.71
MER0308564	MEROPS	0.64	0.50	0.83	1.00	0.89	1.00	0.35
abH21	LED	0.73	0.33	0.83	1.00	0.67	1.00	0.76
CE4	CAZYME	0.91	0.67	1.00	1.00	1.00	1.00	0.88
MER0314821	MEROPS	0.62	1.00	0.67	0.67	1.00	NA	0.41
abH33	LED	0.78	0.50	1.00	0.67	1.00	0.50	0.76
MER0472968	MEROPS	0.82	0.50	1.00	0.67	1.00	0.50	0.88
MER0211021	MEROPS	0.84	0.67	0.83	1.00	1.00	NA	1.00
GT15	CAZYME	0.76	0.83	0.83	NA	0.78	0.25	0.94
GH5_7	NA	0.84	0.67	0.83	NA	1.00	1.00	0.94
MER0035648	MEROPS	0.84	0.67	0.83	NA	1.00	1.00	0.94

MER0032938	MEROPS	0.80	0.67	0.83	0.67	1.00	1.00	0.71
MER0204750	MEROPS	0.76	1.00	0.83	0.67	0.89	1.00	0.53
3004584	CARD	0.13	NA	0.17	NA	0.11	0.25	0.18
MER0496069	MEROPS	0.07	NA	NA	NA	NA	NA	0.18
MER1007435	MEROPS	0.04	NA	NA	NA	NA	NA	0.12
E9EJV1_METAR	VIRULENCE	0.04	NA	NA	NA	NA	NA	0.12
MER0064151	MEROPS	0.04	NA	NA	NA	NA	NA	0.12
3004035	CARD	0.04	NA	NA	NA	NA	NA	0.12
MER0064130	MEROPS	0.07	NA	NA	NA	NA	NA	0.18
MER1175858	MEROPS	0.04	NA	NA	NA	NA	NA	0.12
MER1073104	MEROPS	0.04	NA	NA	NA	NA	NA	0.12
3002522	CARD	0.04	NA	NA	NA	NA	NA	0.12
MER0976651	MEROPS	0.04	NA	NA	NA	NA	NA	0.12
MER1178639	MEROPS	0.04	NA	NA	NA	NA	NA	0.12
SUB5_ARTBC	VIRULENCE	0.07	NA	NA	NA	NA	NA	0.18
MER0064233	MEROPS	0.07	NA	NA	NA	NA	NA	0.18
MER1179079	MEROPS	0.07	NA	NA	NA	NA	NA	0.18
MER0064746	MEROPS	0.11	NA	NA	NA	NA	NA	0.29
MER0975454	MEROPS	0.09	NA	NA	NA	NA	NA	0.24
Q6TDT0_CRYGA	VIRULENCE	0.09	NA	NA	NA	NA	NA	0.24

MER0983684	MEROPS	0.11	NA	NA	NA	NA	NA	0.29
MER0536151	MEROPS	0.11	NA	NA	NA	NA	NA	0.29
MER1073477	MEROPS	0.13	NA	NA	NA	NA	NA	0.35
CTSD_ARTBC	VIRULENCE	0.27	NA	NA	NA	0.11	0.50	0.53
LAP1_TRIVH	VIRULENCE	0.31	0.33	NA	0.33	NA	0.25	0.59
MER0032162	MEROPS	0.20	NA	NA	NA	NA	NA	0.53
MER0378848	MEROPS	0.27	0.67	NA	0.33	NA	NA	0.41
OPSB_TRIVH	VIRULENCE	0.22	0.33	0.17	NA	NA	NA	0.41
MER0383686	MEROPS	0.27	NA	0.17	0.67	NA	0.50	0.41
MER0383724	MEROPS	0.22	NA	0.17	0.33	NA	NA	0.47
MER0625115	MEROPS	0.22	NA	NA	0.33	NA	NA	0.53
MER0998302	MEROPS	0.16	NA	NA	NA	NA	NA	0.41
MER0167059	MEROPS	0.20	NA	NA	0.33	NA	NA	0.47
MER0625808	MEROPS	0.18	NA	NA	NA	NA	NA	0.47
MER0109473	MEROPS	0.16	NA	NA	NA	NA	NA	0.41
MER0511361	MEROPS	0.16	NA	NA	NA	NA	NA	0.41
MER0383713	MEROPS	0.18	NA	NA	0.33	NA	NA	0.41
MER0496070	MEROPS	0.18	NA	NA	0.33	NA	NA	0.41
MER0761149	MEROPS	0.16	NA	NA	NA	NA	NA	0.41
MER1248093	MEROPS	0.16	NA	NA	NA	NA	NA	0.41

SUB7_ARTBC	VIRULENCE	0.18	NA	NA	NA	0.22	NA	0.35
MER0131500	MEROPS	0.11	NA	NA	NA	NA	NA	0.29
AA3	CAZYME	0.13	NA	NA	NA	NA	NA	0.35
GH45	CAZYME	0.11	NA	NA	NA	NA	NA	0.29
MER1138037	MEROPS	0.11	NA	NA	NA	NA	NA	0.29
MER0118505	MEROPS	0.11	NA	NA	NA	NA	NA	0.29
MER1005478	MEROPS	0.11	NA	NA	NA	NA	NA	0.29
MER0099136	MEROPS	0.13	NA	NA	NA	NA	NA	0.35
MER1069374	MEROPS	0.13	NA	NA	NA	NA	NA	0.35
CUTI1_COLGL	VIRULENCE	0.11	NA	NA	NA	NA	NA	0.29
Q9C2Y1_BOTFU	VIRULENCE	0.13	NA	NA	NA	NA	NA	0.35
MER1073214	MEROPS	0.16	NA	NA	NA	NA	NA	0.41
MER0970662	MEROPS	0.16	NA	NA	NA	NA	NA	0.41
MER0384193	MEROPS	0.16	NA	NA	NA	NA	NA	0.41
MER0384133	MEROPS	0.16	NA	NA	NA	NA	NA	0.41
MER0295895	MEROPS	0.16	NA	NA	NA	NA	NA	0.41
MER0383832	MEROPS	0.16	NA	NA	NA	NA	NA	0.41
MER1070132	MEROPS	0.18	NA	NA	NA	NA	NA	0.47
MER1065333	MEROPS	0.18	NA	NA	NA	NA	NA	0.47
MER0985130	MEROPS	0.18	NA	NA	NA	NA	NA	0.47

MER0968917	MEROPS	0.18	NA	NA	NA	NA	NA	0.47
MER0383470	MEROPS	0.18	NA	NA	NA	NA	NA	0.47
MER0297012	MEROPS	0.18	NA	NA	NA	NA	NA	0.47
MER0349865	MEROPS	0.18	NA	NA	NA	NA	NA	0.47
3004290	CARD	0.07	NA	NA	NA	NA	NA	0.18
MER1010109	MEROPS	0.07	NA	NA	NA	NA	NA	0.18
GH26	CAZYME	0.11	NA	NA	NA	NA	NA	0.29
3004591	CARD	0.09	NA	NA	NA	NA	NA	0.24
MER0032867	MEROPS	0.09	NA	NA	NA	NA	NA	0.24
A7ULH9_CANGY	VIRULENCE	0.16	NA	NA	0.33	NA	NA	0.35
MER0383344	MEROPS	0.11	NA	NA	0.33	NA	NA	0.24
MER0130181	MEROPS	0.16	NA	NA	NA	NA	NA	0.41
MER0173931	MEROPS	0.16	NA	NA	NA	NA	NA	0.41
MER1074102	MEROPS	0.11	NA	NA	NA	NA	NA	0.29
MER0118072	MEROPS	0.11	NA	NA	NA	NA	NA	0.29
MER0974079	MEROPS	0.11	NA	NA	NA	NA	NA	0.29
3002516	CARD	0.11	NA	NA	0.33	NA	NA	0.24
MER1005208	MEROPS	0.09	NA	NA	NA	NA	NA	0.24
MER0031546	MEROPS	0.07	NA	NA	NA	NA	NA	0.18
MER1230312	MEROPS	0.09	NA	NA	NA	NA	NA	0.24

MER1228585	MEROPS	0.09	NA	NA	NA	NA	NA	0.24
MER0350221	MEROPS	0.09	NA	NA	NA	NA	NA	0.24
MER0625803	MEROPS	0.09	NA	NA	NA	NA	NA	0.24
MER0281239	MEROPS	0.13	NA	NA	NA	NA	NA	0.35
MER0314866	MEROPS	0.13	NA	NA	NA	NA	NA	0.35
MER1177284	MEROPS	0.11	NA	NA	NA	NA	NA	0.29
MER1286490	MEROPS	0.09	NA	NA	NA	NA	NA	0.24
GH43_13	NA	0.09	NA	NA	NA	NA	NA	0.24
MER1027628	MEROPS	0.09	NA	NA	NA	NA	NA	0.24
3003854	CARD	0.07	NA	NA	NA	NA	NA	0.18
MER0033386	MEROPS	0.09	NA	NA	NA	NA	NA	0.24
SCPA_ARTBC	VIRULENCE	0.04	NA	NA	NA	NA	NA	0.12
abH14	LED	0.09	NA	NA	NA	NA	0.50	0.12
Q5ANE1_CANAL	VIRULENCE	0.07	NA	0.17	NA	NA	NA	0.12
MER1179045	MEROPS	0.07	NA	NA	NA	NA	NA	0.18
MER0624524	MEROPS	0.07	NA	NA	NA	NA	NA	0.18
MER0096282	MEROPS	0.07	NA	NA	NA	NA	NA	0.18
MER1125240	MEROPS	0.04	NA	NA	NA	NA	NA	0.12
abH30	LED	0.04	NA	NA	NA	0.11	NA	0.06
3000844	CARD	0.04	NA	NA	NA	NA	NA	0.12

MER0902462	MEROPS	0.07	NA	NA	NA	NA	NA	0.18
MER0258435	MEROPS	0.16	NA	NA	NA	NA	NA	0.41
MER0209177	MEROPS	0.16	NA	NA	NA	NA	NA	0.41
3004582	CARD	0.18	NA	NA	NA	NA	NA	0.47
SUB7_ARTOC	VIRULENCE	0.13	NA	NA	NA	NA	NA	0.35
MER0208727	MEROPS	0.13	NA	NA	NA	NA	NA	0.35
MER1074437	MEROPS	0.16	NA	NA	NA	NA	NA	0.41
3004289	CARD	0.20	NA	NA	NA	NA	NA	0.53
MER0425752	MEROPS	0.16	NA	NA	NA	NA	NA	0.41
GH106	CAZYME	0.18	NA	NA	NA	NA	NA	0.47
SUB10_ARTBC	VIRULENCE	0.20	NA	NA	NA	NA	NA	0.53
MER0167067	MEROPS	0.24	NA	NA	NA	NA	NA	0.65
MER0972305	MEROPS	0.22	NA	NA	NA	NA	NA	0.59
MER0213217	MEROPS	0.29	NA	NA	NA	NA	NA	0.76
GH93	CAZYME	0.27	NA	NA	NA	NA	NA	0.71
MER0064128	MEROPS	0.29	NA	NA	NA	NA	NA	0.76
CE8	CAZYME	0.20	NA	NA	NA	NA	NA	0.53
MER0064533	MEROPS	0.22	NA	NA	NA	NA	NA	0.59
Q00351_COCCA	VIRULENCE	0.24	0.17	NA	NA	NA	NA	0.59
Q5GFD3_PHAND	VIRULENCE	0.27	NA	NA	0.33	NA	0.50	0.53

GH6	CAZYME	0.38	0.33	NA	NA	NA	1.00	0.65
NPIIC_ASPFU	VIRULENCE	0.42	NA	0.33	0.67	NA	1.00	0.65
MER0384170	MEROPS	0.27	NA	NA	0.67	NA	0.25	0.53
MER0210110	MEROPS	0.29	NA	NA	1.00	NA	NA	0.59
MER0214202	MEROPS	0.29	NA	NA	1.00	NA	NA	0.59
PEPA_COCP7	VIRULENCE	0.36	NA	NA	1.00	NA	NA	0.76
Q59PP4_CANAL	VIRULENCE	0.29	NA	NA	1.00	NA	NA	0.59
MER0970307	MEROPS	0.22	NA	NA	0.67	NA	NA	0.47
GH1	CAZYME	0.22	NA	NA	0.33	NA	NA	0.53
MEP_NEOFI	VIRULENCE	0.24	NA	NA	0.67	NA	NA	0.53
A1CIY3_ASPCL	VIRULENCE	0.27	NA	NA	0.67	NA	NA	0.59
MER0273140	MEROPS	0.33	NA	NA	0.67	NA	NA	0.76
AA5	CAZYME	0.64	0.50	0.67	1.00	0.22	0.50	0.88
GT32	CAZYME	0.69	1.00	0.83	0.67	NA	0.50	0.94
GH11	CAZYME	0.76	0.83	0.67	0.67	0.33	0.75	1.00
MER0242197	MEROPS	0.60	0.67	0.50	0.67	0.22	0.50	0.82
GH67	CAZYME	0.62	0.67	1.00	NA	NA	0.25	1.00
AA3_2	NA	0.64	0.50	NA	1.00	0.44	0.75	0.94
abH17	LED	0.49	0.33	NA	0.33	NA	0.75	0.94
MER0047368	MEROPS	0.47	0.33	0.17	NA	NA	0.50	0.94

Q2LK92_BOTFU	VIRULENCE	0.51	0.33	0.17	1.00	NA	0.50	0.88
GH81	CAZYME	0.56	0.33	NA	1.00	NA	1.00	0.94
MER0408764	MEROPS	0.58	0.33	NA	1.00	NA	1.00	1.00
GT17	CAZYME	0.47	0.33	NA	0.67	0.33	NA	0.82
CE1	CAZYME	0.53	0.67	NA	1.00	NA	NA	1.00
abH38	LED	0.51	0.33	NA	1.00	0.33	NA	0.88
SED2_ASPFU	VIRULENCE	0.44	0.33	0.17	1.00	NA	NA	0.82
GH25	CAZYME	0.47	0.33	NA	1.00	NA	NA	0.94
SPCA_ARTOC	VIRULENCE	0.44	0.17	NA	0.67	NA	NA	1.00
MER0625601	MEROPS	0.29	NA	NA	NA	NA	NA	0.76
GH62	CAZYME	0.33	NA	NA	NA	NA	NA	0.88
GH30_5	NA	0.33	NA	NA	NA	NA	NA	0.88
CEUL_OPHUL	VIRULENCE	0.33	NA	NA	NA	NA	NA	0.88
GH30_7	NA	0.36	NA	NA	NA	NA	NA	0.94
abH26	LED	0.38	NA	NA	0.33	NA	0.25	0.88
CE16	CAZYME	0.44	NA	NA	NA	NA	0.75	1.00
Q5AG71_CANAL	VIRULENCE	0.40	NA	NA	0.33	NA	0.25	0.94
Q01446_NECHA	VIRULENCE	0.33	NA	NA	NA	NA	NA	0.88
Q9Y784_MAGGR	VIRULENCE	0.31	NA	NA	NA	NA	NA	0.82
3002883	CARD	0.38	NA	NA	0.33	NA	NA	0.94

GT1	CAZYME	0.36	NA	NA	NA	NA	NA	0.94
GH78	CAZYME	0.36	NA	NA	NA	NA	NA	0.94
MER0114579	MEROPS	0.33	NA	NA	NA	NA	NA	0.88
MER0424902	MEROPS	0.33	NA	NA	NA	NA	NA	0.88
GH54	CAZYME	0.42	0.33	NA	NA	NA	NA	1.00
GH74	CAZYME	0.38	0.17	NA	NA	NA	NA	0.94
Q5AJC8_CANAL	VIRULENCE	0.38	NA	0.17	NA	NA	NA	0.94
MER0382286	MEROPS	0.36	NA	NA	NA	NA	NA	0.94
MER0511172	MEROPS	0.36	NA	NA	NA	NA	NA	0.94
MER0999770	MEROPS	0.38	NA	NA	NA	NA	NA	1.00
MER0874598	MEROPS	0.38	NA	NA	NA	NA	NA	1.00
GH10	CAZYME	0.38	NA	NA	NA	NA	NA	1.00
MER0275595	MEROPS	0.38	NA	NA	NA	NA	NA	1.00
MER0204230	MEROPS	0.36	NA	NA	NA	NA	NA	0.94
SED4_ASPFU	VIRULENCE	0.36	NA	NA	NA	NA	NA	0.94
MER0087541	MEROPS	0.36	NA	NA	0.67	NA	NA	0.82
3004611	CARD	0.38	NA	NA	0.67	NA	NA	0.88
O94196_MAGGR	VIRULENCE	0.36	NA	NA	0.67	NA	NA	0.82
MER0065244	MEROPS	0.42	NA	NA	1.00	NA	NA	0.94
MER0032561	MEROPS	0.42	NA	NA	1.00	NA	NA	0.94

GH27	CAZYME	0.42	NA	NA	0.67	NA	NA	1.00
GH13_1	CAZYME	0.44	NA	NA	1.00	NA	NA	1.00
PL20	CAZYME	0.44	NA	NA	1.00	NA	NA	1.00
MER0060274	MEROPS	0.40	NA	NA	1.00	NA	NA	0.88
GH5_15	CAZYME	0.40	NA	NA	1.00	NA	NA	0.88
Q7ZA48_9HYPO	VIRULENCE	0.40	NA	NA	1.00	NA	NA	0.88
AA12	CAZYME	0.36	NA	NA	1.00	NA	NA	0.76
GH37	CAZYME	0.36	NA	NA	1.00	NA	NA	0.76
MER0421119	MEROPS	0.27	NA	NA	1.00	NA	NA	0.53
MER0350546	MEROPS	0.29	NA	NA	1.00	NA	NA	0.59
Q4PDC5_USTMA	VIRULENCE	0.36	NA	NA	1.00	NA	NA	0.76
GH105	CAZYME	0.24	NA	NA	1.00	NA	NA	0.47
MER0378941	MEROPS	0.38	0.33	NA	1.00	NA	NA	0.71
Q59VF3_CANAL	VIRULENCE	0.31	NA	NA	1.00	NA	NA	0.65
MER0114300	MEROPS	0.18	NA	NA	NA	NA	NA	0.47
3002135	CARD	0.18	NA	NA	NA	NA	NA	0.47
LAP4_ARTOC	VIRULENCE	0.22	NA	NA	0.33	NA	NA	0.53
MER0032545	MEROPS	0.13	NA	NA	NA	NA	NA	0.35
MER0119691	MEROPS	0.22	NA	NA	NA	NA	NA	0.59
MER1051527	MEROPS	0.18	NA	NA	NA	NA	NA	0.47

CE15	CAZYME	0.24	NA	NA	NA	NA	NA	0.65
MER0214723	MEROPS	0.20	NA	NA	NA	NA	NA	0.53
MER0215489	MEROPS	0.22	NA	NA	NA	NA	NA	0.59
ELM_ASPFU	VIRULENCE	0.22	0.33	NA	0.33	NA	NA	0.41
MER1068763	MEROPS	0.33	0.33	NA	0.33	NA	NA	0.71
MER0214426	MEROPS	0.24	NA	NA	NA	NA	NA	0.65
MCPA_TRIRU	VIRULENCE	0.22	NA	NA	NA	NA	NA	0.59
MER0305009	MEROPS	0.22	NA	NA	NA	NA	NA	0.59
MER0125990	MEROPS	0.33	NA	0.50	0.67	NA	NA	0.59
MER0209012	MEROPS	0.27	NA	NA	NA	NA	NA	0.71
MER0851575	MEROPS	0.31	NA	NA	0.67	NA	NA	0.71
CARP2_CANAL	VIRULENCE	0.36	0.17	NA	0.67	NA	0.50	0.65
E9ETX3_METAR	VIRULENCE	0.31	NA	NA	0.67	NA	0.25	0.65
GH24	CAZYME	0.33	NA	NA	1.00	NA	NA	0.71
MER0093089	MEROPS	0.33	NA	NA	1.00	NA	NA	0.71
MER0384250	MEROPS	0.40	NA	0.50	0.67	0.22	NA	0.65
GH39	CAZYME	0.24	NA	NA	0.33	NA	NA	0.59
MER0626147	MEROPS	0.18	NA	NA	0.67	NA	NA	0.35
MER0114101	MEROPS	0.04	NA	NA	NA	NA	NA	0.12
Q59X54_CANAL	VIRULENCE	0.07	NA	NA	NA	NA	NA	0.18

GT90	CAZYME	0.20	0.17	0.17	NA	NA	0.25	0.35
Q7ZA26_CRYNE	VIRULENCE	0.11	0.17	0.17	NA	NA	NA	0.18
3003026	CARD	0.29	0.33	NA	NA	NA	0.25	0.59
CE3	CAZYME	0.40	0.33	NA	1.00	NA	0.25	0.71
GH43	CAZYME	0.33	0.17	NA	0.67	NA	0.25	0.65
MER0033394	MEROPS	0.20	NA	NA	NA	NA	NA	0.53
GH5_24	NA	0.16	NA	NA	NA	NA	NA	0.41
PEPA_TRIVH	VIRULENCE	0.18	NA	NA	NA	NA	NA	0.47
MER0211573	MEROPS	0.20	NA	NA	NA	NA	NA	0.53
MER0033095	MEROPS	0.20	NA	NA	NA	NA	NA	0.53
MER0033126	MEROPS	0.29	NA	NA	NA	NA	NA	0.76
MCPAL_ARTBC	VIRULENCE	0.20	0.17	NA	0.67	NA	NA	0.35
MER0130678	MEROPS	0.13	NA	NA	1.00	NA	NA	0.18
MER0296885	MEROPS	0.13	NA	NA	1.00	NA	NA	0.18
MER1100667	MEROPS	0.13	NA	NA	0.33	NA	NA	0.29
MER0349890	MEROPS	0.18	0.17	NA	0.67	NA	NA	0.29
MER0383704	MEROPS	0.18	NA	NA	1.00	NA	NA	0.29
GH5_31	CAZYME	0.13	NA	NA	0.67	NA	NA	0.24
MER0295897	MEROPS	0.16	NA	NA	0.67	NA	NA	0.29
CBM1	CAZYME	0.24	0.33	0.17	NA	NA	0.50	0.35

MER0279945	MEROPS	0.22	NA	NA	0.33	NA	0.75	0.35
LAP1_ARTBC	VIRULENCE	0.38	0.33	0.33	0.33	0.22	NA	0.59
MER0853622	MEROPS	0.38	0.33	1.00	NA	0.33	0.25	0.29
MER0296926	MEROPS	0.31	NA	0.67	0.33	0.44	0.25	0.24
MER1073443	MEROPS	0.24	NA	0.50	1.00	NA	0.25	0.24
MER0378947	MEROPS	0.31	NA	0.33	NA	0.67	0.25	0.29
MER0383780	MEROPS	0.31	0.17	0.83	NA	0.33	NA	0.29
LAP2_TRIRU	VIRULENCE	0.11	0.33	NA	0.33	NA	NA	0.12
MER0850829	MEROPS	0.11	0.33	NA	0.33	NA	NA	0.12
MER0101148	MEROPS	0.22	0.50	NA	0.33	NA	NA	0.35
MER0296714	MEROPS	0.16	0.33	0.17	NA	NA	NA	0.24
abH25	LED	0.22	0.67	NA	0.33	NA	NA	0.29
MER0064512	MEROPS	0.31	0.67	NA	1.00	NA	0.50	0.29
3001816	CARD	0.07	NA	NA	NA	NA	NA	0.18
O94100_BOTFU	VIRULENCE	0.11	NA	NA	NA	NA	NA	0.29
MER0624725	MEROPS	0.07	NA	NA	NA	NA	NA	0.18
GT4	CAZYME	0.07	NA	0.17	NA	NA	NA	0.12
Q4WLS1_ASPFU	VIRULENCE	0.04	NA	NA	NA	NA	NA	0.12
3002878	CARD	0.04	NA	NA	NA	NA	NA	0.12
MER0383788	MEROPS	0.04	NA	NA	NA	NA	NA	0.12

MER1047980	MEROPS	0.13	NA	NA	NA	NA	NA	0.35
MER0276430	MEROPS	0.13	0.33	NA	NA	NA	NA	0.24
MER0496059	MEROPS	0.09	NA	NA	NA	NA	NA	0.24
MER1060383	MEROPS	0.04	NA	NA	NA	NA	NA	0.12
MER0656118	MEROPS	0.07	NA	NA	NA	NA	NA	0.18
MER0295438	MEROPS	0.07	NA	NA	NA	NA	NA	0.18
A4RGG9_MAGO7	VIRULENCE	0.07	NA	NA	NA	NA	NA	0.18
A6R3U9_AJECN	VIRULENCE	0.07	NA	NA	NA	NA	NA	0.18
MER0280243	MEROPS	0.11	NA	0.17	NA	NA	NA	0.24
MER1005925	MEROPS	0.09	NA	NA	NA	NA	NA	0.24
MER0496058	MEROPS	0.09	NA	NA	NA	NA	NA	0.24
MER0988519	MEROPS	0.11	NA	NA	NA	NA	NA	0.29
MER0975957	MEROPS	0.11	NA	NA	NA	NA	NA	0.29
MER0383872	MEROPS	0.11	NA	NA	NA	NA	NA	0.29
MER0383819	MEROPS	0.11	NA	NA	NA	NA	NA	0.29
MER0383736	MEROPS	0.11	NA	NA	NA	NA	NA	0.29
MER0383643	MEROPS	0.11	NA	NA	NA	NA	NA	0.29
MER0365567	MEROPS	0.11	NA	NA	NA	NA	NA	0.29
MER0187519	MEROPS	0.11	NA	NA	NA	NA	NA	0.29
MER0194922	MEROPS	0.11	NA	NA	NA	NA	NA	0.29

MER1070231	MEROPS	0.09	NA	NA	NA	NA	NA	0.24
MER1003490	MEROPS	0.09	NA	NA	NA	NA	NA	0.24
MER0382079	MEROPS	0.09	NA	NA	NA	NA	NA	0.24
MER0202996	MEROPS	0.09	NA	NA	NA	NA	NA	0.24
MER0325030	MEROPS	0.09	NA	NA	NA	NA	NA	0.24
MER0693873	MEROPS	0.11	NA	NA	0.33	NA	NA	0.24
MER0988946	MEROPS	0.04	NA	NA	NA	NA	NA	0.12
MER0384279	MEROPS	0.07	NA	NA	NA	NA	NA	0.18
MER0384301	MEROPS	0.07	NA	NA	NA	NA	NA	0.18
MER1286495	MEROPS	0.04	NA	NA	NA	NA	NA	0.12
MER1230431	MEROPS	0.04	NA	NA	NA	NA	NA	0.12
MER1230022	MEROPS	0.04	NA	NA	NA	NA	NA	0.12
MER1178694	MEROPS	0.04	NA	NA	NA	NA	NA	0.12
MER1177687	MEROPS	0.04	NA	NA	NA	NA	NA	0.12
MER1175936	MEROPS	0.04	NA	NA	NA	NA	NA	0.12
MER1175890	MEROPS	0.04	NA	NA	NA	NA	NA	0.12
MER1146596	MEROPS	0.04	NA	NA	NA	NA	NA	0.12
MER1142693	MEROPS	0.04	NA	NA	NA	NA	NA	0.12
MER1072707	MEROPS	0.04	NA	NA	NA	NA	NA	0.12
MER0845095	MEROPS	0.04	NA	NA	NA	NA	NA	0.12

MER0625950	MEROPS	0.04	NA	NA	NA	NA	NA	0.12
MER0421114	MEROPS	0.04	NA	NA	NA	NA	NA	0.12
MER0414073	MEROPS	0.04	NA	NA	NA	NA	NA	0.12
MER0383915	MEROPS	0.04	NA	NA	NA	NA	NA	0.12
MER0305109	MEROPS	0.04	NA	NA	NA	NA	NA	0.12
MER0220622	MEROPS	0.04	NA	NA	NA	NA	NA	0.12
GH134	CAZYME	0.04	NA	NA	NA	NA	NA	0.12
3000849	CARD	0.04	NA	NA	NA	NA	NA	0.12
CTSD_ARTOC	VIRULENCE	0.04	NA	NA	NA	NA	NA	0.12
MER0383576	MEROPS	0.04	NA	NA	NA	NA	NA	0.12
MER0383474	MEROPS	0.04	NA	NA	NA	NA	NA	0.12
MER0383311	MEROPS	0.04	NA	NA	NA	NA	NA	0.12
MER0382088	MEROPS	0.04	NA	NA	NA	NA	NA	0.12
MER0314882	MEROPS	0.04	NA	NA	NA	NA	NA	0.12
MER0308295	MEROPS	0.04	NA	NA	NA	NA	NA	0.12
MER0188786	MEROPS	0.04	NA	NA	NA	NA	NA	0.12
3001817	CARD	0.04	NA	NA	NA	NA	NA	0.12
MER0187495	MEROPS	0.04	NA	NA	NA	NA	NA	0.12
MER0325032	MEROPS	0.07	NA	NA	NA	NA	NA	0.18
MER0297003	MEROPS	0.07	NA	NA	NA	NA	NA	0.18

MER0187528	MEROPS	0.07	NA	NA	NA	NA	NA	0.18
MER0210192	MEROPS	0.07	NA	NA	NA	NA	NA	0.18
P78607_CLAPU	VIRULENCE	0.09	NA	NA	NA	NA	NA	0.24
MER1074503	MEROPS	0.09	NA	NA	NA	NA	NA	0.24
MER1073341	MEROPS	0.09	NA	NA	NA	NA	NA	0.24
MER1073149	MEROPS	0.09	NA	NA	NA	NA	NA	0.24
MER0983324	MEROPS	0.09	NA	NA	NA	NA	NA	0.24
MER0979320	MEROPS	0.09	NA	NA	NA	NA	NA	0.24
MER0972514	MEROPS	0.09	NA	NA	NA	NA	NA	0.24
MER0402318	MEROPS	0.09	NA	NA	NA	NA	NA	0.24
MER0383625	MEROPS	0.09	NA	NA	NA	NA	NA	0.24
MER0366015	MEROPS	0.09	NA	NA	NA	NA	NA	0.24
MER0349783	MEROPS	0.09	NA	NA	NA	NA	NA	0.24
MER0296717	MEROPS	0.09	NA	NA	NA	NA	NA	0.24
MER0211190	MEROPS	0.09	NA	NA	NA	NA	NA	0.24
GH99	CAZYME	0.09	NA	NA	NA	NA	NA	0.24
MER0123675	MEROPS	0.09	NA	NA	NA	NA	NA	0.24
MER0389931	MEROPS	0.09	NA	NA	NA	NA	0.25	0.18
MER0854697	MEROPS	0.11	NA	NA	NA	NA	0.25	0.24
GH43_29	NA	0.09	NA	NA	NA	NA	NA	0.24

MER0967802	MEROPS	0.07	NA	NA	NA	NA	NA	0.18
MER0401497	MEROPS	0.07	NA	NA	NA	NA	NA	0.18
MER0350469	MEROPS	0.07	NA	NA	NA	NA	NA	0.18
MER0383531	MEROPS	0.07	NA	NA	NA	NA	NA	0.18
MER1073781	MEROPS	0.09	NA	NA	NA	NA	NA	0.24
MER0058016	MEROPS	0.09	NA	NA	NA	NA	NA	0.24
GH43_24	NA	0.07	NA	NA	NA	NA	NA	0.18
MER0355678	MEROPS	0.07	NA	NA	NA	NA	NA	0.18
MER1094922	MEROPS	0.11	0.17	NA	NA	NA	NA	0.24
CBM66	CAZYME	0.07	NA	NA	NA	NA	NA	0.18
MER0688976	MEROPS	0.04	NA	NA	NA	NA	NA	0.12
A1CIY4_ASPCL	VIRULENCE	0.04	NA	NA	0.33	NA	NA	0.06
Q00LS5_PHAND	VIRULENCE	0.04	NA	NA	0.33	NA	NA	0.06
MER1248390	MEROPS	0.04	NA	NA	NA	NA	NA	0.12
MER0215464	MEROPS	0.04	NA	NA	NA	NA	NA	0.12
MER0319665	MEROPS	0.04	NA	NA	NA	NA	NA	0.12
MER0209297	MEROPS	0.07	NA	NA	NA	NA	NA	0.18
MER1074563	MEROPS	0.04	NA	NA	NA	NA	NA	0.12
MER0032537	MEROPS	0.13	NA	NA	0.67	NA	NA	0.24
MER0356205	MEROPS	0.16	NA	NA	0.67	NA	NA	0.29

MER0384103	MEROPS	0.16	NA	NA	0.67	NA	NA	0.29
GH43_14	CAZYME	0.13	NA	NA	0.67	NA	NA	0.24
SED1_ARTOC	VIRULENCE	0.13	NA	NA	0.33	NA	NA	0.29
MER0425754	MEROPS	0.07	NA	NA	0.33	NA	NA	0.12
MER1070883	MEROPS	0.11	NA	NA	0.67	NA	NA	0.18
MER0624820	MEROPS	0.13	NA	NA	1.00	NA	NA	0.18
C0S1U9_PARBP	VIRULENCE	0.11	NA	NA	0.67	NA	NA	0.18
MER0295437	MEROPS	0.13	NA	NA	0.67	NA	NA	0.24
MCPA_ARTBC	VIRULENCE	0.18	NA	NA	NA	0.22	NA	0.35
MER0032566	MEROPS	0.16	NA	NA	NA	NA	NA	0.41
SUB8_ARTOC	VIRULENCE	0.11	NA	NA	NA	NA	NA	0.29
MER0295896	MEROPS	0.16	0.33	NA	0.33	NA	NA	0.24
MER0383814	MEROPS	0.16	0.33	NA	NA	NA	0.25	0.24
abH31	LED	0.29	0.50	NA	0.67	NA	0.25	0.41
CUTI_ERYGR	VIRULENCE	0.27	0.67	0.17	0.67	0.11	NA	0.24
MER1073614	MEROPS	0.09	NA	NA	NA	NA	NA	0.24
MER1058581	MEROPS	0.11	NA	NA	NA	NA	NA	0.29
GH43_30	NA	0.11	NA	NA	NA	NA	NA	0.29
GH51	CAZYME	0.11	NA	NA	NA	NA	NA	0.29
MEP1_ASPFC	VIRULENCE	0.07	NA	NA	NA	NA	NA	0.18

MER0383609	MEROPS	0.09	NA	NA	NA	NA	NA	0.24
MER0881738	MEROPS	0.09	NA	NA	NA	NA	NA	0.24
MER1095177	MEROPS	0.07	NA	NA	NA	NA	NA	0.18
MER1068984	MEROPS	0.07	NA	NA	NA	NA	NA	0.18
MER0975367	MEROPS	0.07	NA	NA	NA	NA	NA	0.18
MER0549739	MEROPS	0.07	NA	NA	NA	NA	NA	0.18
MER0211309	MEROPS	0.07	NA	NA	NA	NA	NA	0.18
MER0383880	MEROPS	0.07	NA	NA	NA	NA	NA	0.18
MER1178638	MEROPS	0.07	NA	NA	NA	NA	NA	0.18
Q5IFQ6_CRYNV	VIRULENCE	0.09	NA	NA	0.33	NA	NA	0.18
A4ULJ0_MYCGR	VIRULENCE	0.07	0.17	NA	NA	NA	NA	0.12
MER0985053	MEROPS	0.07	0.17	NA	NA	NA	NA	0.12
3002892	CARD	0.07	NA	NA	NA	NA	NA	0.18
A3LNY8_PICST	VIRULENCE	0.04	0.17	NA	NA	NA	NA	0.06
MER1047786	MEROPS	0.04	NA	0.17	NA	NA	NA	0.06
MER0425491	MEROPS	0.47	1.00	0.83	0.67	0.67	0.50	NA
Q59WE5_CANAL	VIRULENCE	0.51	0.83	1.00	0.67	0.67	1.00	NA
MER0204874	MEROPS	0.40	0.67	0.83	NA	0.44	0.75	0.12
SUB4A_COCP7	VIRULENCE	0.33	0.50	0.50	0.67	0.33	1.00	NA
MER0065989	MEROPS	0.18	0.17	0.50	0.33	NA	0.75	NA

OPSB_ARTBC	VIRULENCE	0.33	0.83	0.83	0.67	NA	0.50	0.06
PL1_2	NA	0.60	1.00	1.00	NA	1.00	0.50	0.24
PL1_4	NA	0.53	0.83	1.00	NA	0.89	0.50	0.18
MER0383705	MEROPS	0.58	0.33	0.83	0.67	1.00	0.75	0.29
MER0384160	MEROPS	0.67	0.83	1.00	1.00	0.78	1.00	0.29
A4QVD7_MAGO7	VIRULENCE	0.49	0.50	0.83	1.00	0.67	1.00	0.06
O60038_CLAPU	VIRULENCE	0.44	0.83	0.83	0.67	0.89	NA	NA
MER0305119	MEROPS	0.44	0.67	1.00	0.33	0.67	0.75	NA
MER0383730	MEROPS	0.49	0.33	0.83	0.67	1.00	1.00	NA
Q8J0E1_CLAPU	VIRULENCE	0.38	0.50	0.83	NA	0.89	0.25	NA
GH17	CAZYME	0.49	0.83	0.67	NA	1.00	0.75	0.06
MER0228949	MEROPS	0.47	0.83	1.00	NA	1.00	0.25	NA
Q59NP5_CANAL	VIRULENCE	0.49	0.67	0.67	0.33	1.00	1.00	NA
MER1143003	MEROPS	0.51	1.00	0.83	0.33	0.89	0.75	NA
MER1254858	MEROPS	0.53	0.50	1.00	0.67	1.00	1.00	NA
MER0109583	MEROPS	0.53	0.67	1.00	0.33	0.89	1.00	0.06
MER1175944	MEROPS	0.53	1.00	1.00	NA	0.89	1.00	NA
MER1297562	MEROPS	0.58	1.00	1.00	0.33	1.00	1.00	NA
Q2I0M6_CERNC	VIRULENCE	0.07	NA	NA	NA	0.22	NA	0.06
MCPA_TRIEQ	VIRULENCE	0.07	NA	NA	NA	0.33	NA	NA

3004589	CARD	0.04	NA	NA	NA	0.22	NA	NA
MER0067170	MEROPS	0.04	NA	NA	NA	0.22	NA	NA
MEP7_ARTBC	VIRULENCE	0.16	NA	0.17	NA	0.56	NA	0.06
Q4WQJ0_ASPFU	VIRULENCE	0.11	NA	NA	NA	0.56	NA	NA
MER1070091	MEROPS	0.11	NA	NA	NA	0.56	NA	NA
MER1267242	MEROPS	0.11	NA	NA	NA	0.56	NA	NA
MER0979965	MEROPS	0.04	NA	NA	NA	0.22	NA	NA
A4R0W3_MAGO7	VIRULENCE	0.04	NA	NA	NA	0.22	NA	NA
MER0229521	MEROPS	0.07	NA	NA	NA	0.33	NA	NA
Q5A661_CANAL	VIRULENCE	0.09	NA	NA	NA	0.44	NA	NA
3003361	CARD	0.04	NA	NA	NA	0.22	NA	NA
Q59YF3_CANAL	VIRULENCE	0.04	NA	NA	NA	0.22	NA	NA
Q6B971_CRYPA	VIRULENCE	0.04	NA	NA	NA	0.22	NA	NA
Q5A762_CANAL	VIRULENCE	0.16	NA	NA	NA	0.44	NA	0.18
MER0296701	MEROPS	0.16	NA	0.17	NA	0.67	NA	NA
3004032	CARD	0.09	NA	NA	NA	0.44	NA	NA
MER0220675	MEROPS	0.13	NA	0.33	NA	0.44	NA	NA
PLYB_COLGL	VIRULENCE	0.33	0.67	0.67	NA	0.78	NA	NA
MER1228871	MEROPS	0.33	0.33	0.83	NA	0.89	NA	NA
MER0383630	MEROPS	0.42	0.50	1.00	NA	1.00	0.25	NA

MER1286597	MEROPS	0.40	0.50	1.00	NA	1.00	NA	NA
MCPA_ARTOC	VIRULENCE	0.18	NA	0.50	NA	0.56	NA	NA
MER0000339	MEROPS	0.24	NA	0.50	0.33	0.78	NA	NA
DPP4_ASPFU	VIRULENCE	0.33	NA	0.83	0.33	1.00	NA	NA
MER1248328	MEROPS	0.29	NA	0.67	NA	1.00	NA	NA
MER0761007	MEROPS	0.29	NA	0.67	NA	1.00	NA	NA
MER1096997	MEROPS	0.29	NA	0.67	NA	1.00	NA	NA
SED2_ARTOC	VIRULENCE	0.31	NA	0.83	NA	0.56	0.50	0.12
SUB6_ARTGP	VIRULENCE	0.27	0.33	NA	NA	0.56	NA	0.29
MER0296715	MEROPS	0.33	NA	0.50	0.33	0.33	NA	0.47
MER0903139	MEROPS	0.53	0.33	0.67	0.33	1.00	NA	0.47
abH05	LED	0.20	0.33	NA	NA	0.56	NA	0.12
Q5AM49_CANAL	VIRULENCE	0.29	0.33	0.50	NA	0.67	0.25	0.06
MER0626149	MEROPS	0.24	0.33	0.50	NA	0.67	NA	NA
MER0833534	MEROPS	0.22	0.50	0.50	NA	0.33	0.25	NA
MER0024046	MEROPS	0.16	NA	0.17	NA	0.67	NA	NA
MER0977078	MEROPS	0.20	NA	NA	NA	1.00	NA	NA
MER0242200	MEROPS	0.18	NA	0.17	NA	0.78	NA	NA
Q5A747_CANAL	VIRULENCE	0.13	NA	NA	NA	0.67	NA	NA
MER0383910	MEROPS	0.20	NA	NA	NA	0.56	NA	0.24

SED2_ARTBC	VIRULENCE	0.38	NA	0.33	0.33	1.00	0.25	0.24
CARP3_CANAL	VIRULENCE	0.29	NA	NA	NA	0.89	NA	0.29
MER0305143	MEROPS	0.38	0.33	0.33	NA	1.00	NA	0.24
C4YPV8_CANAW	VIRULENCE	0.33	NA	NA	NA	0.78	0.25	0.41
PL8	CAZYME	0.51	NA	0.17	0.67	0.89	1.00	0.47
MER0834757	MEROPS	0.33	0.50	0.50	0.67	0.67	NA	0.06
MER0064864	MEROPS	0.40	0.50	0.17	0.33	0.89	0.50	0.18
MER0979722	MEROPS	0.22	0.33	0.17	NA	0.67	0.25	NA
LAP1_ARTOC	VIRULENCE	0.40	NA	0.50	0.33	0.78	0.50	0.29
CTSD_ASPFU	VIRULENCE	0.49	0.33	0.17	0.67	0.78	0.25	0.53
MER0785864	MEROPS	0.42	0.33	NA	1.00	0.67	0.50	0.35
MER0033389	MEROPS	0.20	NA	0.17	0.67	0.56	NA	0.06
MER0296884	MEROPS	0.38	0.67	0.33	0.67	0.56	0.50	0.12
MER1128390	MEROPS	0.33	0.33	0.17	0.67	0.89	0.50	NA
MER1248034	MEROPS	0.04	NA	NA	0.67	NA	NA	NA
MER1073836	MEROPS	0.04	NA	NA	0.67	NA	NA	NA
MER1009650	MEROPS	0.04	NA	NA	0.67	NA	NA	NA
MER1008241	MEROPS	0.04	NA	NA	0.67	NA	NA	NA
MER0842434	MEROPS	0.04	NA	NA	0.67	NA	NA	NA
MER0834062	MEROPS	0.04	NA	NA	0.67	NA	NA	NA

MER0280073	MEROPS	0.04	NA	NA	0.67	NA	NA	NA
MER0239537	MEROPS	0.04	NA	NA	0.67	NA	NA	NA
MER0220952	MEROPS	0.04	NA	NA	0.67	NA	NA	NA
MER0124599	MEROPS	0.04	NA	NA	0.67	NA	NA	NA
AA13	CAZYME	0.04	NA	NA	0.67	NA	NA	NA
MER0032723	MEROPS	0.04	NA	NA	0.67	NA	NA	NA
MER0004239	MEROPS	0.04	NA	NA	0.67	NA	NA	NA
MER1175938	MEROPS	0.04	NA	NA	0.67	NA	NA	NA
MER0402219	MEROPS	0.04	NA	NA	0.67	NA	NA	NA
MER0761051	MEROPS	0.09	0.17	NA	1.00	NA	NA	NA
MER0882059	MEROPS	0.07	NA	NA	1.00	NA	NA	NA
MER0201858	MEROPS	0.07	NA	NA	1.00	NA	NA	NA
E9F9I6_METAR	VIRULENCE	0.07	NA	NA	1.00	NA	NA	NA
MER0107351	MEROPS	0.07	NA	NA	1.00	NA	NA	NA
PEPA_ARTBC	VIRULENCE	0.04	NA	NA	NA	NA	0.50	NA
MER0848649	MEROPS	0.04	NA	NA	NA	NA	0.50	NA
MER0306630	MEROPS	0.04	NA	NA	NA	NA	0.50	NA
MER0287564	MEROPS	0.04	NA	NA	NA	NA	0.50	NA
MER0213847	MEROPS	0.04	NA	NA	NA	NA	0.50	NA
MER0090158	MEROPS	0.04	NA	NA	NA	NA	0.50	NA

MER0073932	MEROPS	0.04	NA	NA	NA	NA	0.50	NA
MER0064174	MEROPS	0.04	NA	NA	NA	NA	0.50	NA
F0X720_GROCL	VIRULENCE	0.04	NA	NA	NA	NA	0.50	NA
MER0032698	MEROPS	0.04	NA	NA	NA	NA	0.50	NA
AA1_3	NA	0.20	NA	NA	NA	NA	0.75	0.35
MER0314841	MEROPS	0.20	NA	0.17	NA	NA	1.00	0.24
MER0384340	MEROPS	0.18	NA	NA	NA	NA	1.00	0.24
MER0214563	MEROPS	0.09	NA	NA	NA	NA	0.50	0.12
MER0760948	MEROPS	0.11	NA	NA	NA	NA	0.50	0.18
Q00350_COCCA	VIRULENCE	0.09	0.17	0.17	NA	NA	0.50	NA
Q6T7C1_MAGGR	VIRULENCE	0.09	0.33	NA	NA	NA	0.50	NA
Q6IVV6_BOTFU	VIRULENCE	0.16	0.67	0.17	NA	NA	0.50	NA
Q8TGD1_FUSOX	VIRULENCE	0.09	0.33	NA	NA	NA	0.50	NA
MER0019139	MEROPS	0.09	NA	NA	NA	NA	1.00	NA
MER0090831	MEROPS	0.09	NA	NA	NA	0.11	0.75	NA
MER0160806	MEROPS	0.07	NA	NA	0.33	NA	0.50	NA
CARP_ASPFU	VIRULENCE	0.07	NA	NA	0.33	NA	0.50	NA
MER1073604	MEROPS	0.11	NA	NA	0.67	NA	0.75	NA
SUB7A_COCP7	VIRULENCE	0.04	0.33	NA	NA	NA	NA	NA
SED3_TRIVH	VIRULENCE	0.04	0.33	NA	NA	NA	NA	NA

MER1248078	MEROPS	0.04	0.33	NA	NA	NA	NA	NA
MER0976426	MEROPS	0.04	0.33	NA	NA	NA	NA	NA
MER0954117	MEROPS	0.04	0.33	NA	NA	NA	NA	NA
MER0693594	MEROPS	0.04	0.33	NA	NA	NA	NA	NA
MER0313342	MEROPS	0.04	0.33	NA	NA	NA	NA	NA
LAP5_ARTBC	VIRULENCE	0.04	0.33	NA	NA	NA	NA	NA
MER0011060	MEROPS	0.04	0.33	NA	NA	NA	NA	NA
MER0238105	MEROPS	0.09	0.17	NA	0.33	NA	0.50	NA
MER0402352	MEROPS	0.16	0.33	NA	1.00	NA	0.50	NA
MER0881927	MEROPS	0.07	0.33	NA	0.33	NA	NA	NA
MER0947474	MEROPS	0.09	0.33	NA	0.67	NA	NA	NA
C7GMI1_YEAS2	VIRULENCE	0.04	0.17	NA	NA	NA	0.25	NA
MER0028352	MEROPS	0.04	0.17	NA	NA	NA	NA	0.06
MER0694303	MEROPS	0.07	0.33	0.17	NA	NA	NA	NA
MER1251538	MEROPS	0.09	0.33	0.33	NA	NA	NA	NA
MER1069234	MEROPS	0.09	0.33	0.33	NA	NA	NA	NA
Q4P8E7_USTMA	VIRULENCE	0.07	0.33	0.17	NA	NA	NA	NA
CUTI2_FUSSO	VIRULENCE	0.07	0.33	0.17	NA	NA	NA	NA
Q9C1I7_MYCGR	VIRULENCE	0.04	0.33	NA	NA	NA	NA	NA
MER1247538	MEROPS	0.04	0.33	NA	NA	NA	NA	NA

MER1228522	MEROPS	0.04	0.33	NA	NA	NA	NA	NA
MER0383966	MEROPS	0.04	0.33	NA	NA	NA	NA	NA
MER0845695	MEROPS	0.04	0.33	NA	NA	NA	NA	NA
Q6WP53_BOTFU	VIRULENCE	0.13	0.33	0.33	NA	NA	0.50	NA
MER0507688	MEROPS	0.11	0.33	NA	NA	0.11	0.50	NA
Q5AD07_CANAL	VIRULENCE	0.09	0.33	NA	NA	NA	0.50	NA
Q5AMT2_CANAL	VIRULENCE	0.09	0.33	0.17	NA	NA	0.25	NA
MER0625945	MEROPS	0.16	0.33	0.17	NA	NA	1.00	NA
MER1248434	MEROPS	0.11	0.33	NA	NA	NA	0.75	NA
CXT1_CRYNJ	VIRULENCE	0.04	NA	0.17	NA	NA	0.25	NA
MER0209188	MEROPS	0.07	NA	0.17	NA	NA	0.50	NA
3000421	CARD	0.07	NA	0.17	NA	NA	0.50	NA
MER0229183	MEROPS	0.04	NA	NA	NA	NA	0.50	NA
MER0064713	MEROPS	0.04	NA	NA	NA	NA	0.50	NA
abH35	LED	0.04	NA	NA	NA	NA	0.50	NA
A4QRN5_MAGO7	VIRULENCE	0.04	NA	NA	NA	NA	0.50	NA
abH28	LED	0.04	NA	NA	NA	NA	0.50	NA
MEP8_ARTGP	VIRULENCE	0.18	0.17	0.67	NA	0.33	NA	NA
Q9C1R1_FUSOX	VIRULENCE	0.11	NA	0.33	NA	0.33	NA	NA
MER0624541	MEROPS	0.20	0.33	0.67	0.33	0.22	NA	NA

MER0882052	MEROPS	0.44	0.50	0.83	0.33	0.56	NA	0.35
GT69	CAZYME	0.22	0.17	0.67	NA	0.56	NA	NA
Q00523_CRYNE	VIRULENCE	0.18	0.17	0.67	NA	0.33	NA	NA
3004574	CARD	0.13	NA	0.50	NA	NA	NA	0.18
CTSD_TRIVH	VIRULENCE	0.29	0.67	0.67	NA	0.11	NA	0.24
3004581	CARD	0.04	NA	0.17	NA	NA	NA	0.06
B9WDE6_CANDC	VIRULENCE	0.04	0.17	0.17	NA	NA	NA	NA
3004587	CARD	0.11	NA	0.33	0.67	NA	NA	0.06
MER1185140	MEROPS	0.09	NA	0.33	0.33	0.11	NA	NA
MER0121047	MEROPS	0.11	0.33	0.33	NA	NA	NA	0.06
MER0210856	MEROPS	0.13	0.33	0.33	NA	0.22	NA	NA
A4ULI5_MYCGR	VIRULENCE	0.16	0.50	0.67	NA	NA	NA	NA
GH49	CAZYME	0.20	0.67	0.33	NA	NA	0.50	0.06
C0SAT8_PARBP	VIRULENCE	0.09	0.33	0.33	NA	NA	NA	NA
MER1073654	MEROPS	0.07	NA	0.50	NA	NA	NA	NA
GT21	CAZYME	0.07	0.17	0.17	NA	0.11	NA	NA
Q5AMQ4_CANAL	VIRULENCE	0.07	0.17	0.17	NA	0.11	NA	NA
Q9UUS8_COLGL	VIRULENCE	0.07	0.33	0.17	NA	NA	NA	NA
MER0449393	MEROPS	0.07	0.33	NA	NA	0.11	NA	NA
MER0064189	MEROPS	0.07	0.33	NA	0.33	NA	NA	NA

MER0032062	MEROPS	0.04	0.33	NA	NA	NA	NA	NA
MER0242202	MEROPS	0.04	0.33	NA	NA	NA	NA	NA
A6ZYV3_YEAS7	VIRULENCE	0.20	0.67	0.33	NA	0.33	NA	NA
MER0064110	MEROPS	0.09	0.67	NA	NA	NA	NA	NA
O13407_MAGGR	VIRULENCE	0.20	0.33	0.50	NA	NA	1.00	NA
Q5AB91_CANAL	VIRULENCE	0.11	0.33	0.17	NA	0.11	0.25	NA
MER0188710	MEROPS	0.04	NA	NA	NA	NA	NA	0.12
MER0402064	MEROPS	0.04	NA	NA	NA	NA	NA	0.12
Q5XTQ5_BOTFU	VIRULENCE	0.07	NA	0.17	NA	NA	NA	0.12
MER0060939	MEROPS	0.04	NA	NA	NA	NA	NA	0.12
MER0382075	MEROPS	0.07	NA	NA	NA	NA	NA	0.18
A6ZKV8_YEAS7	VIRULENCE	0.07	NA	NA	NA	NA	NA	0.18
abH15	LED	0.07	NA	0.17	NA	NA	NA	0.12
Q09MP5_COCMI	VIRULENCE	0.04	NA	NA	NA	NA	NA	0.12
Q1AMT8_TRIRU	VIRULENCE	0.04	NA	NA	NA	NA	0.25	0.06
MER0626102	MEROPS	0.07	NA	0.17	NA	NA	NA	0.12
MER0474671	MEROPS	0.04	NA	NA	NA	NA	NA	0.12
MER1060381	MEROPS	0.07	NA	NA	NA	NA	NA	0.18
A4QVA7_MAGO7	VIRULENCE	0.09	NA	0.17	NA	NA	NA	0.18
CARP_ARTBC	VIRULENCE	0.07	NA	NA	NA	NA	NA	0.18

Q9P8L8_BOTFU	VIRULENCE	0.11	NA	NA	NA	NA	NA	0.29
MER0212820	MEROPS	0.04	NA	0.17	NA	NA	NA	0.06
MER0215532	MEROPS	0.09	NA	NA	NA	NA	NA	0.24
3002494	CARD	0.04	NA	NA	NA	NA	NA	0.12
3002893	CARD	0.07	NA	NA	NA	NA	NA	0.18
MER0254872	MEROPS	0.07	NA	NA	NA	NA	NA	0.18
MER0511360	MEROPS	0.04	NA	NA	NA	NA	NA	0.12
GH32	CAZYME	0.09	NA	NA	0.33	NA	NA	0.18
SUB1_ARTOC	VIRULENCE	0.09	NA	NA	NA	NA	NA	0.24
3002143	CARD	0.04	NA	NA	0.33	NA	NA	0.06
MER0064120	MEROPS	0.04	NA	0.17	0.33	NA	NA	NA
MER0428589	MEROPS	0.04	NA	NA	NA	NA	NA	0.12
MER0760805	MEROPS	0.09	0.17	NA	NA	NA	0.25	0.12
C5G6Q4_AJEDR	VIRULENCE	0.04	NA	0.33	NA	NA	NA	NA
Q5ABB1_CANAL	VIRULENCE	0.07	NA	0.50	NA	NA	NA	NA
SUB6_ARTOC	VIRULENCE	0.07	NA	0.50	NA	NA	NA	NA
Q0PND8_MAGGR	VIRULENCE	0.04	NA	0.17	NA	NA	NA	0.06
3000193	CARD	0.04	NA	0.17	NA	0.11	NA	NA
MER1096359	MEROPS	0.04	NA	0.17	0.33	NA	NA	NA
AA14	CAZYME	0.16	NA	NA	0.33	NA	NA	0.35

GH43_34	CAZYME	0.16	NA	NA	0.33	NA	NA	0.35
MER0511150	MEROPS	0.11	NA	NA	NA	NA	NA	0.29
PL8_4	CAZYME	0.13	NA	NA	0.33	NA	NA	0.29
MER0975090	MEROPS	0.16	NA	NA	0.67	NA	NA	0.29
MER0383999	MEROPS	0.22	NA	NA	0.67	NA	NA	0.47
MER1073766	MEROPS	0.20	NA	NA	0.67	NA	NA	0.41
abH29	LED	0.18	NA	NA	0.67	0.22	NA	0.24
SUB1_ARTGP	VIRULENCE	0.09	NA	NA	0.33	NA	NA	0.18
3004612	CARD	0.13	NA	NA	0.67	NA	NA	0.24
MER0032575	MEROPS	0.11	NA	NA	0.67	NA	NA	0.18
Q8X1F0_CRYNE	VIRULENCE	0.07	NA	NA	0.67	NA	NA	0.06
E9F9I5_METAR	VIRULENCE	0.07	NA	NA	0.67	NA	NA	0.06
MER0114178	MEROPS	0.13	NA	NA	0.67	NA	NA	0.24
MER0080738	MEROPS	0.20	0.33	NA	0.33	NA	0.25	0.29
SUB8_TRIVH	VIRULENCE	0.18	0.33	NA	0.33	NA	0.50	0.18
MER1096429	MEROPS	0.18	NA	NA	0.67	NA	NA	0.35
MER0374691	MEROPS	0.16	NA	NA	0.67	NA	0.25	0.24
SED3_ASPFU	VIRULENCE	0.18	NA	NA	0.67	NA	0.25	0.29
CUTI_BOTFU	VIRULENCE	0.20	0.33	NA	0.67	NA	0.50	0.18
CARP_TRIVH	VIRULENCE	0.09	NA	NA	0.33	NA	0.50	0.06

MER1073277	MEROPS	0.22	NA	NA	1.00	NA	1.00	0.18
MER0215484	MEROPS	0.16	NA	0.50	1.00	NA	0.25	NA
MER0378835	MEROPS	0.29	NA	0.50	0.67	0.22	0.50	0.24
SED3_ARTBC	VIRULENCE	0.11	NA	0.33	0.67	NA	0.25	NA
MER0305138	MEROPS	0.33	0.33	0.50	0.67	NA	0.75	0.29
MER1073675	MEROPS	0.31	NA	1.00	0.67	NA	0.75	0.18
MER1094825	MEROPS	0.09	0.67	NA	NA	NA	NA	NA
MER0033130	MEROPS	0.29	0.67	0.17	0.33	0.22	0.50	0.18
MER0079834	MEROPS	0.16	0.50	NA	0.67	NA	0.50	NA
DPP4_ARTBC	VIRULENCE	0.27	1.00	0.17	0.33	NA	1.00	NA
ERG2_USTMA	VIRULENCE	0.27	0.50	0.33	0.67	NA	1.00	0.06
GT22	CAZYME	0.49	0.83	0.17	1.00	0.22	1.00	0.41
MEP1_COCP7	VIRULENCE	0.36	0.83	NA	1.00	NA	0.50	0.35
MER0025111	MEROPS	0.36	0.83	NA	0.33	NA	1.00	0.35
MER1178700	MEROPS	0.11	NA	NA	NA	NA	NA	0.29
LAP2_ASPFU	VIRULENCE	0.22	0.33	0.17	NA	NA	NA	0.41
SCPB_ARTOC	VIRULENCE	0.16	0.33	NA	0.67	NA	NA	0.18
Q9UVN5_ALTAL	VIRULENCE	0.07	NA	NA	0.33	0.11	NA	0.06
MER0039492	MEROPS	0.04	0.17	NA	NA	NA	NA	0.06
Q5D6D3_COCHE	VIRULENCE	0.04	0.17	NA	NA	NA	NA	0.06

MER0834156	MEROPS	0.04	NA	NA	0.33	NA	0.25	NA
MER0295435	MEROPS	0.04	NA	NA	0.33	NA	NA	0.06
LAP2_TRIVH	VIRULENCE	0.04	NA	0.17	0.33	NA	NA	NA
3000843	CARD	0.04	NA	NA	0.33	NA	NA	0.06
A6N6J8_FUSOX	VIRULENCE	0.04	0.17	NA	0.33	NA	NA	NA
CARP1_CANAL	VIRULENCE	0.07	0.17	NA	0.33	NA	NA	0.06
MER0122025	MEROPS	0.04	NA	NA	0.33	NA	NA	0.06
A5H456_MYCGR	VIRULENCE	0.04	NA	NA	0.33	NA	NA	0.06
E9DY48_METAQ	VIRULENCE	0.09	NA	NA	0.67	NA	NA	0.12
NPIIC_ARTOC	VIRULENCE	0.53	0.67	0.67	1.00	0.89	NA	0.29
MCPAL_ARTOC	VIRULENCE	0.53	0.67	0.33	0.33	0.44	0.75	0.59
Q2LMP0_BOTFU	VIRULENCE	0.56	0.67	0.17	0.67	NA	0.25	1.00
Q8NJS2_LEPMC	VIRULENCE	0.60	0.67	0.17	0.67	0.89	0.50	0.59
GEL3_ASPFU	VIRULENCE	0.60	0.50	NA	1.00	0.33	0.50	0.94
Q96VZ3_FUSOX	VIRULENCE	0.60	1.00	0.17	0.33	NA	0.50	1.00
LAP2_TRIEQ	VIRULENCE	0.62	0.17	0.50	0.67	0.44	0.50	0.94
CUTI_MONFR	VIRULENCE	0.62	0.67	0.33	0.33	0.11	0.75	1.00
Q7Z868_USTMD	VIRULENCE	0.64	0.50	0.67	1.00	0.22	0.50	0.88
Q9C4A1_9PLEO	VIRULENCE	0.64	0.33	0.83	NA	0.22	0.75	1.00
Q4P8E8_USTMA	VIRULENCE	0.64	0.50	NA	1.00	0.44	0.75	0.94

Q9C1F9_COCCA	VIRULENCE	0.67	0.33	0.50	NA	0.67	0.50	1.00
A6R119_AJECN	VIRULENCE	0.67	0.83	0.33	1.00	NA	1.00	0.94
CUTI_PYRBR	VIRULENCE	0.69	0.33	0.67	1.00	1.00	NA	0.76
LAP2_ARTOC	VIRULENCE	0.69	0.67	1.00	0.33	1.00	0.50	0.53
Q874F3_MAGGR	VIRULENCE	0.71	0.33	0.50	0.67	1.00	NA	0.94
ECM14_ARTOC	VIRULENCE	0.73	0.50	0.83	1.00	0.89	1.00	0.59
Q9P8W9_CRYNE	VIRULENCE	0.76	0.67	0.67	1.00	0.44	0.50	1.00
Q8J1W4_CLAPU	VIRULENCE	0.76	0.33	0.67	1.00	0.89	NA	1.00
PLB1_CANAL	VIRULENCE	0.76	1.00	0.83	1.00	NA	1.00	0.94
B2C6F1_CRYGA	VIRULENCE	0.76	0.50	0.83	1.00	0.22	1.00	1.00
Q705V7_USTMD	VIRULENCE	0.78	0.67	1.00	0.67	1.00	NA	0.82
Q5AEW4_CANAL	VIRULENCE	0.82	0.67	0.83	1.00	0.67	1.00	0.88
D1MGZ7_BEABA	VIRULENCE	0.82	0.33	1.00	1.00	1.00	1.00	0.76
Q5RLJ7_CRYNV	VIRULENCE	0.84	1.00	0.50	1.00	0.56	1.00	1.00
A5HF03_MAGGR	VIRULENCE	0.87	1.00	0.83	1.00	1.00	1.00	0.71
D1MYV6_MAGGR	VIRULENCE	0.87	0.67	1.00	1.00	1.00	1.00	0.76
Y1220_ASPFU	VIRULENCE	0.89	1.00	0.83	1.00	0.78	1.00	0.88
Q5XTQ4_BOTFU	VIRULENCE	0.89	0.67	0.83	1.00	0.78	1.00	1.00
A0ST43_CERNC	VIRULENCE	0.89	0.50	0.67	1.00	1.00	1.00	1.00
Q5APK9_CANAL	VIRULENCE	0.89	0.83	1.00	1.00	1.00	0.50	0.88

A4RJR0_MAGO7	VIRULENCE	0.91	1.00	0.83	0.67	1.00	1.00	0.88
O59937_FUSOX	VIRULENCE	0.91	1.00	0.83	NA	1.00	1.00	1.00
Q8J0U4_LEPMC	VIRULENCE	0.93	0.83	1.00	0.67	1.00	1.00	0.94
Q6WER3_GIBZA	VIRULENCE	0.93	0.83	1.00	0.67	1.00	1.00	0.94
OPSB_ASPFU	VIRULENCE	0.96	0.67	1.00	1.00	1.00	1.00	1.00
Q9HFZ2_CANAL	VIRULENCE	0.96	1.00	1.00	1.00	1.00	0.75	0.94
Q5AJC0_CANAL	VIRULENCE	0.98	1.00	1.00	1.00	1.00	1.00	0.94
KATG_PENMA	VIRULENCE	0.98	1.00	1.00	1.00	1.00	1.00	0.94
Q4PDC7_USTMA	VIRULENCE	0.98	0.83	1.00	1.00	1.00	1.00	1.00
A4QPV0_MAGO7	VIRULENCE	0.98	1.00	1.00	0.67	1.00	1.00	1.00
SED1_ASPFU	VIRULENCE	1.00	1.00	1.00	1.00	1.00	1.00	1.00
Q99324_SEPLY	VIRULENCE	1.00	1.00	1.00	1.00	1.00	1.00	1.00
Q8J1Y3_BEABA	VIRULENCE	1.00	1.00	1.00	1.00	1.00	1.00	1.00
Q59NY2_CANAL	VIRULENCE	1.00	1.00	1.00	1.00	1.00	1.00	1.00
Q2VLJ1_GIBZA	VIRULENCE	1.00	1.00	1.00	1.00	1.00	1.00	1.00
Q2KN79_FUSOX	VIRULENCE	1.00	1.00	1.00	1.00	1.00	1.00	1.00
PEPA_ASPFC	VIRULENCE	1.00	1.00	1.00	1.00	1.00	1.00	1.00
ORYZ_ASPFC	VIRULENCE	1.00	1.00	1.00	1.00	1.00	1.00	1.00
O59928_HYPVI	VIRULENCE	1.00	1.00	1.00	1.00	1.00	1.00	1.00
GEL1_ASPFU	VIRULENCE	1.00	1.00	1.00	1.00	1.00	1.00	1.00

A4R566_MAGO7	VIRULENCE	1.00	1.00	1.00	1.00	1.00	1.00	1.00

Appendix 2: Supplemental Material for Chapter 3

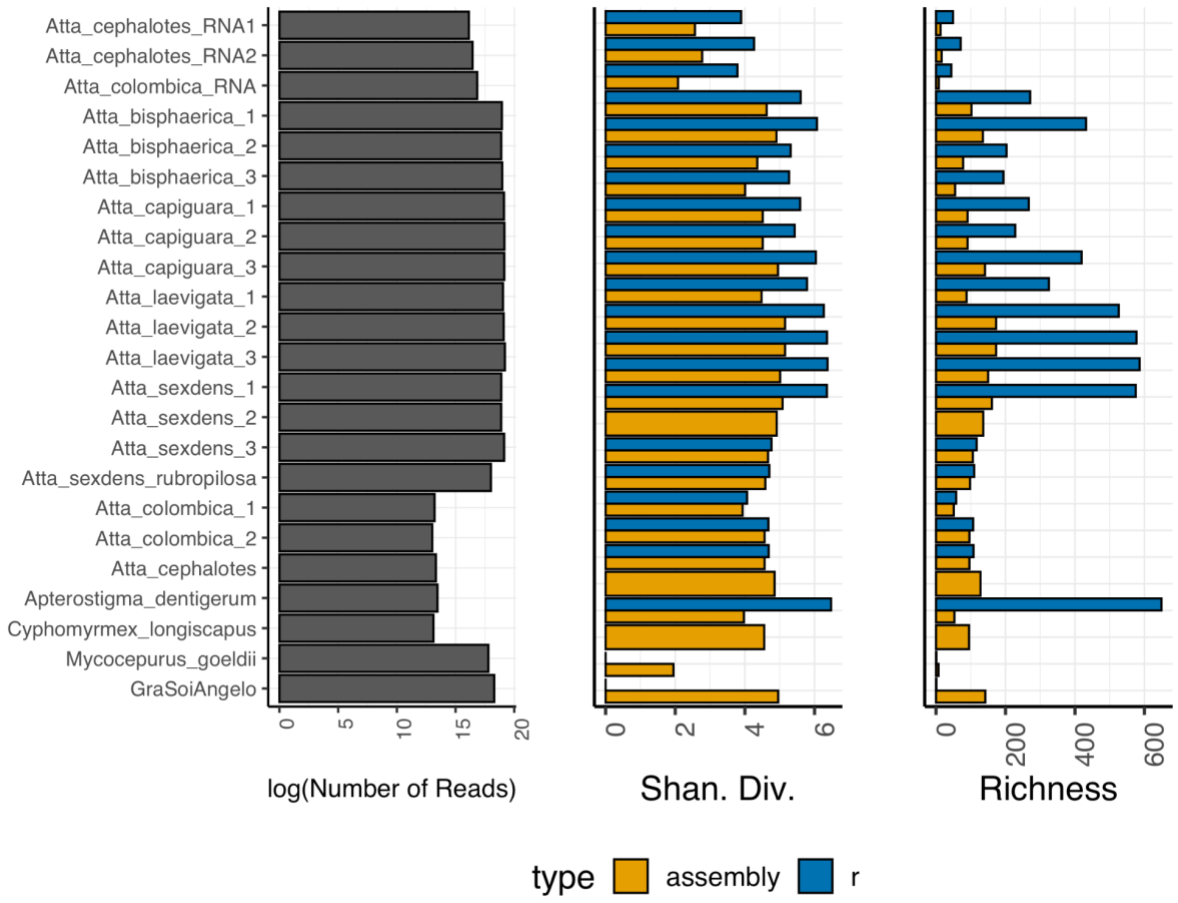

Figure S1. From left to right, read depth sequenced for each sample, Shannon diversity of predicted taxa, richness of predicted taxa.

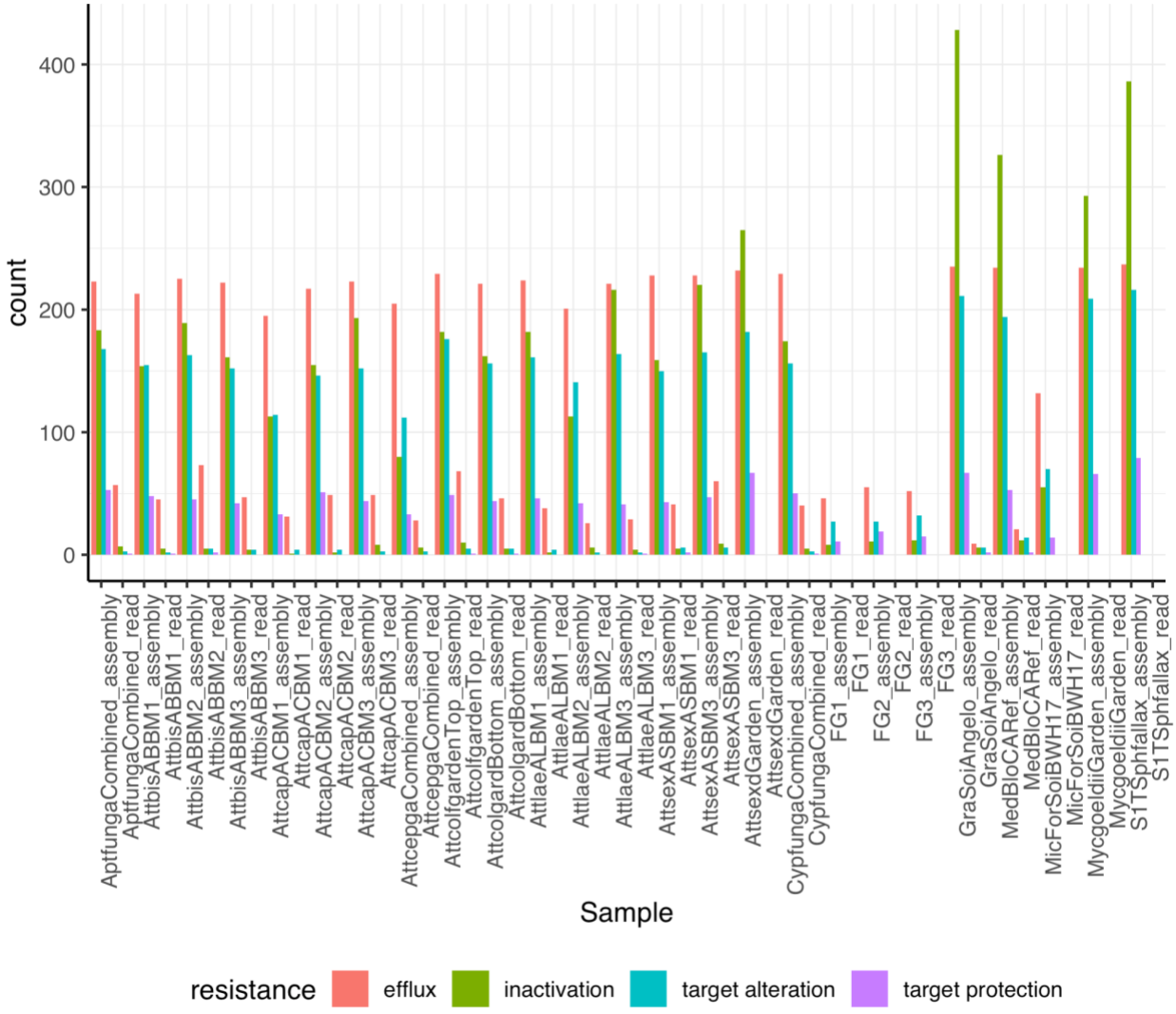

Figure S2. Numbers of resistance genes detected across reads and assemblies for each sample, with colors pertaining to the resistance mechanism predicted for each gene.

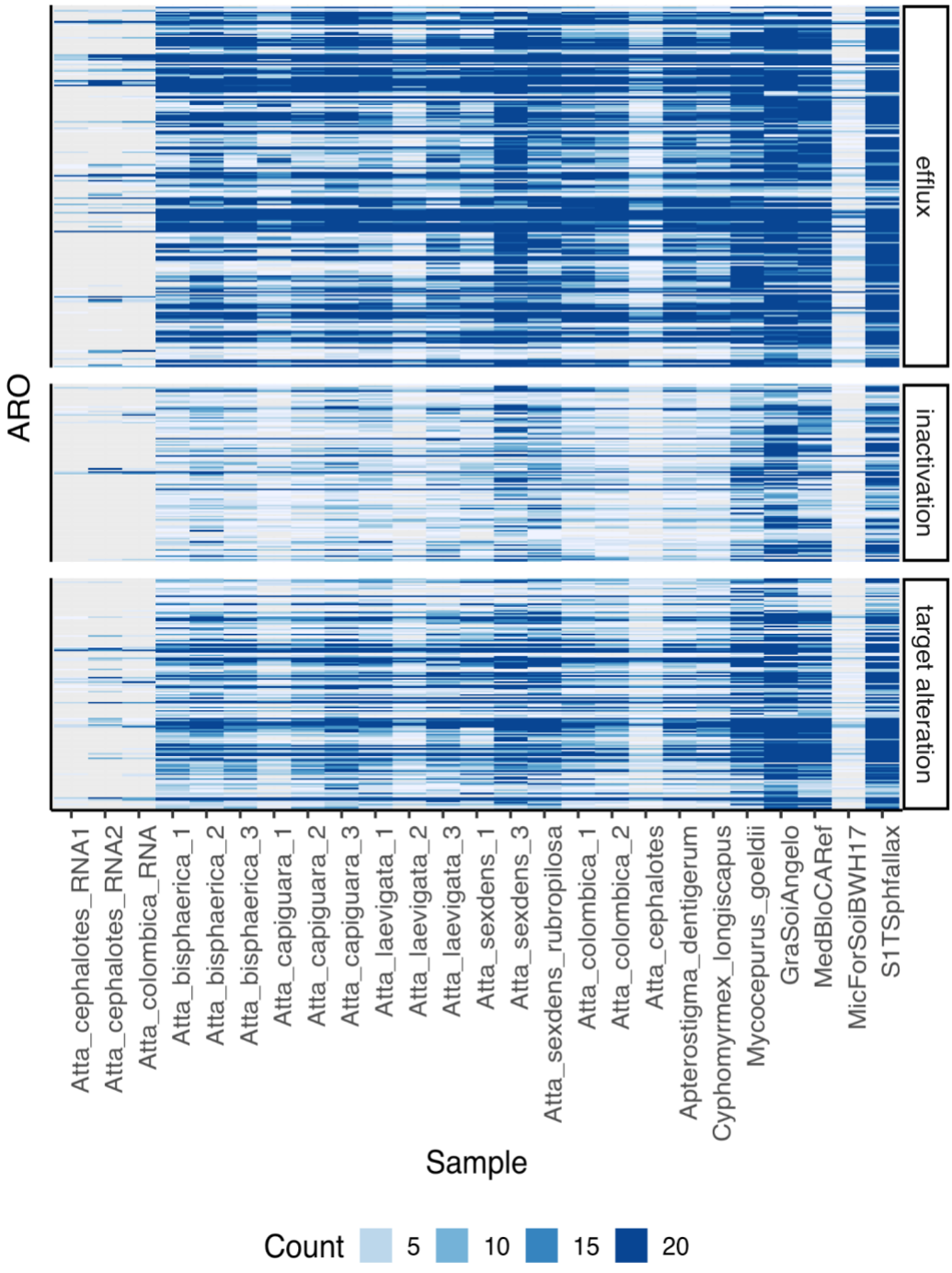

Figure S3. Heatmap of numbers of ARO's associated found in individual metagenomes, with the Resistance Mechanism indicated on the right-side facet.

Appendix 3: Supplemental Material for Chapter 4

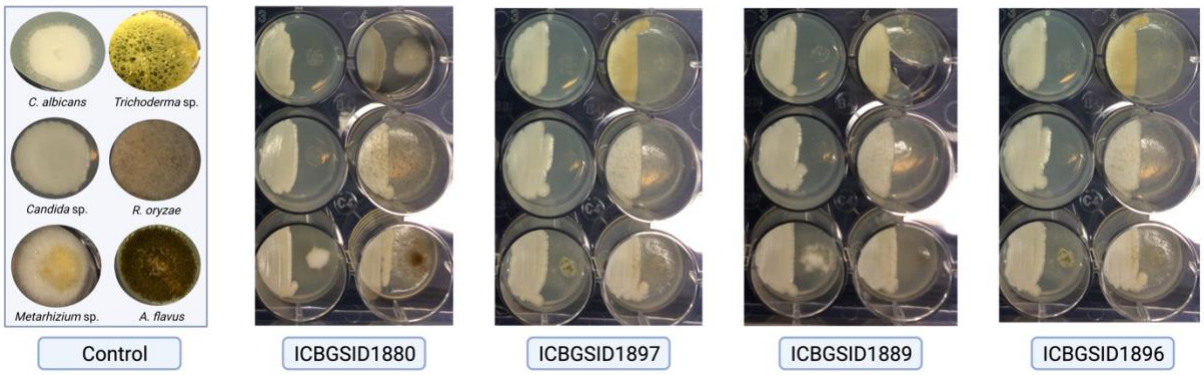

Supplemental Figure 1. Bioassay plates of yeast strains used in this study. The left-most panel indicates control growth for pathogen strains. Test strains are streaked out on left side of the well and grown for five days before inoculation with pathogen strains on the right side.

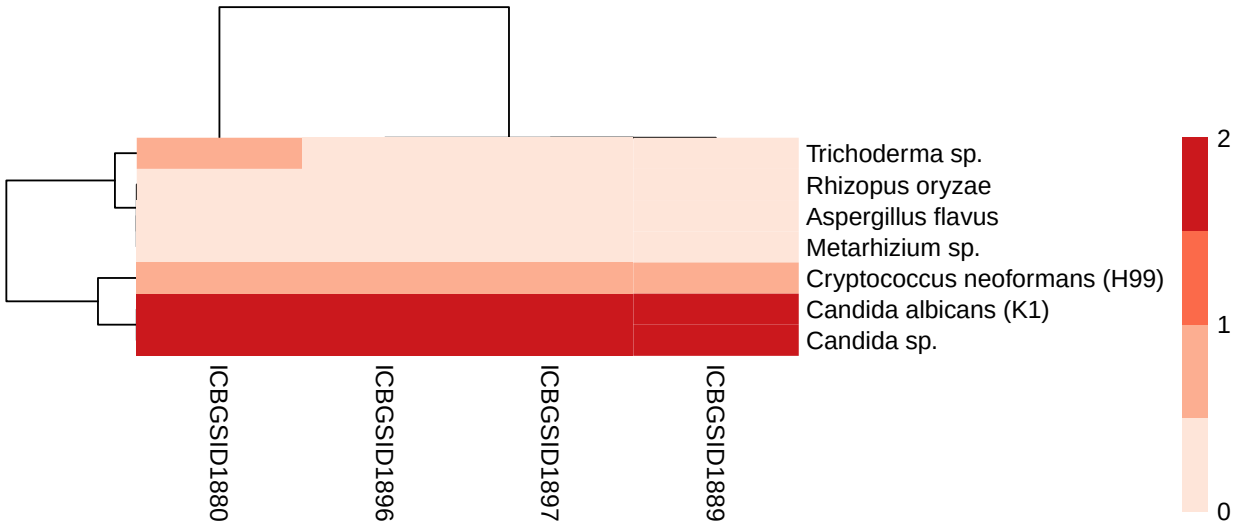

Supplemental Figure 2. Heatmap of scored bioassay data. Darker shades of red indicate a higher bioassay score, ranging from 0 (no-inhibition) to 3 (prominent zone of inhibition).

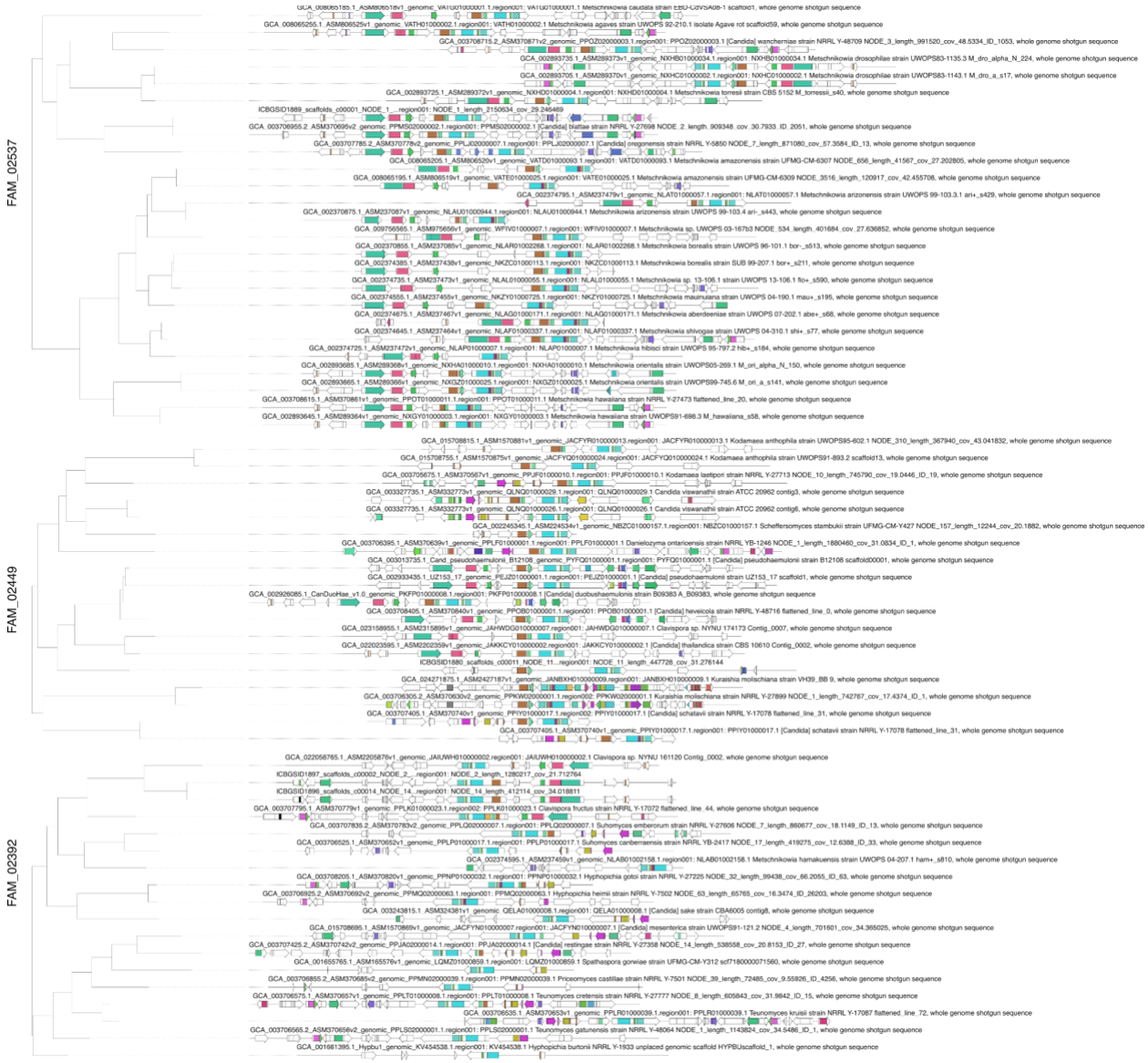

Supplementary figure 3. Full representation of all BGCs in NRPS BGC families. Subsets of these families are presented in Fig. 5.

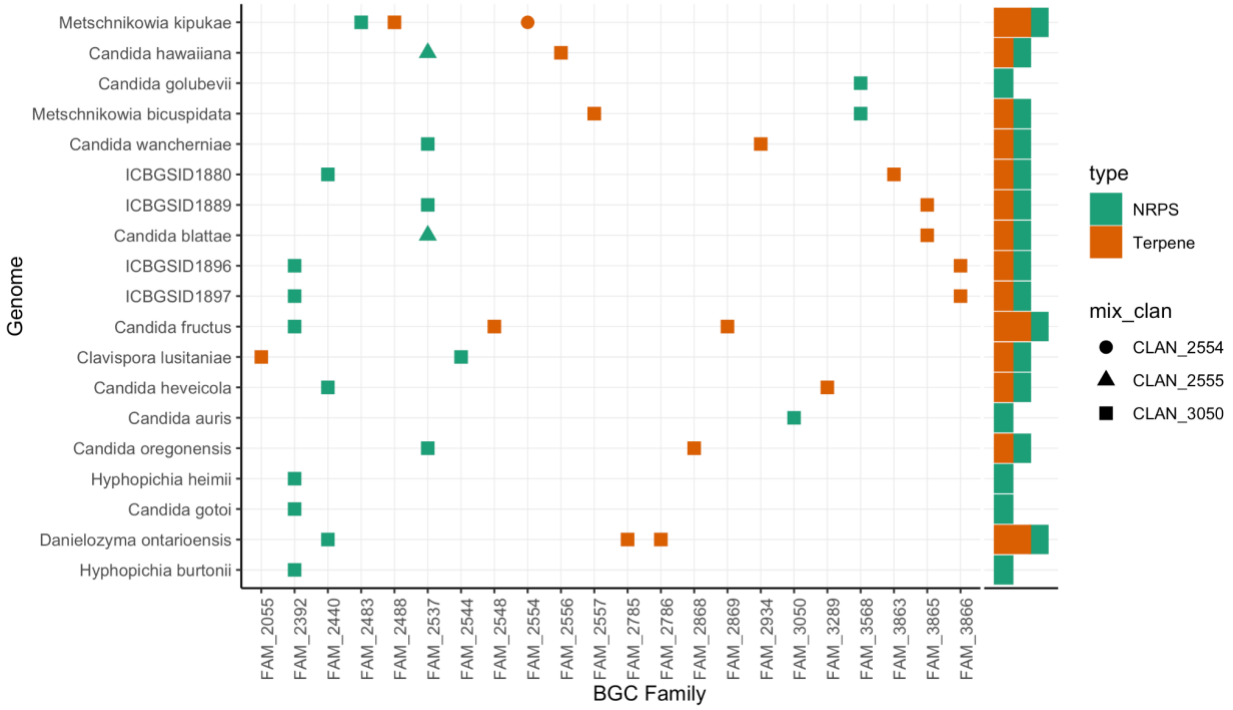

Supplemental figure 4. BGCs across yeasts that are evolutionarily related to yeasts associated with *Azteca* ants are mapped. The x-axis represents a given BGC family, the y-axis is the genome of origin for each BGC. The side bar plot counts the number of BGCs in each genome. The color represents the predicted type of the BGC, either NRPS (green) or terpene (orange). The shape of each point indicates the clan that each BGC would occupy under a 'mixed' analysis.